Novel Concepts Derived From Microbial Biomarkers In The Congo System: Implications For Continental Methane Cycling

Charlotte Louise Spencer-Jones

Supervised by Dr. Helen M. Talbot and Prof. Thomas Wagner

A thesis submitted to Newcastle University in partial fulfilment of the requirements for the degree of Doctor of Philosophy in the Faculty of Science, Agriculture and Engineering

School of Civil Engineering and Geoscience

Drummond Building

Newcastle University

United Kingdom

October 2015

Declaration

I hereby certify that the work presented in this thesis is my original research work, with the exception of a subset of 120 ODP 1075 samples included in Chapters 4, 5, and 7 and 22 ODP 1075 samples in Chapter 6, however, the subsequent interpretation of the results are my own. Total organic carbon measurements (TOC) for 210 ODP 1075 samples were carried out by Holtvoeth et al. (2005) and are cited as such in Chapter 4. Wherever contributions of others are involved, every effort is made to indicate this clearly, with due reference to the literature and acknowledgement of collaborative research and discussions. No part of this work has been submitted previously for a degree at this or any other university.

Charlotte Louise Spencer-Jones

Abstract

Methane is a climatically active gas and is a potential source of rapid global warming. Future climate change scenarios predict increased global temperatures, which, could destabilise large reservoirs of organic carbon currently locked in sediments and soils and further accelerate global warming. Comparable to the Arctic, the tropics store a large proportion of sedimentary carbon that is potentially highly vulnerable to climate change. However, the significance of tropical methane sinks in modifying methane emissions during past climate warm periods remains unresolved. This study focussed on determining the importance of aerobic methane oxidation (AMO) within the Congo during modern conditions and the Pleistocene.

Bacteriohopanepolyols (BHPs), specifically aminobacteriohopane-31,32,33,34-tetrol (aminotetrol) and 35-aminobacteriohopane-30,31,32,33,34-pentol (aminopentol) are diagnostic molecular markers preserved in soils and sediments that can be used to trace AMO and, therefore, CH_4 cycling within both modern and ancient systems (hereafter termed CH_4 oxidation markers). In this project, BHP distributions were determined within modern samples from the Congo catchment, including; 22 soils, 6 Malebo pool wetlands and an estuarine sediment. To complement this work on modern systems, BHPs were also analysed within ancient sediments from the Congo fan (ODP 1075) dated to 2.5 Ma, including high resolution studies of marine isotope stages (MIS) 5, 11 and 13.

Within ODP 1075, high concentrations of CH_4 oxidation markers are observed with no strong down core degradation signature. The study presents the oldest reported occurrence of CH_4 oxidation markers, to date, with these biomarkers detected in sediments dated to 2.5 Ma (226 meters composite depth). Similarly, high concentrations of aminotetrol and aminopentol are also observed within the modern Malebo pool wetland and estuarine sediment, suggesting these sites as likely sources of CH_4 oxidation markers to the Congo Fan.

High concentrations of CH_4 oxidation markers were found during MIS 5, 11 and 13 within ODP 1075 sediments. The CH_4 oxidation marker signature during MIS 5 and MIS 11 coincides with high global CH_4 concentrations (EPICA Dome C), whereas MIS 13 was characterised by low atmospheric CH_4 concentrations. The strong similarities in CH_4 oxidation marker concentrations during all three interglacial suggests a non-linear response in BHP production/burial and global CH_4. This

disparity could be due to the displacement of main sediment supply to the Congo fan and/or the relative similarity of CH_4 sources during these time intervals. Alternatively, these differences could also be due to a threshold behaviour between methanogenesis – methanotrophy and the synthesis of diagnostic BHPs.

A long term reduction in the mean concentration of CH_4 oxidation markers is observed between 1.7 Ma and 0.3 Ma, suggesting a long term trend towards greater continental aridity within the Congo, consistent with changes in vegetation zones. Significant uncertainty still remain about the response of tropical CH_4 sources and sinks during global climate perturbations, however, this study emphasises the large potential of BHPs as powerful novel tracers for methane cycling, both on land and in the ocean and across all climate zones.

Acknowledgements

I would like to start by thanking my supervisors, Helen M. Talbot and Thomas Wagner, who have provided technical and scientific support as well as a large amount of encouragement during this project. I would like to thank the European Research Council (ERC) for funding this PhD as part of a starting grant (258734; awarded to H.M.T.). I would also like to acknowledge the International Ocean Discovery Programme (IODP) for providing access to ODP 1075 and to the Wildlife Conservation Society of Congo (WCS-Congo) for logistical support and invaluable local knowledge during the sampling campaigns. Furthermore, I would also like to thank Bienvenu Jean Dinga, John R. Poulsen, Jose N. Wabakanghanzi, Rob Spencer and Paul Mann for collecting and providing access to such an extensive set of samples. I sincerely hope future research continues to reveal the secrets of the Congo.

I would like to thank Frances R. Sidgwick, Bernard Bowler, Paul Donohoe, Tracy Thompson, and Philip Green for their technical support and patience during this project. I also thank Melissa Ware, Gail de Blaquiere and Yvonne Hall for making my experience at Newcastle University positive.

I also thank members of the AMOprox and Biogeochemistry group for sharing their research and allowing me to think beyond my own narrow field. I would also like to extend my thanks to members of the European Geoscience Union (EGU) Early Career Researcher network and representatives for showing me the wider, social implications of geoscience research and for supporting discussions about diversity and inclusivity within the field.

I would also like to thank Enno Schefuß and Erin McClymont for scientific advice and support during this project. I would also like to thank my Viva Voce examiners, Bart van Dongen and Martin P. Cooke for their valuable comments.

I would like to thank my friends and family for understanding the commitment a PhD takes and supporting me throughout it.

Last, but not least, I would like to thank Liam Pollard who has been my emotional support throughout this process. Thank-you for always putting my PhD-woes into perspective.

Thank-you all so much, I could not have done it without you.

Publication History

The following papers have been either been published or are in preparation.

Published

Spencer-Jones, C.L., Wagner, T., Dinga, B.J., Schefuß, E., Mann, P.J., Poulsen, J.R., Spencer, R.G.M., Wabakanghanzi, J.N., Talbot, H.M. Bacteriohopanepolyols in tropical soils and sediments in the Congo River catchment area. Organic Geochemistry, *In Press*.

Talbot, H.M., Handley, L., Spencer-Jones, C.L., Bienvenu, D.J., Schefuß, E., Mann, P.J., Poulsen, J.R., Spencer, R.G.M., Wabakanghanzi, J.N., Wagner, T., 2014. Variability in aerobic methane oxidation over the past 1.2Myrs recorded in microbial biomarker signatures from Congo fan sediments. Geochimica et Cosmochimica Acta 133, 387-401.

In Preparation

Spencer-Jones, C.L., Wagner, T., Schefuß, E., Talbot, H.M. High resolution record of terrestrial methane cycling in central Africa during MIS 5 and 11-13. *In Preparation*.

Spencer-Jones, C.L., Schefuß, E., Talbot, H.M. Bacteriohopanepolyol signatures in Congo fan sediments (GeoB 6518-1). *In Preparation.*

Schefuß, E., Eglinton, T.I., Spencer-Jones, C.L., Rullkötter, J., De Pol Holz, R., Talbot, H.M., Grootes, P.M., Schneider, R.R., Hydrologic control of carbon release from tropical wetlands". *In Preparation*.

Abbreviations

The following abbreviations are commonly used throughout this thesis

Aerobic methane oxidation	AMO
Anaerobic oxidation of methane	AOM
Bacteriohopanepolyol	BHP
Branched GDGT	br-GDGT
Branched vs Isoprenoid tetraether index	BIT
Glycerol dialkyl glycerol tetraether	GDGT
Intertropical convergence zone	ITCZ
Liquid chromatography - Mass spectrometry	LC-MS
Marine isotope stage	MIS
Mean annual air temperature	MAAT
Organic carbon	OC
Organic matter	OM
Palaeocene-Eocene thermal maximum	PETM
Sea surface temperature	SST
Soil organic matter	SOM
Sulfate reducing bacteria	SRB
Terrestrial derived organic carbon	OC_{ter}
Total lipid extract	TLE
Total organic carbon	TOC

Contents

List of Figures

Chapter 1. Introduction and Literature Review

Chapter 2. Biomarkers and Methodology

Chapter 3. Bacteriohopanepolyol Biomarker Distributions in Tropical Soils

Chapter 4. Determining Soil Organic Carbon Export to Late Quaternary Congo Deep Sea Fan Sediments (ODP Site 1075) Using Microbial Biomarkers

Chapter 5. Are all Bacteriohopanepolyols in ODP 1075 of Terrestrial Origin?

Chapter 6. High Resolution Record of Terrestrial Aerobic Methane Oxidation Reveals Intense Methane Cycling During MIS 11 and 5

List of Tables

Chapter 2 Biomarkers and Methodology

Chapter 3. Bacteriohopanepolyol Biomarker Distributions in Tropical Soils

Chapter 4. Determining Soil Organic Carbon Export to Late Quaternary Congo Deep Sea Fan Sediments (ODP Site 1075) Using Microbial Biomarkers

Chapter 6. High Resolution Record of Terrestrial Aerobic Methane Oxidation Reveals Intense Methane Cycling During MIS 11 and 5

Chapter 7. Exploring Stratigraphic Limits of Aerobic Methane Oxidation Biomarkers: The Pleistocene Record from the Congo Fan

Chapter 1:

Introduction and Literature Review

Chapter 1. Introduction and Literature Review

1.1. Introduction

The relationship between high and low latitude climate change remains a fundamental question in paleoclimate research, specifically, the sensitivity of low latitude climate to glacial – interglacial forcing from high latitudes. Quaternary paleoclimate studies suggest high latitude ice sheets varied with earth orbital periodicities (e.g. Imbrie et al., 1993). Variations in high latitude sea surface temperature (SST), ice rafted debris and deep ocean circulation have all been shown to co-vary to a large degree with late Quaternary ice volume at the 100 Ka and 41 Ka orbital periodicities throughout the last 700 Ka (Boyle and Keigwin, 1982; Ruddiman and McIntyre, 1984; Ruddiman et al., 1989; Raymo et al., 1990). This suggests a high latitude response to orbital insolation variations during the Pliocene – Pleistocene. As radiative forcing, due to eccentricity (100 Ka), does not have a significant impact on climate, the transition to 100 Ka cyclicity suggests a non-linear forced climate system (Imbrie and Imbrie, 1980). Proposed causes of the non-linear forced climate system include; changes in atmospheric CO_2 and CH_4 (Ruddiman, 2003) and long term decline in global temperatures (Zachos et al., 2001).

West Africa is the largest equatorial landmass and has a large range in vegetation and climate zones, including, tropical and extratropical regions. Two models of tropical paleoclimate exist where either (1) African aridity responds primarly to changes in glacial boundary conditons which propigates down from high latitudes (e.g. Parkin and Shackleton, 1973; Müller and Suess, 1979; Pokras and Mix, 1985; Stein, 1985; Gasse et al., 1990), or (2) African ariditiy is mainly controlled by low latitude insolation changes which modulate monsoonal rainfall at 23 – 41 kyr periodicities (e.g. Street and Grove, 1976; Kutzbach, 1981; Rossignol-Strick, 1983; Pokras and Mix, 1985; Prell and Kutzbach, 1987; McIntyre et al., 1989; Molfino and McIntyre, 1990). Both models have the potential to destabilise sedimentary C sources including oceanic (global estimate of 38 400 Pg C; 1 Pg = 10^{15} g) and terrestrial (global estimate of between 3 950 and 5 450 Pg C; Emerson and Hedges, 1988; Eswaran et al., 1993; Post, 1993; Batjes, 1996; Hedges et al., 1997; Prentice et al., 2001; Lal, 2004; Bridgeham et al., 2006; Tarnocai et al., 2009; Figure 1.1). C and therefore further contribute to climate change feedback loops.

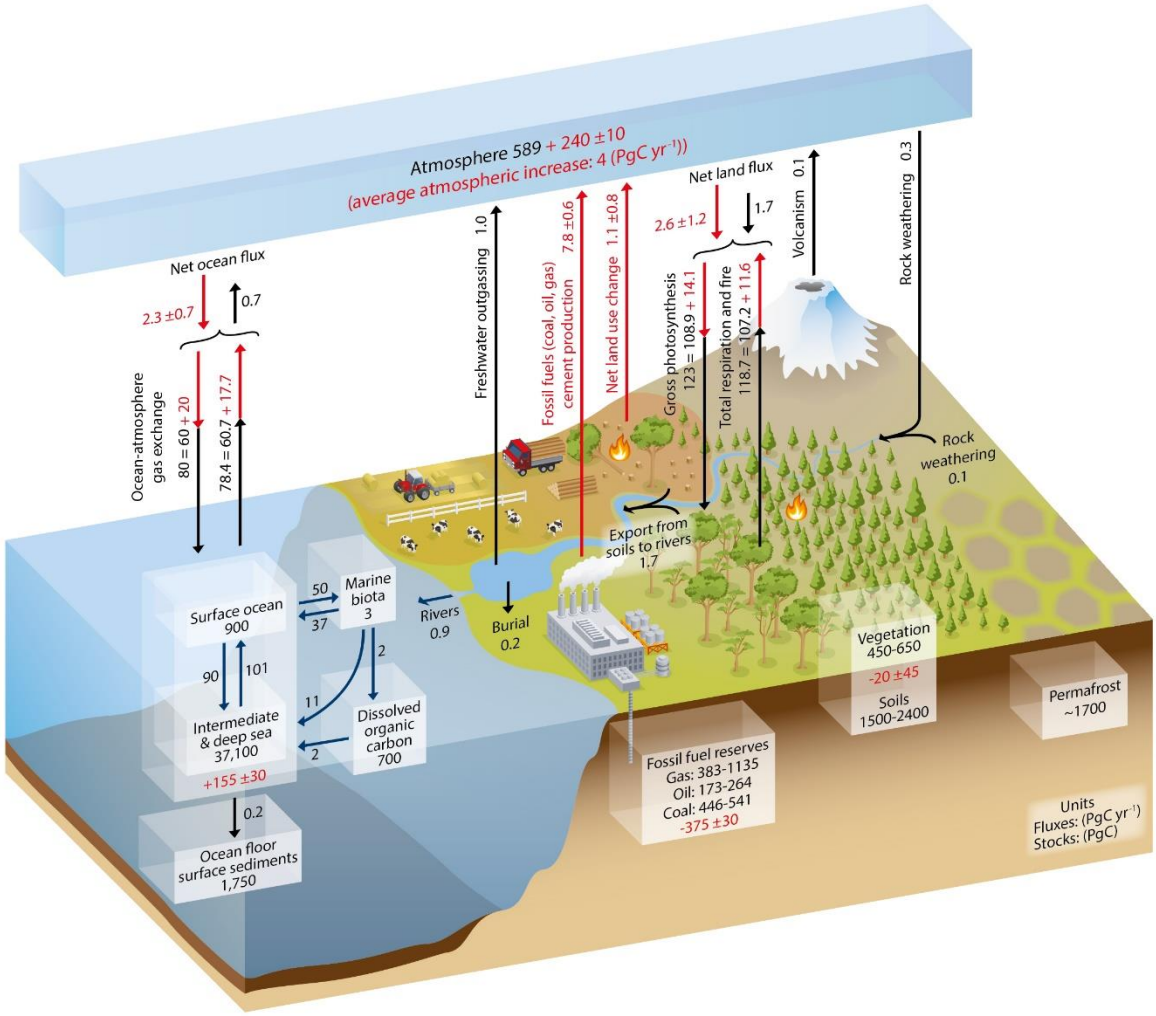

Figure 1.1. Figure taken from IPCC (2013; Figure 6.1). Simplified schematic of the global carbon cycle. Numbers represent reservoir mass, also called 'carbon stocks' in PgC (1 PgC = 10^{15}gC) and annual carbon exchange fluxes (in PgC yr^{-1}). Black numbers and arrows indicate reservoir mass and exchange fluxes estimated for the time prior to the Industrial Era, about 1750 (see IPCC 2013, WGI, Section 6.1.1.1 for references). Fossil fuel reserves are from GEA (2006) and are consistent with numbers used by IPCC WGIII for future scenarios. The sediment storage is a sum of 150 PgC of the organic carbon in the mixed layer (Emerson and Hedges, 1988) and 1600 PgC of the deep-sea $CaCO_3$ sediments available to neutralize fossil fuel CO_2 (Archer et al., 1998). Red arrows and numbers indicate annual 'anthropogenic' fluxes averaged over the 2000–2009 time period. These fluxes are a perturbation of the carbon cycle during Industrial Era post 1750. These fluxes (red arrows) are: Fossil fuel and cement emissions of CO_2 (IPCC, 2013, WGI, Section 6.3.1), Net land use change (IPCC 2013, WGI, Section 6.3.2), and the Average atmospheric increase of CO_2 in the atmosphere, also called 'CO_2 growth rate' (IPCC 2013, WGI, Section 6.3). The uptake of anthropogenic CO_2 by the ocean and by terrestrial ecosystems, often called 'carbon sinks' are the red arrows part of Net land flux and Net ocean flux. Red numbers in the reservoirs denote cumulative changes of anthropogenic carbon over the Industrial Period 1750–2011 (IPCC 2013, WGI, Table 6.1). By convention, a positive cumulative change means that a reservoir has gained carbon since 1750. Uncertainties are reported as 90% confidence intervals. See IPCC (2013) for further detail.

Atmospheric CH_4 is a potent greenhouse gas formed from the mineralisation of organic matter (OM). Ice core records suggest glacial-interglacial transitions experienced maximum CH_4 concentrations of 650-780 ppbv (Petit et al., 1999). Large uncertainties exist surrounding the source of paleo atmospheric CH_4, with several hypotheses proposing gas hydrates (Kennet et al., 2003), permafrost (DeConto et al., 2012), pulses of methane in opal rich sediments (Cook et al., 2011), and high and

low latitude wetlands (Brook et al., 2000; Dallenbach et al, 2000). However, due to a gap in our understanding of the CH_4 cycle and a lack of suitable geologically preserved proxies, large disparities exist between observed CH_4 concentrations from ice core evidence and the geological record. This PhD addresses this major challenge through the application of suitable biomarker proxies within the geological record, focusing on the low latitude CH_4 response to climate purtubations.

1.2. Modern Sources of CH_4

1.2.1. Soils

Soils can be both sources and sinks of CH_4. Methane is produced within soils due to methanogenesis within anoxic microsites, with the CH_4 subsequently consumed by aerobic methane oxidation (AMO) (the dominant form of CH_4 oxidation within soils). Two forms of CH_4 oxidation are recognised within soils (1) high affinity CH_4 oxidation and (2) low affinity CH_4 oxidation (Bender and Conrad, 1992, 1993; Hanson and Hanson, 1996). High affinity CH_4 oxidation occurs when the concentration of CH_4 within the soil is close to atmospheric CH_4 concentration. Low affinity CH_4 oxidation occurs when CH_4 concentration within soil are greater than atmospheric concentrations. Generally, high affinity CH_4 oxidation has been linked to soils that have not been exposed to high NH_4^+ (Bender and Conrad, 1993; Gulledge et al., 2004; Crossman et al., 2006), however, bacterial representatives are still largely unknown with radioactive fingerprinting studies characterising these strains as 'an unknown group of the α-*Proteobacteria'* (Holmes et al., 1999; Bull et al., 2000; Henckel et al., 2000; Crossman et al., 2005).

Soils, and particularly forest soils, are considered a net CH_4 sink (Purbopuspito et al., 2006; Kiese et al., 2008; Wolf et al., 2012). The net CH_4 exchange between soils and the atmosphere is dependent on a range of physical (e.g. soil texture, presence of organic layers, moisture content; Dörr et al., 1993; Topp and Pattey, 1997), chemical (e.g. nutrient availability, soil pH) and microbial parameters (Conrad and Rothfuss, 1991; Wolf et al., 2012). These parameters determine gas diffusivity in addition to the balance between microbial mediated methanogenesis and methanotrophy. For example, within montane forest soils from Ecuador, positive correlation was found between CH_4 uptake rates, mineral nitrogen content of the mineral soil and with CO_2 emissions, indicating CH_4 uptake corresponds to favourable conditions for microbial activity (Wolf et al., 2012).

Tropical forest soils are estimated to account for approximately 28% of annual global soil CH_4 consumption (equivalent to 6.2 Tg CH_4 $year^{-1}$; 1 Tg = 10^{12} g; Dutaur and Verchot, 2007). However, similar studies have found tropical soils to be sources of CH_4 (Martinson et al., 2010). Tathy et al. (1992) measured CH_4 emissions from three soils from the Congo; the dry soil was a CH_4 sink (-8.38 x 10^{10} molecules /cm^2/s) and the flooded soil was a CH_4 source (4.59 x 10^{12} molecules/cm^2/s). This clearly suggests that within tropical soils, the balance between CH_4 source and sink is highly variable with these environments potentially vulnerable to environmental change.

1.2.2. Wetlands

Natural wetlands are, historically, difficult to define. Natural wetlands represent the interface between dry terrestrial systems and deep water aquatic systems. Previous definitions of natural wetlands have been based on three main characteristics which include; shallow or water saturated soil; unique soil conditions that differ from upland soil conditions; and the presence of flood tolerant biota-hydrophytes with bogs, fens, swamps, marshes, mangroves, oxbow lakes, peatlands, salt marshes, riparian ecosystems and mires all categorised as wetlands (Mitsch and Gosselink, 2007). However, wetland environments are more complicated than the Mitsch and Gosselink (2007) definition, where hydrophytes may not be present due to flooding that only occurs seasonally, for example. Single wetlands can also be part of a much larger complex of wetlands and as such the RAMSAR convention (an intergovernmental treaty that provides a framework for the wise use of wetlands and their resources) defines wetlands in the broadest sense to also include floodplains, rivers and lakes, seagrass beds, coral reefs and other marine areas no deeper than 6 m at low tide in addition to those environments included in the Mitch and Gosselink (2007) definition (Ramsar Convention Secretariat, 2013). Natural wetlands have a unique biogeochemistry and are the largest single natural source of CH_4 to the atmosphere (IPCC, 2013) with modern emissions totally around 177 and 284 Tg CH_4 $year^{-1}$ (IPCC, 2013; Mitsch and Gosselink, 2007). However, CH_4 emissions vary on a regional basis, with tropical wetlands (20ºN to 30º S) thought to be the biggest CH_4 producers contributing to 60% of the CH_4 budget while northern (north of 45º N) wetlands are calculated to produce around 38 Tg CH_4 $year^{-1}$ and subtropical and temperate wetlands are calculated as producing considerably less methane (5 Tg CH_4 $year^{-1}$; Bartlett and Harriss, 1993; Ortiz-Llorente and Alvarez-Cobelas, 2012). Modern wetlands cover approximately 5 to 8% of the world's surface (Mitsch and

Gosselink, 2007) with 28 to 56% of the world's modern wetlands located within the tropics (Mitsch and Gosselink, 2007). Bwangoy et al. (2010) estimate that 56% of the Congo basin land cover consists of modern wetlands.

The type of wetland also affects CH_4 emissions, for example, Nahlik and Mitsch (2011) measured CH_4 emissions (sequential gas samples) from three different wetlands in Costa Rica using using nonsteady state plastic chambers during six sampling periods from 2006 to 2009. Higher methane rates were found for the seasonally flooded riverine wetland (719 mg CH_4 cm^{-2} day^{-1}) compared with a stagnant forest flooded wetland (601 mg CH_4 cm^{-2} day^{-1}) and a humid flow through wetland (91 mg CH_4 cm^{-2} day^{-1}; Nahlik and Mitsch, 2011). Temperature is also an important parameter affecting CH_4 cycling within wetlands through its influence on soil respiration. Increases in soil temperatures can increase microbial enzyme activity which can then aid the breakdown of complex polymeric carbon compounds and increase availability of dissolved organic carbon (OC; Freeman et al., 2004). Nahlik and Mitsch (2011) identify mean annual air temperature (MAAT) as affecting CH_4 emissions from three different wetlands in Costa Rica, with greatest CH_4 emissions within seasonally flooded riverine wetland (719 mg CH_4-$cm^{-2}day^{-1}$) which has a MAAT of 28.2 °C (due to the relatively open canopy). However, a similar study with peat mesocosm incubations did not observe a statistically significant increase in CH_4 emissions at high temperatures (Kim et al., 2012).

Within wetlands, CH_4 can bypass the AMO buffer within the surface soil through plant mediated transport resulting in wetlands being a net source of CH_4 to the atmosphere (Torn and Chapin III, 1993). However, within *Sphagnum* peatlands CH_4 can be directly diffused to methanotrophs that are hosted within hyaline cells of the plant and on the stem leaves (Raghoebarsing et al., 2005). Between 10 and 15% that of the sphagnum's C is supplied by symbiotic relationship with the methanotroph, thus, efficiently reducing CH_4 flux to the atmosphere (Raghoebarsing et al., 2005).

In the absence of wetland vegetation AMO removes much of the CH_4 (produced through methanogenesis) reducing emissions to the atmosphere (e.g. King et al., 1990; Conrad and Rothfuss, 1991; Frenzel et al., 1992; Vecherskaya et al., 1993; Van Der Gon and Neue, 1996; Bosse and Frenzel, 1997, 1998; Gilbert and Frenzel, 1998).

1.2.3. Floodplain Lakes

Floodplain lakes are, in essence, wetlands that are subject to seasonal pulsing (Mitsch and Gosselink 2007). Global CH_4 emissions from floodplain lakes are included in wetland CH_4 emission estimates (Wuebbles and Hayhoe 2002). One of the more extensively studied floodplain lake systems is the Amazon basin and can be divided into three habitats; open waters, emergent macrophyte beds and flooded forests (Devol et al., 1990). The total area of the floodplain within the main stem of the Amazon River spans between 100 000 and 180 000 km^2 with CH_4 emission estimates ranging from 3 to 18 Tg CH_4 $year^{-1}$ (Devol et al., 1990) suggesting the Amazon basin as an important source of tropospheric CH_4. Estimates of CH_4 emissions from tropical floodplain lakes are poorly constrained, which, is largely due to the spatial and temporal heterogeneity of these environments. When the full seasonal cycle is considered, CH_4 flux estimates from Amazonian floodplain lakes are around 5.1 Tg CH_4 $year^{-1}$ (Devol et al., 1990). CH_4 emissions for other tropical regions may be lower, e.g. Marani and Alvala (2007) estimate that CH_4 emissions within the Brazilian Pantanal region to be approximately 3.3 Tg CH_4 $year^{-1}$, while Smith et al. (2000) estimates CH_4 emissions from the Orinoco River main stem floodplain lakes to be approximately 0.17 Tg CH_4 $year^{-1}$. Additionally, estimates of CH_4 flux become unreliable due to differences in methodologies employed at each site and short term seasonal differences. For example, Mariani and Alvala (2007) note that their estimates of CH_4 flux from the Brazilian Panatanal region may be conservative as their samples were taken during the regions driest years in recent history.

1.2.4. Marine Sources

Gas hydrates and cold seeps are a significant potential source of CH_4 in marine systems (Kroeger et al., 2011). Gas hydrates are naturally formed in marine sediment when CH_4 saturates pore water in the gas hydrate stability zone (Kvenvolden and Lorenson, 2001). Cold seeps, which occur globally along active margins, represent a source of geologically derived CH_4. Seep formation is driven by (1) plate convergence, (2) sediment loading along passive margins, and (3) by differential compaction related to vertical tectonics (Kvenvolden and Lorenson, 2001). Seeps are usually at ambient sea floor temperature and flow more slowly than hydrothermal vents (Kvenvolden and Lorenson, 2001). Both gas hydrates and cold seeps can

contain either CH_4 derived from thermogenic cracking (characterised by heavy $\delta^{13}C$ isotope ratio) or bacterially mediated organic matter (OM) decomposition (methanogenesis; characterised by lighter $\delta^{13}C$; Kvenvolden and Lorenson, 2001; see Sections 1.3 and 2.2.1 for in-depth discussion).

Gas hydrates represent a significant potential source of marine CH_4, with the world's total gas hydrate inventory thought to be approximately 4.18 to 995 Pg of CH_4 (Burwicz et al., 2011). The dissociation of CH_4 within these reservoirs is dependent on both pressure and temperature gradients. The reduction in pressure, for example, due to ice sheet retreat coupled with an increase in oceanic temperature will reduce the stability of the hydrates and hence increase hydrate decomposition (Formolo et al., 2008), in this case the gas hydrate will decompose starting from the bottom of the stability field. An exception occurs with shallow water hydrates at the top of the stability zone, as they decompose from top to bottom (Reagan and Moridis, 2007). Shallow water hydrates are therefore more vulnerable to changing environmental conditions and are able to undergo rapid dissociation with sea floor temperature fluxes (Reagan and Moridis, 2007; Westbrook et al., 2009).

1.3. Modern CH_4 Cycling and Aerobic/Anaerobic Sinks

There is one major and two minor sinks for CH_4. The major sink for atmospheric CH_4 is the OH radical sink and the 2 minor sinks are the biologically mediated CH_4 sinks; anaerobic oxidation of methane (AOM) and aerobic methane oxidation (AMO). The OH radical sink will not be discussed in great detail, however, the oxidation of CH_4 with OH radicals (in the presence of NOx) leads to the formation of CH_2O, CO and O_3 (Wuebbles and Hayhoe, 2002). Presently, the OH radical sink is responsible for removing approximately 500 Tg CH_4 $year^{-1}$ (approximately 90% of the CH_4 budget) from the atmosphere (Wuebbles and Hayhoe, 2002). Dry soil oxidation is thought to be responsible for the oxidation of approximately 30 Tg CH_4 $year^{-1}$ from the atmosphere (approximately 5% of the CH_4 budget), however, quantification of CH_4 oxidation within soils and sediments (through AMO and AOM), and the prevention of this CH_4 from entering the atmosphere remains uncertain (e.g. Khalil and Shearer, 2000).

1.3.1. Anaerobic Oxidation of Methane (AOM)

Anaerobic oxidation of methane is considered a major marine geochemical process and acts as the dominant CH_4 sink in marine environments. Anaerobic oxidation of methane is hypothesised to consume >50% of the gross annual production of CH_4 in the oceans before it diffuses to the atmosphere (Offre et al., 2013). There are three proposed mechanisms for AOM, including; reverse methanogenesis (Hoehler et al., 1994), acetogenesis (Conrad, 2005; Whalen, 2005) and methylogensis (Conrad et al., 2006), with reverse methanogenesis the most extensively studied. Reverse methanogenesis is thermodynamically favourable when concentrations of CH_4 are higher than H_2 due to sulfate reducing bacteria (SRB) depleting the concentration of H_2 (Equation 1.1; Hoehler et al., 1994). This sulfate dependent methanotrophy is mediated by microbial syntrophic consortia of archaea and SRB (Serrano-Silva et al., 2014 and references therein). The methanotrophic archaea typically consist of the clades ANME-1 and ANME-2 (Strous and Jetten, 2004), with SRB closely related to members of the genera *Desulfosarcina* – *Desulfococcus* (δ-*Proteobacteria*).

Equation 1.1: Balanced equation for the process of anaerobic oxidation of methane (reverse methanogenesis). a, net reaction; b, CH_4 oxidation reaction; c, coupled sulfate reduction reaction.

$$CH_4 + SO_4^{2-} \rightarrow HCO_3^- + HS^- + H_2O \ (net;\ \boldsymbol{a})$$

$$CH_4 + 2H_2O \rightarrow CO_2 + 4H_2 \ (CH_4\ oxidation;\ \boldsymbol{b})$$

$$SO_4^{2-} + 4H_2 + H^+ \rightarrow HS^- + 4H_2O \ (sulfate\ reduction;\boldsymbol{c})$$

Anaerobic oxidation of methane has been shown to occur in a range of marine environments including; recent marine sediments, CH_4 seeps and vents (Vigneron et al., 2013), anoxic waters, soda lakes and deep continental margin sediments (Cambon-Bonavita et al., 2009). AOM is estimated to consume the equivalent of 5 – 20% of the net modern atmospheric CH_4 flux (0.02 – 0.1 Pg C $year^{-1}$) (Valentine and Reeburgh, 2000).

Within marine systems associated with gas hydrates and/or cold seeps, AOM is the dominant CH_4 consuming process due to widespread anoxia (Reeburgh, 2007). For example, high microbial diversity was found in sediments from an active cold seep in the Southeast Atlantic (the REGAB pockmark) including genetic sequences for anaerobic methanotrophic archaea (ANME-2) and bacteria of the *Desulfosarcina*/*Desulfococcus* cluster suggesting the occurrence of AOM 3-5 cm below the surface of the sediment (Cambon-Bonavita et al., 2009). In agreement with

this, Bouloubassi et al. (2009) also found evidence for AOM at the REGAB pockmark; the CH_4 seep sediments contained high concentrations of biomarkers indicative of AOM (archaeol, *sn*-2 hydroxyarchaeol and crocetane) in addition to high concentration of biomarkers for SRB (monoalkylglycerolethers). The occurrence of AOM is further confirmed by highly depleted compound specific $\delta^{13}C$ isotope values as low as -135 ‰ for AOM biomarkers and between -86 and -95 ‰ for SRB biomarkers (Bouloubassi et al., 2009).

However, AMO may still occur in the oxic water column and surface sediments. Valentine et al. (2001) analysed water column CH_4 oxidation adjacent to an area of active hydrate dissociation (Eel River Basin, California) and found AMO activity. High CH_4 oxidation rates of 5.2 mmol CH_4 m^{-2} $year^{-1}$ were measured within the deepest part of the water column (>370 m) compared to CH_4 oxidation rates of 0.14 mmol CH_4 m^{-2} $year^{-1}$ observed within the shallow part of the water column (<370 m) (Valentine et al., 2001). Aerobic methane oxidation was also identified within seep sediments from the Southeast Atlantic Ocean (the REGAB pockmark) where, high concentrations of $\delta^{13}C$ light biomarkers specific for aerobic methanotrophs (diploptene and 4α-methylsterols) were identified (Bouloubassi et al., 2009).

1.3.2. Aerobic Methane Oxidation (AMO)

Aerobic methane oxidation is the oxidation of CH_4 in the presence of O_2 to form CO_2 and H_2O (Equation 1.2). Due to the requirement of O_2, the process of AMO is most common within terrestrial environments and is considered a minor process within marine systems. Aerobic methane oxidation is a bacterially mediated process which utilises the methane monooxygenase enzyme where, the O-O bond of O_2 is split within one O reduced to form H_2O and the second O incorporated into CO_2.

Equation 1.2. Equation for the process of aerobic methane oxidation.

$$CH_4 + 2O_2 \rightarrow CO_2 + 2H_2O$$

Aerobic methane oxidation is performed by a range of aerobic methanotrophs belonging to the *Proteobacteria*. Aerobic methanotrophs are grouped into Type I (RuMP pathway; ɣ-*Proteobacteria*) and Type II (serine pathway; α-*Proteobacteria*) methanotrophs. Type I methanotrophs form a group within the *Methylococcaceae* family and include the genera *Methylomonas, Methylobacter, Methylomicrobium, Methylococcus*, *Methylocaldum*, *Methylosphaera*, *Methylosarcina, Methylohalobius,*

Methylothermus, Methtylosoma (Dedysh, 2009 and references therein), *Methylogaea* (Geymonat et al., 2011; Hoefman et al., 2014), *Methylovulum* (Kip et al., 2011), *Methylomarinum* (Hirayama et al., 2013), *Methyloparacoccus* (Hoefman et al., 2014), *Methylomarinovum* (Hirayama et al., 2014) and type II include the genera *Methylosinus*, *Methylocystis, Methylocella* and *Methylocapsa* (Bowman et al., 1993, 1995; Dedysh, 2009 and references therein). Methanotrophic bacteria have also been identified as endosymbionts within marine animals including *Bathymodiolin* mussels (Distel and Cavanaugh, 1994; Jahnke et al., 1995; Raggi et al., 2013), vent snails (*Ifremoria nautiles*; Borowski et al., 2002; Dubilier et al., 2008) and tube worms (*Siboglinum poseidoni*, *Sclerolinum contortum*; Pimenov et al., 2000). To date, all currently published sequences of endosymbiont methanotrophs are from the ɣ-proterobacteria, with free living CH_4 oxidisers of the genera *Methylobacter* and *Methylomicrobium* (Dubilier et al., 2008 and references therein).

Globally, AMO is thought to consume 7 – 10% of the net total annual global emission of CH_4 (Lowe, 2006; Chowdhury and Dick, 2013). While this estimate is lower than the net modern CH_4 flux consumed through AOM (Valentine and Reeburgh, 2000), AMO has been demonstrated to be a quantitatively important process during massive CH_4 release (e.g. Kessler et al., 2011). During the Deepwater Horizon oil spill (Gulf of Mexico, 2010), CH_4 was the most abundant hydrocarbon released. Kessler et al. (2011) determined that after ~120 days almost all the CH_4 had been consumed and between ~3.0 x 10^{10} and ~3.9 x 10^{10} moles of O_2 were respired. Kessler et al. (2011) suggest a bacterial bloom during this period was responsible for consuming the CH_4. Furthermore, large scale release of CH_4 from gas hydrates is hypothesised to stimulate a similar rapid methanotrophic response (Kessler et al., 2011). Methanotrophs and AMO have been identified in water columns associated with methane seeps (laterally and vertically through benthic water column (e.g.Tavormina et al., 2010); peatlands (e.g. Deng et al., 2013); tropical wetlands; tropical soils (Dedysh et al., 2007); and in aerosol samples (Šantl-Temkiv et al., 2013).

1.3.3. Key Microbial Biomarkers

Biological markers or biomarkers are derived from living organisms. Following the death of these organisms, biomarkers may be preserved in soils or sediments and thus become molecular fossils (Peters et al., 2005). Specific organic biomarkers can be used to trace CH_4 cycling in soils and sediments. Bacteriohopanepolyols (BHPs)

are recalcitrant pentacyclic triterpenoids and are the precursor compounds to geohopanoids. Specific BHPs are produced by aerobic methanotrophs, making these biomarkers highly specialist proxies for AMO; previous studies have used BHPs to trace AMO in both modern and ancient samples (Coolen et al., 2008; Zhu et al., 2010; Berndmeyer et al., 2013; Wagner et al., 2014). However, there exists few studies applying these biomarkers to the tropics during the Pleistocene. It is critically important to understand CH_4 cycling within the tropics and identify if these biomarkers can be used to distinguish the source of paleo CH_4 (see further discussion in Section 2.1).

1.4. Methane Cycling During Past Climates

Concentrations of atmospheric CH_4 are thought to have significantly varied during earth history. The O_2 free world of the late Archean is thought to have hosted the highest concentrations of atmospheric CH_4 in earth history, with CH_4 concentrations predicted to be around 1000 ppm (Kasting, 2005). The rise in atmospheric O_2 concentrations at ~2.3 Ga would have eliminated much of the CH_4. This reduction in atmospheric CH_4 could have triggered the Paleoproterozoic glaciations (Kasting, 2005). Similarly, high atmospheric concentrations of CH_4 are suggested to have occurred during the Palaeocene Eocene Thermal Maximum (PETM). Around 55.5 and 52 Ma the earth experienced a series of extreme hyperthermals superimposed on a long term warming trend. PETM was the first of these hyperthermals and was characterised by massive C input (a shift of >3‰ $\delta^{13}C$; Dickens et al., 1995), ocean acidification and an increase in global temperature by 5°C (Zachos et al., 2003). Large scale fluctuations in atmospheric CH_4 have also been recorded in ice core records from Vostok station and EPICA Dome C in Antarctica spanning the past 800 000 years with minimum concentrations of CH_4 within ice core records ranging from 320 to 350 ppbv and maximum methane concentrations between 650 to 800 ppbv (Petit et al., 1999; Loulergue et al., 2008). High CH_4 concentrations were found to coincide with interglacial periods in both Vostok and Epica Dome C ice core records (Petit et al., 1999; Loulergue et al., 2008).

Sources of CH_4 and the importance these contributions make to shifting climate conditions is still largely unknown. Several sources have been proposed for the rise in atmospheric CH_4 during climates of the past, including gas hydrates (Dickens et al., 1997; Kennet et al., 2003), permafrost (DeConto et al., 2012), pulses of methane

in opal rich sediments (Cook et al., 2011), and high and low latitude wetlands (Brook et al., 2000; Dallenbach et al, 2000). The cause of CH_4 release during the hyperthermals of the PETM has been the most extensively studied. The clathrate gun hypothesis proposes large scale massive release of sedimentary CH_4 from gas hydrates (Kennet et al., 2003) as a source of isotopically depleted $\delta^{13}C$. Numerical models of climate scenarios similar to the PETM where $1.12x10^{18}$ g CH_4 is released within the framework of the modern C cycle show $\delta^{13}C$ excursions of a similar magnitude observed in the geological record, suggesting massive release of CH_4 from marine hydrates as a plausible source of CH_4 during the PETM (Dickens et al., 1997). However, modern gas hydrates have an isotopic composition of approximately -60‰ suggesting a C release of approximately 2000 Pg, which is too small to cause between 5 and 6 °C of warming (Dickens et al., 1997). Additionally, a 2000 Pg C release could not cause a 2 km rise in the depth of the calcite compensation depth (CCD; Zachos et al., 2005) suggesting that gas hydrates alone could not be responsible for the PETM (Higgins and Schrag, 2006).

DeConto et al. (2012) propose the decomposition of high latitude permafrost as a massive source of CH_4 during the PETM. Orbitally triggered decomposition of soil organic matter (SOM) reservoirs in permafrost could have released the necessary C flux for the 6°C warming of the PETM (3434 Pg C ± 951 over 10^4 year timescale).

In further contrast to the permafrost hypothesis, Pancost et al. (2007) suggest that the release of CH_4 from the terrestrial biosphere through wetlands could be responsible for the C flux. Enhanced CH_4 production from tropical wetlands is thought to be responsible for the 70% increase in atmospheric CH_4 since the last deglaciation (Maslin and Thomas, 2003). While this accounts for only 250 Pg of carbon (a far smaller flux than is required for the magnitude of the PETM hyperthermals) increased C burial in wetlands during the Palaeocene could have resulted in a greater CH_4 flux. Maslin and Thomas (2003) also argue that increases in atmospheric CH_4 concentrations could result from a CH_4 flux from a combination of sources. Pre-industrial CH_4 emissions are estimated between ~ 200 and 250 Tg $year^{-1}$ with wetlands suggested to have contributed ~ 85% to the CH_4 budget (IPCC, 2013), adding further weight to the wetland hypothesis.

Potentially, large scale CH_4 emissions could have come from a mixture of all these proposed sources (Maslin and Thomas, 2003), however, the influence of high vs. low latitude sources is also much debated. Within modern wetlands two thirds of the CH_4

flux is from tropical sources suggesting tropical wetlands as a major contributor to atmospheric CH_4 concentrations and a potential driver of climate. Ice records from EPICA Dome C reveal CH_4 emissions during the past 800 000 Ka which are influenced by both high latitude boreal wetland/permafrost and low latitude tropical wetlands extent (Loulergue et al., 2008). At high latitudes, variations in ice sheet extent contribute to the decomposition of peat and the thawing and refreezing of permafrost active layers (Schmidt et al., 2004). Within EPICA Dome C ice core records, CH_4 signal and global ice volume signal show an in phase relationship and a strong coherency with 100 Ka cycle (Loulergue et al., 2008). Tropical wetland extent is modulated through the tropical monsoon system and position of the intertropical convergence zone (ITCZ), which, is modulated through orbitally driven variations in the latitudinal and land sea temperature gradient (Chiang et al., 2003; Liu et al., 2003). CH_4 signals from EPICA Dome C show an in phase variation with summer monsoon and show an increasing variance in the precessional band starting at 420 Ka, thus suggesting a dominant contribution of monsoon – related processes in the CH_4 variability at precessional periodicities (Loulergue et al., 2008). Loulergue et al. (2008) suggest a dominant contribution of tropical wetlands to atmospheric CH_4 in the preindustrial budget. Boreal wetlands are suggested to have a switch-on response when ice sheets decay and an amplification of the OH sink (Loulergue et al., 2008). Climate and wetland simulations of the global CH_4 cycle for the past 130 Ka are able to recreate CH_4 signals within the ice core records (Singarayer et al., 2011). Further suggesting that variations in CH_4 emissions from tropical sources are important in past climate modulation. Therefore, the focus of this PhD will be on tropical CH_4 cycling.

1.5. Tropical Africa and the Pleistocene

1.5.1. Modern West African Climate

The equatorial Atlantic is a key position for the investigation of climatic development and its fluctuations with land – ocean interactions (Zabel et al., 2004). The equatorial Atlantic represents a corridor for global water mass circulation. The global water mass circulation is a significant process of the interhemispheric and latitudinal heat transfer around the Earth (Zabel et al., 2004). At the equatorial Atlantic, Northern and Southern Hemisphere meteorological cycles meet at the ITCZ. The ITCZ is a highly

dynamic climate system which is greatly impacted by global water cycle (Zabel et al., 2004).

West African continental moisture is controlled through wind and pressure patterns which govern the regions climate. Three major air streams (Congo air with Westerly and South-Westerly flow; the Southeast (SE) monsoon and the Northeast (NE) monsoon) and 3 convergence zones balance the humidity and aridity cycles. Both the NE and SE monsoon are thermally stable and associated with subsiding air and are, therefore, relatively dry. In contrast, the flow from the Congo is relatively humid, convergent and thermally unstable and, therefore, associated with rainfall. These air streams are separated by 2 surface convergence zones, the ITCZ (separates the 2 monsoons) and the Congo air boundary (separates the Easterlies and Westerlies). A third convergence zone separates the dry, stable, northerly flow of the Sahara and the moister southerly flow (Nicholson, 1996; Figure 1.2). The contrast in land – ocean temperatures and air pressure gradients, atmospheric circulation controlled climate and marine sedimentation give rise to highly complex interacting sub-processes (Zabel et al., 2004).

1.5.1. Pleistocene Climate Dynamics

Quaternary climate is defined as periods of warm/temperate interglacials with cold glacial periods often with the build-up of ice sheets (Imbrie et al., 1992). Interglacials are highly complex periods with variable duration, intensity and stability. In the early Pleistocene (2.5 to 1.4 Ma) glacial-interglacial cycling was controlled by orbital cycles (Imbrie et al., 1992). Orbital cycles (Milankovitch theory) describes parameters (orbital elements) which influence the amount of solar energy the Earth can absorb and therefore influence Earth climate. Milankovitch theory describes three orbital elements: eccentricity, obliquity and precession. Eccentricity describes the variation in the elliptical orbit of the Earth with the main periods of eccentricity occurring on a 400 and 101 Ka cycle. Obliquity is a measure of the angle between the polar North Pole and celestial north and varies on a 41 Ka cycle. Insolation has a periodicity of 23 Ka and is a measure of the amount of solar radiation the planet receives whereby its intensity is inversely proportional to the square of the distance of the planet to the Sun. Solar radiation is party absorbed and partly reflected back into space (albedo). Insolation, and therefore the solar radiation that is absorbed/reflected by the earth, is sensitive to changes in both eccentricity and obliquity. Precession sensitivity and

asymmetry of glacial (saw toothed) cycles begin to increase sometime between 3 and 2.5 Ma (Lisiecki and Raymo, 2007). The onset of the northern hemisphere glaciation appears to be associated with the start of a gradual change in the dynamics of glacial cycles.

Both glacial asymmetry and precession sensitivity are either controlled by the dynamics of the northern ice sheets directly or by the same factor which determines the glacial maximum in northern ice volume (Ashkenazy and Tziperman, 2004; Liu and Herbert, 2004; Huybers, 2007; Lisiecki and Raymo, 2007). During the past 300 Ka the influence of precession modulated variations in seasonal incoming radiation significantly affected the tropical climate both on land and in the surface ocean (deMenocal et al., 1993).

The Mid Pleistocene transition (MPT) is a major transitional period in Earth history (Head and Gibbard, 2005). During the Pliocene – early Pleistocene, glacial – interglacial cycles were dominated by low amplitude obliquity forced 41 Ka cycles. However, at the onset of the MPT glacial interglacial cycles were dominated by high amplitude 100 kyr cycles. The MPT spans a period from 1.2 Ma to 0.5 Ma with much debate still surrounding the timing (Head and Gibbard, 2005). The 100 kyr cycles that define the MPT have been thought to be related to eccentricity cycles, however, the MPT is more closely linked with precessional cycles which have a period of 23 Ka, with each cycle defined by the fourth or fifth precessional cycle (Maslin and Ridgwell, 2005). At the beginning of the MPT at 940-890 Ka a significant increase global ice volume with 41 Ka cyclicity occurred. The second phase of the MPT began approximately 725-65 Ka and is characterised by high amplitude 100 Ka cyclicity (Head and Gibbard, 2005). The 100 Ka cycles of the MPT are indicative of slow ice build-up and subsequent rapid melting, which, implies a transition to a strongly non-linear forced climate system (Head and Gibbard, 2005). Proposed causes of the non-linear forced climate system include; changes in atmospheric CO_2 and CH_4 (Ruddiman, 2003) and long term decline in global temperatures (Zachos et al., 2001). Within the tropics, the dominance of 100 Ka and 41 Ka variations after the MPT suggest increased high-latitude climatic influence under the growth and decay of large continental ice sheets over the last 0.9 Ma (Jahn et al., 2005).

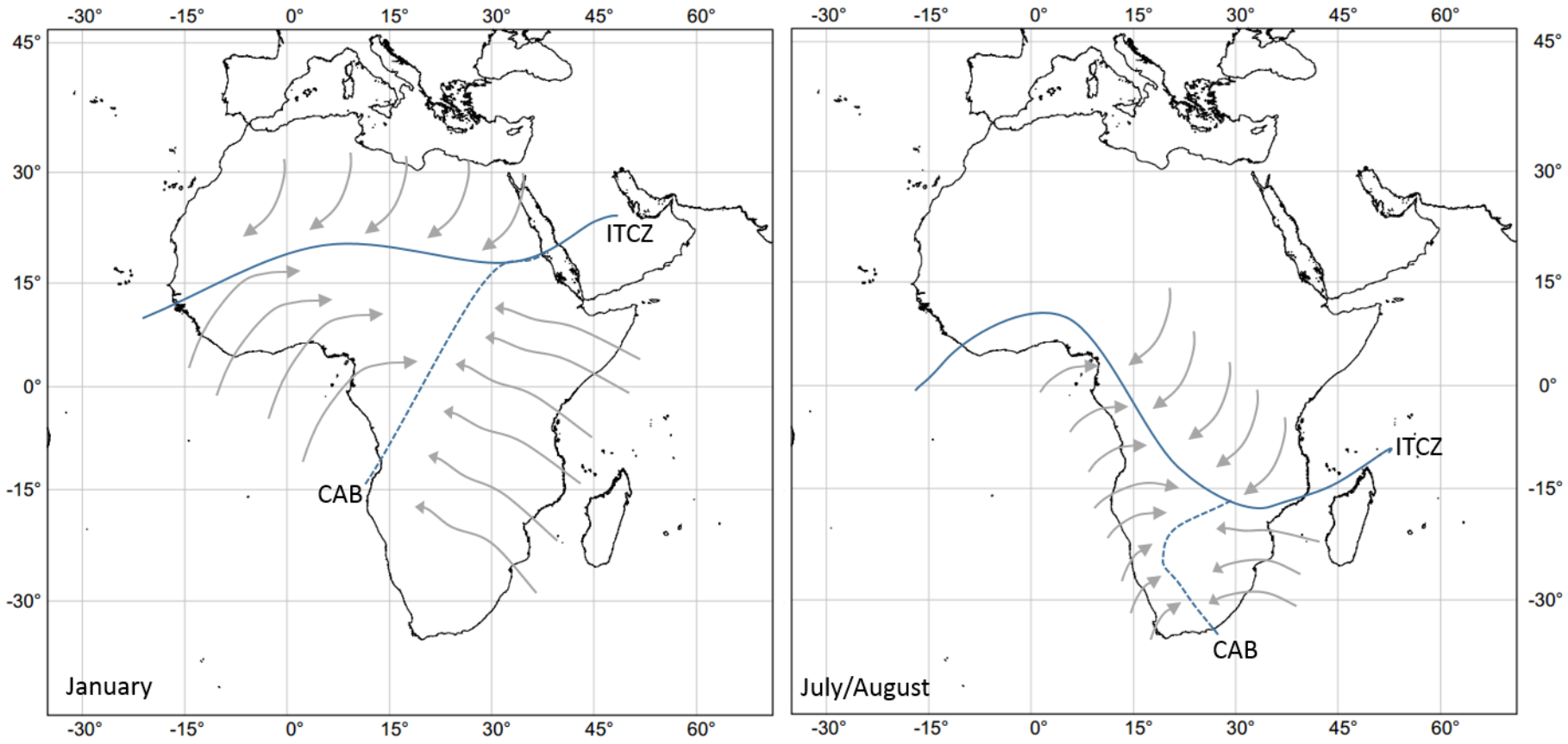

Figure 1.2. Approximate position of the Intertropical Convergence Zone (ITCZ) and Congo air boundary (CAB) in January and July/August, grey arrows show Easterly and Westerly winds. Figure modified from Schefuß et al, (2011) and Nicholson, (1996).

1.5.2. Terrestrial CH_4 Cycling During the Pleistocene

The global water cycle, which impacts on CH_4 cycling in wetland and soil environments, is modulated through glacial – interglacial cycles, insolation driven tropical monsoon change and by millennial frequencies (Guo et al., 2012). Analysis of plant waxes records from West African sedimentary archives (ODP 1077) reveals a significant increase in trade wind strength and zonality with the onset of the 100 Ka cyclicity (Schefuß et al., 2003). Sea surface temperature (SST) was controlled through atmospheric water balance, leading to highest continental aridity when SSTs were lowest, with the destabilisation of vegetation by increasing wind strength (Schefuß et al., 2004a,b). Increased dust accumulation in West Africa agrees with records from Northwest Africa (deMenocal et al., 1993) and the equatorial Atlantic (Ruddiman and Janecek, 1989; Tiedemann et al., 1994; Wagner, 2000). In contrast, plant wax records from Southwest Africa (ODP 1085) suggest no significant change in moisture availability to the continent over the past 2.5 Ma (Maslin et al., 2012).

Changes in atmospheric moisture content during the mid-Pleistocene are found to coincide with large scale vegetation change in the Congo, which, is driven by SST, the intensity of the African monsoon and ocean circulation (Schefuß et al., 2003; 2005). Dupont et al. (2000) analysed palynology records from West African marine and terrestrial cores for the past 150 000 years and found expansion of mangrove swamps and tropical rainforest typically during warm – humid marine isotope stages (MIS) with an expansion in dry savannahs and grasslands during cool – dry MIS. At the onset of the cooler MIS 5d at approximately 115 Ka a small reduction in rain forest was observed but not at the same magnitude as during glacial MIS (Dupont et al., 2000).

Tropical African climate has been suggested as wetter than present day during the Pleistocene. Beuning and Russell (2004) analysed palynology records from Lake Edward (Uganda – Democratic Republic of Congo border) and found wetter climate than present with the rift valley floor suggested to contain extensive semi-deciduous forest compared to typically drier grassland type environments that are present today. This shift in vegetation would require a 25-60% increase in annual precipitation (Beuning and Russell, 2004). However, the terrestrial CH_4 cycling remains poorly characterised, largely due to a lack of appropriate biomarkers/proxies.

1.6. Hypotheses, Aims and Objectives of This Thesis

High anthropogenic induced greenhouse gas emissions have the potential to cause a catastrophic environmental disaster. This flux of CH_4 to the atmosphere highlights the importance of identifying all potential greenhouse gas sources and sinks. Approximately 41 460 Pg C is stored in the terrestrial and oceanic realm (Emerson and Hedges, 1988; Eswaran et al., 1993; Post, 1993; Hedges et al., 1997; Lal, 2004) with both these stores increasingly vulnerable to changes in climate. While the massive global release of CH_4 observed in ice core and geological records has yet to be reconciled with a source, paleo tropical CH_4 emissions have the potential to induce large scale environmental change.

To date, there exists few studies applying biomarkers specific to CH_4 cycling to the tropics during the entire Pleistocene. It is critically important to understand CH_4 cycling within the tropics and identify if these biomarkers can be used to distinguish the source of paleo CH_4.

This project builds on existing biomarker records from the Congo Fan, which, suggest intense AMO (high concentration of BHP CH_4 oxidation markers; see Section 2.6 for definition) from an unknown source during Pleistocene interglacials (see Talbot et al., 2014). The overall aim of this project was to identify the sedimentary microbial response to short term climate fluctuations within the continental catchment of the Congo fan. This project was divided into five specific sub-projects, each with specific hypothesis and objectives:

Hypothesis 1: Paleo CH_4 oxidation biomarkers in Congo fan sediments are of terrestrial origin (Chapter 3).

This sub-project assessed and compared BHP signatures from a range of soil and wetland samples and 1 estuarine sediment from the Congo hinterland and estuary and to determine factors that control BHP distributions in these environments.

Hypothesis 2. The Congo fan is influenced by terrestrial organic carbon transport (Chapter 4)

This sub-project analysed terrestrial inputs to the Congo fan to a maximum depth of 226.7 mcd within ODP 1075 and to determine fluctuations in R_{soil} and BIT indices.

Hypothesis 3: All BHPs found in ODP 1075 are of terrestrial origin (Chapter 5)

This sub-project analysed the origins of different BHP biomarkers within the Congo fan with comparison of these results with existing modern terrestrial, culture, coastal and marine sediment data.

Hypothesis 4: Temporal changes in R_{soil} and BIT indices within ODP 1075 occur due to variations in orbital cycling (Chapter 6).

This sub-project determined CH_4 oxidation marker signatures (BHPs) within high resolution ODP 1075 sediments from the Congo Fan between MIS 10 and 14 to determine short term variations in CH_4 oxidation.

Hypothesis 5: Ancient marine sediments record past terrestrial aerobic methane oxidation activity (Chapter 7).

This sub-project determined CH_4 oxidation marker signatures within ODP 1075 sediment from the Congo Fan to a depth of 234 meters below sea floor (m.b.s.f) to determine long scale fluctuations in CH_4 oxidation.

Chapter 2:

Biomarkers and Methodology

Chapter 2. Biomarkers and Methodology

2.1. Selected Biomarkers

Biomarkers are complex organic compounds that originate from a formerly living organism. Following the death of this organism, biomarkers can be traced back to their original source organism thus becoming molecular fossils. These biomarkers are preserved in soils, sediments, rocks and crude oil and can be distinguished from other organic compounds by three main characteristics: (1) Biomarkers have structures composed of repeating subunits, indicating that their origins are from previously living organisms; (2) each parent biomarker is common in a specific organism/s; and (3) the biomarkers are chemically stable and can be well preserved following deposition and burial (Peters et al., 2005). A biomarker – proxy approach is beneficial in understanding past biogeochemical cycling where it is not possible to perform direct measurements (e.g. paleo soils and sediments). It is critically important to understand CH_4 cycling within the tropics and a biomarker approach could aid in distinguishing the source of CH_4 emissions during past periods of climate change particularly the Pleistocene.

2.2. Bacteriohopanepolyols (BHPs)

Bacteriohopanepolyols are highly functionalised pentacyclic triterpenoids produced by many aerobic as well as a number of obligate and facultative anaerobic bacteria (e.g. Eickhoff et al., 2013a; Rohmer et al., 1984; Talbot et al., 2008b and references therein). Hopanoids are found in the cytoplasmic and outer membranes of bacteria (Ourisson et al., 1987; Kannenberg and Poralla, 1999; Sáenz et al., 2012). Only bacteria containing the gene encoding for squalene hopene cyclase (*sqhC*; Ochs et al., 1992) are able to biosynthesise hopanoids. Biosynthesis of BHPs is believed to be limited to less than 10% of all bacteria in most communities (Pearson et al., 2007). The initial step in BHP synthesis is the cyclisation of squalene (controlled via the *sqhC* gene) followed by the addition of the hopanoid side chain (via the *hpnH* gene) and leading to the production of 30-(5'-adenosyl)hopane (adenosylhopane; **1a**; Figure 2.1; Bradley et al., 2010). It is believed that all hopanoid producing bacteria synthesise adenosylhopane as a BHP precursor compound, however, few hopanoid producers have been observed accumulating adenosylhopane (Talbot et al., 2007a and references therein; van Winden et al., 2012b). Following the formation of

adenosylhopane, the adenine group is cleaved off to yield ribosylhopane (Duvold and Rohmer, 1999; Liu et al., 2014; Rohmer, 1993). However, ribosylhopane has never been identified in cultures or environmental samples as most bacterial species further modify the hopanoid structure by the addition of -OH, -NH_2, sugar and ether moieties at the C-35 position (e.g. Rohmer, 1993; Talbot et al., 2007b; Figure 2.1)

BHPs are thought to have a stabilising effect on the cell membrane similar to eukaryotic sterols (Ourisson et al., 1987) although the exact role of BHPs within bacterial cells remains poorly understood. BHPs have been suggested to promote the liquid ordered phase within the cell membrane (Sáenz et al., 2012), however, hopanoids vary in abundance within different bacterial species (Rohmer et al., 1984) suggesting additional roles for BHPs within bacteria (Poger and Mark, 2013). BHPs have been shown in pure culture to aid bacteria under pH stress (e.g. Sáenz et al., 2012; Welander et al., 2009; Schmerk et al., 2011). In support of this, Kim et al. (2011) determined soil pH to be the most important environmental factor influencing the production of BHPs, along with growth temperature and growth phase (e.g. Joyeux et al., 2004; Doughty et al., 2009; Welander and Summons, 2012), and anoxia and ferrous environmental conditions (Eickhoff et al., 2013b).

2.2.1. BHPs as Biomarkers

Hopanes including C-3 methylated hopanes have been used as biomarkers for AMO (e.g. Collister et al., 1992; Pancost et al., 2007). Hopanes are highly recalcitrant compounds and are the defunctionalised diagenetic products of BHPs (Farrimond et al., 2004). Hopanes have been reported in sediments dating back to the late Archaean (Eigenbrode et al., 2008). Similarly, the hopanoids diploptene and diplopterol are also used as biomarkers for AMO and have been reported in sediments from the Santa Barbara Basin (Hinrichs et al., 2001, 2003), the western North Pacific (Uchida et al., 2004) and the Sea of Marmara (North-eastern Mediterranean; Menot and Bard, 2010).

However, a persistent issue with using hopanes and hopanoids as biomarkers for AMO is that these compounds are not specific enough for methanotrophy. As hopanes are diagenetic products of BHP degradation hopanes have multiple bacterial sources. Similarly, diploptene and diplopterol are produced by all hopanoid producing bacteria (Bradley et al., 2010). In order to confirm the methanotrophic origin, compound specific carbon isotopes of hopanes and hopanoids can be

analysed. Therefore, as with methylated C30 hopanes, compound specific $\delta^{13}C$ analysis is required to confirm the source of diploptene and diplopterol. Isotopes are elements with the same number of protons and electrons but with a different number of neutrons. C has two stable isotopes, ^{12}C and ^{13}C, which are present in the environment at a ratio of 99:1. The kinetic isotope effect (KIE) is a process associated with isotopically substituted molecules exhibiting different reaction rates and impacts all biological reactions. In biological systems, the KIE impacts on the $\delta^{13}C$ value of the resulting OM. The KIE is normally associated with fast, incomplete, or unidirectional processes such as evaporation, diffusion, dissociation reactions and almost all biological reactions (Sharp, 2007). Molecules containing heavier isotopes (e.g. $^{13}CH_4$) are more stable and have higher dissociation energies than those containing light isotopes (e.g. $^{12}CH_4$). As a consequence it is easier to break ^{12}C-H bonds then to break ^{13}C-H bonds (Sharp, 2007). KIE arising from differences in dissociation energies can be large in bacterial reactions that occur in nature. Therefore, methanotrophs will preferentially incorporate ^{12}C in to membrane lipids resulting in hopanes and hopanoids that are formed through methanotrophy (Equation 1.2) having lower $^{13}C/^{12}C$ ratio due to the KIE during formation. However, a number of issues arise when using KIE to confirm a methanotrophy source of hopanes and hopanoids. In freshwater environments CH_4 is formed through acetate fermentation (Equation 2.1) while in saline environments CH_4 is formed through CO_2 reduction which (Equation 2.2). CH_4 formed through acetate reduction results in a smaller fractionation between acetate and CH_4 (Sharp, 2007). Comparatively, CH_4 formed through CO_2 reduction results in a larger fractionation and will result in CH_4 with a much lower $\delta^{13}C$.

Equation 2.1. Reaction for CH_4 production through acetate fermentation in freshwater environments.

$$CH_3\mathrm{COOH} \rightarrow CH_4 + CO_2$$

Equation 2.2. Reaction for CH_4 production through CO_2 reduction in saline environments.

$$CO_2 + 8H^+ \rightarrow CH_4 + 2H_2O$$

Additionally, significant differences in $\delta^{13}C$ fractionation exist due to differences in C assimilation pathway. Type I methanotrophs utilise the ribulose monophosphate (RuMP) pathway and type II methanotrophs utilise the serine pathway (e.g. Hanson and Hanson, 1996). However, a group of Type I methanotrophs (formally known as Type X) utilise both the RuMP and serine pathways in addition to the reductive pentose phosphate pathways (Jahnke et al., 1999). Differences in $\delta^{13}C$ fractionation

are also linked to the type of methane monooxygenase (MMO) expressed by the methanotroph. The membrane bound particulate MMO (pMMO) typically results in greater fractionation leading to lighter $\delta^{13}C$ lipids in type I and X methanotrophs (Summons et al., 1994; Jahnke et al., 1999). Type II methanotrophs are capable of expressing both pMMO and soluble MMO (sMMO) and can range from 10‰ enriched or 12‰ depleted (Summons et al., 1994; Jahnke et al., 1999). Additionally some type I *Methylomonas* like species isolated from freshwater environments contain both pMMO and sMMO (Auman et al., 2000; Auman and Lidstrom, 2002).

In contrast, BHPs with an amine at the C-35 position are biomarkers that are specific for aerobic methane oxidation (AMO). 35-aminobacteriohopane-31,32,33,34–tetrol (aminotetrol; **1c**; Figure 2.1); 35-aminobacteriohopane-30,31,32,33,34-pentol (aminopentol; **1d**), unsaturated aminopentol (**4/5d**) and aminopentol isomer (**1d'**; van Winden et al., 2012b) are almost exclusively produced by aerobic methanotrophs (Berndmeyer et al., 2013; Talbot and Farrimond, 2007; Talbot et al., 2014; van Winden et al., 2012b; Zhu et al., 2010; hearafter referred to as CH_4 oxidation biomarkers) eliminating the need for compound specific $\delta^{13}C$ measurements. CH_4 oxidation biomarkers have been identified in many terrestrial and marine settings including; peatlands (van Winden et al., 2012a,b), a stratified post glacial lake in Antarctica (Coolen et al., 2008), tropical rice-paddy soils (Cooke, 2010), forest and farm soils (Cooke, 2010), geothermal microbial mats and sinters (Zhang et al., 2007; Gibson et al., 2008), suspended particulate matter in ocean settings (Blumenberg et al., 2007; Wakeham et al., 2007; Sáenz et al., 2011), pelagic sub-oxic zones of the water column in the Baltic sea (Berndmeyer et al., 2013), Yangtze river sediments (Zhu et al., 2010), and sediments from the Amazon Fan (Wagner et al., 2014).

Bacteriohopanepolyols are also biomarkers for soil organic carbon transport specifically, BHPs **1a**, **2a**, **1e**, **2e**, **1f**, **2f** (hereafter referred to as soil marker BHPs). High concentrations of soil marker BHPs have been observed in soils, including soils from Northern England (Cooke et al., 2008a), the Têt watershed (Kim et al., 2011), Arctic permafrost (Rethemeyer et al., 2010) and Western Canadian soils (Xu et al., 2009). Soil marker BHP abundance was found to vary with depth in the Congo deep sea fan suggesting the potential of these biomarkers as terrestrial OC (OC_{ter}) transport proxies (Cooke et al., 2008b).

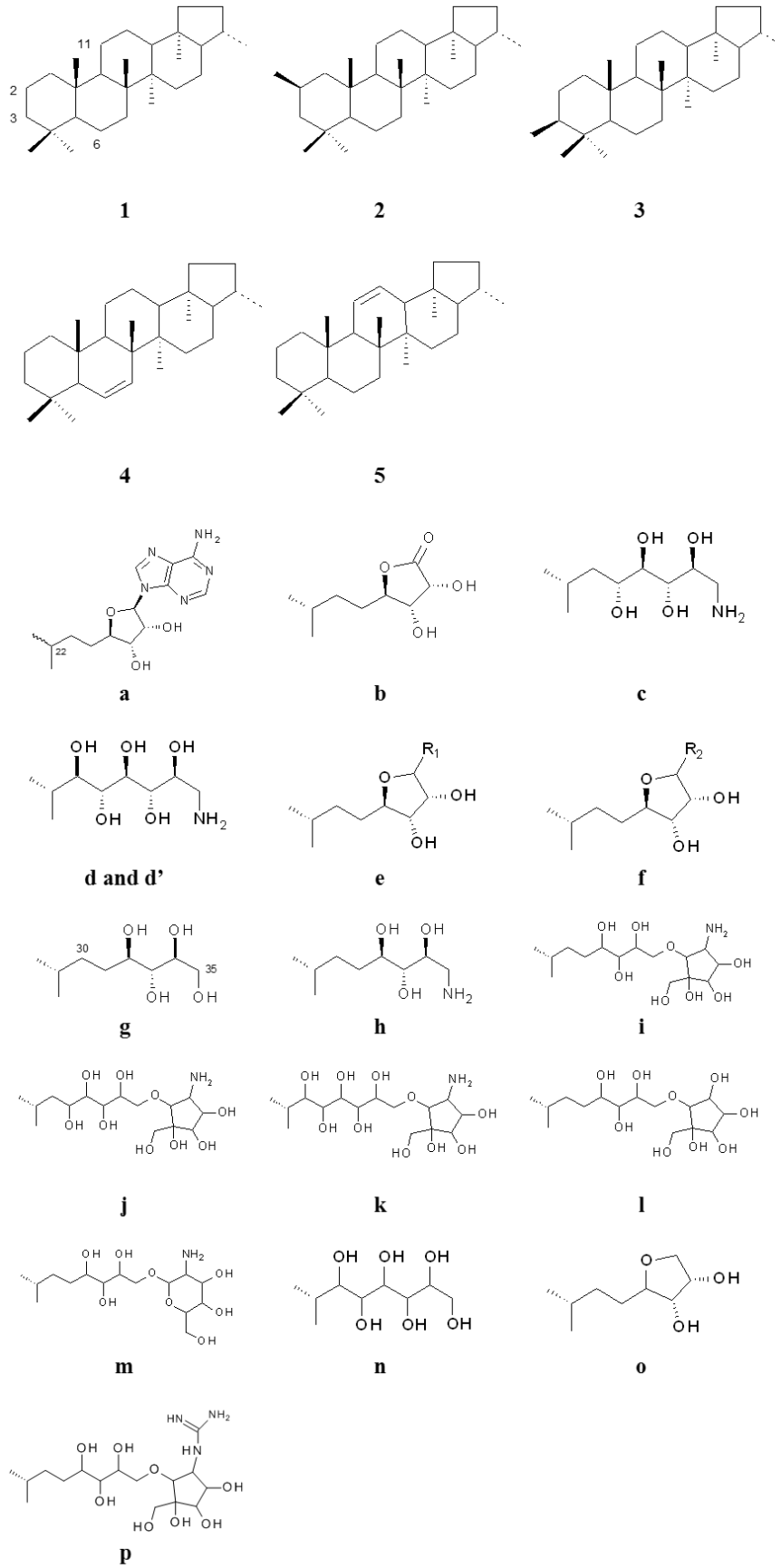

Figure 2.1. Structures of bacteriohopanepolyols.

Furthermore, Zhu et al. (2011) proposed the R_{soil} (Equation 2.3) index which uses a simple two-end member mixing model approach, where, soil marker BHPs are the terrestrial BHP end member and bacteriohopanetetrol (BHT; **1g**) is the marine end member. Moderate to strong correlation has been observed between the R_{soil} index and other OC_{ter} proxies, including, bulk $\delta^{13}C_{org}$ and the BIT index suggesting that the R_{soil} index behaves similarly to other OC_{ter} proxies (Zhu et al., 2011; Doğrul Selver et al., 2012, 2015). However, methylated group II (**2e**) and methylated group III (**2f**) soil marker compounds are not observed in all soils or sediment samples, therefore, Doğrul Selver et al. (2012) proposed excluding methylated soil marker BHPs from the OC_{ter} proxy and suggested the R'_{soil} index (Equation 2.4). Exclusion of the methylated soil marker compounds in the R'_{soil} index results in a significant increase in the correlation between the BIT index and $\delta^{13}C_{org}$ proxies (Doğrul Selver et al., 2012). To date, the R'_{soil} index has only been applied within arctic sediments.

Equation 2.3. R_{soil} index equation (Zhu et al., 2011).

$$R_{soil}\ index = \frac{(1_a + 2_a + 1_e + 2_e + 1_f + 2_f)}{(1_a + 2_a + 1_e + 2_e + 1_f + 2_f + 1_{g)}}$$

Equation 2.4. R'_{soil} index equation (Doğrul Selver et al., 2012).

$$R'_{soil}\ index = \frac{(1_a + 1_e + 1_f)}{(1_a + 1_e + 1_f + 1_g)}$$

2.2.2. Outlook

BHPs are ubiquitous and have been identified in many environmental samples (Table 2.1). As with most biomarkers, interpretation of the BHP record is restricted by degradation and thermal maturity of sediments they are deposited in. Degradation of adenosylhopane in a sediment core from the Congo deep sea fan (ODP 1075) limits interpretation (Handley et al., 2010). However, degradation signatures of other BHPs were not evident in the same core within the Congo deep sea fan, suggesting adenosylhopane to be highly labile in comparison to BHPs with C-35 amines and cyclitol ethers.

Table 2.1. List of different environments that have been tested for BHPs.

Environment	Reference
Terrestrial	
Soils	Cooke et al. (2008a); Redshaw et al. (2008); Pearson et al. (2009); Xu et al. (2009); Cooke (2010); Kim et al. (2011); Zhu et al. (2011); Ricci et al. (2014); Talbot et al. (2014); Wagner et al. (2014)
Peat	Kim et al. (2011); van Winden et al. (2012a,b); Taylor and Harvey (2011)
Lignite	Talbot et al. (*in prep*).
Permafrost	Rethemeyer et al. (2010); Doğrul Selver et al. (2015); Höfle et al. (2015)
Lakes/ponds/wetlands	Talbot et al. (2003a); Talbot and Farrimond (2007); Talbot et al. (2008a,b); Coolen et al. (2008); Talbot et al. (2014); Wagner et al. (2014)
Geothermal environments & microbial mats	Talbot et al. (2005); Pancost et al. (2006); Zhang et al. (2007); Gibson et al. (2008); Talbot et al. (2008a); Gibson (2010); Blumenberg et al. (2013); Gibson et al. (2014); Ricci et al. (2014).
Stream, River, Estuary and harbour sediments	Cooke et al. (2009); Pearson et al. (2009); Rethemeyer et al. (2010); Zhu et al. (2010); Taylor and Harvey (2011); Zhu et al. (2011); De Jonge et al. (2015)
Water column particulates (River + marine)	Blumenberg et al. (2007); Wakeham et al. (2007); Sáenz et al. (2011a,b); Berndmeyer et al. (2013); De Jonge et al. (2015).
Marine	
Microbial mat	Blumenberg et al. (2006)
Black Sea Sediment	Blumenberg et al. (2006); Blumenberg et al. (2009)
Deep sea Fans	Cooke et al. (2008b); Handley et al. (2010); Talbot et al. (2014); Wagner et al. (2014);
Authigenic Carbonates	Pancost et al. (2005); Birgel et al. (2011)
Marine sediments	van Dongen et al. (2006); Blumenberg et al. (2010); Zhu et al. (2011); Doğrul Selver et al. (2012); Berndmeyer et al. (2013, 2014); Rush et al. (2014)
Arctic Rivers/marine sediments	Cooke et al. (2009); Taylor and Harvey (2011); De Jonge et al. (2015); Doğrul Selver et al. (2015)
Other	Mondamert et al. (2011)

An additional issue with the interpretation of BHP data is that many of the compounds have multiple sources. A range of non-methanotroph sources have been identified for 35-aminobacteriohopane-32,33,34–triol (aminotriol; **1h**; see Talbot et al., 2007a and references therein). *Desulfovibrio* (Δ-proteobacteria, SRB) have been found to produce low concentrations of aminotetrol at a range of 20-100:1 (aminotriol : aminotetrol; Blumenberg et al., 2006, 2009, 2012). Additionally, trace levels of aminopentol have been observed in *D. salexigens* at a ratio of 1352:1 (aminotriol : aminopentol; Blumenberg et al., 2012). Despite these extremely low concentrations, aminopentol remains an excellent biomarker for AMO (Berndmeyer et al., 2013).

Another problem is that while *sqhC* gene is widespread within bacteria (Pearson et al., 2007) not all bacteria capable of producing BHPs do so at all growth phases (e.g. Poralla et al., 2000) and not all methanotrophs produce aminopentol and/or aminotetrol (e.g. van Winden et al., 2012b and references therein). For example, *Methylocella* spp. is thought to be one of the most important methanotroph groups within peat bogs (Dedysh, 2009), however, analysis of pure cultures found that *Methylocella* spp. do not produce diagnostic aminopentol or aminotetrol, they do, however, produce aminotriol (van Winden et al., 2012b), which is much less diagnostic as it is also produced by some SRB (Blumenberg et al., 2006), cyanobacteria, acetic acid bacteria, purple non-sulfur bacteria as well as methanotrophs (Talbot et al., 2008b and references therein).

2.2.3. Glycerol Dialkyl Glycerol Tetraether Lipids (GDGT)

Glycerol dialkyl glycerol tetraether (GDGTs) are membrane spanning lipids found within anaerobic archaea and some anaerobic bacteria (Schouten et al., 2013b and references therein). These lipids form a membrane monolayer which is kept taught by the bipolar nature of the GDGT compound (Valentine, 2007). The formation of a lipid monolayer over a bilayer membrane is suggested to add stability to the cell membrane at high temperature and low pH (De Rosa *et al*., 1986). However, GDGT production is not limited to the hyperthermophiles (growing at temperatures greater than 60°C) as there is evidence for the wide spread occurrence of structurally diverse GDGTs in low temperature environments (less than 20°C) (e.g. Schouten et al., 2000). Archaea produce isoprenoid GDGTs (iso-GDGTs) while bacteria produce branched GDGTs (br-GDGTs; see Figure 2.2 for structures; Weijers et al., 2006a).

Br-GDGTs have been identified as being of bacterial origin due to their 1,2-di-*O*-alkyl-*sn*-glycerol stereochemistry and not the 2,3-di-*O*-alkyl-*sn*-glycerol configuration of archaea (Weijers et al., 2006a). Both br- and iso- GDGTs are structurally diverse containing up to 8 cyclopentyl moieties and alkyl chains (br-GDGTs only). Viable (living) archaeal and bacterial GDGTs contain a polar head group and are known as intact GDGTs (I-GDGT). The polar head group often consist of sugars or phosphosugars attached to the glycerol moiety, which is enzymatically cleaved following cell death and are subsequently known as core GDGTs (C-GDGTs) (Schouten et al*.,* 2008). Due to this there is a large quantity of relict C-GDGTs present within environmental samples.

2.2.4. GDGT Sources

Specific groups of archaea have been identified as sources of iso-GDGTs following isolation in pure culture. Thaumarchaeota (previously classified as Crenarchaeota) and Euryarchaeota are the main groups of archaea that are known to produce GDGTs (Schouten et al., 2013b and references therein). Methanogenic archaea and archaea involved in the AOM (Pancost *et al*., 2001) have also been identified as likely producers of iso-GDGTs (Weijers *et al*., 2006a).

A source of br-GDGTs has been difficult to elucidate with br-GDGTs not reported as abundant lipids in any cultured organism, except for minor amounts of **GDGT-I** in cultures of 2 members of *Acidobacteria* (Sinninghe Damsté et al., 2011). Br-GDGTs are also thought to have anaerobic sources due to the predominance of these compounds in anaerobic niches. Weijers *et al.* (2006a) found a distinct lack of br-GDGTs in upper oxic parts of soils cores while high concentrations of branched GDGTs were found in lower parts of the soil core that were permanently saturated with water and therefore anoxic. GDGTs (both br- and iso-) have been found in a number of different environments, including; deep sea sediments (e.g. Weijers *et al*., 2006b), tropical lakes (e.g. Berke et al., 2012), temperate, arctic and Antarctic lakes (Pearson et al., 2011), soils and peats (Weijers et al., 2006b; Kim et al., 2011), cold seep sediments (Zhang et al., 2011), and microbial mats and sediments associated with hot springs (e.g. Schouten et al., 2007; see review by Schouten et al., 2013b for further details).

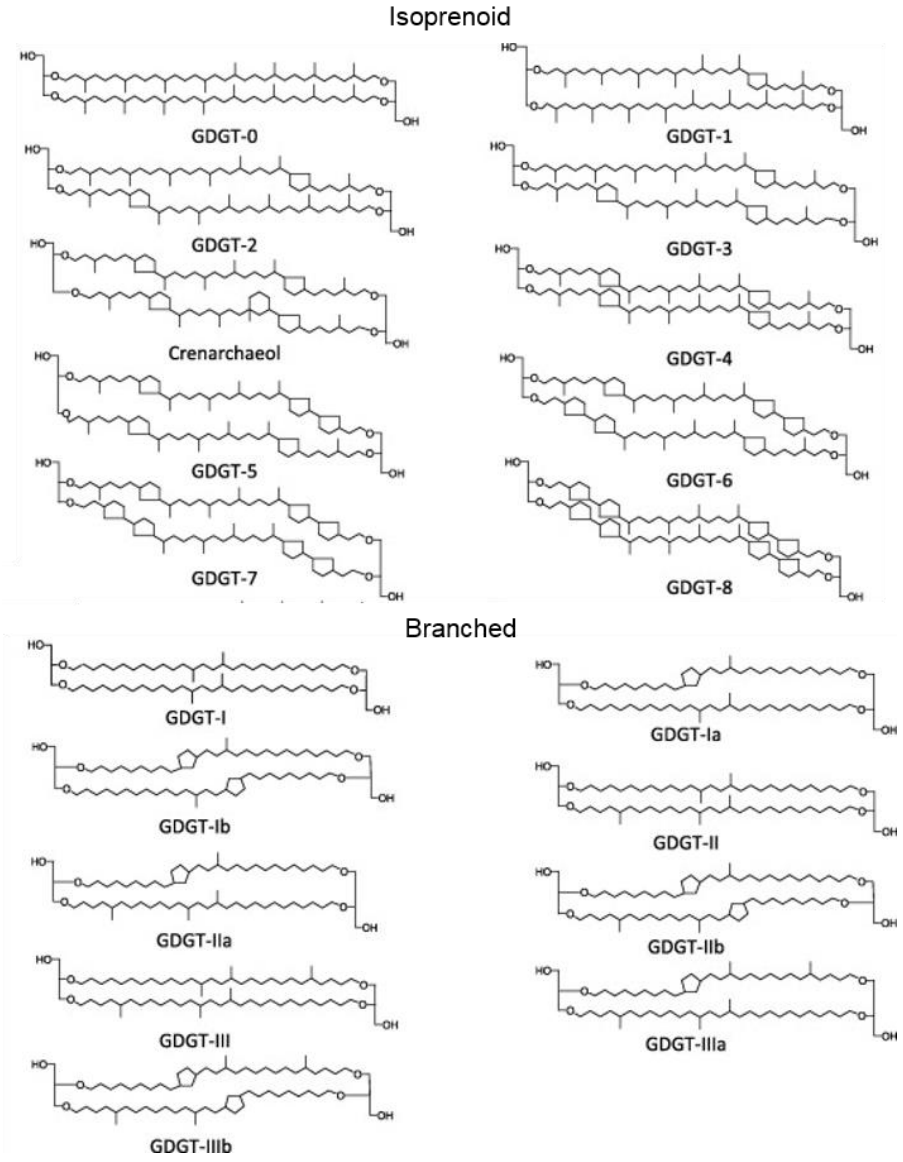

Figure 2.2: Isoprenoid and branched glycerol dialkyl glycerol tetraether lipid (GDGT) structures figure modified from Schouten *et al*. (2013b).

2.2.5. GDGTs as Environmental Biomarkers

Bacteria and archaea both undergo homeoviscous adaptation; a mechanism which allows the cell membrane to remain fluid at changing temperatures. Iso-GDGT producing archaea increase number of cyclopentane moieties in the carbon chain with increasing growth temperature (Schouten et al., 2013b and references therein). Environmental studies have observed an increase in methylation on the branched alkyl chains of br-GDGT with decreasing temperature and pH and an increase in the number of cyclopentane moieties with decreasing pH (Schouten et al., 2013b and references therein). Marine pelagic Thaumarchaeota can further modify the GDGT lipids by the addition of a cyclohexyl moiety resulting in a compound called crenarchaeol (Figure 2.2), and its regio-isomer. As a result a number of indices have

been developed to model paleo environmental temperature conditions (TEX_{86} and associated calibrations; see Schouten et al., 2013b for further details).

Iso- and br- GDGT distribution can also be used to trace soil OC transport; this is known as the Branched vs. Isoprenoid Tetraether index (BIT; Hopmans et al., 2004) (Equation 2.5). The BIT index compares the proportional amount of terrestrially derived br-GDGTs with marine-sourced crenarchaeol within sediments.

Equation 2.5. Branched vs. Isoprenoid Tetraether index (BIT) (Hopmans et al., 2004).

$$BIT = \frac{(GDGT\ I + GDGT\ II + GDGT\ III)}{(GDGT\ I + GDGT\ II + GDGT\ III + Crenarchaeol)}$$

2.2.6. Outlook

Degradation of GDGTs is observed within sediments with a strong oxic-anoxic transition, with selective preservation of core GDGT components. Huguet et al. (2008) determined the concentration of GDGTs within Madeira Abyssal Plain turbidites that have a strong oxic-anoxic transition. Relative to the anoxic part of the sediment, 7-20% of branched GDGTs were preserved in the oxic part of the sediment while 0.2-3% of the marine iso-GDGT crenarchaeol was preserved (Huguet et al., 2008). Selective preservation of br-GDGTs in oxic sediment is particularly interesting as the anoxic sediment was found to contain iso-GDGT crenarchaeol at concentration two orders of magnitude higher than the soil derived br-GDGTs (Huguet et al., 2008). Despite the relatively small changes in br-GDGT concentration within oxic sediments, the larger variation in crenarchaeol concentration can have a large effect on the BIT index. Huguet et al. (2008) found the BIT index increase from 0.02 to 0.4 within the anoxic to oxic sediment. Despite potentially important GDGT degradation signatures observed in Pliocene – Miocene deposits, oxic degradation is not expected to significantly impact Pleistocene sediments from the Congo fan.

Low concentrations of crenarchaeol have been observed in soils (Weijers et al., 2006b). As crenarchaeol is the marine end member within the BIT index, the presence of crenarchaeol within terrestrial soils could artificially reduce the BIT index. Additionally, br-GDGTs and terrestrial crenarchaeol are thought to be protected from degradation during deposition due to the soil matrix (Huguet et al., 2008) which could lead to inconsistencies in the BIT index. Furthermore, the R_{soil} and BIT indices cannot be compared in down core studies, largely due to the different rates of degradation

between the indices (Kim et al., 2011; Zhu et al., 2013), however, they show good correlation in surface transects (Doğrul Selver et al., 2012; 2015).

Furthermore, br-GDGTs production has been identified within aquatic environments, including lakes (Sinninghe Damsté et al., 2009; Tierney and Russell, 2009; Bechtel et al., 2010; Tierney et al., 2010; 2012; Zink et al., 2010; Loomis et al., 2011; Buckles et al., 2014) and rivers (Zhu et al., 2011; Kim et al., 2012; Zhang et al., 2012; Yang et al., 2013; Zell et al., 2013a,b; 2014a,b; De Jonge et al., 2014).

2.2.7. Alkenones

Alkenones are long chain compounds comprising of a series of C_{37} to C_{39} di, tri and tetra unsaturated ketones. They are abundant organic compounds found in marine (e.g. Brassell et al., 1986; Prahl et al., 1993; Hoefs et al., 1998; Müller et al., 1998; Rosell-Melé, 1998; Bentaleb et al., 1999) and lacustrine sediments (e.g. Sun et al., 2012; Randlett et al., 2014; Zhao et al., 2014). In marine systems the main producers of alkenones are *Emiliana huxleyi* (de Leeuw et al., 1980) and *Gephyrocapsa oceanica* (Conte et al., 1994; Volkman et al., 1995). Alkenones are also reported in the coastal species *Isochrysis galbana* and *Chrysotila lamellosa* (Marlowe et al., 1984). These haptophyte algae belong to a class of photosynthetic organisms called *Prymnesiophyceae*. Due to the requirement of sunlight, *Prymnesiophyceae* live in the upper photic zone. A positive relationship between growth temperature and alkenone saturation has been observed in haptophytes where increasing growth temperature results in decrease in the relative proportion of tri unsaturated ketones (Brassell et al., 1986). As a result, the proportion of alkenones with different degrees of saturation can be used as temperature proxies. Brassell et al. (1986) devised the U^{K}_{37} index, which uses the relative proportions of C_{37} di, tri and tetra unsaturated alkenones to reconstruct temperature (Equation 2.6). However, growth culture experiments using *E. huxleyi* found there to be no advantage of using tetra unsaturated alkenones in the U^{K}_{37} index and thus the $U^{K'}_{37}$ index using the relative proportions of $C_{37:2}$ and $C_{37:3}$ was devised (Prahl and Wakeham, 1987). U^{K}_{37} and $U^{K'}_{37}$ estimated temperatures are thought to represent the annual SST despite strong seasonal temperature contrasts. A possible reason for this could be due to maximal haptophyte algae blooms occurring during the time of year when temperature is close to the mean annual temperature (Müller et al., 1998).

Equation 2.6. U^{K}_{37} temperature proxy using C_{37} di, tri and tetra unsaturated alkenones (Brassell et al., 1986).

$$\mathbf{U}^{\mathbf{K}}_{\mathbf{37}} = \frac{(\boldsymbol{C}_{\mathbf{37:2}} - \boldsymbol{C}_{\mathbf{37:4}})}{(\boldsymbol{C}_{\mathbf{37:2}} + \boldsymbol{C}_{\mathbf{37:3}} + \boldsymbol{C}_{\mathbf{37:4}})}$$

Another reason could be that during haptophyte algae blooms a large amount of material is transported from the water column to the sediments, while outside of the algae blooms, transport of alkenones to the sediment is decreased (Prahl et al., 1993).

Equation 2.7. $U^{K'}_{37}$ temperature proxy using C37 di and tri unsaturated alkenones (Prahl and Wakeman 1987).

$$\mathbf{U}^{\mathbf{K'}}_{\mathbf{37}} = \frac{(\boldsymbol{C}_{\mathbf{37:2}})}{(\boldsymbol{C}_{\mathbf{37:2}} + \boldsymbol{C}_{\mathbf{37:3}})}$$

This suggests that $U^{K'}_{37}$ records the SST during algae blooms rather than an integrated annual signal. Finally, alkenones appear to be fairly robust to degradation with no clear evidence for the preferential loss of tri unsaturated alkenones over di unsaturated alkenones (Gong and Hollander, 1999; Hoefs et al., 1998). Additionally, there exists no clear evidence for microbial (Teece et al., 1998), photochemical (Rontani et al., 1997) or grazing degradation (Grice et al., 1998; Volkman et al., 1980).

2.3. Site Location and Sample Description

2.3.1. The Modern Congo Fan

The Congo River is the largest river in Africa and the second largest river in the world in terms of drainage basin size (~3.7 x 10^6 Km^2; Runge, 2007; Laraque et al., 2009) and supplies freshwater, nutrients (including large amounts of SiO_2) and sediment to the ocean. The Congo River plume extends 800 Km offshore and can be detected during austral summer when monsoon/precipitation reach their maximum seasonal intensity (Anka and Séranne 2004). The rapid outflow of the Congo River is caused by the small river mouth and a large canyon head (Berger et al., 2002). As a result of coastal, oceanic and river induced upwelling, modern primary production is very high in the surface waters of the Congo fan (Anka and Séranne 2004).

Sedimentation within the Congo fan is dominated by rainout of suspended clays derived from the Congo River and by pelagic settings of biogenic debris (Berger et al., 2002). The lower Congo basin sediments lack a significant river borne sand and

silt fraction, due to most of the coarse debris being deposited before the ocean (Spencer et al., 2012).

2.3.2. The Angola – Benguela Current

The Congo fan is influenced by the Angola – Benguela front (ABF; Figure 2.3). The ABF is an oceanic front caused by the confluence of the southward flowing Angola current and northward flowing Benguela current presently at 16°S off the African coast between the Angola – Namibia boarder at the mouth of the Kunene River (Shannon et al., 1987). The ABF can be detected in the temperature of the upper 50 m of the water column and in the salinity to at least 200 m depth of the fan. However, the exact location of the ABF has oscillated as part of the natural cycle of climate and associated oceanic current change (Shannon et al., 1987). A number of factors affect the location of the ABF, including; wind stress; coastal orientation; bottom topography; and the north and south movements of the warm and cold water associated with the ABF (Shannon et al., 1987).

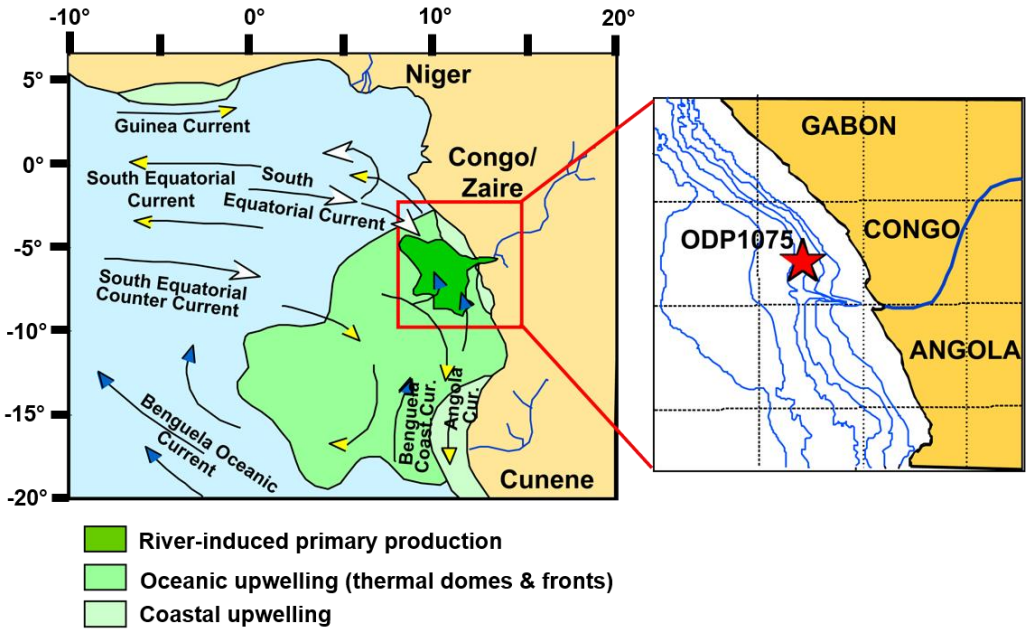

Figure 2.3. Approximate positions of the Benguela current, Angola current and, equatorial counter current and upwelling regions. Figure adapted from Holtvoeth et al. (2001).

The controls and drivers on the Benguela current (BG) have been extensively studied by Hart and Currie (1960). The BG originates at the confluence of the Indian Ocean and South Atlantic with subtropical thermocline water; saline, low oxygen tropical water; and cooler, fresher deep water. The 200 – 300 m wide BG current is characterized by cool temperature, leading to a cold dry wind driven to the coast of

the Namib Desert. The western seaward edge of the BG is poorly defined with many fluctuating seasonal eddies and meanders. The BG current has a well-defined thermal front between the waters associated with the Benguela upwelling system and the Southeast Atlantic Ocean. The Angola current (AG) flows southward between north of the Kunene river and Angola/Namibia boarder. The AG is warmer than the BG and can be viewed as an extension of the Guinea current flowing near central and northern western Africa's coast. The AG manifests similar effects to the El Nino, however, the AG is notably weaker.

2.3.3. Ocean Drilling Program Leg 175 and Congo Estuary Sampling

During the Ocean Drilling Program (ODP) leg 175, 13 sites were drilled off the West African coast (Aug-1997; Shipboard Scientific Party, 1998). ODP site 1075 is a deep water drill site on a depth transect in the lower Congo basin (Figure 2.4). ODP 1075 is located at 2995 m water depth and is dominated by (1) freshwater input from the Congo River, (2) seasonal coast upwelling activity and associated filaments and eddies moving offshore, and (3) incursions of open-ocean waters from the South Equatorial Countercurrent (Berger et al., 2002). Sediments from ODP 1075 and neighboring cores (e.g. ODP 1077) have been closely correlate with climatic signaling (Jahn et al., 2005) and large scale shifts in terrestrial vegetation relating to humidity – aridity cycles (Dupont et al., 2000; Schefuß et al., 2003, 2004a). The sediments of ODP 1075 have low $CaCO_3$ (Lin et al., 2001). ODP 1075 is approximately 234 meters below sea floor (m.b.s.f.) with a sedimentation rate of 100 m/Ma. Organic matter in ODP 1075 is of both terrestrial and marine origin, with SOM being an important contributor (Holtvoeth et al., 2001).

Sediment cores from ODP 1075 were stored at Integrated Ocean Discovery Program (IODP) Bremen Core Repository (MARUM, Universität Bremen) in a refrigerated storage area at 4°C. Samples between 1.65 and 126 meters composite depth (mcd) were previously collected by Holtvoeth et al. (2001). During April 2013, lower section sediments of ODP 1075 (core A, working half; 126.9 to 226.7 mcd) were collected at 1 m intervals, resolving ~ 13 to 18 Ka between samples. Approximately 20 ml of sediment was removed from the core using a plastic scoop. The sample was then stored in a polypropylene bag and shipped to Newcastle University (UK) where the samples were frozen immediately upon arrival.

The sediment sample from the estuary of the Congo River ('Anker 24') was taken as grab sample (Eisma et al., 1978) and stored as dried sediment before analyses. Additional lipid data were published earlier (Schefuß et al., 2004b; Figure 2.4; square).

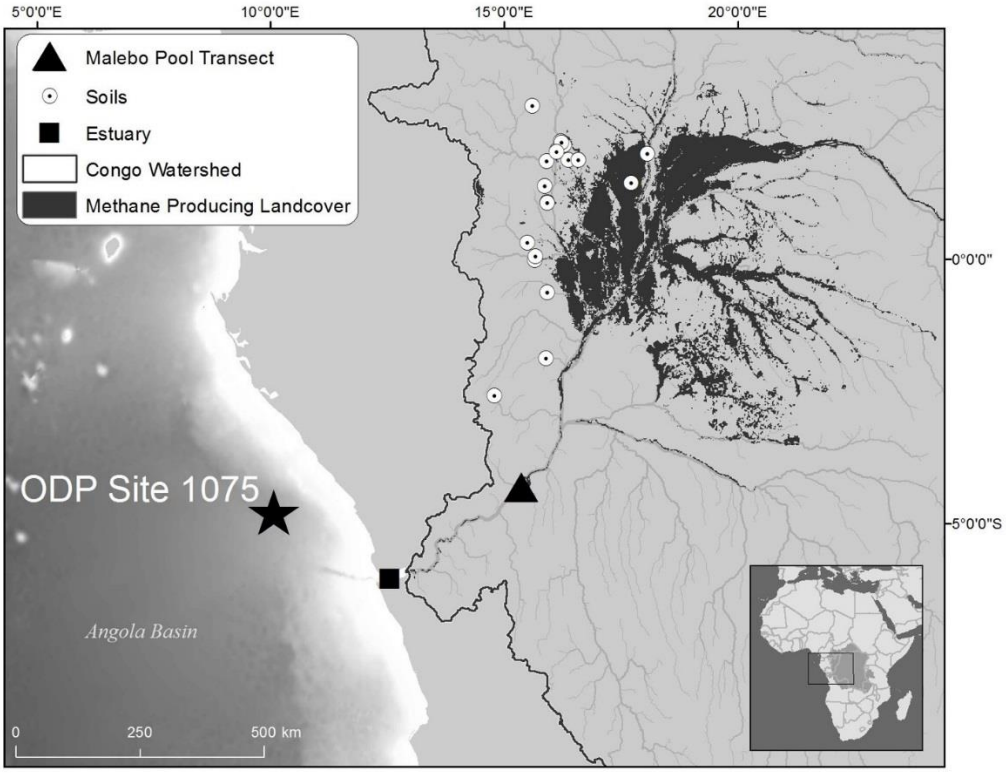

Figure 2.4. Geographical locations of the study site in the Congo. The map shows the locations of 22 soil samples (circles), 6 floodplain wetland sediment samples (Malebo pool; triangle) and the Congo estuary sediment sample (square). The map was generated using the planiglobe beta online plotting service (http://www.planiglobe.com) and is modified from Talbot et al (2014).

2.3.4. Congo River

The Congo River is the second largest exporter of C to the ocean, draining both pristine tropical rainforest and savannah. Spencer et al. (2012) analysed water samples from five stations down the Congo River including two stations before and after Malebo pool (a widening in the Congo River; Figure 2.4; triangle). The Congo River was found to have relatively low total suspended solids (TSS) compared to other major river systems with an organic rich character as demonstrated by the high relative abundance of coarse particulate OC (CPOC; >63 µm), fine POC (FPOC; 0.7-63 µm) and dissolved OC (DOC; <0.7 µm). Modern radiocarbon ages are found for both the Δ^{14}C-DOC and Δ^{14}C-CPOC indicating a coupling between recently fixed terrestrial C and C exported to the Atlantic Ocean. Conversely, Δ^{14}C-FPOC shows a depleted radiocarbon age suggesting source from mineral associated OM of tropical

soils. Furthermore, sediment records from the Congo fan (Pleistocene) show a thermally stable organic fraction, which, relates to strongly degraded SOM of old and highly developed, Kaolinite-rich ferallitic soils (Oxisols) that are abundant in the Congo River basin (Holtvoeth et al., 2005). Spencer et al. (2012) shows that OM exported from Malebo Pool is geochemically similar to OM at the head of the estuary (~ 350 km downstream) with no major tributaries join the Congo River between this site and the Atlantic Ocean.

2.3.4.1. Congo Soils

Soil samples were collected by our local partners at Congo Atomic Energy Commission (Democratic Republic of Congo) and Ministere de la Recherche Scientifique (Congo) from 22 sites spanning a wide range of land cover types, ranging from scrub savannah and grasslands, secondary forest and pristine tropical mixed forest, to seasonally flooded and swamp forest environments within the Congo Basin (Figure 2.4; circle; Figure 2.5; Table 2.2). Sites were located approximately 5-30 m from nearby streams and rivers. Samples were wrapped in clean foil and shipped to Newcastle University within three weeks of collection. Samples were stored frozen on arrival and were freeze-dried and ground prior to lipid extraction. Surface soils (0 – 5 cm) were collected during the months of November 2010 and August 2011.

Table 2.2. Sample name, abbreviated name and location of soil, Malebo pool and estuarine samples.

Sample name	Abbreviated name	Longitude	Latitude	Sampling date
Soil				
Closed evergreen lowland forest	CELF (JP6)	1.86184	16.56118	Nov-2011
Closed evergreen lowland forest	CELF (C6B)	-0.63315	15.90448	Nov-2011
Closed evergreen lowland forest	CELF (C17B)	2.056971	16.12198	Nov-2011
Closed evergreen lowland forest	CELF (C18B)	2.14825	16.26329	Nov-2011
Closed evergreen lowland forest	CELF (C19B)	2.22453	16.19214	Nov-2011
Closed evergreen lowland forest	CELF (C27B)	1.871608	16.35349	Nov-2011
Logged tropical mixed forest	LTF (7-1)	1.37373	15.85108	Aug-2011
Logged tropical mixed forest	LTF (8-1)	2.19816	16.2047	Aug-2011
Logged tropical mixed forest	LTF (10-1)	1.86195	16.56124	Aug-2011
Tropical mixed forest	TMF (12-1)	1.98281	18.04926	Aug-2011
Gilbertiodendron forest	GF (9-1)	2.01899	16.10091	Aug-2011
Swamp forest	SF (11-1)	1.43347	17.69439	Aug-2011
Tropical seasonally flooded forest	TSFF (6-1c)	0.30442	15.47285	Aug-2011
Secondary forest in savanna-forest mosaic	SFS (3-1)	1.06335	15.89473	Aug-2011
Field in savanna-forest mosaic	FSFM (4-1)	1.06291	15.89512	Aug-2011
Mosaic Forest/Croplands	MF (C8B)	-0.01805	15.62952	Nov-2011
Swamp bushland and grassland	SB (C38B)	1.36756	17.48491	Nov-2011
Closed grassland	CG (C46B)	-2.58107	14.78071	Nov-2011
Savanna outside of BZV	SBZV (1-1)	2.88896	15.58278	Aug-2011
Scrub savanna	SS (2-1)	1.84152	15.89446	Aug-2011
Scrub savanna	SS (5-1)	0.05104	15.64404	Aug-2011
Field	F (13-1)	1.9827	18.04992	Aug-2011
Malebo pool				
Permanently submerged sediment	PS (0-5)	-4.27111	15.54361	Jul-2013
Permanently submerged sediment	PS (5-15)	-4.27111	15.54361	Jul-2013
Recently exposed sediment	RE (0-5)	-4.27111	15.54361	Jul-2013
Recently exposed sediment	RE (5-15)	-4.27111	15.54361	Jul-2013
Exposed floodplain with occasional submersion	EF (0-5)	-4.27111	15.54361	Jul-2013
Exposed floodplain with occasional submersion	EF (5-15)	-4.27111	15.54361	Jul-2013
Estuarine sediment				
Estuary	Estuary	-0.10056	0.20944	Sep-1989

2.3.4.2. Malebo Pool Wetland Sediments

Malebo Pool floodplain wetland sediments were collected during July 2013 along a transect at three sites encompassing sediment that is permanently flooded, sediment inundated during high discharge months only and sediment from above the seasonal high water point (Figure 2.4; triangle). At each of the three sites sediment was collected at two distinct depths (0 – 5 cm and 5 – 15 cm), i.e. a surface and sub-surface sample. Samples were shipped to Newcastle University and were immediately frozen.

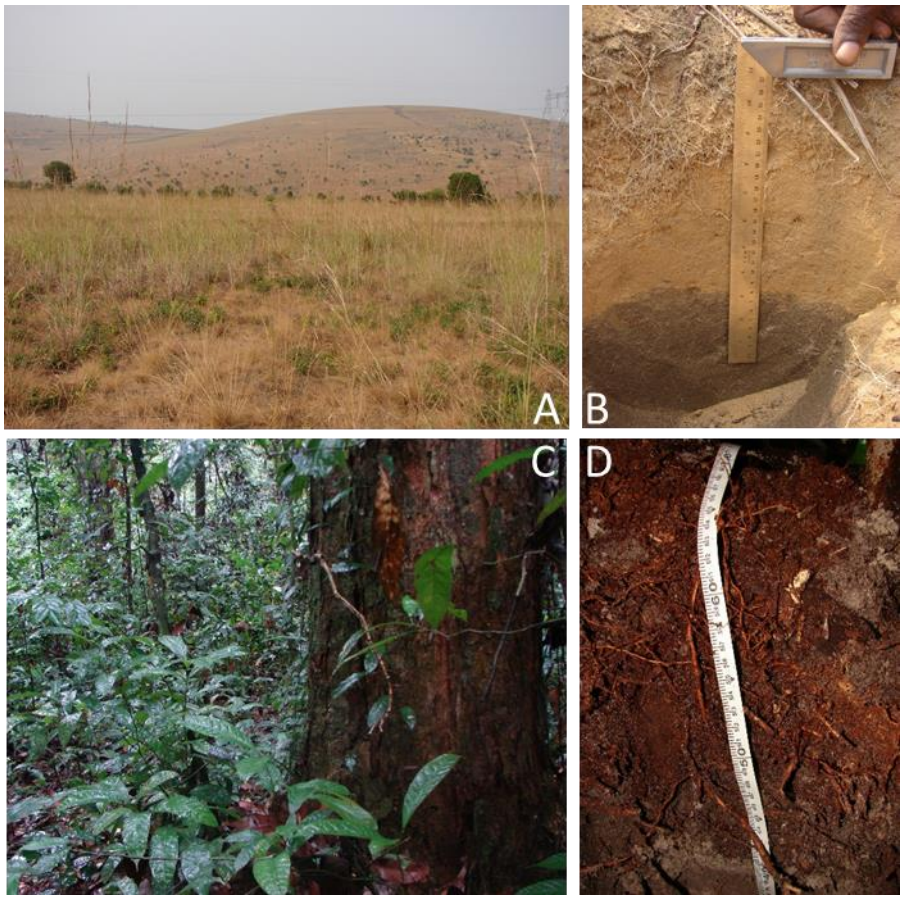

Figure 2.5. Examples of different sampling locations including Savannah outside Brazzaville (SBZV 1-1) site (A) and soil sample (B), Gilbertiodendron forest (GF 9-1) site (C) and soil sample (D).

2.4. Bulk Measurements

2.4.1. Total Organic Carbon (TOC)

Total OC (%) content of the soils, Malebo Pool and lower section of ODP 1075 (126.9 to 226.7 mcd) samples was measured at Newcastle University. Approximately 0.1 g of sample was treated with 4 mol/L HCl (60-70 °C) for removal of inorganic carbon. Following which, HCl was allowed to drain from each sample. Deionised

water was added to each sample to neutralise the acid and allowed to drain. The samples were then dried in an oven at 65 °C for between 16 and 24 hours. TOC was measured using a LECO CS244 Carbon/Sulfur Analyser. Precision based on repeat sample analysis was 4.5 % (relative standard deviation). Accuracy based on repeated measurements of a standard reference material (Chinese stream sediment, NCS DC 73307; LGC, Teddington, UK) was within the permissible ± 0.05 % TOC. An instrument calibration standard (Carbon in steel, part no 501-506, Leco) was analysed and was found to be within the nominal 0.8% permissible range.

TOC of the upper section of ODP 1075 was reported by Holtvoeth et al. (2003). TOC of the estuarine sediment was reported by Schefuß et al. (2004b).

2.4.2. pH

The pH was measured following the standard method described in BS ISO 10390 (2005). Briefly 5 mL freeze dried soil was shaken with 25 mL water for 1 h and the resulting soil-water suspension left to equilibrate for 1 to 3 h. The pH-H_2O of the suspension was measured using a pH electrode (VWR 662-1761, combination double junction with BNC connector ATC temperature probe, Dutscher Scientific, part no. 027-017) and meter (Jenway 3020, serial no. 2539), calibrated using standard buffer solutions of pH 4 and 7.

2.5. BHP, GDGT and Alkenone Analysis

2.5.1. Solvents

Dichloromethane (DCM) and methanol (MeOH) were purchased as technical grade (unless otherwise stated in methodology) and then redistilled using a 30-plate Oldenshaw fractionation column. Solvent purity was checked by LC analysis prior to use and procedural blanks were analysed with each batch of samples.

2.5.2. Bligh Dyer Extraction for BHP and GDGT Analysis

Total lipids were extracted using an adaptation of the method published in Talbot et al. (2007a) and further modified by Osborne, (PhD thesis, submitted), which, is based on the Kates modification (Kates, 1972) of the Bligh and Dyer (Bligh and Dyer, 1959) extraction. Total lipids were extracted from between 1g and 3g of freeze dried and homogenised soil and sediment. Sediment/soil was extracted in a Teflon centrifuge

tube (50 ml; Oak Ridge Thermo Scientific Nalgene CFT-648-K) with a monophasic mixture of bi-distilled water (4 ml), methanol (10 ml) and chloroform (5 ml; Fisher Scientific, Distol, C/4963/17, for residue analysis). The sample was agitated vigorously via sonication for 15 min at 40ºC followed by centrifugation for 15 min at 12000 rpm. The supernatant was collected and added to a second 50 ml centrifuge tube. This extraction was repeated three times with the supernatant collected at the end of each extraction cycle.

The monophasic extract was phase separated via addition of chloroform (5 ml) and bi-distilled water (5 ml) to each of the supernatants. The sample was gently inverted and centrifuged for 5 minutes (12000 rpm) to break the emulsion. The organic layer from each tube was removed using a 20 ml glass syringe fitted with a steel blunt ended 14 gauge needle and transferred to a round bottom flask (100 ml).

The organic extract within the round bottom flask was concentrated using a rotary evaporator under vacuum with a water bath heated to 40ºC. The concentrated TLE was transferred to a 3.5 ml glass vial using chloroform/methanol at a ratio of 2:1 (v/v) and evaporated to dryness under a stream of N_2 with heating from below (40ºC). Total lipid extracts were then separated into aliquots where 1/3 of the TLE was acetylated for analysis of BHPs and 1/3 of the TLE was used for GDGT purification. Total lipid extracts were then stored at 4ºC prior to further processing.

2.5.3. GDGT Purification

An aliquot (1/3) of the TLE was purified into apolar and polar fractions by column chromatography using Pastor Pipette columns containing Soxhlet extracted cotton wool and approximately 4 cm of activated Al_2O_3 (Aluminium oxide 90, standardised; Merck KGaA, Germany, 1.01097.1000; particle size 1-3 mm) as the stationary phase using the method reported in Huguet et al. (2006). Elution of the apolar fraction was achieved by loading the TLE sample onto the column in of hexane/DCM (300 µl, 9:1 v/v). The sample vial was rinsed three times to ensure complete removal of the apolar fraction. Three column volumes of hexane (Fisher Scientific, 95% n-Hexane for HPLC)/DCM (9:1 v/v) were used to ensure complete elution of the fraction.

For elution of the polar fraction, the TLE was dissolved in DCM/methanol (300 µl, 1:2 v/v) and loaded onto the column. The TLE vial was rinsed with DCM:methanol (300 µl, 1:2 v/v) three times to ensure complete transfer of polar compounds. Three

column volumes were added of DCM/methanol (1:2 v/v) were used to ensure complete elution of the polar fraction. Both the apolar and polar fractions were evaporated to dryness under a stream of N_2 and stored at 4ºC. The polar fraction was dissolved in a hexane/propanol (99:1 v/v) mixture and filtered through a 13 mm syringe filter with a 0.22 µm PTFE membrane (VWR, 514-0070). This was repeated three times to ensure complete transfer of the polar fraction. The resulting filtered polar fraction was evaporated to dryness under a stream of N_2 with a hot plate (40 °C) and stored at 4ºC.

2.5.4. Acetylation for BHP Analysis

A third of the TLE was acetylated using 250 µl acetic anhydride (Sigma-Aldrich, ReagentPlus, 99%; 320102-1L) and 250 µl of pyridine (Fisher Scientific, Certified for AR analysis 99.5%, 10102110; see Section 2.7 for method development). Following the addition of the acetic anhydride and pyridine, the sample was heated for 1 hour at 50ºC and left overnight at room temperature. Samples were dried under a stream of N_2 with heating from below (40ºC).

2.5.5. HPLC-APCI-MS

2.5.5.1. BHP Analysis

The method has been described previously (Talbot et al., 2003a). Briefly, BHP analysis was performed by reversed-phase high performance liquid chromatography-atmospheric pressure chemical ionisation-mass spectrometry (HPLC-APCI-MS^n) using a ThermoFinnigan surveyor HPLC system fitted with a Phenomenex Gemini C_{18} column (150 mm; 3.0 mm i.d.; 5 µm particle size) and a security guard column cartridge of the same material coupled to a Finnigan LCQ ion-trap mass spectrometer equipped with an APCI source operated in positive ion mode. Chromatographic separation was accomplished at 30°C with a flow rate of 0.5 ml min^{-1} and the following mobile phase solvent gradient: 90% MeOH (VWR, HiPerSolv Chromanorm for LC-MS; 83638.320), 10% water (0 min; VWR, HiPerSolv Chromanorm for LC-MS; 83645.320); 59% MeOH, 1% water, 40% propan-2-ol (at 25 min; HiPerSolv Chromanorm for HPLC; 20880.320); isocratic to 45 min returning to the starting conditions in 5 min and stabilising for 10 min. MS conditions were 155°C capillary temperature and 490°C APCI vaporiser temperature with a corona discharge current of 8 µA, sheath and auxiliary gas flow of 40 and 10, respectively

(arbitrary units). MS^n analysis was carried out in data-dependent mode with three scan events: SCAN 1: full mass spectrum, *m/z* 300–1300; SCAN 2: data-dependent MS^2 spectrum of most intense ion from SCAN 1; SCAN 3: data-dependent MS^3 spectrum of most intense ion from SCAN 2. Detection was achieved at an isolation width of *m/z* 5.0 and fragmentation (scans 2 and 3) with normalised collisional dissociation energy of 35% and an activation Q value (parameter determining the *m/z* range of the observed fragment ions) of 0.15. The semi-quantitative estimate of BHP concentrations was achieved employing the characteristic base peak ion peak areas of individual BHPs in mass chromatograms (from SCAN 1) relative to the *m/z* 345 mass chromatogram base peak area of the acetylated 5α-pregnane-3β,20β-diol internal standard (0.236 μg/μl). Averaged relative response factors relative to the internal standard, determined from a suite of acetylated BHP standards, were used to adjust the BHP peak areas. Typical error in absolute quantification was ± 20%, based on selected replicate analyses and BHP standards of known concentration (Cooke, 2010; van Winden et al., 2012b).

2.5.5.2. GDGT analysis

GDGT data presented here were analysed on two different instruments and prior to the availability of crenarchaeol standard therefore results should be interpreted with caution. 54 GDGT samples were analysed by normal-phase LC/MSn using a Surveyor HPLC system (ThermoFinnigan, Hemel Hempstead, UK) interfaced to a ThermoFinnigan LCQ ion trap mass spectrometer. The HPLC system was fitted with a Grace Prevail Cyano HPLC column (3µm, 150 mm x 2.1 mm i.d.) and a guard column of the same material. Separation was achieved at 30°C with a flow-rate of 0.2 ml min^{-1} and the following gradient profile described in Table 2.3.

The ThermoFinnigan LCQ MS was equipped with an atmospheric pressure chemical ionisation interface (APCI) source operated in positive ion mode. LC/MS settings were as follows: Vaporiser 400°C, capillary temperature 200°C, discharge current 5 µA, sheath gas flow 40 and auxiliary gas 6 (arbitrary units). Detection of GDGTs was achieved using the mass ranges m/z 1280-1310 for isoprenoid GDGTs and m/z 1015-1055 for branched GDGTs. Peak areas were integrated as combined area of ($[M+H]^+$ and $[M+H+1]^+$).

Table 2.3. Gradient profile for separation of GDGTs using ThermoFinnigan LCQ HPLC; all HPLC grade purchased from Fisher (Loughborough, UK).

Time	1% Propan-2-ol in Hexane	2% Propan-2-ol in Hexane	10% Propan-2-ol in Hexane
0	100	0	0
5	100	0	0
25	10	90	0
30	0	0	100
40	0	0	100
60	100	0	0

All other samples (218) were analysed for GDGTs by normal-phase LC/MS using a Waters Xevo TQ-S ACQUITY UPLC. The UPLC system was fitted with a Grace Prevail Cyano HPLC column (3 µm, 150x 2.1 mm i.d.) and an in line filter (Waters Acquity UPLC in-line filter, 0.2µm; 700002775). Separation was achieved at 40 °C with a flow rate of 0.2 ml min^{-1} and the gradient profile in Table 2.4 using hexane and propan-2-ol (Greyhound Chromatography ULC/MS; BIO-162641-2.5L).

Table 2.4. Gradient profile for separation of GDGTs using Waters Xevo TQ-S ACQUITY UPLC.

Time (minutes	Hexane (%)	Propan-2-ol (%)
0	99	1
5	99	1
50	98.2	1.8
55	90	10
65	90	10
66	99	1
80	99	1

Waters Xevo TQ-S triple Quad is equipped with an atmospheric pressure chemical ionisation interface (APCI) source (Ion Saber II) operated in positive ion mode. LC/MS settings were as follows: Source offset 50 V, capillary 1.5 KV, Desolvation

temperature 200 °C, cone voltage 30 V, Desolvation gas (N_2) 800 L/hour, cone gas 150 L/hour, nebulizer 7.0 bar. Detection of GDGTs was achieved using selected ion monitoring (SIM) of targeted $[M+H]^+$ ions (dwell time 50 ms; see Table 2.5 for selected masses).

Table 2.5. GDGT structures (see Figure 2.2) and SIM of targeted [M+H]+.

GDGT structure	$[M+H]^+$
GDGT-0	1302
GDGT-1	1300
GDGT-2	1298
GDGT-3	1296
Crenarchaeol and regio isomer	1292
GDGT-I	1050
GDGT-Ia	1048
GDGT-Ib	1046
GDGT-II	1036
GDGT-IIa	1034
GDGT-IIb	1032
GDGT-III	1022
GDGT-IIIa	1020
GDGT-IIIb	1018

The two ODP 1075 data sets from the LCQ and the Xevo have been combined, however, there is a clear offset between BIT values calculated for the LCQ (open circles; Figure 2.6) compared with the Xevo (black circles). To ensure data quality, 10 samples (including 2 samples from an interlaboratory study; see Schouten et al. (2013a) were analysed on both the LCQ and the Xevo (Table 2.6). An offset is observed between data analysed on the LCQ and the Xevo (Table 2.6). The offset between the two sample sets is observed to be linear and could therefore be corrected for. The LCQ data (Figure 2.6; open circles) was, therefore, corrected using a calibration curve generated by comparing analysis of 10 samples on both the LCQ and Xevo TQ-S.

Table 2.6. BIT index for samples analysed on LCQ HPLC and Xevo UPLC, Ali 1 to 8 are marine sediment samples, RR D and RR E are samples from the interlaboratory study Schouten et al. (2013a)

Sample	BIT from LCQ	BIT from Xevo
Ali 1	0.99	0.98
Ali 2	1.00	1.00
Ali 3	0.45	0.80
Ali 4	0.41	0.84
Ali 5	0.00	0.09
Ali 6	0.00	0.17
Ali 7	0.10	0.26
Ali 8	0.06	0.16
RR D	0.50	0.84
RR E	0.22	0.57

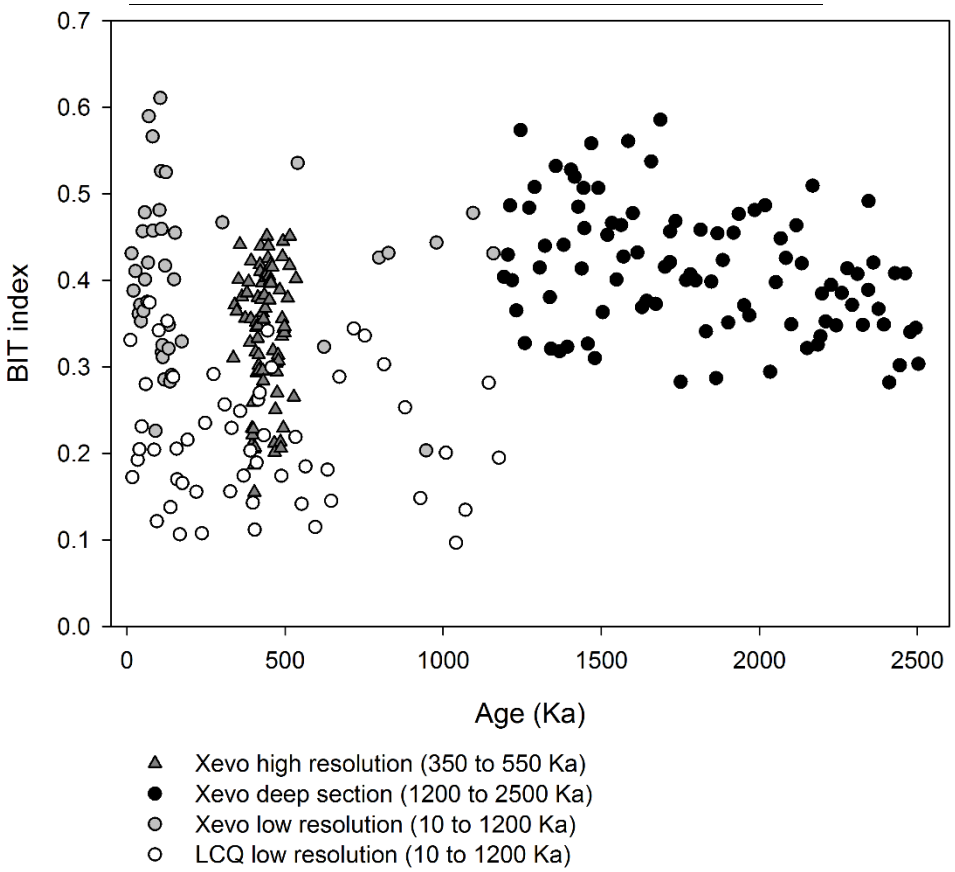

Figure 2.6 BIT index plotted with age (Ka) for 4 sets of samples, high resolution section (500 Ka to 600 Ka; grey triangle), deep section (1.2 Ma to 2.5 Ma; black circle), and low resolution section (10 Ka to 1.2 Ma; grey circle) all analysed on Xevo UPLC. Low resolution section (10 Ka to 1.2 Ma) analysed on LCQ HPLC.

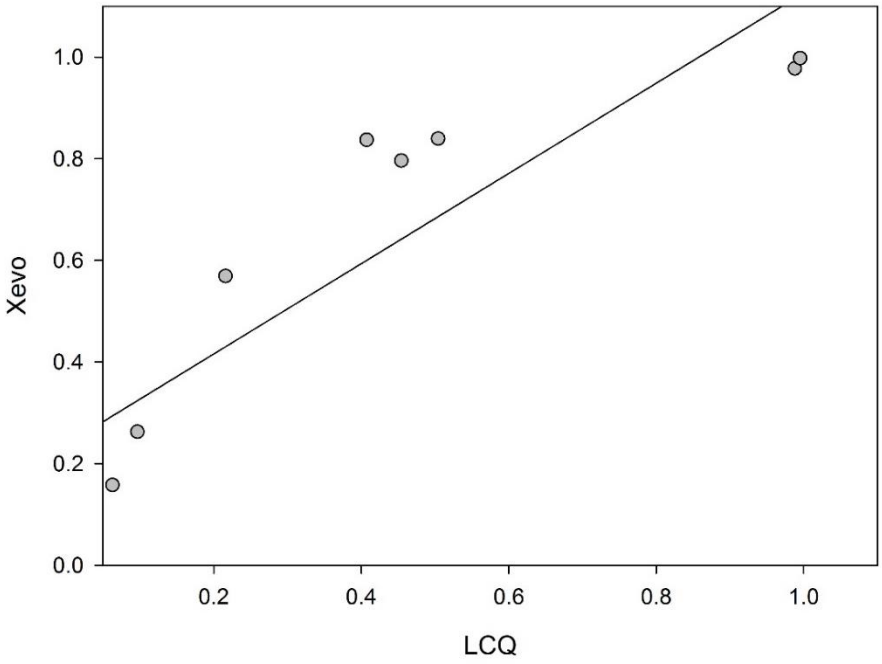

Figure 2.7. BIT index for 10 samples analysed on both LCQ HPLC and Xevo UPLC. R^2 = 0.83, y = 0.8879x + 0.238.

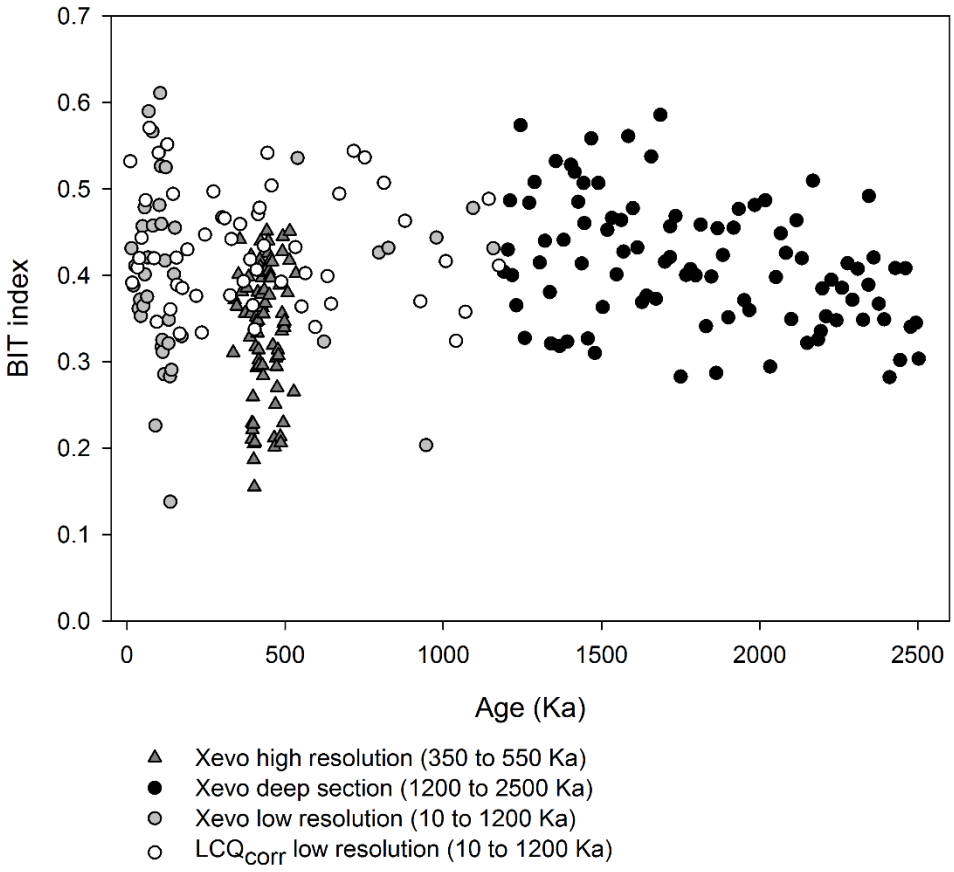

Figure 2.8. BIT index plotted with age (Ka) for; high resolution section (grey triangle), deep section (black circle), and low resolution section (grey circle) all analysed on Xevo UPLC. Low resolution section (LCQ_{corr}) analysed on LCQ HPLC corrected using calibration curve in Figure 2.7.

An additional 10 samples from ODP 1075 that were originally analysed on the Xevo were also analysed at The Royal Netherlands Institute for Sea Research (NIOZ; as detailed in Hopmans et al., 2000). A linear correlation between the Xevo data and NIOZ data are observed validating the trends in the BIT index reported here (Figure 2.9).

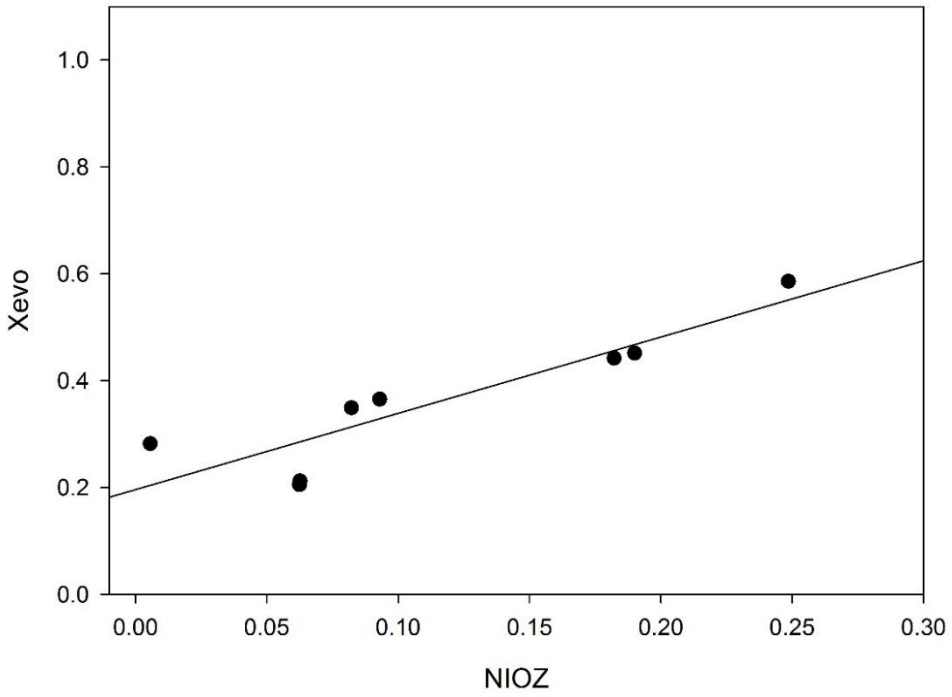

Figure 2.9. BIT index for 8 samples analysed on Xevo UPLC and at the Royal Netherlands Institute for Sea Research (NIOZ), $R^2 = 0.81$.

2.6. Compound Classification and Statistics

2.6.1. BHPs

The abbreviated names of the compounds identified, characteristic base peak ions (*m/z*) and structure numbers are given in Table 2.7, Table 2.8, Table 2.9, and Table 2.10). The term tetrafunctionalised compounds refers to BHPs with four functional groups at the C-32, C-33, C-34 and C-35 positions (Figure 2.1). Pentafunctionalised compounds have an additional fifth functional groups located at the C-31 position and hexafunctionalised compounds have 2 additional functional groups located at the C-30 and C-31. All concentration data are presented to 2 significant figures. Specific statistical details can be found in the methodology of each results chapter.

Table 2.7. List of polyols and pentose compounds identified in samples with corresponding abbreviated names, structure references and base peak (m/z) values.

Compound name	Abbreviated name	Structure	Base peak (m/z)	Assignment
Anhydrobacteiohopanetetrol	Anhydro BHT	1o	613	$[M+H]^+$
Ribonylhopane	Ribonylhopane	1b	627	$[M+H]^+$
Unsaturated Bacteriohopane-32,33,34,35-tetrol	Unsaturated BHT	4/5g	653	$[M+H-CH_3COOH]^+$
Bacteriohopane-32,33,34,35-tetrol	BHT	1g	655	$[M+H-CH_3COOH]^+$
2-methylbacteriohopane-32,33,34,35-tetrol	2-methyl BHT	2g	669	$[M+H-CH_3COOH]^+$
Bacteriohopane-30,31,32,33,34,35-hexol	BHhexol	1n	771	$[M+H-CH_3COOH]^+$
Bacteriohopene-32,33,34,35-tetrol pseudopentose	unsaturated BHT pentose	4/5l	941	$[M+H-CH_3COOH]^+$
Bacteriohopane-32,33,34,35-tetrol pseudopentose	BHT pentose	1l	943	$[M+H-CH_3COOH]^+$
2-methylbacteriohopane-32,33,34,35-tetrol pseudopentose	2-methyl BHT pentose	2l	957	$[M+H-CH_3COOH]^+$

Table 2.8. List of C35 amine containing compounds identified in samples with corresponding abbreviated names, structure references and base peak (m/z) values.

Compound name	Abbreviated name	Structure	Base peak m/z	m/z
aminobacteriohopene-32,33,34-triol	unsaturated aminotriol	4/5h	712	$[M+H]^+$
aminobacteriohopane-32,33,34-triol	aminotriol	1h	714	$[M+H]^+$
2-methylaminobacteriohopane-32,33,34-triol	2-methyl aminotriol	2h	728	$[M+H]^+$
3-methylaminobacteriohopane-32,33,34-triol	3-methyl aminotriol	3h	728	$[M+H]^+$
35-aminobacteriohopene-31,32,33,34–tetrol	unsaturated aminotetrol	4/5c	770	$[M+H]^+$
35-aminobacteriohopane-31,32,33,34–tetrol	aminotetrol	1c	772	$[M+H]^+$
35-aminobacteriohopene-30,31,32,33,34-pentol	unsaturated aminopentol	4/5d	828	$[M+H]^+$
35-aminobacteriohopane-30,31,32,33,34-pentol	aminopentol	1d	830	$[M+H]^+$
35-aminobacteriohopane-30,31,32,33,34-pentol isomer	aminopentol isomer	1d’	788	$[M+H]^+$

Table 2.9. List of soil marker compounds identified in samples with corresponding abbreviated names, structure references and base peak (m/z) values.

Compound name	Abbreviated name	Structure	Base peak m/z	m/z
30-(5'-adenosyl)hopane	G1	1a	788	$[M+H]^+$
2-methyl-30-(5'-adenosyl)hopane	2-Me G1	2a	802	$[M+H]^+$
Adenosylhopane type 2	G2	1e	761	$[M+H]^+$
2-methyladenosylhopane type 2	2-Me G2	2e	775	$[M+H]^+$
Adenosylhopane type 3	G3	1f	802	$[M+H]^+$
2-Methyladenosylhopane type 3	2-Me G3	2f	816	$[M+H]^+$

Table 2.10. List of cyclitol ethers identified in samples with corresponding abbreviated names, structure references and base peak (m/z) values.

Compound name	Abbreviated name	Structure	Base peak m/z	m/z
Bacteriohopanetetrol carbopseudopentose ether	BHT cyclitol ether	1i	1002	$[M+H]^+$
2-methylbacteriohopanetetrol carbopseudopentose ether	BHT cyclitol ether isomer	1i	1002	$[M+H]^+$
Bacteriohopanetetrol carbopseudopentose ether	2-methyl BHT cyclitol ether	2i	1016	$[M+H]^+$
Bacteriohopanetetrol carbopseudopentose ether	3-methyl BHT cyclitol ether	3i	1016	$[M+H]^+$
Bacteriohopanetetrol carbopseudopentose ether glucosamine	BHT glucosamine	1m	1002	$[M+H]^+$
Bacteriohopanepentol carbopseudopentose ether	BHpentol cyclitol ether	1j	1060	$[M+H]^+$
Bacteriohopanepentol carbopseudopentose ether (isomer)	BHpentol cyclitol ether (isomer)	1j	1060	$[M+H]^+$
2-methylbacteriohopanepentol carbopseudopentose ether (isomer)	2-methylBHpentol cyclitol ether	2j	1074	$[M+H]^+$
3-methylbacteriohopanepentol carbopseudopentose ether (isomer)	3-methyl BHpentol cyclitol ether	3j	1074	$[M+H]^+$
Bacteriohopane-30,31,32,33,34,35-hexol carbopseudopentose ether	BHhexol cyclitol ether	1k	1118	$[M+H]^+$
Bacteriohopane-30,31,32,33,34,35-hexol carbopseudopentose ether (isomer)	BHhexol cyclitol ether (isomer)	1k	1118	$[M+H]^+$
2-methylbacteriohopane-30,31,32,33,34,35-hexol carbopseudopentose ether	2-methyl BHhexol cyclitol ether	2k	1132	$[M+H]^+$
3-methylbacteriohopane-30,31,32,33,34,35-hexol carbopseudopentose ether	3-methyl BHhexol cyclitol ether	3k	1132	$[M+H]^+$
Guanidine substituted Bacteriohopanetetrol carbopseudopentose ether	Guanidine substituted BHT cyclitol ether	1p	1086	$[M+H]^+$

2.7. Method Development

Derivatization of BHPs is required for the analysis of these compounds through either GC-MS or LC-MS. BHPs are primarily analysed following a simple acetylation of the dried TLE extract using an excess volume of acetic anhydride and pyridine at a ratio of 1:1 (v/v; e.g. Talbot et al., 2007a; Cooke, 2010). Other derivatization techniques have been found to be less effective than acetylation in the quantification of BHPs, for example, hydrolysis has been found to produce many artifactual hopanoids (Sessions et al., 2013). Acetylation is the addition of an acetyl group to an active hydrogen atom. Acetylation involves the use of an acid and a base, commonly acetic anhydride and pyridine are used. Pyridine is a catalyst in acetylation and forms an acetyl-pyridinium cation intermediate through an equilibrium reaction. The acetyl-pyridinium ion then reacts with the alcohol and forms an alcohol-acetate compound and a protonated pyridine compound in the rate determining second step (Fersht and Jencks, 1970; Reaction 2.1 and Reaction 2.2). Pyridine is an efficient catalyst in these reactions as it is a highly effective nucleophile for acyl compounds with good leaving groups. Similarly pyridine is a highly effective catalyst as the amine cannot lose a proton to form a resonance stabilised amide.

Bacteriohopanepolyols are highly polar compounds which require acetylation prior to HPLC analysis. Acetylation aids in chromatographic separation by allowing the elution of amine containing compounds and reducing interaction of amine groups with the free silanols present on the HPLC column. Additionally acetylation enhances ionisation of BHPs by APCI-MS analysis. The aim of this work was to reduce and standardise the amount of acetic anhydride and pyridine required for BHP analysis. The specific objectives of this work were to (1) identify the optimum acetic anhydride and pyridine volume and (2) to identify to optimum acetylation duration.

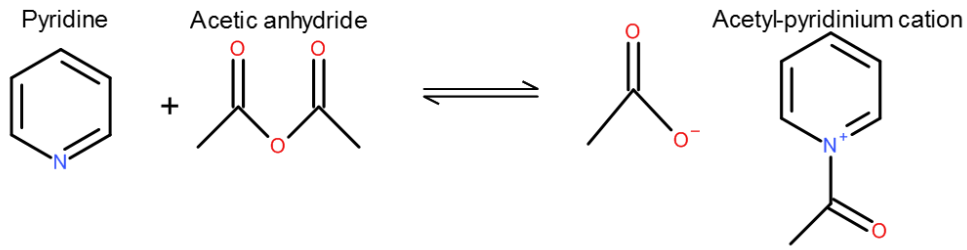

Reaction 2.1. Formation of acetyl-pyridinium cation from acetic anhydride and pyridine. Acetic anhydride and pyridine are in excess.

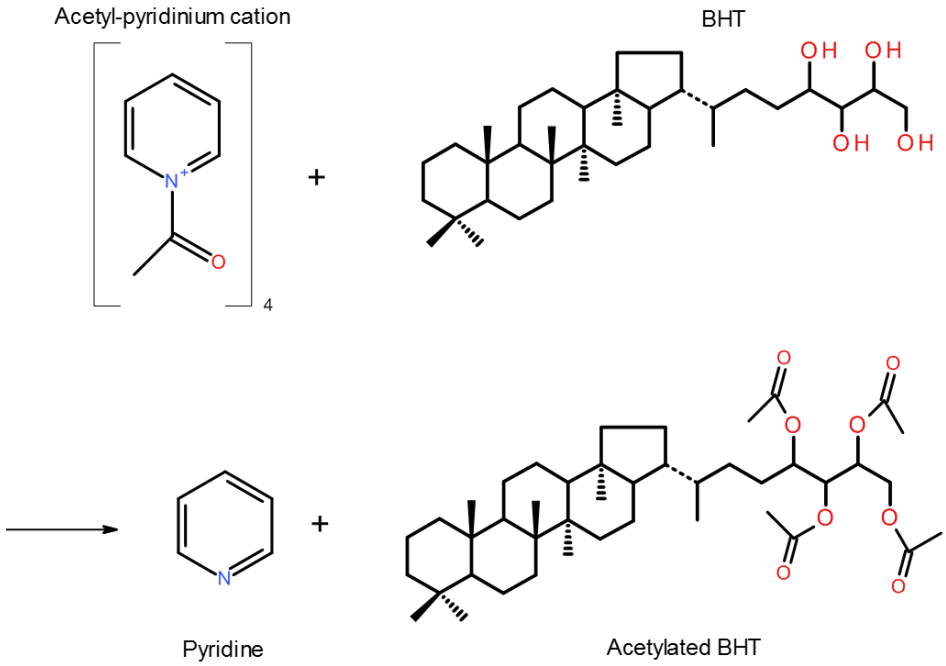

Reaction 2.2. Acetylation of a hopanoid (BHT) with acetyl-pyridinium cation formed in reaction 2.1.

2.7.1. Methodology

A stock of River Tyne (UK) sediment TLE (approximately 0.12 g) was divided into 32 aliquots. Each aliquot was treated as detailed in Table 2.11 (3 replicates for each treatment).

River Tyne sediment TLE aliquots were acetylated using either 100 µl, 500 µl, 1000 µl or 1.5 ml of acetic anhydride: pyridine (1:1 v/v). Aliquots were then heated for (1 h) on a 50 °C heating block. Half of the treatments were then evaporated to dryness under a stream of N_2 with a heating block at 40 °C. The other set of treatments were left overnight at room temperature and evaporated to dryness under a stream of N_2 with a heating block (40 °C) the following day. All samples were then filtered through a 13 mm syringe filter with a 0.45 µm PTFE membrane. Samples were analysed for BHPs as described in section 2.5.5.1. Statistical analysis was performed using

Minitab 17.1.0. Total BHP concentration (μg/g TOC) was found to have a normal distribution (Anderson Darling test statistic 0.369, P = 0.402) and to have equal variance (Levene's test statistic 0.48, P = 0.838). A 2 – way ANOVA was performed to test the response of total BHP concentration against volume of acetic anhydride and pyridine and acetylation time including comparisons using Tukey.

Table 2.11: Acetylation treatment matrix for River Tyne sediment.

Acetic anhydride (μl)	Pyridine (μl)	Heat	Overnight treatment	Dry
50	50	Heat (1 h) on heating block at 50°C	Do not leave samples overnight	Dry under a stream of N_2 on heating block at 50°C
250	250			
500	500			
750	750			
50	50		Leave samples overnight at room temperature	
250	250			
500	500			
750	750			

2.7.2. Results and Discussion of Tyne Sediments

A range of BHPs are observed in Tyne sediment, including; BHT (**1g**), aminotriol (**1h**), adenosylhopane (**1a**), group 2 adenosylhopane (**1e**), methylated group 2 adenosylhopane (**2e**), BHT pentose (**1l**), BHT cyclitol ether (**1i**), BHpentol cyclitol ether (**1j**) and BHhexol cyclitol ether (**1k**). Total BHP concentration measurements ranged from 250 to 350 μg/g TOC (Figure 2.10). Statistical analysis suggest acetylation volume (100 μl, 500 μl, 100 μl or 1500 μl) has a significant effect on measured total BHP concentration (F = 7.19, P = 0.002), conversely, acetylation time (overnight vs. no overnight treatment) does not have a significant effect on acetylation efficiency (F = 1.32, P = 0.266). However, the interaction between volume of acetic anhydride and pyridine and acetylation time does have a significant effect on total BHP concentration (volume x time interaction F = 6.76, P = 0.003). When samples are acetylated overnight, acetylation reagent volume does not have a significant impact on total BHP concentrations (Figure 2.11).

However, when samples are not left overnight the volume of acetic anhydride and pyridine added to the sample has a significant impact on the total BHP concentration; significantly higher total BHP concentrations are observed for samples acetylated with 1500 μl of acetic anhydride and pyridine compared with samples acetylated with

100 µl (T = 5.89, P = 0.001). Differences in total BHPs concentration was observed for the 1500 µl acetic anhydride and pyridine overnight (M, 300 µg/g TOC; SD, 9.3 µg/g TOC) vs not overnight treatments (M, 350 µg/g TOC; SD, 18 µg/g TOC), however, this difference was not found to be significant (T = -2.63, P = 0.207).

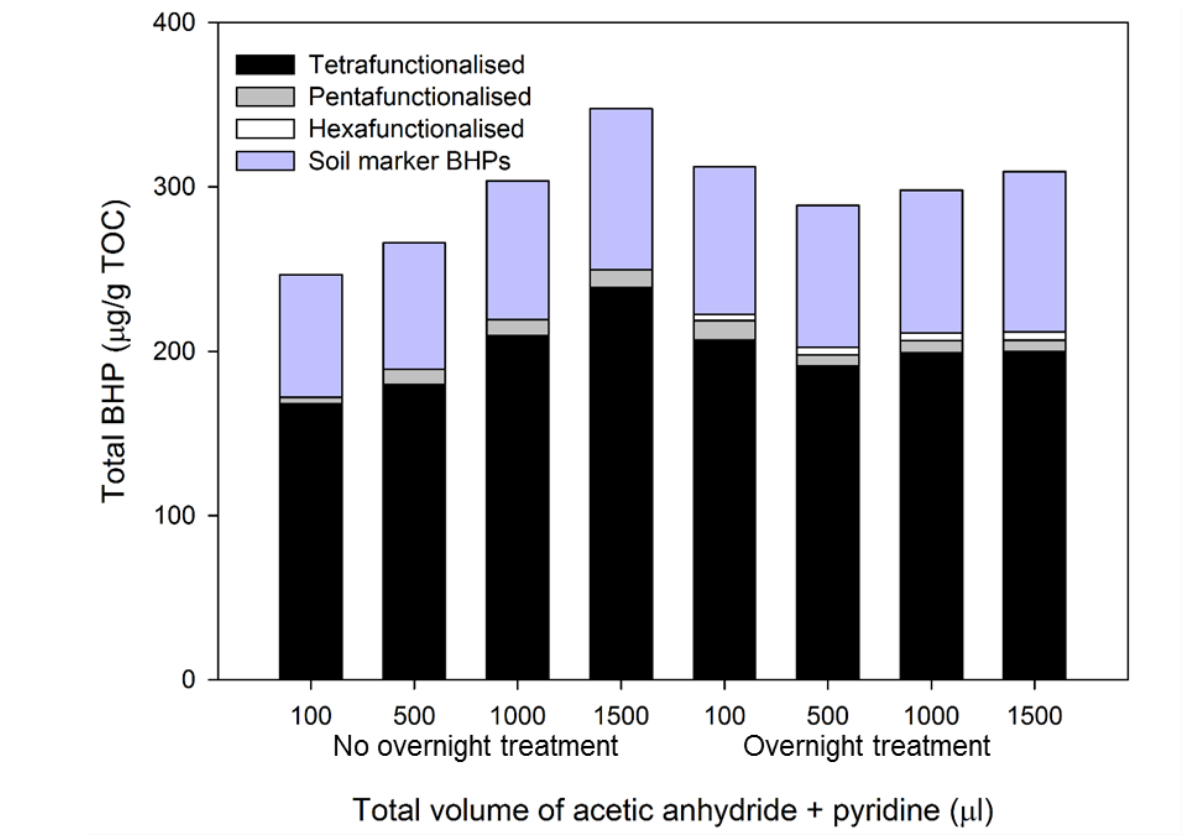

Figure 2.10. Concentration (µg/g TOC) of tetra- (black), penta- (grey) and hexafunctionalised (white) BHPs and soil marker BHPs (blue) within samples treated 4 different volumes of acetic anhydride and pyridine (1:1 vol; 100 µl, 500 µl, 1000 µl, 1500 µl) and overnight treatments).

Relative standard deviation was below the 20% threshold quoted in literature (Figure 2.11; e.g. Cooke, 2010; van Winden et al., 2012b; Talbot et al., 2014). The same suite of tetra- and pentafunctionalised BHPs and soil marker BHPs were found in all treatments (Figure 2.10). However, BHhexol cyclitol ether (**1k**) was the only hexafunctionalised BHP compound to be identified and was only found to be present in samples that had been treated with acetic anhydride and pyridine overnight. The absence of hexafunctionalised BHP compounds in samples that have not been treated overnight suggests BHhexol cyclitol ether and potentially other more highly functionalised BHPs require a long (preferably overnight) acetylation reaction for full quantification of these compounds.

Therefore the 500 µl volume (250 µl acetic anhydride : 250 µl pyridine) with overnight treatment was selected for all subsequent analyses. Results of this method show

high concentrations of BHPs combined with the full suite of BHPs including hexafunctionalised compounds. While RSD (%) is higher for the 500 µl treatments (12%) compared with the 100 µl (6.3%), 1000 µl (5.7%) and 1500 µl (3.1%) treatments it is still lower than the 20% instrumental reproducibility threshold previously reported (e.g. Cooke, 2010; van Winden et al., 2012b; Talbot et al., 2014). Additionally, the 500 µl overnight treatment was selected at as this is a large enough volume to adequately dissolve TLE samples.

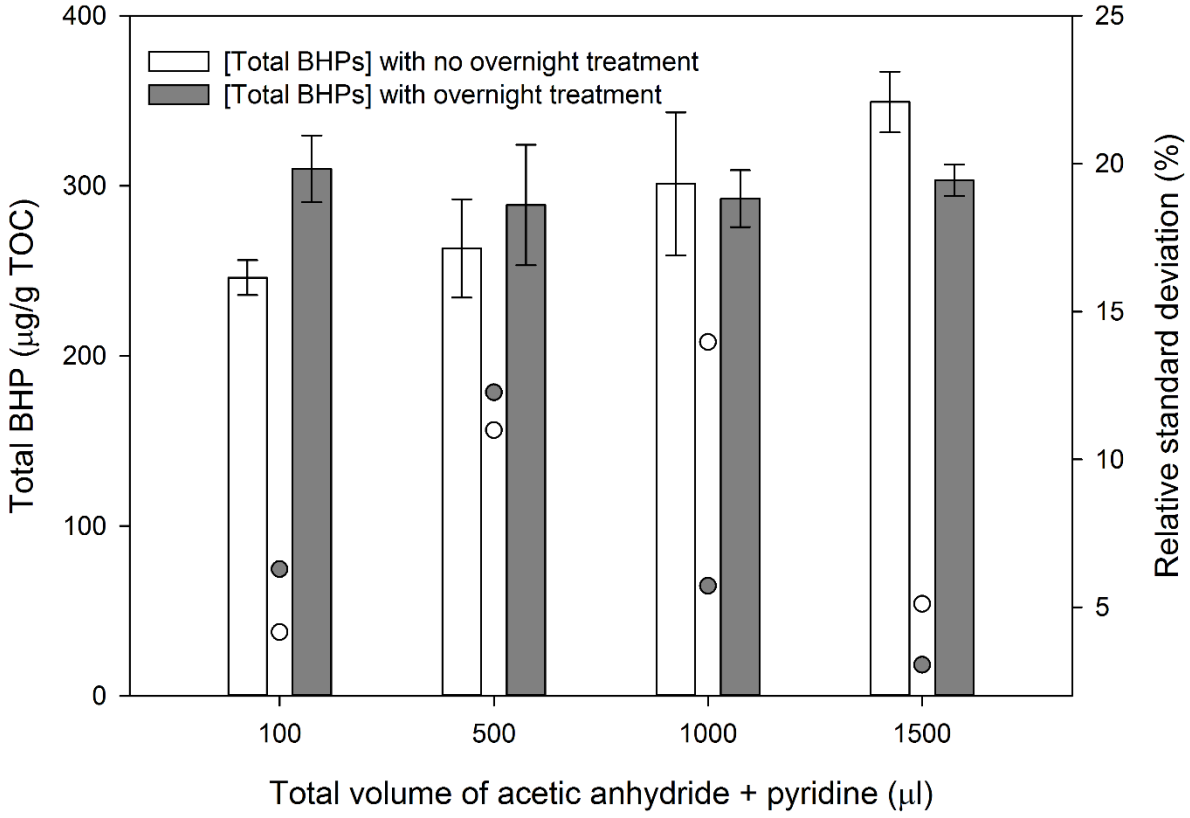

Figure 2.11. Concentration (µg/g TOC) of total BHPs between samples with no overnight treatment (open bar) and samples with an overnight treatment (grey bar) including 4 different volumes of acetic anhydride and pyridine (1:1 vol; 100 µl, 500 µl, 1000 µl, 1500 µl). Error bars are 1 standard deviation. Relative standard deviation shown in open circles (no overnight treatment) and grey circles (overnight treatment).

Chapter 3:

Bacteriohopanepolyol Biomarker Distributions in Tropical Soils

Chapter 3. Bacteriohopanepolyol Biomarker Distributions in Tropical Soils

3.1. Introduction

BHP signatures in the marine geological record are thought to reflect changes in microbial communities at the time of deposition, with multiple factors controlling their distribution. However, relatively little is known about the distribution of these compounds within modern terrestrial environments. Previous studies of soil BHP distributions have mainly focused on Northern hemisphere sites (Cooke et al., 2008a; Xu et al., 2009; Cooke, 2010; Rethemeyer et al., 2010; Kim et al., 2011) with comparatively few studies detailing BHP distributions in modern tropical soils (Pearson et al., 2009; Wagner et al., 2014). As tropical wetlands and soils are understudied, large uncertainties in BHP end members likely exists.

3.2. BHPs as Biomarkers

BHPs have been hypothesised as environmental proxies for *in situ* soil parameters. For example, Kim et al., (2011) found correlation between soil marker BHP distributions and MAAT, pH and precipitation within soils and peats from the Têt watershed. Similarly, BHP distributions have been correlated to pH (Poralla et al., 1984; Schmerk et al., 2011; Welander et al., 2009) and temperature (Joyeux et al., 2004) within pure culture experiments. BHPs have also been hypothesised as proxies for biogeochemical cycling; for example, adenosylhopane (**1a**) and related compounds including C-2 methylated homologues (**2a**, **1e**, **2e**, **1f** and **2f**) have been suggested as biomarkers for soil OC_{ter} (Cooke et al., 2008b, 2009; Zhu et al., 2011; Doğrul Selver et al., 2012, 2015). Another group of highly diagnostic markers are those produced by AMO bacteria (methanotrophs) including aminotetrol (**1c**), aminopentol (**1d**), unsaturated aminopentol (**4/5d**) and aminopentol isomer (**1d';** Talbot and Farrimond, 2007; Zhu et al., 2010; van Winden et al., 2012b; Berndmeyer et al., 2013; Talbot et al., 2014). Lastly, BHPs have been hypothesised as proxies for a specific ecological bacterial niche, where 2-methylhopanoids are enriched in sessile microbial communities inhabiting environments low in oxygen and fixed nitrogen with high osmolarity (Ricci et al., 2014).

3.3. Environmental Sources of BHPs

Terrestrial BHPs may be an important contributor to shelf and fan sediments. An investigation of suspended particulate matter along a tropical river-ocean water column transect suggests that terrigenous OM exported to marine sediments could provide a significant contribution to the marine sedimentary hopanoid inventory (Sáenz et al., 2011a). Additionally, a recent study from the Amazon found high concentration and structural diversity of BHPs within surface wetland sediments suggesting wetlands as possibly significant sources of BHPs to shelf and fan systems (Wagner et al., 2014). In this study we attempt to fill a gap in the research by determining BHP signatures within tropical wetland sediments and soils from the Congo hinterland. The Congo basin consists of a large contrast in tropical environments with humid tropical rainforest, extensive wetlands and savannah environments (Spencer et al., 2012; 2014). Previous work on sediments from the Congo fan suggests that terrestrial OC inputs may be an important source of BHPs to these coastal marine sediments, with greater OC_{ter} during interglacial warm periods (Jahn et al., 2005).

3.3.1. Aims, Objectives and Scope

In this chapter we test the hypothesis; “Paleo CH_4 oxidation biomarkers in Congo fan sediments are of terrestrial origin”. The aim of this chapter is to elucidate the modern terrestrial BHP end members for tropical soils. The specific objectives are; to determine BHP signatures within a range of Congo soil environments and to determine factors that control BHP signatures in these samples.

The scope of this chapter will be to;

- Determine the full BHP inventory for 22 soils (16 forest and 6 savannah/field soils), 6 wetland type sediments (Malebo pool) and an estuarine sediment from the Congo fan.
- To determine pH of the soils and sediments.
- Correlate the distribution of individual BHPs with soil/sediment pH.
- Compare the distribution of C-35 amine BHPs in the Congo soil/sediment samples with ODP 1075 fan samples.
- Compare R_{soil} with R'_{soil} of soils and wetland sediments.

- Compare distribution of BHPs in samples from the Congo with other reported data.
- Discuss the importance of BHP reservoirs in the Congo system.
- Hypothesise factors that control BHP distributions with regards to the global BHP dataset.

3.4. Overview of Methodology and Sites

3.4.1. Study site

Full details of the study site and sample collection can be found in Chapter 2. Briefly, the sediment sample from the estuary of the Congo River ('Anker 24') was taken as grab sample (Eisma et al., 1978) and stored as dried sediment before analyses. Additional lipid data has been published earlier (Schefuß et al., 2004b). Soil samples were collected from 22 sites spanning a wide range of land cover types, ranging from scrub savannah and grasslands, secondary forest and pristine tropical mixed forest, to seasonally flooded and swamp forest environments within the Congo Basin (Figure 2.4). Malebo Pool floodplain wetland sediments were collected along a transect at three sites encompassing sediment that is permanently flooded, sediment inundated during high discharge months only and sediment from above the seasonal high water point (Figure 2.4).

3.4.2. Bulk and Geochemical Analysis

Full details of the bulk parameter, geochemical and LC-MS methodology can be found in Chapter 2. Briefly, soil/sediment pH was measured following the standard method described in BS ISO 10390 (2005). TOC (%) of the soils and Malebo Pool samples was measured at Newcastle University using a LECO CS244 Carbon/Sulfur Analyser after removal of inorganic carbon by treatment with hydrochloric acid. Total lipids were extracted from approximately 3 g of freeze-dried sediment using a modified Bligh and Dyer extraction method as described by Talbot et al. (2007a) and further modified by Osborne, (PhD thesis, Submitted). An aliquot (one third) of the TLE was used for BHP analysis. Semi-quantification of BHP concentrations was achieved using an internal standard (see section 2.5 for further details).

3.4.3. Compound Classification and Statistics

The abbreviated names of the compounds identified, characteristic base peak ions (*m/z*) and structure numbers are given in Table 2.7, Table 2.8, Table 2.9 and Table 2.10.

The term tetrafunctionalised compounds refers to BHPs with four functional groups at the C-32, C-33, C-34 and C-35 positions (Chapter 2). Pentafunctionalised compounds have an additional fifth functional groups located at the C-31 position and hexafunctionalised compounds have 2 additional functional groups located at the C-30 and C-31.

BHPs that are diagnostic for soil organic carbon input (hereafter referred to as "soil marker BHPs" include adenosylhopane (**1a**), C-2 methylated adenosylhopane (**2a**), adenosylhopane type 2 (**1e**) C-2 methylated adenosylhopane type 2 (**2e**), adenosylhopane type 3 (**1f**) and its C-2 methylated homologue (**2f**). The structure of the terminal functional groups in adenosylhopane type 2 and type 3 remain to be elucidated so identification of these compounds is based on retention time and comparison of APCI mass spectra with previously published data (see Cooke et al., 2008a; Rethemeyer et al., 2010).

The R_{soil} index (as defined by Zhu et al., 2011; Equation 2.3) was calculated according to the relative concentrations of BHT (**1g**) and all soil marker BHPs. The R'_{soil} (Equation 2.4) index was later proposed as an alternative index excluding methylated homologues for settings where the C-2 methylated soil marker BHPs were only infrequently/intermittently present (Doğrul Selver et al., 2012) and is calculated according to the relative concentrations of BHT (**1g**) and adenosylhopane (**1a**), adenosylhopane type 2 (**1e**) and adenosylhopane type 3 (**1f**).

AminoBHPs include aminotriol (**1h**), unsaturated (**4/5h**) and methylated aminotriol (**2/3h**), aminotetrol (**1c**), unsaturated aminotetrol (**4/5c**), aminopentol (**1d**), unsaturated aminopentol (**4/5d**) and aminopentol isomer (**1d'**; van Winden et al., 2012b).

BHPs diagnostic for AMO (hereafter referred to as "CH_4 oxidation markers") include aminotetrol (**1c**), aminopentol (**1d**), unsaturated aminopentol (**4/5d**) and aminopentol isomer (**1d'**; van Winden et al., 2012b).

All data are presented to 2 significant figures (Appendices II, III and IV). The data was found to have a non-parametric distribution and was not mathematically transformed prior to statistical analysis. Spearmans rho (r_s) was calculated using IBM SPSS statistics version 21 software. Strong correlation between two variables would result in an r_s of 0.9 and above. Subsurface sediment samples (PS 5-15; RE 5-15; EF 5-15) were excluded from statistical analysis as all other samples were surface samples. The estuary sample and one surface wetland sample (RE 0-5) were also excluded from statistical analysis due to the small sample size and pH data was not collected for either sample.

3.4.4. Data Citation

Published BHP data was used to populate Table 3.2, Table 3.3, Figure 3.6, and Figure 3.8. Sample information can be found in Appendix I.

3.5. Results

3.5.1. TOC and Soil pH

TOC and soil pH values are presented in Table 3.1. TOC values ranged from 0.23 to 6.11% in the soils and 1.10 to 2.68 % in wetland sediment samples. pH values ranged from 3.09 to 5.75 for soils and 4.27 to 4.8 for wetland sediments (pH was not measured for recently exposed sediment 0-5 and the estuary sample due to insufficient sample material).

Table 3.1: Soil and sediment sample names and corresponding abbreviated names with TOC (%) and pH (nm = not measured)

	Sample name	Abbreviated name	TOC (%)	pH
Forest	Closed evergreen lowland forest	CELF JP6	3.40	3.82
	Closed evergreen lowland forest	CELF C6B	0.23	4.71
	Closed evergreen lowland forest	CELF C17B	1.08	4.60
	Closed evergreen lowland forest	CELF C18B	1.59	4.31
	Closed evergreen lowland forest	CELF C19B	2.04	3.73
	Closed evergreen lowland forest	CELF C27B	4.48	3.97
	Logged tropical mixed forest	LTF 7-1	2.95	3.78
	Logged tropical mixed forest	LTF 8-1	2.60	3.66
	Logged tropical mixed forest	LTF 10-1	1.47	3.09
	Tropical mixed forest	TMF 12-1	2.68	3.61
	Gilbertiodendron forest	GF 9-1	6.11	3.81
	Swamp forest	SF 11-1	2.51	3.72
	Tropical seasonally flooded forest	TSFF 6-1	1.28	4.57
	Secondary forest in savannah-forest mosaic	SFS 3-1	2.23	3.76
	Field in savannah-forest mosaic	FSFM 4-1	1.23	4.72
	Mosaic Forest/Croplands	MF C8B	0.71	4.74
Savannah/Field	Swamp bushland and grassland	SB C38B	1.26	5.21
	Closed grassland	CG C46B	2.05	5.07
	Savannah outside of BZV	SBZV 1-1	0.36	5.75
	Scrub savannah	SS 1-1	0.60	4.58
	Scrub savannah	SS 5-1	1.17	3.98
	Field	F 13-1	1.07	4.36
Wetland	Permanently submerged sediment	PS 0-5	1.34	4.27
	Permanently submerged sediment	PS 5-15	1.32	4.53
	Recently exposed sediment	RE 0-5	2.68	nm
	Recently exposed sediment	RE 5-15	2.51	4.38
	Exposed floodplain with occasional submersion	EF 0-5	1.10	4.47
	Exposed floodplain with occasional submersion	EF 5-15	1.62	4.80
	Estuary	Estuary	2.90	nm

3.5.2. BHPs in Congo Soils

Full details of BHP concentrations (µg/g TOC) can be found in Appendices II to IV. A total of 35 BHPs were detected within 22 tropical soils from the Congo hinterland, including tetra-, penta- and hexafunctionalised compounds as well as BHPs with a cyclised side chain. The Swamp bushland/grassland (SB C38B) sample was found to contain the lowest concentrations of BHPs (total of 620 µg/g TOC) while logged tropical mixed forest (LTF 8-1 and LTF 10-1) contained the highest concentrations of BHPs (total of 5700 µg/g TOC). Aminotriol (**1h**) and BHT cyclitol ether (**1i**) are the dominant compounds in most of the soil samples (36% to 68% of aminotriol and BHT cyclitol ether in total BHPs). C2 and C3-methylated BHpentol cyclitol ethers (**2j** and **3j**) and BHhexol cyclitol (**2k** and **3k**) ethers were also found in the soil samples though present as minor components.

In addition to aminotriol, soils were found to contain aminotetrol (**1c**) and in some cases aminopentol (**1d**). Aminotriol was the most dominant C-35 amine BHP with concentrations ranging from 210 µg/g TOC to 1600 µg/g TOC (12% to 50% of total BHPs) within the soils. Aminotetrol was found in all samples, except in the savannah outside of Brazzaville (BZV) (SBZV 1-1), at low concentration and low relative abundance ranging from 2.1 µg/g TOC to 87 µg/g TOC (0.17% to 3.0% of total BHPs). Aminopentol was present as a minor component of the BHP suite with concentrations ranging from 0.92 µg/g TOC to 47 µg/g TOC within six soils. However, aminopentol was found in high concentration (260 µg/g TOC) and high relative abundance (8.8% of total BHPs) in one outlier soil (Closed evergreen lowland forest sample C18B; CELF C18B). Low relative abundance (%) of CH_4 oxidation markers were identified in the soil samples (Figure 3.1). Low concentrations of unsaturated and methylated homologues of C-35 amine BHPs were found intermittently in the soil samples including $\Delta^{6 \text{ or } 11 \text{ or side chain}}$ aminotriol (unsaturated aminotriol; **4/5h**), C-2 and C-3 methylated aminotriol (**2h** and **3h**), $\Delta^{6 \text{ or } 11}$ aminotetrol (unsaturated aminotetrol; **4/5c**), $\Delta^{6 \text{ or } 11}$ aminopentol (unsaturated aminopentol; **4/5d**) and aminopentol isomer (**1d'**; van Winden et al., 2012b).

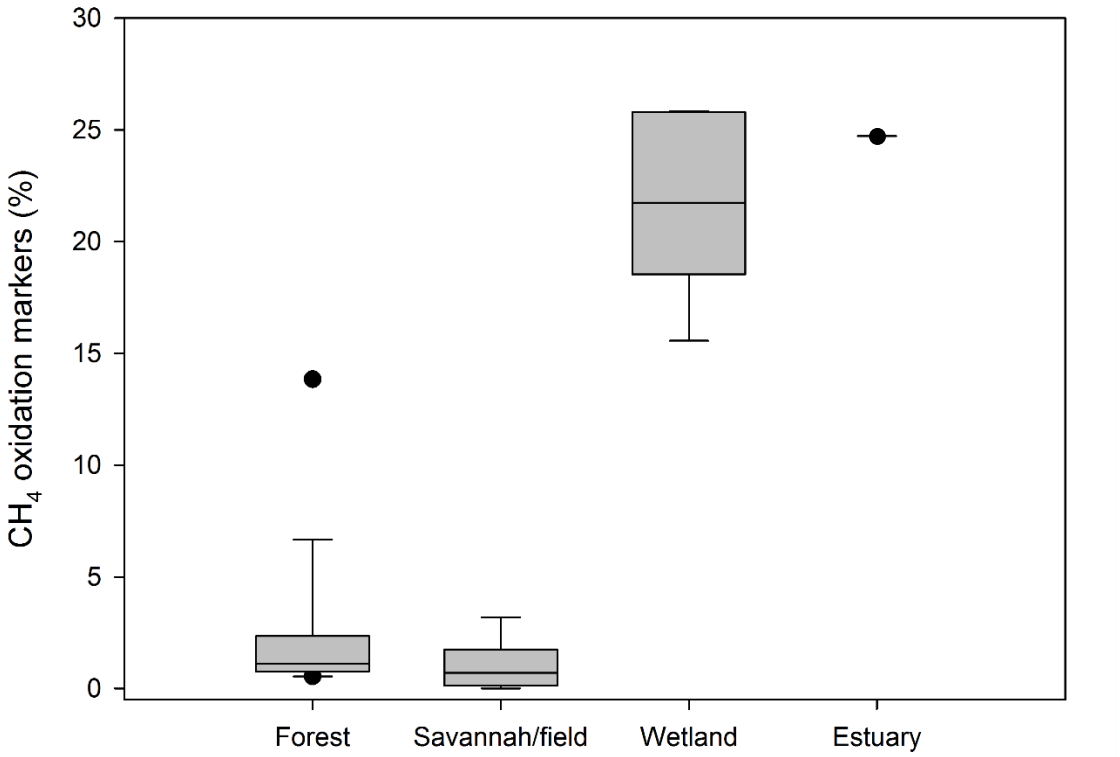

Figure 3.1: Relative abundance (% of total BHPs) of CH_4 oxidation markers within forest, savannah/field soils and wetland and estuarine sediments from the Congo Fan.

Soils were also found to contain a range of other minor BHP compounds. Low concentrations of ribonylhopane (**1b**) were found in 13 of the 22 samples ranging from 2.0 to 20 µg/g TOC (0.14 to 0.46% of total BHPs). Low concentrations of 32,35-anhydro BHT (1o) were found in seven of the 22 soils ranging from 5.0 to 20 µg/g TOC (0.087 to 0.42% of total BHPs; Figure 3.2a)

Composite BHPs with a terminal carbopseudopentose group were present in low abundance in 17 of the 22 soils. Bacteriohopane-32,33,34,35-tetrol pseudopentose (BHT pentose; **1l**) was the most common non-amino sugar BHP to be detected in 17 of the 22 soils with concentrations ranging from 3.9 to 130 µg/g TOC and contributing between 0.35% and 3.0% of total BHPs (Figure 3.2b). $\Delta^{6 \text{ or } 11}$ BHT pentose (unsaturated BHT pentose; **4/5l**) and 2-methyl BHT pentose (**2l**) were identified in 11 and 6 samples respectively.

Similar concentrations of unsaturated- and 2-methyl BHT pentose were observed ranging from 15 to 68 and 26 to 100 µg/g TOC respectively (with relative abundance ranging from 0.62 and 2.28% of total BHPs and between 0.45 and 2.23% of total BHPs respectively).

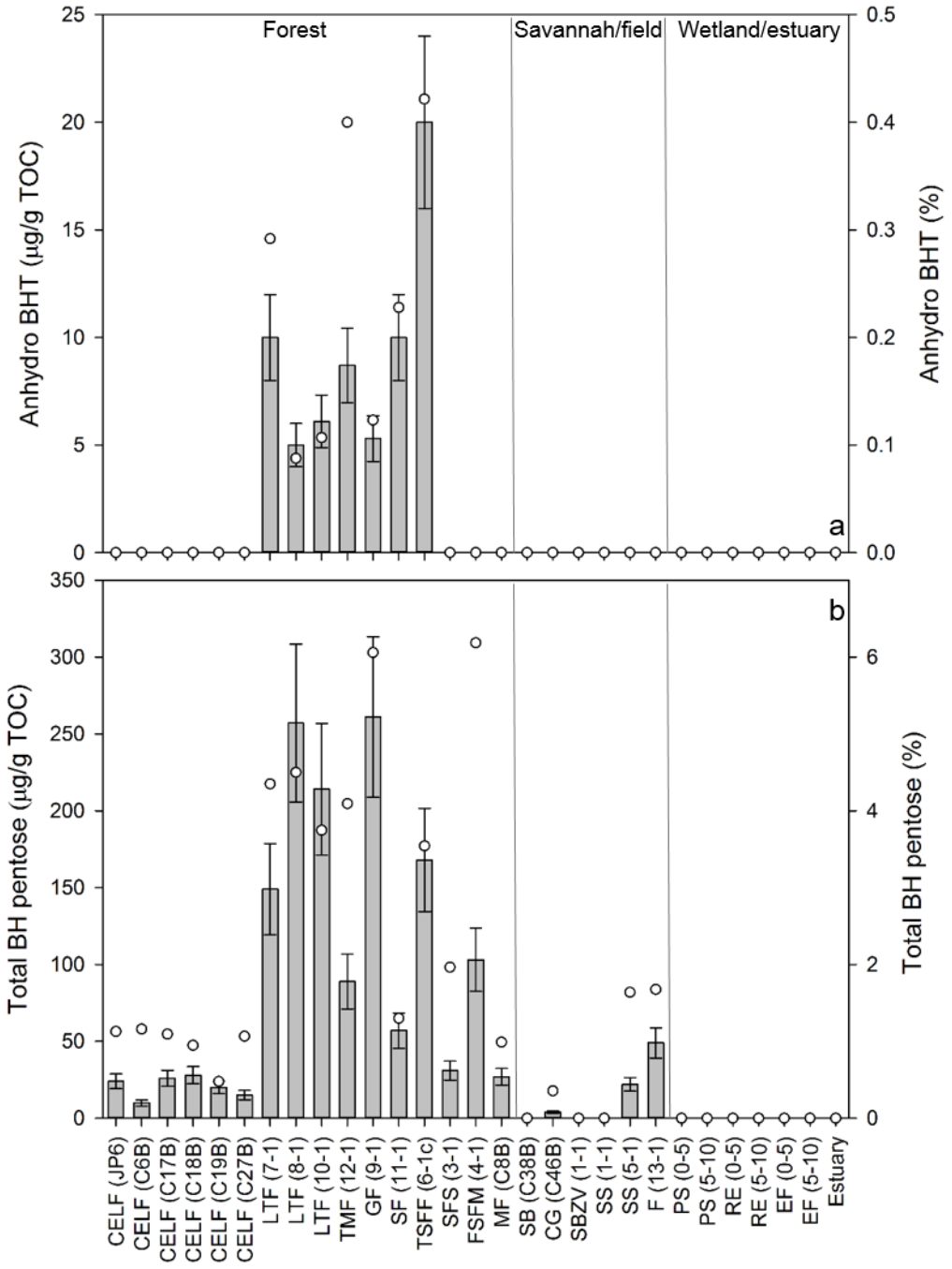

Figure 3.2. Concentration (µg/g TOC) and relative abundance (% of total BHPs) of total anhydro BHT (a) and BH pentose (b) within soil and sediment.

The distribution of individual soil marker BHPs varies across the 22 soils with adenosylhopane (**1a**) consistently being the most abundant of the soil marker BHP with concentrations ranging from 33 to 800 µg/g TOC. Mosaic forest/ cropland; MF C8B is the only soil where 'adenosylhopane type 2' (**1e**) is the most abundant soil marker BHP. C-2 methylated adenosylhopane (**2a**), 'adenosylhopane type 2' and C-2 methylated 'adenosylhopane type 2' (**2e**) are identified in all the soils with 'adenosylhopane type 3' (**1f**) identified in all samples except swamp bushland and grassland C38B (SB C38B), CELF C27B and Gilbertiodendron forest (GF 9-1). C-2

methylated ‘adenosylhopane type 3’ (**2f**) is identified only intermittently. Soil marker BHPs range from 10% to 36% within the forest soils and 7.9% to 36% within the savannah/grassland samples (Figure 3.3). R_{soil} and R'_{soil} indices were calculated for the 22 Congo soils (see section 2.4 for definition). R_{soil} index ranged from 0.58 to 0.92 (average 0.77) and the R'_{soil} index ranged from 0.48 to 0.91 (average 0.74) across the 22 soils (Table 3.2).

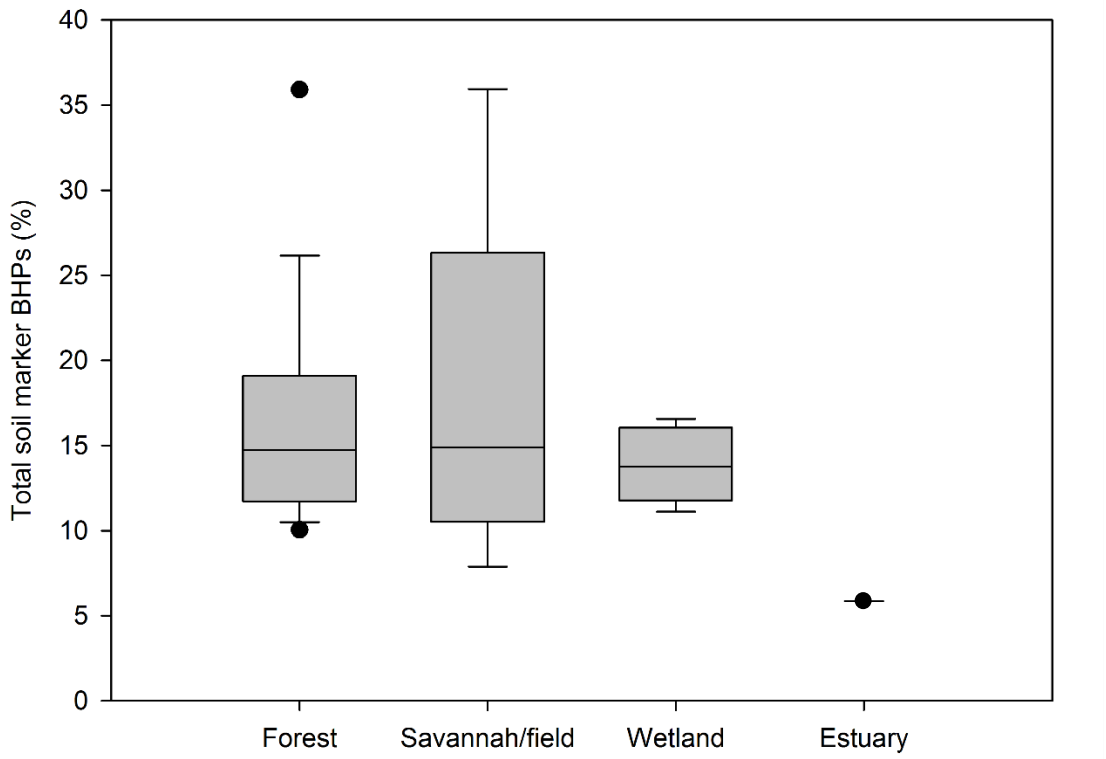

Figure 3.3. Distribution of total soil marker BHPs (% of total BHPs) in forest and savannah/field soils and wetland and estuarine sediment.

3.5.3. BHPs in Wetland Sediments

A total of 19 BHPs were identified in the 6 wetland sediments. High BHP concentrations were found within the wetland samples with values ranging from 4300 µg/g TOC (recently exposed surface and sub-surface sample, RE 0-5 and RE 5-15) to 7500 µg/g TOC (permanently submerged sub surface sample, PS 5-15). Aminopentol (**1d**) and adenosylhopane (**1a**) were the dominant BHPs along with BHT cyclitol ether (**1i**) and aminotriol (**1h**). These samples also contained other CH_4 oxidation markers including aminotetrol (**1c**), aminopentol isomer (**1d’**) and unsaturated aminopentol (**4/5d**: reported in Talbot et al., 2014; Figure 3.1).

Concentrations of soil marker BHPs ranged from 620 µg/g TOC (exposed with occasional flooding sub surface sample; EF 5-15) to 1100 µg/g TOC (PS 5-15).

Relative abundance of soil marker BHPs ranged from 11% and 17% of total BHPs (Figure 3.3). R_{soil} index ranged from 0.61 to 0.66 (average 0.63; Table 3.2) and the R'_{soil} index ranged from 0.59 to 0.62 (average 0.60).

3.5.4. Estuarine Sediment

The estuarine samples was found to contain 12 BHP compounds. Total BHP concentration was 1400 µg/g TOC. Aminopentol and adenosylhopane were the dominant BHPs. Adenosylhopane was the only soil marker BHP detected at concentrations of 81 µg/g TOC (relative abundance of 6% of total BHPs; Figure 3.3). The R_{soil} and R'_{soil} index was 0.20.

3.6. Discussion

3.6.1. BHP Distributions

The soils analysed in this study are dominated by non-source specific BHPs. Greater BHP diversity was found within soils compared to the wetland and estuarine samples, which is consistent with other studies (e.g. Pearson et al., 2009; Zhu et al., 2011). Soils are thought to contain a greater proportion of hopanoid producers than aquatic systems, where BHP synthesis may be limited to approximately 10% of the bacterial community within soils compared to 5% within aquatic environments (Pearson et al., 2007). BHT cyclitol ether (**1i**) is one of the most dominant BHPs within the soils, wetlands and the estuarine sediments. Previous studies have shown that within surface soils where AMO (as indicated by aminopentol; **1d**) is not a dominant process, soils are dominated by non-source specific BHPs; aminotriol (**1h**), BHT cyclitol ether, BHT (**1g**) and adenosylhopane (**1a**) (Cooke, 2010; Cooke et al., 2008a; Pearson et al., 2009; Zhu et al., 2011).

3.6.2. Soil Marker BHPs

A large range of soil marker BHP relative abundance is observed for soils (7.9% to 36% of total BHPs) and wetland sediments (11 to 17% of total BHPs; Figure 3.3). However, the Congo soils have a low mean soil marker BHP abundance of 16% for forest soils (n = 16) and 19% for savannah/field soils (n = 6) compared with samples from other studies (Table 3.2 and Figure 3.8). Surface soils from temperate regions show a larger range in soil marker BHP relative abundance of 0% to 66% (Cooke et al., 2008; Xu et al., 2009; Kim et al., 2010; Rethemeyer et al., 2010; Zhu et al., 2011;

n = 28; Table 3.2). This is compared to a smaller range of soil marker BHP relative abundance in tropical surface soils of 7.9 to 36% (Pearson et al., 2009; Wagner et al., 2014; this study; n = 25) and in tropical wetlands of 2.6 to 17% (surface and subsurface samples; Wagner et al., 2014; this study; n = 11;Table 3.2). This difference in soil marker BHP relative abundance could be due to local environmental parameters. For example, previous studies have shown that changes in pH can affect BHP distributions (concentration normalised to TOC and relative abundance) in environmental samples (Kim et al., 2011) and in laboratory culture experiments where changes in the amount and/or type of BHPs produced are altered (Poralla et al., 1984; Welander et al., 2009; Schmerk et al., 2011). Correlation was not found between the soil marker BHP concentration and sample pH (µg/g TOC; r_s -0.600, p 0.002), R_{soil} (r_s -0.203, p 0.341) or R'_{soil} (r_s -0.266, p 0.209), suggesting that pH is not a key factor influencing soil marker BHP distributions within the Congo samples. However, it should be noted that the soils studied here were from a narrower pH range (pH 3.09 to 5.75; Table 3.1) than those in the Kim et al. (2011; pH 4.6 to 8.9) study.

3.6.2.1. R_{soil} and R'_{soil}

The R_{soil} and R'_{soil} indices have been proposed as SOM input proxies that use adenosylhopane and related compounds as indicators of soil OC. The R_{soil} index (Equation 2.1) uses a 2- endmember mixing model approach based on the relative proportions of soil marker BHPs (**1a**, **2a**, **1e**, **2e**, **1f**, **2f**; Zhu et al., 2011), with BHT utilised as a pseudo marine end member due to the abundance of this compound in both soils and open marine sediments. However, methylated group II (**2e**) and methylated group III (**2f**) soil marker compounds are not observed in all soils or sediment samples, therefore, Doğrul Selver et al. (2012) proposed excluding methylated soil marker BHPs from the OC_{ter} proxy and suggested the R'_{soil} index (Equation 2.4). To date, the R'_{soil} index has only been applied in arctic environments. A wide range in R_{soil} and R'_{soil} indices are observed for the Congo forest and savannah/field soils with a smaller range for the wetland samples (Figure 3.3). The R_{soil} and R'_{soil} indices show significant correlation (Rs 0.98, $p<0.05$; Figure 3.4a). However, as the savannah/field samples have high relative abundance of methylated soil marker BHPs (Figure 3.4b), these samples plot below the regression line.

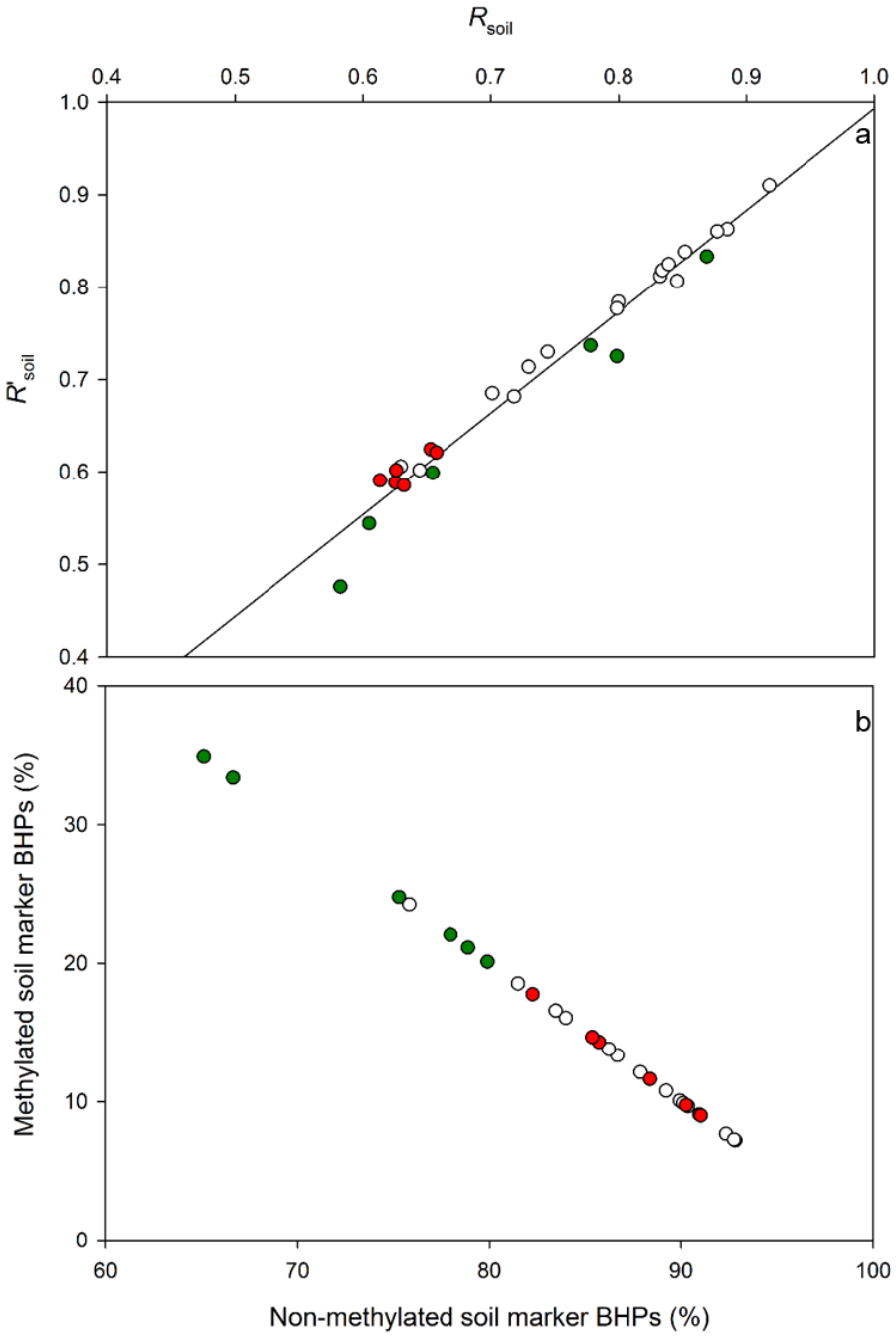

Figure 3.4. a; Correlation between R_{soil} and R'_{soil} indices within Congo forest soils (open), Congo savannah/field soils (green) and Malebo pool wetland samples (red), R_s 0.98 p <0.05. b; Abundance (% of total soil marker BHPs) of non-methylated (1a, 1e, 1f) and methylated (2a, 2e, 2f) soil marker BHPs within Congo forest, savannah/field and Malebo pool wetland samples.

While a clear difference in R_{soil} index can be seen between the catchment and the estuary, the R_{soil} and R'_{soil} indices cannot be used to distinguish between the catchment sub-environments. Data collated from previous tropical BHP studies report R_{soil}/R'_{soil} indices ranging from 0.43 to 0.83 (R_{soil}) and 0.41 to 0.81 (R'_{soil}) for tropical soils (Pearson et al., 2009; Wagner et al., 2014; n = 3) and 0.27 to 0.68 (R_{soil}), 0.21 to 0.64 (R'_{soil}) for Amazon wetlands (Wagner et al., 2014; n = 5; Table 3.2). Arctic and temperate surface soils are also found to have a wide range in R_{soil}/R'_{soil} ranging from

0 to 0.85 and 0 to 0.81, respectively (n = 28; Cooke et al., 2008a; Xu et al., 2009; Kim et al., 2010; Rethemeyer et al., 2010; Zhu et al., 2011; Table 3.2). These results suggest that there is no globally consistent pattern in the R_{soil}/R'_{soil} indices with the application of these proxies strongly dependent on local end members (Zhu et al., 2011). The R_{soil}/R'_{soil} indices of the Congo samples were found to weakly correlate with BHT (R_{soil} r_s -0.616, p 0.001; R'_{soil} r_s -0.519, p 0.009; µg/g TOC) but not with total soil marker BHP concentration (R_{soil} r_s -0.092, p 0.671; µg/g TOC) or with total non-methylated soil marker BHP concentration (R'_{soil} r_s 0.062, p 0.774; µg/g TOC). This suggests that variations in BHT are the most significant influence on R_{soil}/R'_{soil} indices, however, other parameters could also be affecting the R_{soil}/R'_{soil} indices. Furthermore, due to the intermittent presence of methylated soil marker BHPs within the Congo hinterland samples and the relative similarity between the trends in the Rsoil/R'soil indices we will exclude the R_{soil} index from further analyses.

Table 3.2: Summary of relative abundance (%) of soil marker BHPs, R_{soil} and R'_{soil} within this study and published studies.

Location	N	Soil marker BHPs (%)		R_{soil} (R'_{soil})		Reference
		Mean	Range	Mean	Range	
Congo Forest soils	16	16	10 - 36	0.79 (0.77)	0.63 - 0.92 (0.60 - 0.91)	This study
Congo savannah/fields	6	19	7.9 - 36	0.71 (0.65)	0.58 - 0.87 (0.48 - 0.83)	This study
Congo wetlands (surface and subsurface)	6	14	11 - 17	0.63 (0.60)	0.61 - 0.66 (0.59 - 0.62)	This study
Amazon soils	2	23	18 - 28	0.64 (0.61)	0.44 - 0.84 (0.41 - 0.81)	Wagner et al., 2014
Amazon wetlands (surface and subsurface)	5	6.0	2.6 - 11	0.45 (0.43)	0.27 - 0.68 (0.21 - 0.64)	Wagner et al., 2014
Tropical soil San Salvador	1	21		0.48 (0.48)		Pearson et al, 2009
Têt (surface soils)	12	41	0 - 66	0.54 (0.52)	0 - 0.87 (0 - 0.85)	Kim et al., 2011
Têt peat (surface)	2	27	24 - 31	0.62 (0.60)	0.53 - 0.71 (0.51 - 0.68)	Kim et al., 2011
East China (Mid catchment surface soils)	3	20	12 - 30	0.74 (0.70)	0.60 - 0.82 (0.57 - 0.80)	Zhu et al., 2011
Canada	5	43	35 - 52	0.79 (0.76)	0.67 - 0.85 (0.65 - 0.81)	Xu et al., 2009
Arctic permafrost	6	40	27 - 55	0.64 (0.60)	0.53 - 0.75 (0.48 - 0.72)	Rethemeyer et al., 2010
Northern UK (surface)	4	23	20 - 27	0.48 (0.42)	0.36 -0.64 (0.30 - 0.58)	Cooke et al., 2008a

A prominent issue with using BHT as a marine end member in SOM proxies is that this BHP has a wide range of potential sources in soils (e.g. Talbot et al., 2008) and can be a dominant component of the BHP profile in soils (Cooke et al., 2008a; Xu et al., 2009; Kim et al., 2011, Rethemeyer et al., 2010). Furthermore, relatively little is known about possible marine sources of BHT other than some species of SRB (e.g. Blumenberg et al., 2006). Finally, BHT and adenosylhopane have different reactivities and therefore may degrade at different rates upon deposition (e.g. Cooke et al., 2008b; Handley et al., 2010) suggesting, at least in some settings, the R_{soil}/R'$_{soil}$ index could instead be used to describe relative rates of degradation.

3.6.3. Biomarkers for AMO

Aerobic methane oxidation is a CH_4 sink in the terrestrial realm, occurring in peatlands (e.g. Deng et al., 2013), soils (e.g. Wolf et al., 2012), rice paddy fields (e.g. Vishwakarma and Dubey, 2010) and lakes (e.g. Dumont et al., 2013). Aminopentol (**1d**) is a biomarker for type I methanotrophs (Neunlist and Rohmer, 1985a; Rohmer et al., 1984; Cvejic et al., 2000b; Talbot et al., 2001; Coolen et al., 2008; van Winden et al., 2012b) with only one report of a non-methanotroph source; a species of *Desulfovibrio* SRB which synthesised extremely low concentrations of aminopentol when grown in pure culture (Blumenberg et al., 2012). Concentrations of CH_4 oxidation markers (see section 3.4.3; **1c, 1d**, **4/5d**, **1d'**) vary between the different samples analysed in this study. High concentrations and relative abundances of CH_4 oxidation markers are identified in the wetland samples, where aminopentol is the second most dominant BHP compound after BHT cyclitol ether (**1i**) confirming the occurrence of AMO (Figure 3.1). The high concentrations and high relative abundance of CH_4 oxidation markers is in contrast to the soil samples, where aminotetrol is the most dominant CH_4 oxidation marker, but a minor compound in the BHP suite overall (Figure 3.1 and Table 3.3). This is unexpected as 2 soils were sampled within an area of CH_4 producing land cover (Figure 2.4; swamp forest 11-1; tropical mixed forest 12-1) suggesting AMO should be identifiable from the BHP biomarker suite.

Table 3.3: Summary of relative abundance (%) of CH_4 oxidation markers within this study and published studies.

Location	N	% CH_4 oxidation markers		Reference
		Mean	Range	
Congo Forest soils	16	2.3	0.53 - 14	This study
Congo savannah/fields	6	1.0	0 - 3.2	This study
Congo wetlands (surface and subsurface)	6	22	16 - 26	This study
Amazon soils	2	4.3	0.94 - 7.7	Wagner et al., 2014
Amazon wetlands (surface and subsurface)	5	37	24 - 45	Wagner et al., 2014
Tropical soil San Salvador	1	5.8		Pearson et al, 2009
Têt (surface soils)	12	1.0	0 - 5.8	Kim et al., 2011
Têt peat (surface)	2	1.3	0 - 2.5	Kim et al., 2011
East China (Mid catchment surface soils)	3	2.4	0.52 - 6.1	Zhu et al., 2011
Canada	5	1.4	0.96 - 2.0	Xu et al., 2009
Arctic permafrost	6	0	0	Rethemeyer et al., 2010
Northern UK (surface)	4	0.85	0 - 2.0	Cooke et al., 2008a

Low levels of aminopentol in soils could be due to low AMO activity in these samples. Alternatively, the soil samples could have been collected when the oxic – anoxic boundary was shallowest. A previous study by van Winden et al. (2012a) found CH_4 oxidation markers in peatlands, specifically at the oxic – anoxic boundary where AMO is thought to occur. Additionally, Henckel et al. (2001) found that AMO increased during the drying out of CH_4 producing wetland type environments, presumably due to the extension of the oxic –anoxic boundary. Lastly, the lack of CH_4 oxidation markers in the soil samples could be due to a disparity in our understanding of the source organisms of aminopentol and related compounds. Many Type I methanotrophs synthesise aminopentol as a dominant membrane component followed by minor amounts of aminotetrol and aminotriol. Type II methanotroph membranes are dominated by aminotetrol and aminotriol (e.g. van Winden et al., 2012b and references therein). However, aminotriol was found as the

dominant BHP within the Type I methanotroph *Methylomicrobium album* (Talbot et al., 2001). Additionally, Coolen et al. (2008) found a dominance of type I methanotrophs within sediments from Ace Lake (unit 1 of sediment profile, Antarctica) despite the absence of aminopentol and dominance of aminotriol and aminotetrol within the sedimentary BHP distribution.

3.6.4. Transport of AMO Biomarkers to Congo Fan

High concentrations of aminoBHPs in particular CH_4 oxidation markers were identified in the Congo fan (ODP 1075; see Talbot et al., 2014). The origin of CH_4 oxidation markers on the Congo fan could be due to (1) allochthonous production of these biomarkers due to intense AMO occurring within wetlands/flood plain lakes, or (2) autochthonous production of CH_4 oxidation markers due to the destabilisation of shallow gas hydrates.

3.6.4.1. Wetlands

Wetlands are a major CH_4 sink (Wuebbles and Hayhoe, 2002) due to AMO by a diverse group of methanotrophs, including many hopanoid synthesising bacteria (Dedysh 2009; Henckel et al., 2001; van Winden et al., 2012a,b). Sediment from Malebo pool wetland was found to contain high concentration and high relative abundance of CH_4 oxidation markers, suggesting this site as a location of intense AMO. Furthermore, similarities between in CH_4 oxidation marker signatures in Malebo pool and ODP 1075 could suggest Malebo pool as a possible site of intense AMO within both modern and past climate phases (Figure 3.5).

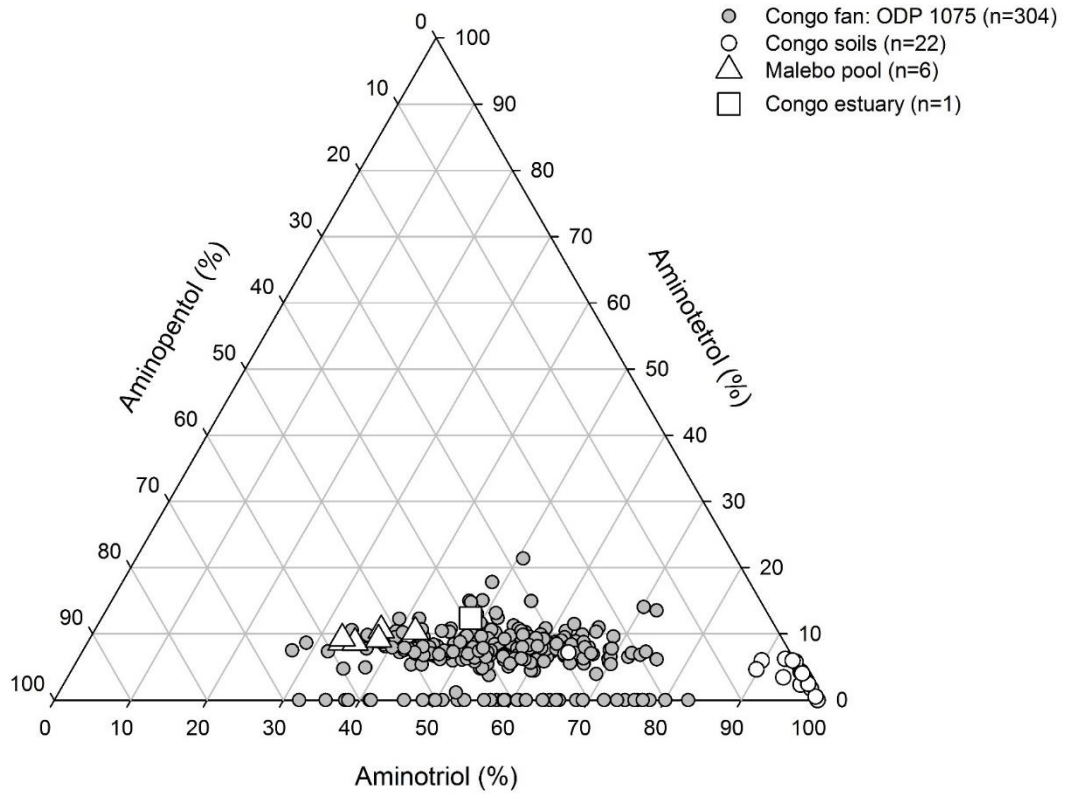

Figure 3.5. Relative abundance (% of total aminoBHPs) of aminotriol, aminotetrol and aminopentol (including unsaturated aminopentol and aminopentol isomer) in ODP 1075 sediments, soils, wetland (Malebo pool) and estuarine sediment from the Congo. Modified from Talbot et al. (2014).

Organic matter exported from Malebo Pool is geochemically similar to OM at the head of the estuary (~ 350 km downstream) and no major tributaries join the Congo River between this site and the Atlantic Ocean (Spencer et al., 2012). In agreement with this, the estuary sample was found to contain high concentrations of CH_4 oxidation markers. The wetland and ODP 1075 data set is also compared with 22 soils from the Congo hinterland (Figure 3.5). As can be seen, the majority of the soils have a low relative abundance of aminopentol suggesting that these soils are not the source of CH_4 oxidation biomarkers to the Congo fan. The data also agrees with recent investigations of BHP signatures within the Amazon where Wagner et al. (2014) suggests wetland type environments as source areas for BHP CH_4 oxidation markers signatures. Thus, our Congo study is the second to document such high abundance of CH_4 oxidation markers within tropical wetland samples (Table 3.3). Furthermore, high concentrations of CH_4 oxidation markers may be a more general feature of tropical and possibly other wetlands.

3.6.4.2. Marine CH_4 Sources

The presence of CH_4 oxidation markers identified on the Congo fan could also be due to in situ production. The destabilisation of shallow gas hydrates and/or CH_4 outgassing from pockmark structures could result in intense AMO leading to the synthesis of CH_4 oxidation markers. Destabilisation of gas hydrates has been hypothesised as a potential climate forcing source of paleo CH_4 to the atmosphere ('the clathrate gun hypothesis'; Kennet et al., 2003). However, the real potential of CH_4 hydrates as a climate forcing source has yet to be actualised. Both modelling and geochemical studies suggest CH_4 release from gas hydrates may be insufficient to cause global climate perturbations (e.g. Brock et al., 2010). The Congo fan hosts CH_4 rich gas hydrates (Charlou et al., 2004 and references therein) and giant pockmark structures (more than 800m diameter; Gay et al., 2006). Within these gas hydrates, AOM is hypothesised to be the major CH_4 sink due to the dominance of Mg-calcite, Aragonite and Pyrite in the associated sediments (Charlou et al., 2004). To date, gas hydrates and pockmarks hosted in the Congo fan have not been analysed for biomarkers specific for AMO. However, previous biomarker analysis of similar marine structures in other locations, suggests the Congo fan pockmarks and gas hydrates may not be key sources of BHPs found on the Fan (Rush et al., *in prep*). While there are few studies determining BHP signatures within marine CH_4 structures, those that have been published do not report high concentrations of CH_4 oxidation markers, these studies include; cold-seep sediments (Alaminos Canyon, Gulf of Mexico; Birgel et al., 2011); hydrate associated authigenic carbonate rocks (Green Canyon, Gulf of Mexico; Pancost et al., 2005); and OM from CH_4 seeps from Be'eri sulphur deposit (Israel; Burhan et al., 2002). In addition to this, a methanotrophic cold-seep mytilid mussel gill symbiont collected from the Louisiana slope off the Gulf of Mexico was found to only produce aminotriol and aminotetrol (Jahnke et al., 1995), potentially further suggesting marine methanotrophs may not synthesise aminopentol as a dominant cell membrane BHP.

Isotopic evidence suggests a terrestrial rather than a marine source for CH_4 oxidation markers identified on the Congo fan. Charlou et al. (2004) reports relatively light $\delta^{13}C$ values of -69.3‰ for CH_4 associated with gas hydrates in the Congo fan, which, is in agreement with other studies from similar regions (e.g. Jahnke et al., 1995; Burhan et al., 2002; Peckmann and Thiel, 2004; Birgel et al., 2006a,b). However, compound specific carbon isotope values for BHPs derived from aminopentol within ODP 1075

show relatively heavy $\delta^{13}C$ of -41‰ (Talbot et al., 2014). This evidence further suggests that if AMO does occur within marine sediments, these biomarkers make only a minor contribution to the Congo fan hopanoid inventory.

3.6.5. Degradation Products Anhydro BHT

Low and trace amounts of anhydro BHT was found within seven tropical forest samples (Figure 3.2). Anhydro BHT is a degradation product of BHT (Talbot et al., 2005; Saito & Suzuki, 2007; Schaeffer et al., 2008), BHT cyclitol ether, BHT glucosamine (Schaeffer et al., 2010) and possibly adenosylhopane (Cooke et al, 2008b; Handley et al., 2010; Eickhoff et al., 2014) and is commonly found within modern and ancient sediments from marine (Sáenz et al., 2011a; Handley et al., 2010; Wagner et al., 2014), riverine (Pearson et al., 2009; Zhu et al., 2011) and coastal regions (Pearson et al., 2009; Sáenz et al., 2011a; Zhu et al., 2011; Wagner et al., 2014). Anhydro BHT can be formed through acid treatment (Schaeffer et al., 2008, 2010) and in high temperature and pressure treatments (Eickhoff et al., 2014). The presence of anhydro BHT in the soils could be due to tropical forest samples being sites of rapid carbon turnover. Additionally, as anhydro BHT formation is aided in acidic environments (due to the acid hydrolysis mechanism; Schaeffer et al., 2008, 2010) the production of this compound could be due to the acidic nature of the soils (see Table 3.1).

3.6.6. Distribution of Cyclitol Ethers

Strong correlation between BHT cyclitol ether and BHpentol cyclitol ether (r_s 0.903, $p < 0.05$) and BHT cyclitol ether and BHhexol cyclitol ether (r_s 0.921, $p < 0.05$) in both the soil and Malebo pool samples is identified in this study (Appendix V). Correlation between BHT cyclitol ether, BHpentol cyclitol ether and BHhexol cyclitol ether could suggest similar sources of composite BHPs in soil environments. BHT cyclitol ether and BHpentol cyclitol ether have similar soil bacterial sources including *Burkholderia* spp. (Cvejic et al., 2000b), *Azotobacter vinelandii* (Vilcheze et al., 1994) and *Acetobacter xylinum* (Herrmann et al., 1996b). A source organism for BHhexol cyclitol ether has yet to be identified, however, the strong correlation between BHT cyclitol ether and BHhexol cyclitol ether in the samples suggests these compounds to have a similar bacterial source.

C2 and C3 methylated BHpentol and BHhexol cyclitol ethers are identified in the soils. C3 methylated cyclitol ethers have been rarely reported in soils with the only other examples from the Yangtze River (Zhu et al., 2011). Malebo pool samples contain C2 and C3 methylated BHpentol cyclitol ethers as minor components of the BHP suite. C2 and C3 methylated BH cyclitol ethers show significant correlation with non-methylated BH cyclitol ethers. BHT cyclitol ether was found to strongly correlate with 2-methyl BHT cyclitol ether (r_s 0.864, $p < 0.05$), 2-methyl BHpentol cyclitol ether (r_s 0.864, $p < 0.05$) and weakly correlate with 3-methyl BHpentol cyclitol ether (r_s 0.443, $p < 0.05$). BHpentol cyclitol ether was found to strongly correlate with 2-methyl BHT cyclitol ether (r_s 0.830, $p < 0.05$), and weakly correlate with 2-methyl BHpentol cyclitol ether (r_s 0.686, $p < 0.05$). BHhexol cyclitol ether was found to strongly correlate with 2-methyl BHT cyclitol ether (r_s 0.833, $p < 0.05$), 2-methyl BHpentol cyclitol ether (r_s 0.758, $p < 0.05$), and weakly correlate with 3-methyl BHpentol cyclitol ether (r_s 0.491, $p < 0.05$). Weaker but significant correlation was found between the methylated cyclitol ethers. This correlation between methylated and non-methylated homologues could suggest similar controls on the occurrence of these compounds within the soils and sediments. Factors affecting the distribution of methylated and non-methylated cyclitol ethers include (1) similarities in bacterial sources, and (2) bacterial sources of these compounds affected in a similar way by environmental parameters. Synthesis of hopanoids has been linked to pH sensitivity where a bacterial strain lacking the ability to synthesise hopanoids (*Rhodopseudomonas palustris* TIE-1) was observed to have severe morphological damage when cells were grown under acidic and alkaline conditions (Welander et al., 2009). Additionally when hopanoid synthesis was restored to *R. palustris* TIE-1 a significant increase in methylated BHPs was observed (Welander et al., 2009). Similarly, *Burkholderia cenocepacia* K56-2 mutants with the inability to produce BHPs were also found to be sensitive to low pH, detergent, and various antibiotics (Schmerk et al., 2011). Furthermore, a significant increase in BHP production has been observed when *Bacillus acidocaldarius* was grown at increasing temperature with a moderate increase in extended hopanoid production when these cells were grown at decreasing pH (Poralla et al., 1984). Hopanoid producers have also been observed to be sensitive to nitrogen concentration where *Nostoc punctiforme* vegetative cells starved of nitrogen showed an initial 3 fold increase in 2-methylhopanoids, however, hopanoid synthesis returned to control levels within 2 weeks (Doughty et al., 2009). A more in-depth environmental study, including full analysis of environmental

parameters and molecular microbiology would be required to fully explore the correlations reported here.

3.6.7. Distribution of Non-Nitrogen Containing Pseudopentose Compounds

BHT pentose, including unsaturated and C2 methylated homologues, were identified in the soil samples (Figure 3.2) and are synthesised by cyanobacteria (Talbot et al., 2008). BHT pentose, unsaturated and methylated homologues were not identified in either the Malebo pool samples or the estuary sample. Lack of BHT pentose compounds in both the Malebo pool and estuary samples could suggest these compounds are not readily transported through the Congo catchment and may be subject to enhanced (riverine) degradation. Degradation of BH pentose is aided in highly acidic environments leading to degradation of the labile sugar moiety (van Winden et al., 2012a) and could suggest the intermitted and low concentrations of these compounds in the Congo samples.

3.6.8. BHP Reservoirs

The Congo River drains the second largest basin in the world (~3.7 x 10^6 Km^2). Soil derived OM is an important component of sediments deposited on the Congo fan (Holtvoeth et al., 2005). The organic fraction of ODP 1075 sediments relates to strongly degraded SOM of old highly developed, Kaolinite-rich ferallitic soils (Oxisols) that cover large areas of the Congo river basin (Holtvoeth et al., 2005). The OC from the soils analysed in this study is transported through the Congo River and deposited in Malebo pool (Hughes et al., 2011; Spencer et al., 2012). Similarity between the spread in R'_{soil} indices for the soils and Malebo pool (Figure 3.6) further suggests that BHPs are also subject to this transport mechanism. Due to the position of Malebo pool in the Congo River, OM and therefore BHP signatures in the wetlands are representative of BHPs from the Congo watershed (Hughes et al., 2011; Spencer et al., 2012).

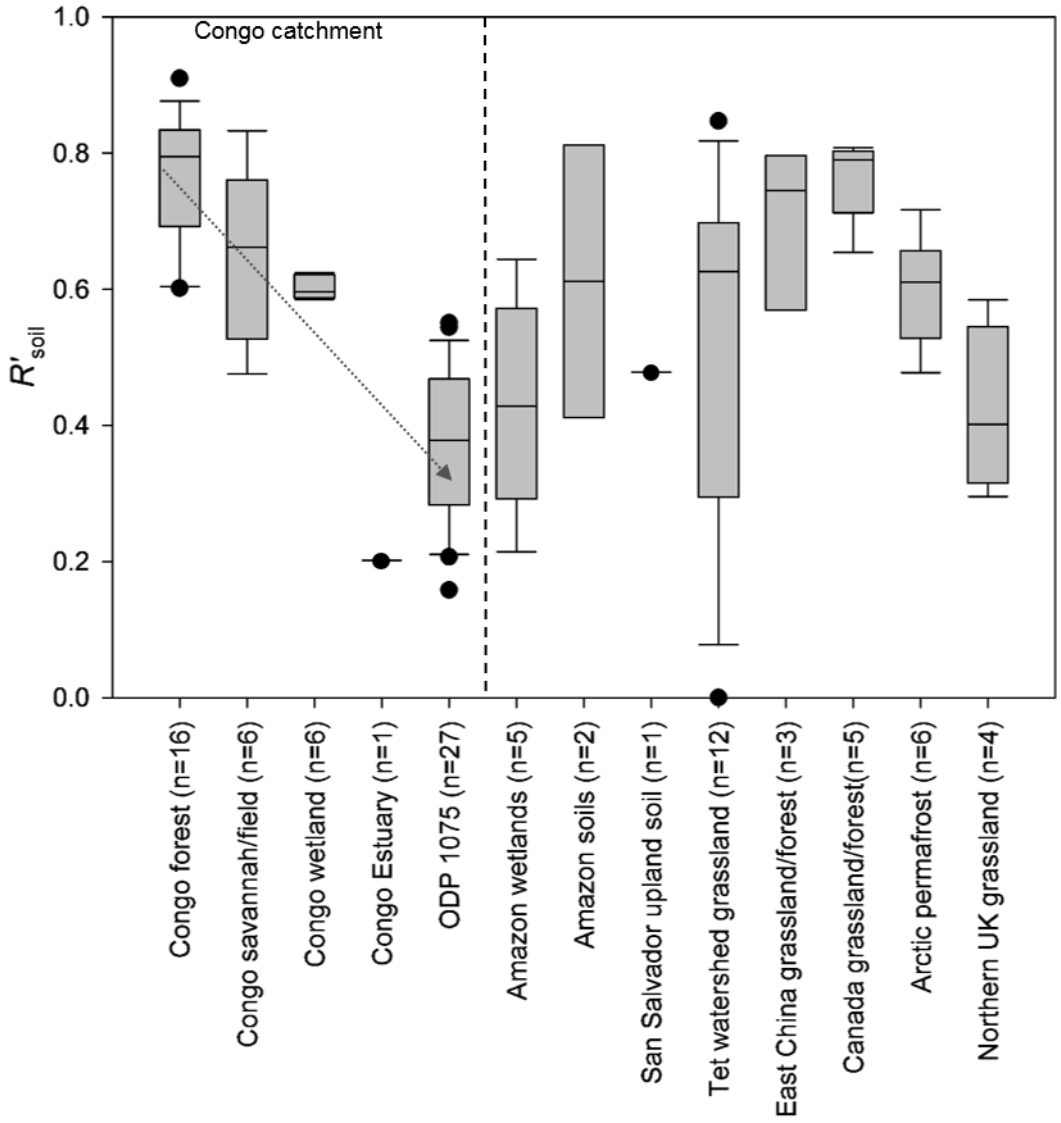

Figure 3.6. Box plots showing range of *R'*$_{soil}$ values for soils and sediments including: forest soil (this study; n=16); savannah/Field soil (this study; n=6); estuary (this study; n = 1); Congo fan (ODP 1075) paleo sediments (Handley et al., 2010; and Chapter 4; n=27); wetland surface and subsurface sediment (this study; n=6); Amazon wetlands (surface and subsurface; Wagner et al., 2014; n=5); Amazon soil (Wagner et al., 2014; n = 2) San Salvador soils (Pearson et al., 2009; n=1); Têt watershed surface soils (Kim et al., 2011; n=12); East China soil (Zhu et al., 2011; n=3) Canadian surface soils (Xu et al., 2009; n=5); surface Permafrost (Rethemeyer et al., 2010; n=6); Surface soils from Northern UK (Cooke et al., 2008a; n=4); grey arrow indicates a general decreasing trend in *R'*$_{soil}$ from source (Congo soils and wetlands) to sink (Congo estuary and fan).

Therefore, a terrestrial *R'*$_{soil}$ end member of 0.60 (Malebo pool mean; Table 3.2) is representative of fluvially transported soils within the Congo watershed in combination with BHPs produced in Malebo Pool. Sediments deposited at Malebo pool are flushed into the estuary and then on to the Congo shelf and fan. As only one grab sample from the estuary was analysed in this study, the reported *R'*$_{soil}$ value of 0.2 (Table 3.2) may not represent the true mean of the Congo estuary. However, BHT and adenosylhopane concentrations for ODP 1075 have previously been reported by Handley et al. (2010). Calculation of the *R'*$_{soil}$ index for sediments

between 10 and 100 Ka (n = 27) show the R'_{soil} index for the estuary is within the range of 0.16-0.55 (interglacial 0.16-0.55; glacial 0.21-0.52) for ODP 1075 sediments (n = 27; Figure 3.6). The mean R'_{soil} index for ODP 1075 is 0.37 which is approximately half of the terrestrial end member of Malebo pool, suggesting, that soil OM is a significant contributor to marine OM. This is in accordance with other studies from the Congo deep-sea fan. Holtvoeth et al. (2003) used a binary mixing model approach to determine that between 18 and 61% of bulk OM in ODP 1075 is of continental origin. Similarly, Weijers et al. (2009) used a 3 end member mixing model to determine that between 38 and 52 % of OC within GeoB 6518-1 is of terrestrial (soil) origin.

Furthermore, strong similarities are found between the distribution of BHPs identified in the soils, wetlands, estuarine and ODP 1075 samples (Figure 3.7 a, b). A suite of common BHPs are identified within the forest and savannah/field and Malebo pool samples with more than half of the BHPs identified in the soils also found in the wetlands. In addition, the common BHPs identified in the hinterland soils and the wetlands represent a major component of the soil BHP profile, contributing an average of 88% (forests) and 94% (savannah/field) of total BHPs (based on concentration; Figure 3.7 a). Strong similarities are also found between the BHP profiles of the hinterland soils, wetlands, estuary, and ODP 1075 sediments. Lower BHP diversity is reported for samples from the Congo fan (Handley et al., 2010; Talbot et al., 2014) with many of the methylated and pentose compounds below detection limit. Between 7 and 10 of the 12 BHP compounds identified in ODP 1075 are also found in the wetlands and soils, and are a major component of all of the BHP profiles representing over 90% of the total BHPs found in the wetland and estuary samples (Figure 3.7 b). Strong similarities between BHPs identified in the Congo hinterland and wetland samples and those identified in ODP 1075 suggests a link between BHP reservoirs. High concentrations of aminotetrol and aminopentol (including unsaturated aminopentol and aminopentol isomer) found in ODP 1075 sediments have previously been linked to fluvial transport of these biomarkers to the Congo fan from Malebo pool and potentially similar wetlands (Talbot et al., 2014; section 3.6.4) with similar mechanisms also reported in the Amazon (Wagner et al., 2014). Due to the ubiquitous nature of BHT, aminotriol, BHT-, BHpentol and BHhexol cyclitol ether it is likely that the source of these compounds in the Congo fan will be both marine and terrestrial derived (see Chapter 5 for further discussion). The

notable absence of methylated and unsaturated BHPs from ODP 1075 which represent no more than 18% of total BHPs in the soils and wetland sediments, is likely due to a dilution effect.

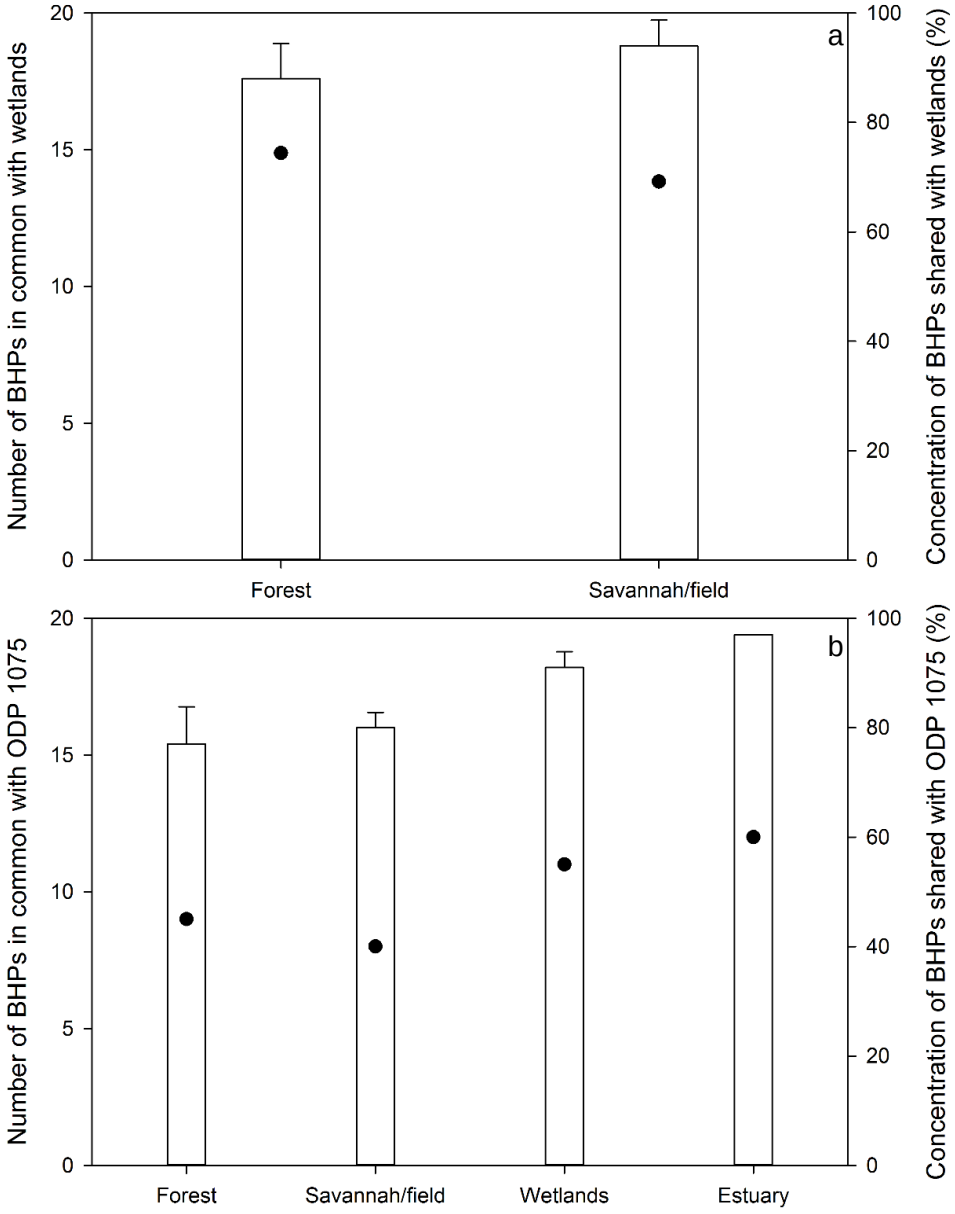

Figure 3.7. a; Mean number of BHPs identified in forest and savannah/field samples in common with wetlands (a) and in common with ODP 1075 (b; circles). Relative abundance (% based on µg/g TOC) of BHPs in forest and savannah/field samples in common with wetlands (a) and ODP 1075 (b; bars).

3.6.9. Trends in Global Distribution

The data presented here suggest that BHP relative abundance may be controlled by large scale climate trends. Within the soils and wetlands from the Congo Basin, a narrow range in soil marker BHP relative abundance (7.9-36% of total BHPs) and tetrafunctionalised BHP relative abundance (52-81% of total BHPs) was observed (Figure 3.8). The range is much smaller in comparison with studies from other less

stable climatic zones, where surface soil marker BHP relative abundance varies between 0% and 66% of total BHPs and tetrafunctionalised BHP relative abundance varies between 34% and 100% of total BHPs (Cooke et al., 2008a; Xu et al., 2009; Rethemeyer et al., 2010; Kim et al., 2011; Figure 3.8).

Additionally, mean soil marker BHP relative abundance for Congo soils (17%) is lower than that for temperate soils from northern and eastern Europe (28%; Cooke et al., 2008a; Redshaw et al., 2008). These differences may suggest that the main factors controlling BHP distributions in tropical climate zones are different from those in temperate and polar climate zones. Kim et al. (2011) found MAAT and precipitation to influence soil marker BHP distribution in samples from the Mediterranean (Têt watershed). Soils from the Têt watershed were collected along a transect with strong environmental contrasts in altitude, MAAT, precipitation and a wide pH range, including some low pH peat samples.

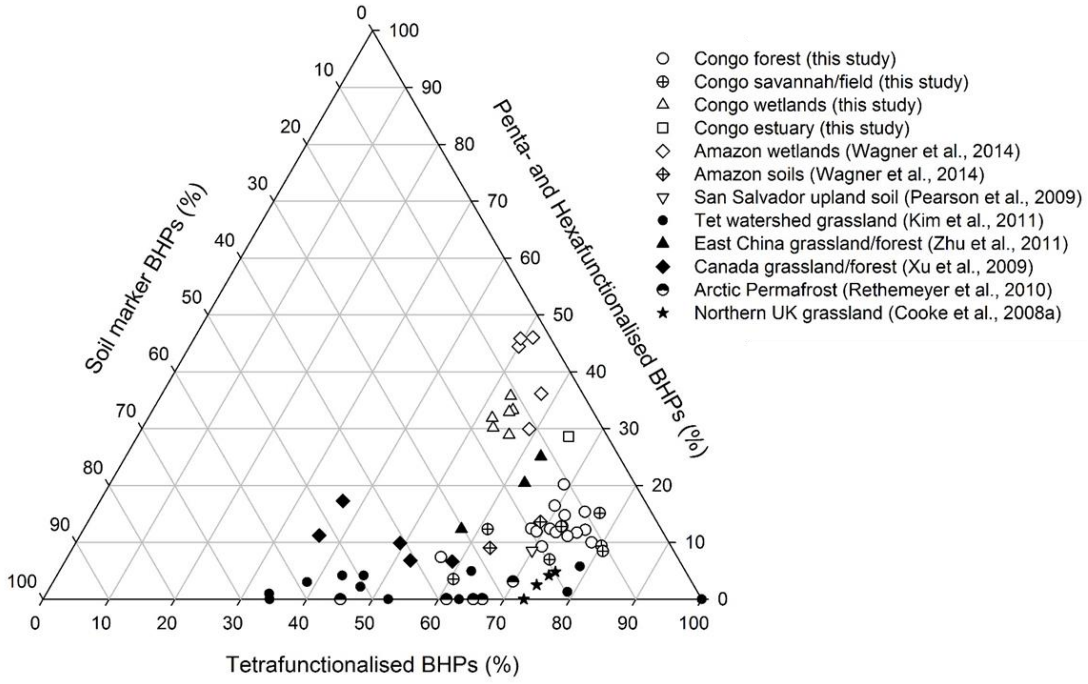

Figure 3.8: Ternary plot with relative abundance of tetrafunctionalised BHPs (%), sum of penta- and hexafunctionalised BHPs (%) and soil marker BHPs (%) in soils/sediments from this study and from published data (see section 3.4.4 for details).

Kim et al. (2011) found that the lowest relative abundance of adenosylhopane (the dominant soil marker BHP) occurred at low altitude where MAAT was high, pH more alkaline and precipitation lowest. This could suggest that, during BHP synthesis, adenosylhopane (an intermediate in hopanoid biosynthesis) is converted to other

BHPs when environmental conditions are favourable for microbial activity (e.g. warmer).

High relative abundance of soil marker BHPs are found in soils from polar climates, with values between 27% and 55% of total BHPs for Svalbard (Rethemeyer et al., 2010) and 69-82% for surface and subsurface Yedoma permafrost from Siberia (Doğrul Selver et al., 2015). Xu et al. (2009) also observed abundances ranging from 35-52% of total BHPs in Alberta (Canada).

Hopanoids are thought to maintain cell membrane fluidity and preserve liquid order within the cell (Sáenz et al., 2012) and could therefore potentially be important cell membrane constituents for cold tolerance within bacteria (Seipke and Loria, 2009). Physiological alteration of the bacterial cell membrane during cold stress is an important prokaryotic adaptation, with rapid temperature downshift of bacterial cells causing phase separation of the cell membrane phospholipids and consequently decreasing cell membrane fluidity and permeability (Cao-Hoang et al., 2010). However, mesophilic and psychrophilic bacteria respond differently to cold stress depending on whether the cold stress is below or above 0 °C. At sub – zero temperatures the response of most prokaryotes is passive and eventually leads to cell death (Haines, 1938; Weiser and Osterud, 1945), whereas, outside the optimal growth range temperature and above 0 °C the bacterial response is active, with typically the synthesis of specific proteins (Jones et al., 1994; Graumann et al., 1996). Mesophiles adapt to cold stress through physiology and have been observed to reduce synthesis of 'housekeeping' proteins and increase synthesis of cold-shock proteins during cold stress (Graumann et al., 1996). Psychrophiles are adapted to low temperature due to evolutionary pressure and continue to produce housekeeping proteins, as well as cold-shock proteins and cold acclimation proteins during cold stress (Hébraud and Potier, 1999). Very few studies exist that systematically examine cold stress responses and regulation of hopanoid biosynthesis. Jahnke et al. (1999) investigated the hopanoid composition of a psychrotolerant methanotroph (designated CEL1923) grown at a range of temperatures between 10 and 35 °C and found a higher concentration of total hopanoids (BHPs and the C_{30} compounds diploptene and diplopterol) at the lowest temperature. Kulkarni et al. (2013) found that C-2 methylated hopanoid gene expression (hpnP; Welander et al., 2010) is regulated by the general stress response factor of alpha proteobacteria (EcfG), however, there are no studies analysing the role of EcfG in the regulation of other

hopanoid synthesis. Additionally, maximal hopanoid production has been observed in *Nostoc punctiforme* cells that had differentiated into akinetes (Doughty et al., 2009), which are thought to form during cold stress and desiccation, again suggesting the importance of these compounds in bacterial cold stress. However, the organisms in these studies either do not accumulate adenosylhopane (**1a**; methanotrophs, *Nostoc* sp. cyanobacterium; Jahnke et al., 1999; Doughty et al., 2009) or the methods used were not appropriate for the detection of adenosylhopane (Jahnke et al., 1999, Kulkarni et al., 2013), so the specific role of this BHP in cold adaptation remains to be elucidated. The role of hopanoids in bacterial stress tolerance could also be suggested by the structural diversity of BHPs observed both in environmental samples and in bacterial cultures (e.g. Kannenberg and Poralla, 1999). Poger and Mark (2013) observed key differences in the orientation of BHT compared with diploptene within a bacterial lipid bilayer molecular dynamics simulation, suggesting that the diversity of BHPs may lead to a broader range of functional roles in bacterial membranes than sterols in eukaryotic cells.

The temperatures at Ny-Ålesund are much lower than those at the Têt watershed, which, may imply that there is a threshold where cool temperatures reduce BHP diversity due to differences in bacterial response to cold stress above and below 0 °C. In contrast, low relative abundances of soil marker BHPs occur in samples from tropical climate zones. Soil marker BHPs in the Congo soils range from 7.9-36% of total BHPs and within Amazon soils between 18% and 28% of total BHPs (Wagner et al., 2014; Table 3.2). Wetland sediments from tropical climate zones have the lowest relative abundance of soil marker BHPs of between 11 and 17% in the Congo and between 2.6% and 11% in wetland samples from the Amazon (Wagner et al., 2014). MAAT and precipitation data are not available for the exact locations of the Congo soils or Amazon samples; however, as the Congo samples were all from locations with similar elevation and the Congo Basin has high temperatures year round (Spencer et al., 2014), MAAT is also relatively comparable. The small range in soil marker BHP relative abundance in the Congo and Amazon samples is therefore likely due to the small range in seasonal temperature contrasts that are always above 0 °C. Long term soil temperature studies for Cameroon and South Africa show a temperature range from 18-30 °C (Fan et al., 2015; Sugihara et al., 2015), however, more comparable studies within the Congo are unavailable. Additionally, fluctuation in seasonal precipitation in the Congo catchment could also impact on BHP relative

abundance; however, such a link cannot be identified from the current data. Long term seasonality studies are required to constrain the interrelationship between BHP distributions and seasonal variation in tropical precipitation and temperature. Two soils from east China (28°N; Zhu et al., 2011; soils from a rice farm and from an afforested area) plot close to the wetland samples (Figure 3.8) with high relative abundance of penta- and hexafunctionalised BHPs and low relative abundance of soil marker compounds. These BHP signatures could possibly be linked to the subtropical (warm–wet) climate conditions of the Yangtze.

The Kim et al. (2011) study suggests BHP responses based on local temperature variation. On a much larger scale, BHP abundances between climate zones could be controlled by seasonal temperature contrasts. Our initial observations on BHP variation across climate zones leads us to propose the following hypothesis: "Variation in BHP relative abundance in soils is controlled by the magnitude of local seasonal temperature contrasts". Specifically, within Arctic and temperate regions which experience strong seasonality, a wide range of BHP relative abundances is observed, including the highest relative contributions from soil marker BHPs observed to date. Conversely, within tropical regions, seasonal temperatures remain high, resulting in a more constrained range in BHP relative abundance. This hypothesis would suggest that, in addition to *in situ* environmental parameters (e.g. pH), contrasts in MAAT would impact on hopanoid producing microbial communities and their BHP signatures preserved in soils, on a regional scale. BHP data from a wide range of depositional and climatic settings, including seasonal time series are needed to test this hypothesis.

3.7. Conclusions

The aim of this chapter was to test the hypothesis "Paleo CH_4 oxidation biomarkers in Congo fan sediments are of terrestrial origin". Modern terrestrial soil end members were defined with up to 35 different BHP structures identified in 22 soils, 6 wetland and one estuarine sediment from the Congo. Dominant compounds in the soil samples were typically BHT, aminotriol and BHT cyclitol ether while in the wetland sediment from Malebo Pool, BHP signatures produced by AMO bacteria (including aminopentol and aminotetrol) were also important, representing up to 26% of total BHPs. This indicates that taxonomic controls, specifically related to the type and activity of aerobic methanotrophs, can be an important source of variability within the

Congo samples. This study is the second reported example of these highly specific biomarkers occurring in high concentrations within tropical environmental samples.

Soil marker BHP relative abundances in the soils and wetland sediments were very similar. However, the relative proportion of soil marker BHPs in the Congo soils (mean, 16% of total BHPs in forest soils; 19% of total BHPs in savannah/field soils) was lower than values for temperate and Arctic surface soils calculated from the available literature data. We speculate that differences in soil marker BHP relative abundance between climate zones may be controlled by seasonal temperature variability, however, the full significance of adenosylhopane (and related compounds) in microbial cold stress adaptation remains to be elucidated. R_{soil} and R'_{soil} indices for the soils show a large range of 0.58-0.92 and 0.48-0.91, respectively, with savannah/field samples typically showing greater variation than forest soils. This is in accord with other R_{soil} and R'_{soil} values calculated from the literature and reinforces the need for local end members to be determined before any interpretation of the index values is undertaken. These results indicate a clear link between BHP reservoirs within the Congo catchment with similar BHPs identified within the Congo fan and in soils and sediments from the Congo fan. Furthermore and in agreement with other studies, R_{soil} indices from ODP 1075 suggest a significant contribution of soil derived OM in the Congo fan.

Overall, these results clearly indicate that tropical wetlands could have been an important source of CH_4 oxidation markers to the Congo fan during the Pleistocene. This suggests that C-35 amine signatures identified in Congo fan sediments are a record of terrestrial CH_4 cycling.

Chapter 4:

Determining Soil Organic Carbon Export to Late Quaternary Congo Deep Sea Fan Sediments (ODP Site 1075) Using Microbial Biomarkers

Chapter 4. Determining Soil Organic Carbon Export to Late Quaternary Congo Deep Sea Fan Sediments (ODP Site 1075) Using Microbial Biomarkers

4.1. Introduction

Fluvial transport of C represents an important connection between the terrestrial and oceanic reservoirs. Current estimates suggest between 0.8 and 1.33 Pg C is fluvially transported to the world's oceans every year (Huang et al., 2012 and references therein). Tropical rivers (30° N – 30° S) are critially important in OC_{ter} due to a disproportionately high freshwater outflow (66.2%), relatively high sediment load (73.2%) and high terrestrial net primary production (61%; Milliman and Syvitski, 1992; Syvitski et al., 2005). Investigations of sediments off major river mouths have shown that fluvial systems make a more important contribution to the supply and accumulation of OC in deep sea settings than previously considered (e.g. Meyers, 1997; Goñi et al., 1998). The Congo River, for example, is the second largest exporter of C to the ocean and the largest river in Africa (drainage basin size; ~3.7 x 10^6 Km^2; Runge, 2007; Laraque et al., 2009). Previous studies suggest soil derived OC to be an important component of Congo fan sediments (Holtvoeth et al., 2001; 2005). However, to date, fluctuations in OC during the entire Pleistocene have yet to be determined.

4.1.1. Modern Organic Carbon transport in the Congo

The Congo River contributes 3.9% (approx. 0.13 Pg C/yr) to the global annual supply of terrigenous OC into the ocean (Martins and Probst, 1991), thereby strongly influencing near shore sedimentation in the eastern equatorial Atlantic (Martins and Probst, 1991). However, in contrast to other major rivers, the Congo River has a relatively low sediment load with 11 to 17 times lower suspension loads compared to the Mississippi or Amazon rivers (Ludwig et al. 1996). Within the modern system, OC_{ter} is a significant input to Congo deep-sea fan sediments with large contributions from plant and soil OM (Spencer et al., 2012). The supply of OC to the Congo deep-sea fan is further complicated by the geomorphology of the river mouth, which is characterised by an exceptionally narrow continental shelf in front of the mouth (approx. 50 Km), and the presence of a canyon which begins within the estuary of the river. It is therefore anticipated that climate induced changes in the supply and

composition of terrigenous OM are well preserved in late Quaternary sediments of the Congo deep sea fan (e.g. Chapter 3; Talbot et al., 2014).

4.1.2. Organic Carbon Transport During the Pleistocene

Geochemical analysis of Quaternary sediments suggests Congo fan OC is a mixture of terrestrially derived soil, vegetative, and marine OC (Holtvoeth et al., 2005; Weijers et al., 2009). Sediments from the Congo contain thermally stable OC which relates to strongly degraded SOM of old and highly developed, kaolinite-rich ferallitic soils (Oxisols) that are common in the Congo basin (Holtvoeth et al., 2005). Fluctuations in the composition of OC observed in the Congo fan are intimately linked to African climate, river drainage and marine sedimentation. Holtvoeth et al. (2001) suggested a close link between OM supply to the Congo deep sea fan and late Quaternary fluctuations in precessional insolation with superimposed lower frequency orbital variations (e.g. eccentricity and obliquity). OM accumulation, OC isotopic composition and Fe content from the past 1.7 Ma within the Congo fan and also found that TOC MAR fluctuations are controlled by precessional variations, indicating that African climate was strongly controlled by low latitude insolation changes (Jahn et al., 2005). However, relatively little is known about the contribution of terrestrial microbial OC to Congo fan records and to what extent patterns in microbial OC may be controlled by orbital scale cycles.

4.1.3. Challenges Tracing Microbial Organic Carbon Pools

Molecular proxies for OC_{ter} transport offer a unique insight into microbial derived soil OC. The GDGT derived BIT index (Hopmans et al., 2004) and the BHP derived R_{soil} index (Zhu et al., 2011) have both been proposed as proxies for OC_{ter} transport. The BIT index has been used in many studies to trace microbial derived soil OC_{ter} (Schouten et al., 2013b and references therein). Previous studies applying the BIT index in the Congo fan have shown a significant proportion of microbial OC_{ter} preserved in sediments dating to the past 20 Ka (Weijers et al., 2009). Similarly, high concentrations of adenosylhopane in Congo fan sediments also reveals microbial derived OC_{ter} during similar time intervals (Cooke et al., 2008b; Handley et al., 2010). However, terrestrial microbial derived OC in Congo fan has yet to be reconstructed in sediments older than the late Pleistocene.

Additionally, the suitability of the BIT and R_{soil} indices in estimating OC_{ter} transport remains to be validated. A previous study comparing the BIT and R_{soil} index in modern soils from the River Têt watershed in southern France revealed clear differences in these proxies suggesting that both indices could be tracing different microbial communities (Kim et al., 2011). This was also supported by recent studies of Arctic surface sediments where R'_{soil} index values closely track bulk $\delta^{13}C$ whilst BIT values were decoupled, suggesting different sources and/or transport mechanisms (Doğrul Selver et al., 2015). Additionally, adenosylhopane, the terrestrial end member of the R_{soil} index shows clear differences in stability over longer time scales with Handley et al. (2010) reporting highly degraded signatures within ODP 1075 dated to the Pleistocene. Comparatively, the BIT index (Schouten et al., 2013b and references therein) has been shown as highly recalcitrant with oldest application of this index within sediments dated to the Jurassic (Jenkyns et al., 2012). Both R_{soil} and BIT indices show uncertainty with terrestrial and marine endmembers. The marine endmembers for both the BIT (crenarchaeol) and R_{soil} (BHT; **Ig**) indices have been identified in soil environments (Weijers et al., 2008: Spencer-Jones et al., 2015), which, can result in an artificial decrease in the indices respectively. However, within soils, crenarchaeol has consistently been reported in low concentrations and, therefore, will potentially have a negligable affect on the BIT index (Weijers et al., 2008). Additionally, while BHT has been reported in higher concentrations within soils compared with crenarchaeol, the R_{soil} index has been shown to be of use when the terrestrial endmember is known (Chapter 3; Spencer-Jones et al., 2015). To date, the terrestrial endmember for the R_{soil} index, adenosylhopane, has not been identified within a marine BHP producing bacteria and is not known to be synthesised within aquatic environments. However, br-GDGTs (the BIT index terrestrial endmember) have been found to be produced within aquatic environments, including lakes (Sinninghe Damsté et al., 2009; Tierney and Russell, 2009; Bechtel et al., 2010; Tierney et al., 2010; 2012; Zink et al., 2010; Loomis et al., 2011; Buckles et al., 2014) and rivers (Zhu et al., 2011; Kim et al., 2012; Zhang et al., 2012; Yang et al., 2013; Zell et al., 2013a,b; 2014a,b; De Jonge et al., 2014). These clear differences in the provenence of the R_{soil} and BIT indices further complicating the interpretation and comparison of both indices in deeper buried sediments.

4.1.4. Aims, Objectives and Scope

Previous work has shown significant variations in OC_{ter} composition and export to the Congo deep sea fan with soil OM thought to dominate during the Pleistocene (Holtvoeth et al., 2003). Terrestrial derived OC transport to the Congo fan has been shown to correlate with insolation changes suggesting large scale climate driven control with increased OC_{ter} transport during interglacial / warm periods (Jahn et al., 2005). However, the contribution of microbial OC to the Congo fan during the Pleistocene remains to be elucidated. Furthermore, to date, no complete R_{soil} or BIT record covering the entire Pleistocene has been constructed for the Congo fan.

In this chapter we test the hypothesis that "*Temporal changes in R_{soil} and BIT indices within ODP 1075 occur due to variations in orbital cycling*".

To address this hypothesis we determine the short term and long term variability in OC_{ter} for the Pleistocene using a molecular biomarker approach. The specific objectives are to (1) expand the maximum sampling depth in ODP 1075 to 2.5 Ma (226 mcd) to address the long term variability, and (2) to increase sampling resolution around MIS 11 and 5 to address the short term climate variability.

The scope of this chapter are;

- Determine soil marker BHP inventory within ODP 1075.
- Determine distribution of anhydro BHT within ODP 1075.
- Determine diagenetic controls on soil marker BHPs indices.
- Calculate R_{soil} and BIT indices for ODP 1075.
- Determine the suitability of R_{soil} and BIT indices for paleoclimate reconstructions.
- Determine if orbital forced climate signals influence R_{soil} and BIT indices during MIS 11 and 5.

4.2. Overview of Methodology and Sites

4.2.1. Sample Collection and Geochemical Analysis

Full details of the study site and sample collection can be found in Chapter 2. Briefly, all samples analysed in this chapter are from ODP 1075. Full details of the bulk parameter, geochemical and LC-MS methodology can be found in Chapter 2. Geochemical analysis described in this chapter include TOC, GDGTs and BHPs.

BHP analyses for 120 samples has previously been published in Handley et al. (2010). TOC for samples between 10 Ka and 1.2 Ma have previously been published by Holtvoeth et al. (2001).

The abbreviated names of the compounds identified, characteristic base peak ions (*m/z*) and structure numbers are given in Table 2.8.

4.2.2. Statistical Analysis

The R_{soil} index (as defined by Zhu et al., 2011) was calculated according to the relative concentrations of BHT (**1g**) and all soil marker BHPs (Equation 2.3). The BIT index was calculated according to the relative concentrations of crenarchaeol and Br-GDGTs (Hopmans et al., 2004; Equation 2.5).

Previous analysis within the Congo fan identified and increase in OC_{ter} between 1.7 Ma and present (Jahn et al., 2005). Jahn et al. (2005) suggested three key intervals where OC_{ter} in the Congo fan significantly changed. Data shown in Table 4.1 and Figure 4.5 is divided into these three intervals (1.7-1.1 Ma; 1.1-0.3 Ma; 0.3-0 Ma). Statistical analysis was performed using Minitab 17.1.0. TOC and BIT index was found to agree with a statistically normal distribution. A One-way ANOVA (post hoc Tukey) was performed on both TOC and BIT used to compare in the means between different intervals (sections 4.3.1). Pearson's correlation index (R) was performed on GDGT relative abundances. Spearmans Rho (R_s) correlation index was performed on BHP abundances.

4.3. Results

4.3.1. Total Organic Carbon and Soil Marker Inventory

Two TOC records are combined including a 10 Ka to 1.2 Ma record reported by Holtvoeth et al. (2001) and a new 1.2 Ma to 2.5 Ma record generated in this study. TOC in ODP 1075 ranges from 0.74 % to 4.15%, with a mean of 2.02% and standard deviation of 0.59% (n = 504; Figure 4.1).

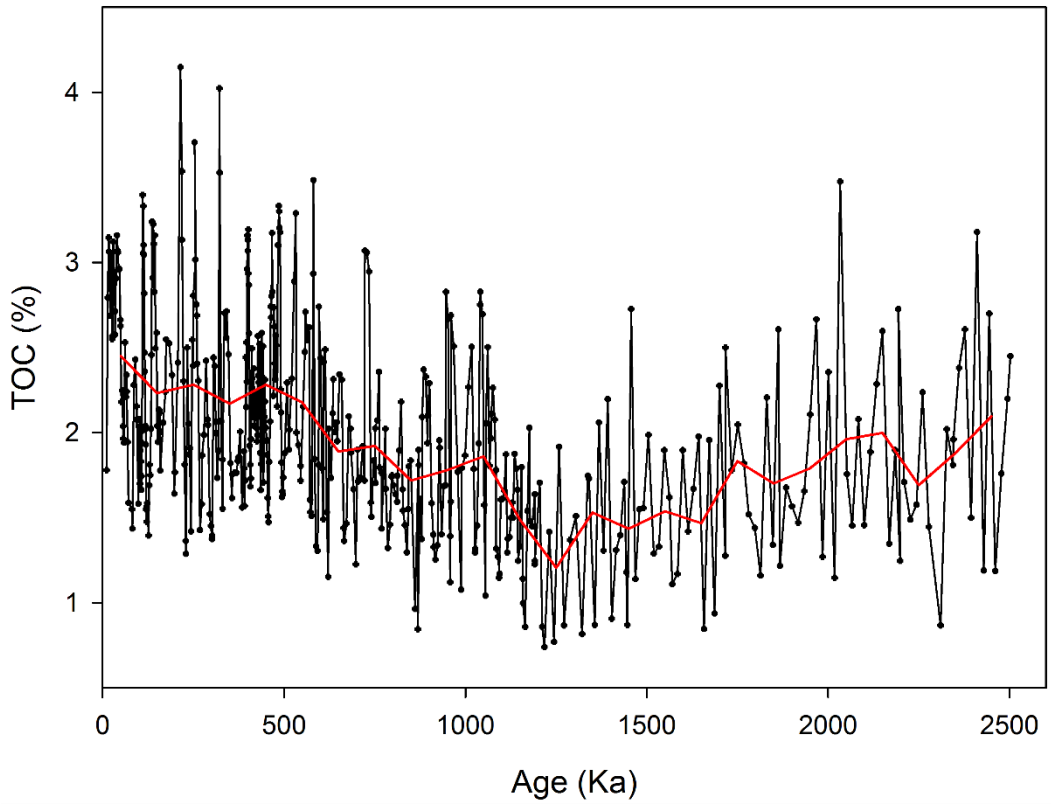

Figure 4.1. TOC (%) record for ODP 1075, including Holtvoeth et al. (2001) record (10 Ka to 1.2 Ma) and new data from 1.2 Ma to 2.5 Ma (black circles). Red line indicates mean TOC (%) for 100 Ka intervals.

Adenosylhopane (**1a**) was the only soil marker BHP identified in ODP 1075 with adenosylhopane type 2 (**1e**), type 3 (**1f**) or methylated adenosylhopane (**2a**, **2e** and **2f**; e.g. Cooke et al., 2008a; Rethemeyer et al., 2010) absent. Adenosylhopane (**1a**) concentrations range from 0 µg/g TOC to 120 µg/g TOC (Figure 4.2), and was found to be absent below 900 Ka. Adenosylhopane (µg/g dry sediment) was not found to clearly correlate with TOC (Figure 4.3). High concentrations of anhydro BHT (**1o**) were observed in ODP 1075 ranging between 5 and 240 µg/g TOC. No clear correlation between anhydro BHT and adenosylhopane are observed down core within ODP 1075 (Figure 4.3b).

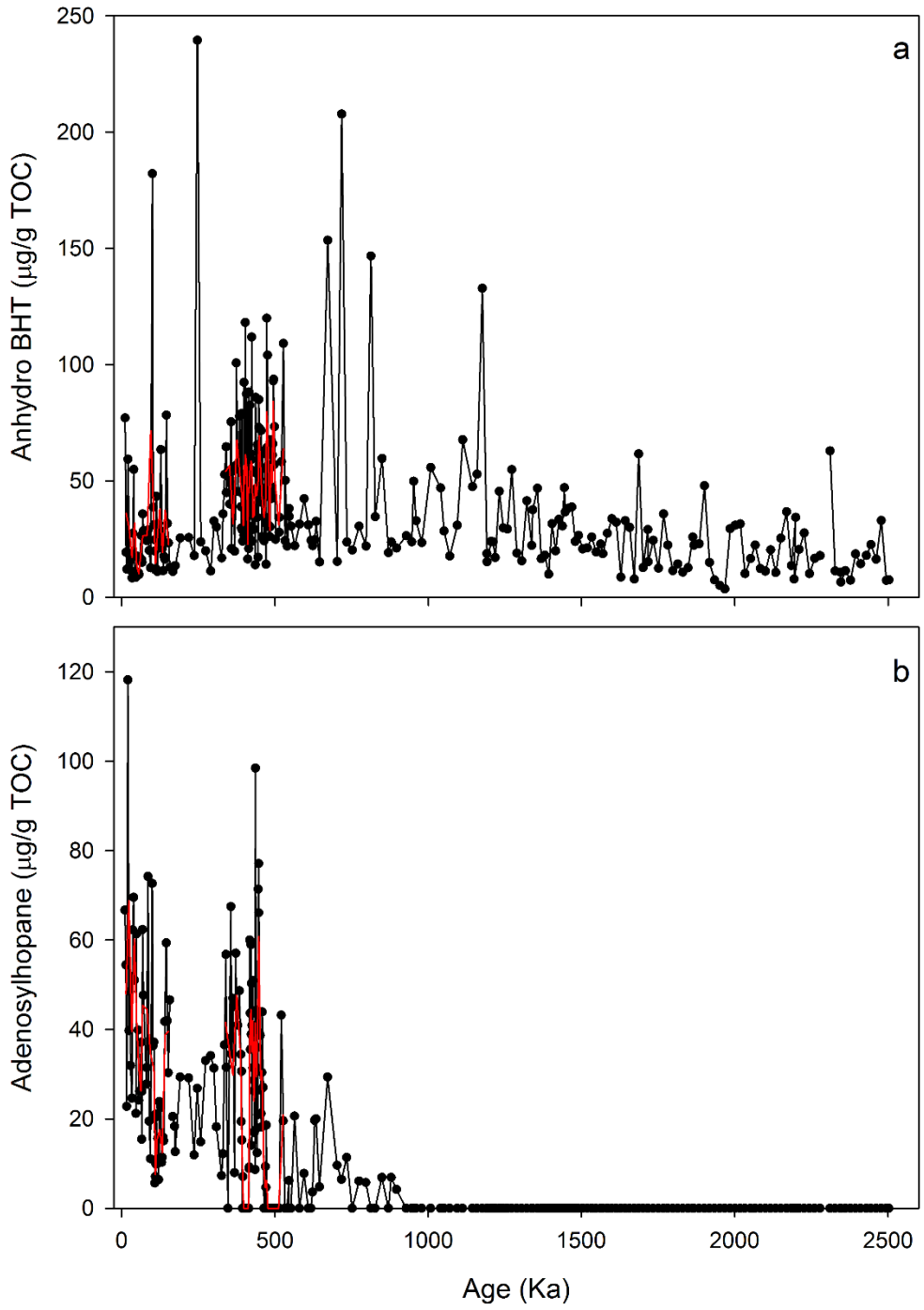

Figure 4.2. Concentration of anhydro BHT and adenosylhopane (µg/g TOC) in ODP 1075.

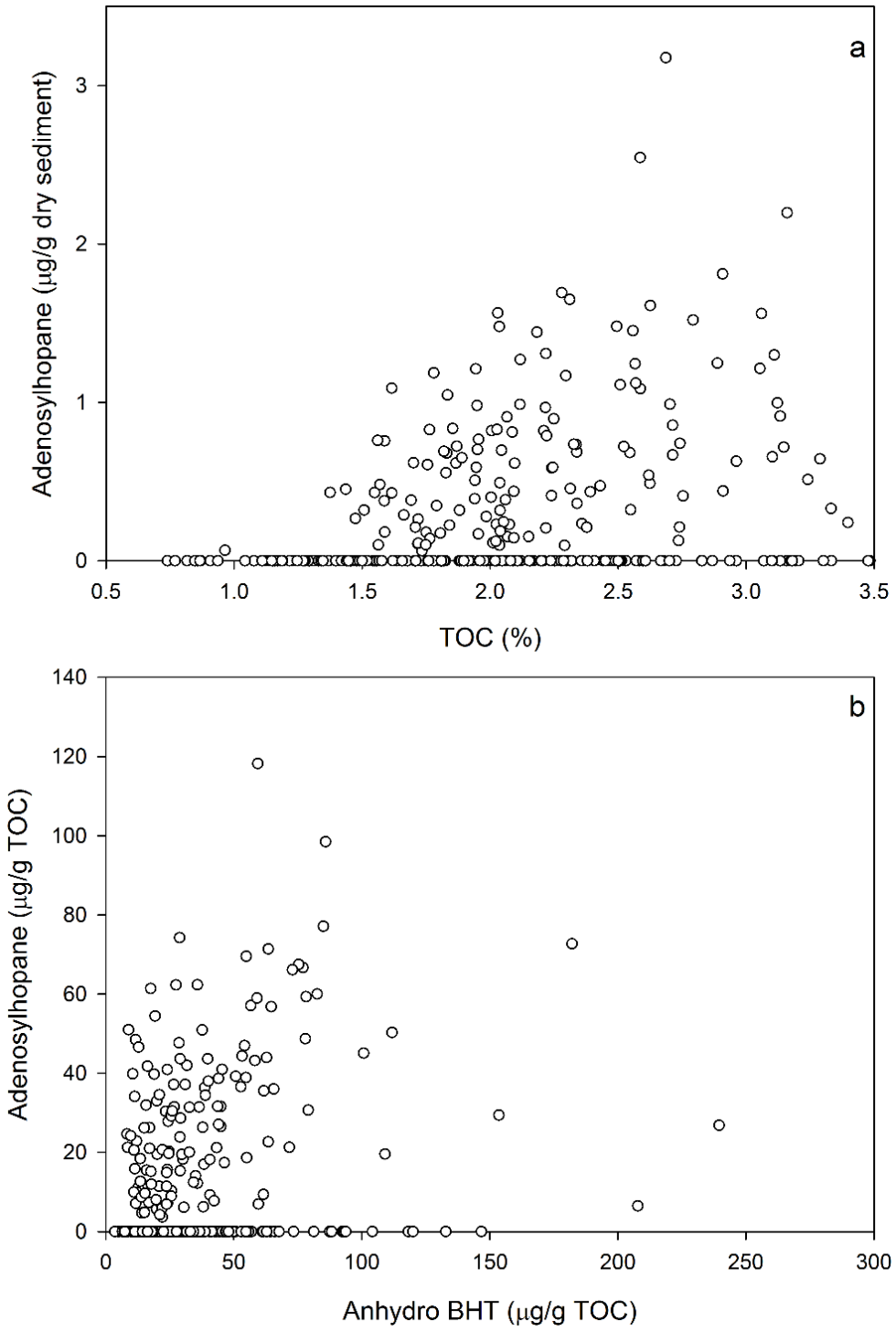

Figure 4.3. a; TOC (%) correlated with adenosylhopane (µg/g dry sediment). b; Anhydro BHT (µg/g TOC) correlated with adenosylhopane (µg/gTOC) in ODP 1075 from 10 Ka to 2.5 Ma.

4.3.2. R_{soil} *and BIT in Complete ODP 1075 Record*

R_{soil} and BIT indices were determined for the ODP 1075 record from 10 Ka to 2.5 Ma (Figure 4.4). R_{soil} index ranges from 0 to 0.7 with the highest R_{soil} value observed at 219 Ka. R_{soil} index decreases over time with R_{soil} = 0 from 900 Ka. The BIT index is highly variable down core ranging from 0.16 (402 Ka) to 0.61 (105 Ka).

Mean BIT index values vary significantly down core (ANOVA F 12.77, P <0.05, df 3; Figure 4.5). Higher mean BIT index values are observed during the deeper/older intervals compared with the shallower/younger intervals (Table 4.1; Figure 4.5; Appendix IV).

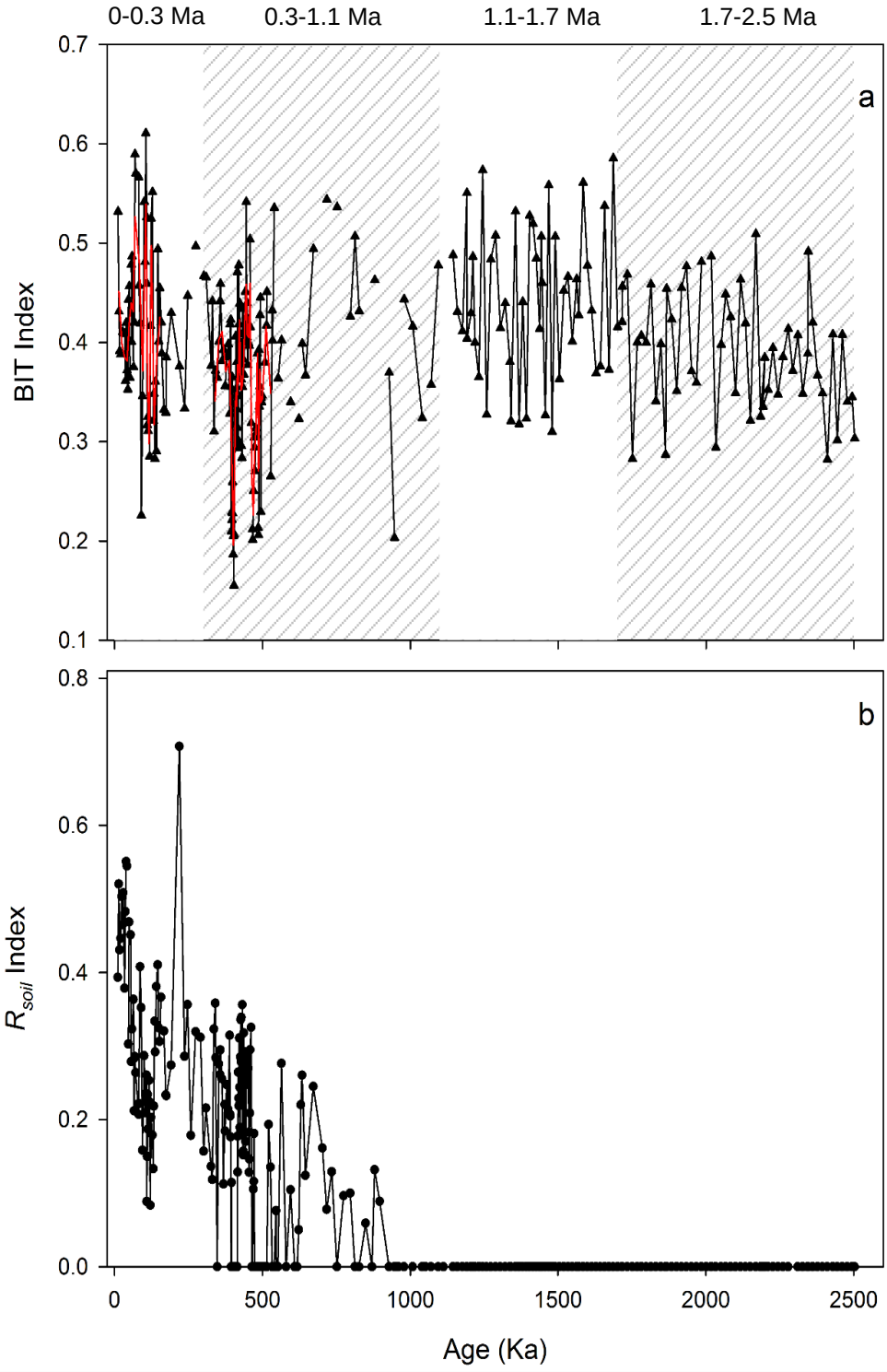

Figure 4.4. a; BIT indices (open triangles) and three point rolling average during high resolution sections (red line). b; R_{soil} (open circles) in ODP 1075 over the past 2.5 Ma. Hatched panels on BIT index graph indicate intervals described in section 4.3.2 and 4.4.5.2.

Table 4.1. Mean BIT index of four ODP 1075 intervals (Ma), including standard deviation (SD) and number of samples in each interval (N).

Interval (Ma)	Mean BIT	SD	N
2.5 to 1.7	0.39	0.06	53
1.7 to 1.1	0.44	0.076	50
1.1 to 0.3	0.36	0.084	146
0 to 0.3	0.42	0.086	62

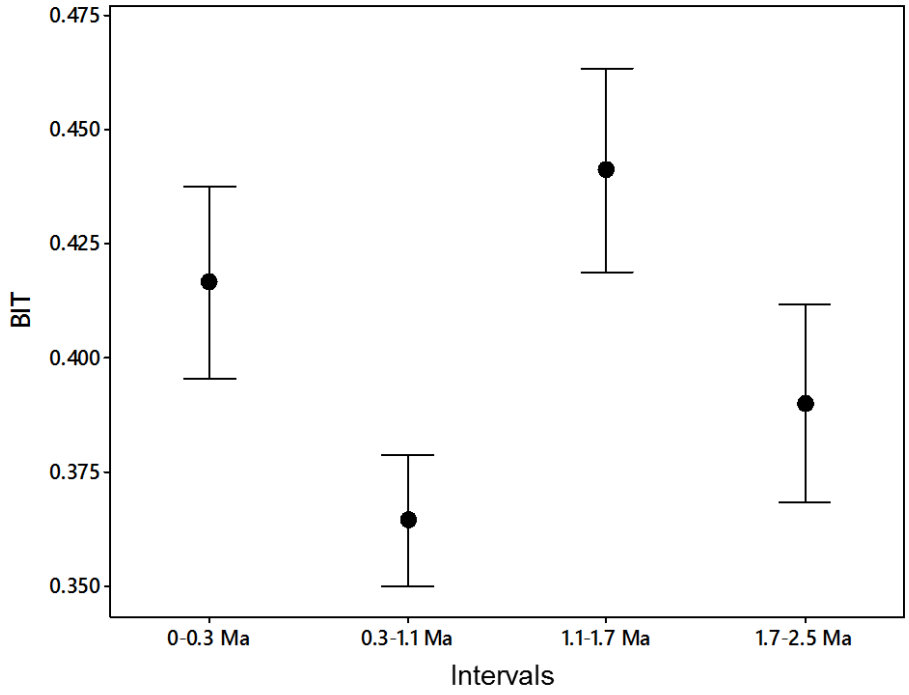

Figure 4.5. Interval plot of mean BIT index and 95% confidence interval of 4 BIT intervals (0 – 0.3 Ma, n = 62; 3.1 – 1.1 Ma, n = 146; 1.1 – 1.7 Ma, n = 50; 1.7 – 2.5 Ma, n = 53).

4.3.2.1. R_{soil} and BIT in High Resolution Sections of ODP 1075 Record

Two intervals, 10 Ka – 200 Ka (MIS 3 – 6) and 350 – 540 Ka (MIS 10 – 13) were analysed in high resolution. Within the high resolution section ranging from MIS 3 to MIS 6 the R_{soil} index ranges from 0 to 0. 54 (Figure 4.6a) and the BIT index ranges from 0.23 to 0.61 (Figure 4.6b). Within the high resolution section ranging from MIS 10 to MIS 13 the R_{soil} index ranges from 0 to 0.34 (Figure 4.7a) and the BIT index ranges from 0.16 to 0.54 (Figure 4.7b).

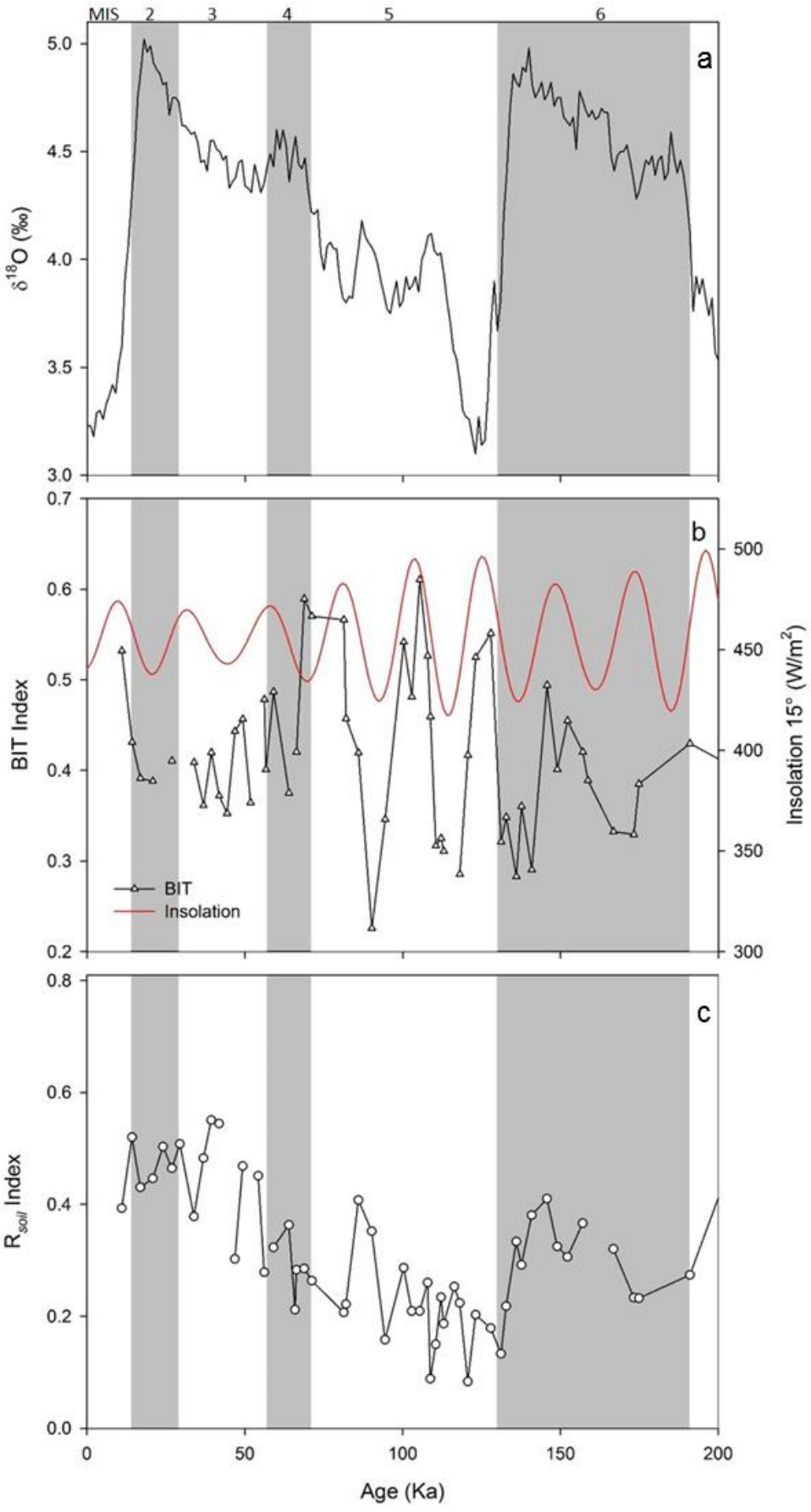

Figure 4.6. Benthic $\delta^{18}O$ stack (Lisiecki and Raymo, 2005; black; a), insolation (15° N, W/m^2; red; b), BIT indices (open triangles; b) and R_{soil} (open circles; c) in a high resolution section of OPD 1075 during 10 Ka to 300 Ka (MIS 2 to 6). Grey bars indicate glacial stages.

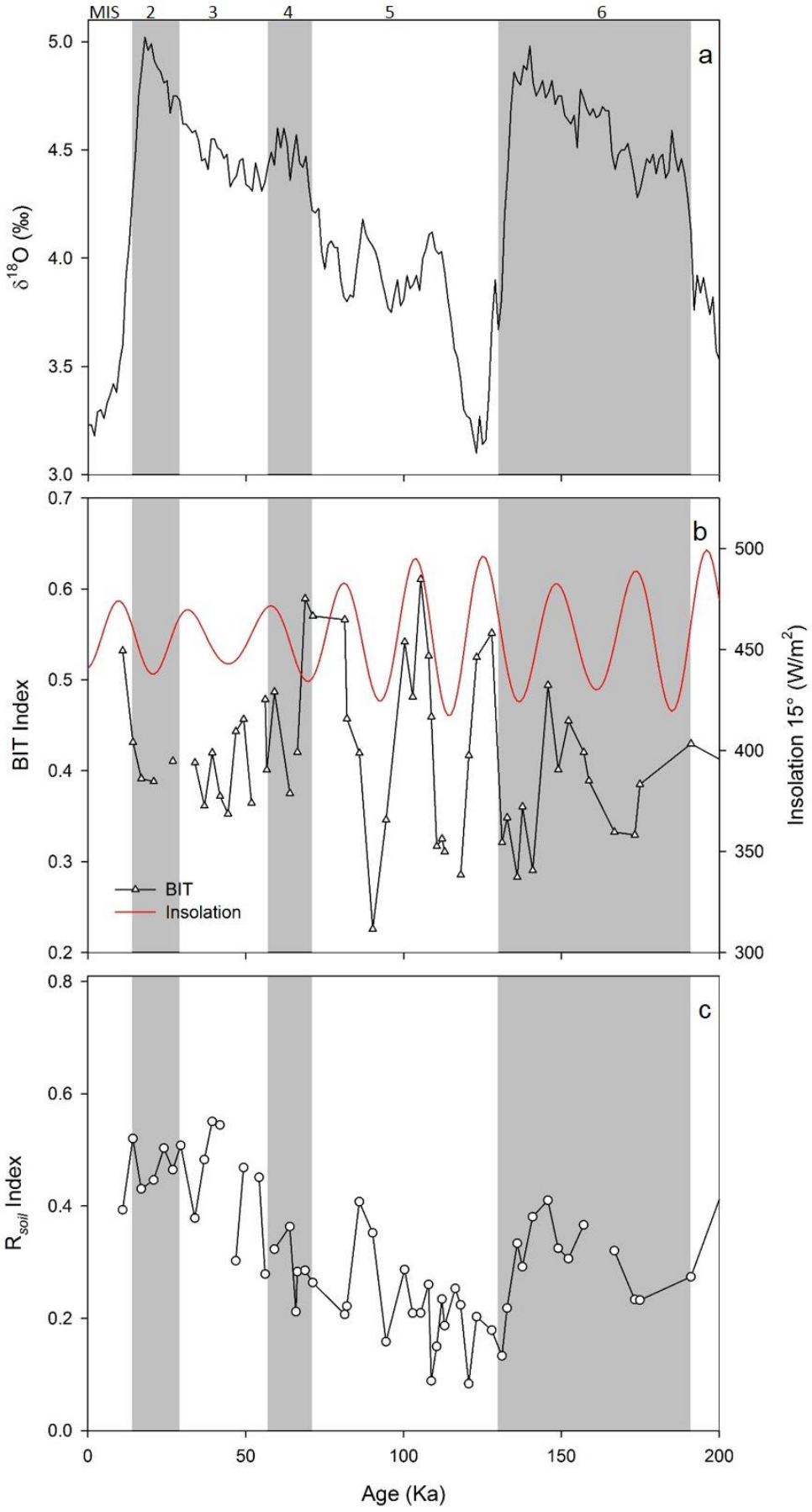

Figure 4.7. Benthic $\delta^{18}O$ stack (Lisiecki and Raymo, 2005; black; a), insolation (15° N, W/m^2; red; b), BIT indices (open triangles; b), R_{soil} (open circles; a) in a high resolution section of ODP 1075 during 350 Ka to 540 Ka (MIS 10 to 13).). Grey bars indicate glacial periods.

4.4. Discussion

4.4.1. Total Organic Carbon

To assess general trends in TOC over the 2.5 Ma study interval, the TOC data was divided into 100 Ka intervals with the mean and standard deviation for each interval presented in Figure 4.1 (red line). The TOC shows a general decreasing trend with higher TOC present in the top 10 Ka to 600 Ka interval compared to the lower 1700 to 2500 Ka interval (Figure 4.1). However, the lowest average TOC (%) of the profile is observed for the middle interval between 1100 to 1500 Ka (ANOVA, $F = 7.2$, $P = <0.05$, df 24; Appendix IV-VI). This gradual reduction in the mean TOC (%) has previously been suggested to be due to progressive diagenesis of OC with burial depth (Holtvoeth et al., 2001; Jahn et al., 2005). This is the first report of TOC from 1.2 to 2.5 Ma within ODP 1075. The decrease in TOC in the middle of ODP 1075 suggests a change in TOC deposition during this time interval. However, further analysis would be required to fully elucidate the cause(s) of this feature.

4.4.2. Soil Marker BHPs Inventory

High concentrations of adenosylhopane persist until ~500 Ka after which a strong diagenetic signature is observed (Figure 4.2). This is in agreement with results from modern Congo samples where adenosylhopane was the only soil marker BHP to be identified in the one available estuarine sediment (see Chapter 3). In contrast, a full suite of soil marker BHPs, including methylated and group 2 and 3 adenosylhopanes, were observed in the Congo soil and wetland samples (see Chapter 3). Mechanisms responsible for the terrestrial transport of adenosylhopane are expected to similarly influence the transport of other) soil marker BHPs (e.g. methylated and group 2/3 adenosylhopanes. Therefore, the absence of methylated adenosylhopane, group 2 and group 3 soil marker compounds could be due to enhanced riverine degradation (Zhu et al., 2013) and/or degradation of these compounds following deposition (Handley et al., 2010). In addition, no clear correlation between TOC and adenosylhopane (µg/g dry sediment; Figure 4.3) is observed. This suggests that adenosylhopane degradation specifically affects this BHP and is not part of overall TOC diagenesis as no other BHPs were previously shown to follow the same trend (Handley et al., 2010). It remains unclear, why adenosylhopane is specifically

affected by post depositional diagenesis. One possible reason could be due to adenosylhopanes role as the first BHP intermediate during BHP synthesis (Bradley et al., 2010). Following synthesis of adenosylhopane, BHP producers can accumulate adenosylhopane and/or cleave the adenine head group and synthesise other BHPs. It is hypothesised that all BHP producing bacteria use this pathway for the synthesis of BHPs (Bradley et al., 2010), therefore, adenosylhopane may be a highly labile compound.

4.4.3. Diagenetic Controls on Soil Marker BHPs

Anhydro BHT (**1o**) was first observed in the sponge *Plakortis simplex* and was hypothesised to be a biogenic product (Costantino et al., 2001). However, *Zymomonas mobilis,* a bacterium that usually synthesises diploptene, diplopterol, BHT (**1g**), BHT cyclitol ether (**1i**) and BHT glucosamine (**1m**)*,* has also been shown to form anhydro BHT when subjected to acid treatment (Schaeffer et al., 2010). Adenosylhopane has also been hypothesised to degrade to anhydro BHT (Cooke et al., 2008b; Handley et al., 2010; Eickhoff et al., 2014) but has yet to be conclusively demonstrated. Therefore, sedimentary anhydro BHT is likely formed from the diagenetic transformation of BHPs from intramolecular acid catalysed cyclization of the hopanoid side chain, possibly aided in the presence of clay mineral (Schaeffer et al., 2008, 2010).

Sedimentary evidence for anhydro BHT was first reported in hypersaline sediments (Realmonte, Italy) by Schaeffer (1993), following which, this compound has been identified in a number of other environments including, sediments from South East Atlantic (Schefuß et al., 2001); Benguela current sediments (Watson, 2002); and the Congo fan (Handley et al., 2010). Watson (2002) found anhydro BHT (putatively assigned C_{32}ββ hopane-keto-diol) to increase in abundance relative to other hopanoids (based on peak areas) with depth in ODP 1084. Furthermore, Cooke et al. (2008b) and Handley et al. (2010) observe correlation between adenosylhopane and anhydro BHT concentrations in ODP 1075 suggesting that adenosylhopane also degrades to anhydro BHT. However, adenosylhopane and anhydro BHT concentrations are not observed to correlate within this study (Figure 4.3 b). These results suggest that within ODP 1075, anhydro BHT is not exclusively produced from the degradation of adenosylhopane but is likely also derived from (additional) BHPs with an oxygen functionality located at C-35. Concentrations of adenosylhopane and

BHT impact on the R_{soil} index. In ODP 1075, relative abundance of adenosylhopane primarily controls the R_{soil} index (R_s 0.912; $p < 0.05$; samples below 900 Ka excluded due to consistent absence of adenosylhopane, N = 195).

4.4.4. Suitability of R_{soil} and BIT indices for Paleoclimate Reconstructions.

Due to strong degradation signatures observed in adenosylhopane concentration, we suggest the application of the R_{soil} proxy within Congo fan sediments is limited to < 500 Ka with OC_{ter} interpretations based of R_{soil} to be treated with caution and always in combination with other, independent proxy evidence. Analysis of R_{soil} index in sediments <500 Ka will ensure the data shows an environmental signature and is not over printed with a degradation trend.

Significant correlation between total br-GDGT and crenarchaeol peak areas (Pearson's correlation R 0.851, $P < 0.05$) is observed confirming a relationship between these groups of compounds (Figure 4.8 b). Significant correlation could suggest br-GDGTs and crenarchaeol to be affected by a common physical process (e.g. terrestrial organic transport of br-GDGTs coupled with increased flux of nutrients to the Congo fan resulting in site fertilization) or that these compounds have a mixed source (Feitz et al., 2012). Previous studies have found crenarchaeol to be produced in soils (Weijers et al., 2008) and for br-GDGTs to be produced within aquatic environments (Zell et al., 2013; Naeher et al., 2014). Therefore, correlation between br-GDGTs and crenarchaeol could suggest these GDGTs to be from mixed marine and terrestrial sources. The BIT index, which uses the relative abundance of Br-GDGT compounds (terrestrial end members; GDGT I, II and III; see Chapter 2, Equation 2.5) and crenarchaeol (the marine end member) is a proxy for OC_{ter} transport (Hopmans et al., 2004). Significant but weak correlation is observed between total br-GDGT (GDGT I, II, and III) and BIT index (Pearson's correlation R 0.426, $P < 0.05$; Figure 4.8 c). This suggests that fluctuations in the BIT index may be controlled by flux of terrestrially derived br-GDGT compounds, however, lack of strong correlation between br-GDGTs and BIT, and crenarchaeol and BIT (Pearson's correlation R -0.047, P 0.494; Figure 4.8 d) suggest that br-GDGTs and crenarchaeol probably have a mixed source within the Congo fan, with potentially significant contributions of these compounds from terrestrial aquatic environments, e.g. flood plain lakes. Therefore, a high BIT index primarily results from increased supply of br-

GDGT compounds from the Congo hinterland, rather than fluctuations in marine primary production.

GDGTs are highly recalcitrant compounds with no clear diagenetic trends observed in the BIT profile of ODP 1075 (Figure 4.4). To date, their oldest reported geological occurrence as core lipids is in Late Jurassic marine sediment of the Kashpir oil shale (Carrillo-Hernandez et al., 2003) and in ODP core 511 (Jenkyns et al., 2012). We therefore suggest that while the BIT index is a robust proxy for OC_{ter}, this proxy should be interpreted with care within Congo fan sediments.

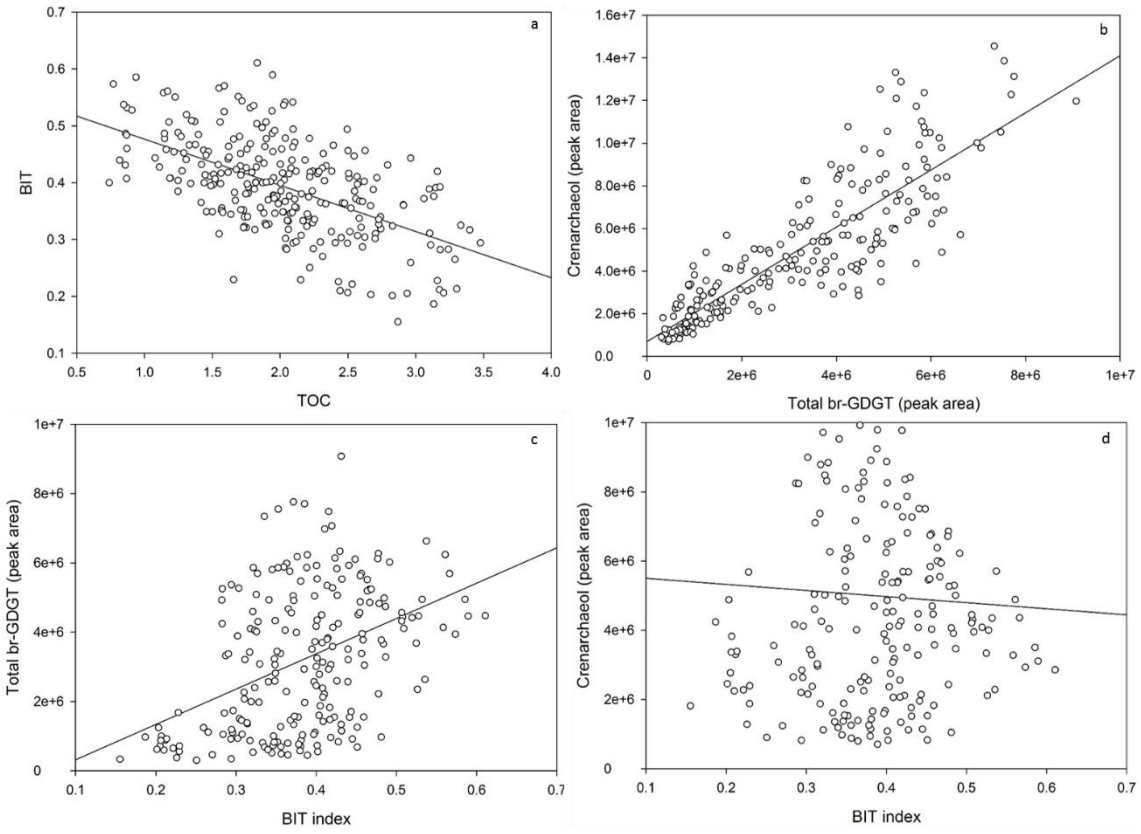

Figure 4.8.Correlation between; TOC (%) and BIT index (a), total br-GDGT (peak area) and crenarchaeol (peak area; b), BIT index and total br-GDGT (peak area; c), BIT index and crenarchaeol (peak area; d).

4.4.5. Climatic Controls on BIT and R_{soil} Indices

4.4.5.1. Marine Isotope Stage 11 and 5

A high R_{soil} index is observed during MIS 12 and 10 while during MIS 13 and 11, due to the absence of adenosylhopane, an R_{soil} index of 0 is observed (Figure 4.7). This unusual pattern in R_{soil} could be due the preferential degradation of adenosylhopane during warm climate conditions. Similarly, a decrease in BIT values are also

observed during MIS 11 and 13. A decrease in both R_{soil} and BIT may, therefore, suggest a decrease in the proportion of terrestrial soil OC export to the fan. Possible reasons for this could be due to either displacement of OC deposition areas (Holtvoeth et al., 2001; Dupont, 2009) and/or changes in the type of OC_{ter} deposited on the Congo Fan. A low BIT index during the high resolution interglacial-warm intervals (Figure 4.6 and Figure 4.7) suggests a reduction in soil OC transport and deposition on the Congo fan. However, Jahn et al. (2005) observes generally high terrestrial OC transport (as indicated by low $\delta^{13}C_{org}$) during interglacial – warm periods within samples from the Congo fan. This disparity is clearly due to a difference in source material deposited on the Congo fan and could indicate a large scale shift in vegetation zones (Holtvoeth et al., 2001, 2003; Schefuß et al., 2005). The $\delta^{13}C_{org}$ is a general biomarker for terrestrial OC transport and includes inputs from vegetation, soil and aeolian OC (Hedges et al., 1997), whereas the BIT index may be specific for soil OC transport (Schouten et al., 2013b and references therein). Within the Congo system, orbital-forced fluctuations in atmospheric circulation primarily control upwelling and productivity along equatorial Africa (Holtvoeth et al., 2001). Additionally, these fluctuations also impacted on aridity/humidity cycles in central Africa, which ultimately caused displacement of vegetation zones and influenced the export of terrigenous material through the Congo River (Holtvoeth et al., 2001; Jahn et al., 2005). The occurrence of humid intervals, promotes the development of tropical rainforests within the Congo fan (Dupont et al., 2000; Versteegh et al., 2004; Miller and Gosling, 2014), which, further stabilises soil structures. The overall increase in depleted $\delta^{13}C_{org}$ and the relative decrease in BIT index during interglacial – warm periods within the Congo fan could suggest an increase in OC derived from vegetation (Holtvoeth et al., 2001) and a reduction in soil derived OC due to the expansion of tropical forests and the subsequent stabilisation of soil matrices.

During MIS 10 – 13 fluctuations in BIT and R_{soil} indices correspond with benthic $\delta^{18}O$ stack (LR04; Lisiecki and Raymo, 2005; Figure 4.7). A correlation between BIT and R_{soil} indices and the LR04 stack is clearly observed during MIS 2 - 6 (Figure 4.6) suggesting that fluctuations in Congo OC_{ter} are controlled by similar mechanisms that modulate global ice volume. In addition, the BIT record shows strong correlation with insolation changes during MIS 5 (70 Ka to 130 Ka); i.e. three high OC_{ter} events are observed in the BIT record, occurring during MIS 5.5 (123 Ka), MIS 5.4 (103 Ka) and

MIS 5.1 (71 Ka; Figure 4.6). These three periods of enhanced OC_{ter} supply/burial coincide with peak insolation (15°N July) arguing for a direct precessional climate control on GDGT production and supply to the Congo fan, in agreement with Holtvoeth et al. (2001) and Jahn et al. (2005). However, similar strong correlation with insolation is not observed during MIS 11, despite this interval also being a high resolution section in this study. Disparity between MIS 5 and 11 could be due to a threshold behaviour in BIT index or related to insolation amplitude, which is higher during MIS 5 than during MIS 11 and should translate into stronger seasonal contrasts during MIS 5. However, disparity between BIT and insolation variations between MIS 5 and 11 could be due to variations in terrestrial BIT source areas with a change in GDGT contributions from soil and aquatic environments. We consequently propose that high amplitude contrasts in insolation are required to translate into BIT biomarker records. These conclusions are in agreement with other studies which find fluctuations in OC_{ter} corresponding to precessional forcing (Holtvoeth et al., 2001; Jahn et al., 2005).

4.4.5.2. Record of Pleistocene Organic Carbon Transport

In section 4.4.5.1 analysis of high resolution records of ODP 1075 suggests that OC_{ter} is may be controlled by variations in precession and obliquity. Large fluctuations in OC_{ter}, as observed via the BIT index, are identified during the entire Pleistocene (see Figure 4.4), which is in agreement with other studies (Sparkes et al., 2015). Holtvoeth et al. (2001, 2003) identifies strong fluctuations in OC_{ter} supply during the late Pleistocene (past 1.2 Ma). Similarly, Jahn et al. (2005) analysed TOC mass accumulation rates (TOC MAR) and $\delta^{13}C_{org}$ over the past 0 to 1.7 Ma and found OC_{ter} signatures to be highly dynamic. Jahn et al. (2005) identifies three intervals within Congo fan deposits that show a trend towards higher contributions of marine OM to Congo fan sediments during the Pleistocene. The first interval from 1.7 to 1.1 Ma is characterised by lower $\delta^{13}C_{org}$ values (-23 ‰ to -21.5 ‰), suggesting high contributions from terrestrial OM sources. The second interval from 1.1 to 0.3 Ma is characterised by $\delta^{13}C_{org}$ values of between -22.5 ‰ to -20 ‰, indicative of both terrestrial and marine contributions. The youngest interval between 0.3 and 0 Ma with $\delta^{13}C_{org}$ ranges from -22 to -19 ‰ suggests increased contributions of OM from marine sources (Jahn et al., 2005). Within this study, mean BIT index during the Jahn et al. (2005) intervals do not show clear correlation with $\delta^{13}C_{org}$ (Figure 4.5) suggesting that these two proxies track different OC reservoirs. Previous studies have reported no

clear correlation between $\delta^{13}C_{org}$ and the BIT index (Huguet et al., 2007; Walsh et al., 2008), largely due to $\delta^{13}C_{org}$ being a bulk OC proxy and BIT index being a specific proxy for soil OC transport.

4.5. Conclusions

The overall aim of this chapter was to test the hypothesis; "*Temporal changes in R_{soil} and BIT indices within ODP 1075 occur due to variations in orbital cycling*".

Adenosylhopane was the only soil marker BHP to be identified in ODP 1075. The presence of other soil marker BHPs were notably absent from ODP 1075 sediments despite high concentrations in the modern soil samples (see Chapter 3). As previously reported in Handley et al. (2010), adenosylhopane shows a strong diagenetic signature in ODP 1075 from ~500 Ka (55 metres below sea floor; msbf), with this compound being completely absent beyond 900 Ka (89 mbsf). Additionally, group 2 and 3 adenosylhopanes (and methylated homologues) may also have been subject to enhanced degradation, although the mechanism for this remains to be elucidated. We anticipate that the strong diagenetic trends of soil marker BHPs in the Congo fan sediments may also be evident in other sedimentary systems. We therefore suggest caution when interpreting adenosylhopane signatures in sediments deeper than 55 msbf. The BIT index does not show a clear diagenetic trend, arguing that GDGTs are more recalcitrant than soil marker BHPs, at least in the Congo fan system.

We propose that the suitability of adenosylhopane, and therefore the R_{soil} index, is limited to sediments down to a depth of 55 mbsf (aged < 500 Ka in case for the Congo fan). However, as no diagenetic trends were evident within the BIT index signatures, we propose this proxy to be more suitable for reconstructing paleoenvironmental conditions. The depth boundary below which the R_{soil} index can no longer be used for pelaoenvironmental reconstructions may shift from location to location, but this study provides first solid evidence to constrain the depth range to look at.

As anticipated variations in BIT and R_{soil} indices correspond with orbital cycling, as a result of large scale changes in Congo hydrology and vegetation zones, which in combination, subsequently impact on the type and abundance of OC_{ter} exported to the Congo fan.

Chapter 5:

Are All Bacteriohopanepolyols in ODP 1075 of Terrestrial Origin?

Chapter 5. Are all Bacteriohopanepolyols in ODP 1075 of Terrestrial Origin?

5.1. Introduction

Hopanes are one of the most abundant natural products on earth (Ourisson and Albrecht, 1992; Brocks et al., 2005). Bacteriohopanepolyols, the intact precursor compounds of hopanes, have been found in many environments including soils, permafrost, river and estuarine sediments and suspended particulate matter from water columns (see Table 2.1 for full details).

Despite their ubiquitous occurrence in modern environments, molecular ecology studies of *sqhC*, the gene encoding for hopanoid biosynthesis, suggests that less than 10% of bacteria have the potential to produce these compounds (Pearson et al., 2007). Environmental *sqhC* sequences reveal only 60% translated amino acids identity to their closest relatives in public databases, suggesting, that the sources of these important biomarkers are largely unknown (Pearson et al., 2007). Culture dependent screening studies have found hopanoids to be synthesised by a variety of bacteria (e.g. Rohmer et al., 1984; Farrimond et al., 2004; Talbot et al., 2008b). Generally, BHPs that are widespread in environmental samples are found to be widespread in hopanoid producing bacteria. For example, BHT (**1g**) has been identified in almost all environmental samples studied (for examples see Table 2.1), and is biosynthesised by a wide variety of marine and terrestrial bacteria including; cyanobacteria, methylotrophic bacteria, thermoacidophilic bacteria, purple non-sulfur bacteria and nitrogen fixing bacteria (e.g. Knani et al., 1994; Vilcheze et al., 1994; Talbot and Farrimond, 2007). Conversely, the occurrence of some BHPs have been found to be limited to specific groups of bacteria or organisms involved in certain biogeochemical processes and, therefore, can be used to indicate these sources or processes when identified in environmental samples. For example, the biosynthesis of aminopentol (**1d**) is limited to aerobic methanotrophic bacteria (see review in Talbot et al., 2014). Therefore, identification of aminopentol is commonly used as an indication of AMO activity (e.g. Talbot and Farrimond, 2007; van Winden et al., 2012a; Berndmeyer et al., 2013; Talbot et al., 2014; Wagner et al., 2014).

Generally, greater BHP diversity has been reported in soils and wetland sediments over marine sediments (e.g. Pearson et al., 2009; Zhu et al., 2011). However, coastal and deep-sea fan samples (Handley et al., 2010; Wagner et al., 2014) have higher BHP diversity than entirely marine samples (e.g. Blumenberg et al., 2010; Sáenz et

al., 2011b; Zhu et al., 2011). High BHP diversity within coastal and fan sediments could be due to terrestrial export of BHPs to these sediments (e.g. Sáenz et al., 2011a; Zhu et al., 2011; Doğrul Selver et al., 2012, 2015). To date, the influence of OC_{ter} on BHP transport remains unclear. BHP archives within coastal and marine sediments could represent an integrated signature between terrestrial and marine BHP realms. Previous work has shown that two of the most commonly occurring groups of BHPs found in Congo fan sediments, soil marker - (**1a**, **2a**, **1e**, **2e**, **1f**, **2f**) and C-35 amine BHPs (**4/5h**, **1h**, **2h**, **3h**, **4/5c**, **1c**, **4/5d**, **1d**, **1d'**) largely have terrestrial origins (Chapter 3 and 4).

In this Chapter, the origins of the remaining major BHP group (BH cyclitol ethers; **1i**, **1j**, **1k**) and a minor unsaturated BHP (BHT; **4/5g**) identified in ODP 1075 will be discussed, testing the hypothesis; "*All BHPs found in ODP 1075 are of terrestrial origin*". The aim of this chapter is to understand the origins of BHPs deposited within tropical fan sites during the Pleistocene. The specific objectives are to determine the full BHP inventory within sediments from the Congo fan and to compare these results with existing modern terrestrial, culture, coastal and marine sediment data. The scope of this chapter is to:

- Analyse the full BHP inventory in ODP 1075, with a specific focus on the distribution of BH cyclitol ethers.
- Determine similarities between BH cyclitol ether distributions within the soils/sediments from the Congo hinterland soils and ODP 1075 sediments.
- Compare the distribution of BH cyclitol ethers with other published BHP data including, culture, soil, and sediments data.
- Determine the influence of fluvial inputs by correlation of BH cyclitol ethers with OC_{ter} proxies (R_{soil} and BIT indices). In order to eliminate the effect of diagenesis (Chapter 4), comparisons with adenosylhopane will be limited to the initial 500 Ka ODP 1075 record.

5.2. Overview of Methodology and Study Site

Bulk and geochemical analysis has previously been described in Chapter 2. Briefly, TOC (%) of ODP 1075 sediments was measured as detailed in Holtvoeth et al. (2001) and chapter 2. Total lipids were extracted from approximately 3 g of freeze-dried sediment using a modified Bligh and Dyer extraction method as described by Talbot et al. (2007a) and further modified by Osborne, (PhD thesis, Submitted). An

aliquot (one third) of the TLE was used for BHP analysis (Chapter 2, section 2.5) and one third was used for GDGT analysis (Chapter 2, section 2.5).

5.2.1. Compound Classification and Statistics

The abbreviated names of the compounds identified, characteristic base peak ions (*m/z*) and structure numbers are given in Chapter 2 (Table 2.7, Table 2.8, Table 2.9, and Table 2.10). Statistical analysis was performed using Minitab 17.1.0. Spearmans Rho (R_S) correlation index was performed on BHP abundances. The 'cyclitol ether index' refers to the ratio of BHpentol cyclitol ether and BHhexol cyclitol ether to the sum of all 3 saturated BH Cyclitol ethers (Equation 5.1) and is applied here to visualise the relative differences between BHT cyclitol ether and BHpentol cyclitol ether, and BHhexol cyclitol ether.

Equation 5.1. Cyclitol ether index.

$$Cyclitol\ ether\ index = \frac{BHpentol\ cyclitol\ ether\ + BHhexol\ cyclitol\ ether}{BHpentol\ cyclitol\ ether\ + BHhexol\ cyclitol\ ether + BHT\ cyclitol\ ether}$$

5.3. Results

BHT (**1g;** Figure 5.1), BHT cyclitol ether (**1i**), BHpentol cyclitol ether (**1j**) and BHhexol cyclitol ethers (**1k**) are present throughout ODP 1075 (Figure 5.2). Additionally, unsaturated BHT (**4/5g**), unsaturated BHT cyclitol ether (**4/5i**), and guanidine substituted BHT cyclitol ether (**1p**) are intermittently present throughout ODP 1075 (Figure 5.3).

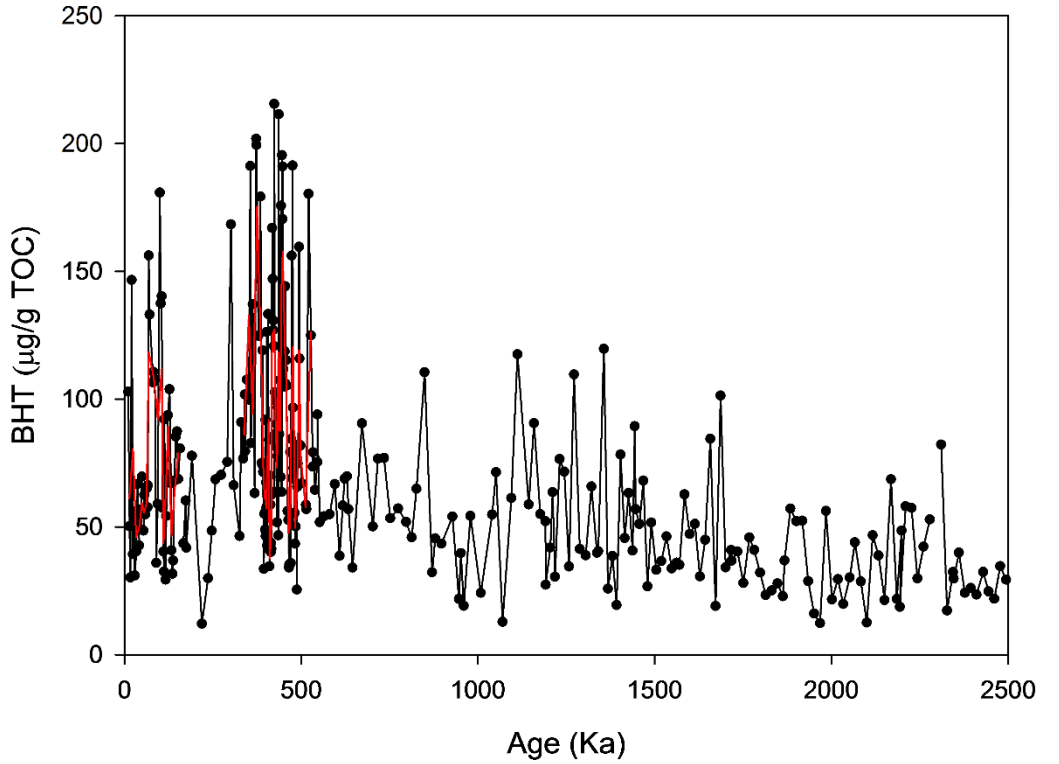

Figure 5.1. Concentration (µg/g TOC) of BHT within ODP 1075, red line indicates three-point rolling average within high resolution sections (error is ±20%).

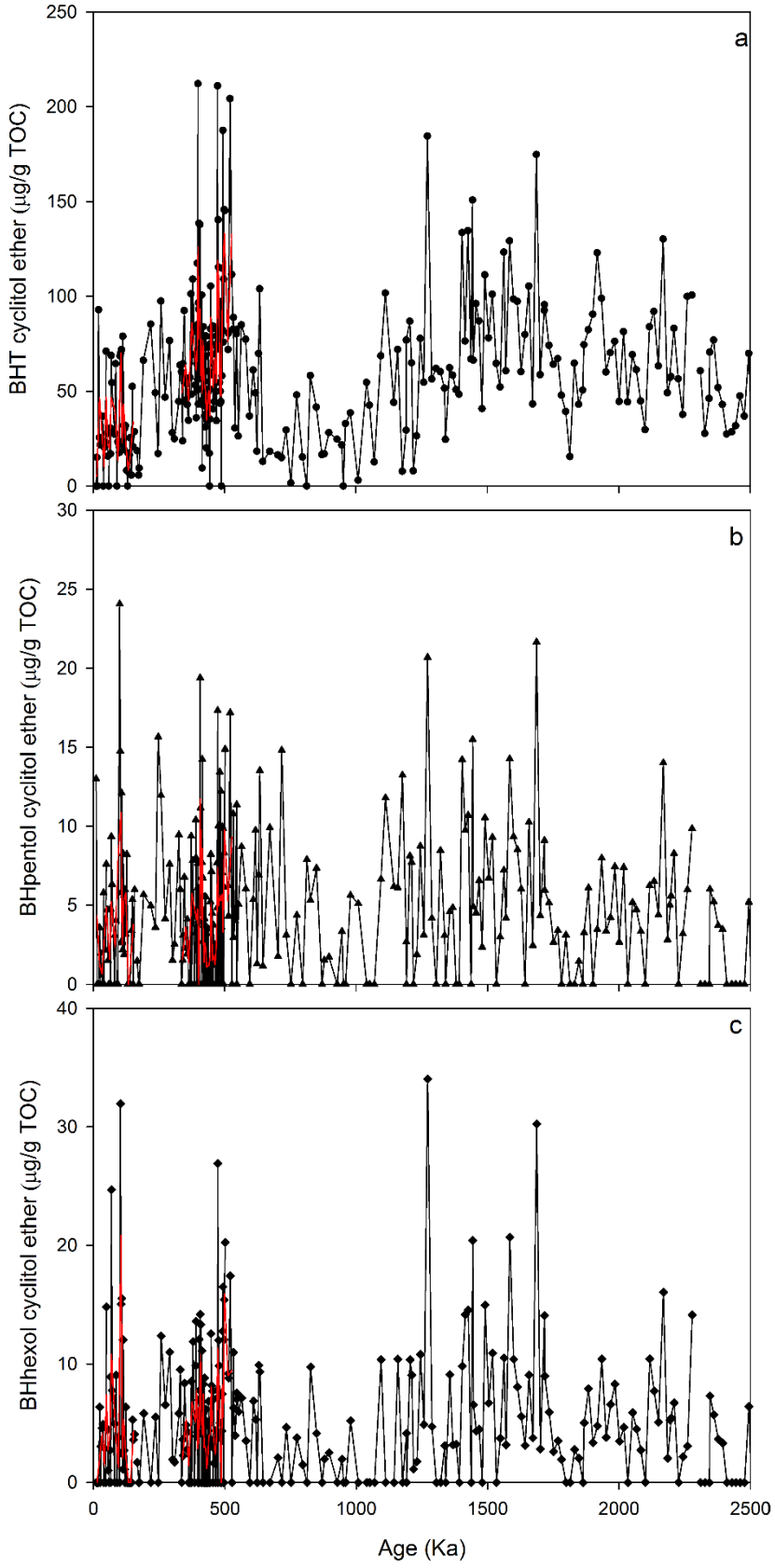

Figure 5.2. Concentration (µg/g TOC) of BHT cyclitol ether (a), BHpentol cyclitol ether (b), and BHhexol cyclitol ether (c) during past 2.5 Ma in ODP 1075, red line indicated three-point rolling average within high resolution sections (error is ±20%).

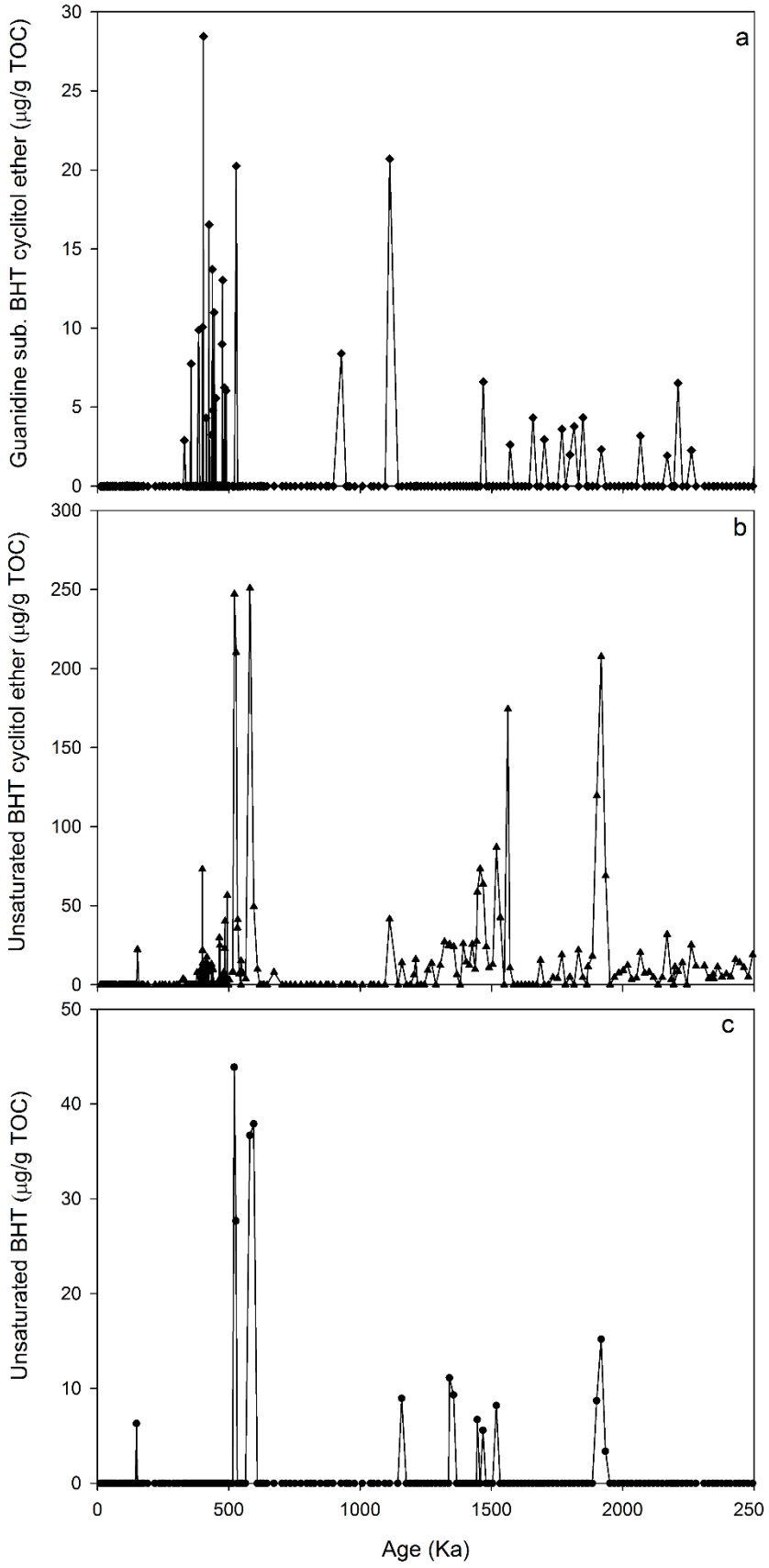

Figure 5.3. Concentration (µg/g TOC) of Guanidine substituted cyclitol ether (a), unsaturated BHT cyclitol ether (b), and unsaturated BHT (c), during past 2.5 Ma in ODP 1075.

BHT cyclitol ether (**1i**) is the most abundant of the cyclitol ethers within the ODP 1075 (0 to 100% of total saturated cyclitol ethers). In addition, this BHP is one of the dominant BHPs within the Congo Fan with concentrations ranging between 0 and 212 µg/g TOC (0-30%). Lower concentrations of BHpentol cyclitol ether (range 0 to 24 µg/g TOC) and BHhexol cyclitol ether (range 0-34 µg/g TOC) are observed throughout ODP 1075.

Unsaturated BHT (**4/5g**), unsaturated BHT cyclitol ether (**4/5i**) and guanidine substituted cyclitol ether (**1p**) are intermittently present within ODP 1075. Peak concentrations of both unsaturated BHT and unsaturated BHT cyclitol occur at 521, 580, 1562 and 1917 Ka. Peak concentrations of guanidine substituted BHT cyclitol ether occur at 402 Ka, 527 Ka and 1111 Ka.

Methylated BHT cyclitol ether (**2i**) is present at low concentrations in 2 samples (3.7 and 6.9 µg/g TOC at 564 and 501 Ka respectively). Due to the absence of this compound throughout much of ODP 1075, methylated BHT cyclitol ether distribution will not be discussed further.

5.4. Discussion

5.4.1. Microbial Sources of BHPs

5.4.1.1. BHT and Unsaturated BHT

High concentrations of BHT are found throughout ODP 1075. BHT and has been identified in many bacteria including N fixing bacteria (Berry et al., 1991; Bravo et al., 2001; Rosa-Putra et al., 2001), cyanobacteria (Bisseret et al., 1985), methylobacteria (Renoux and Rohmer, 1985; Flesch and Rohmer, 1988; Knani et al., 1994), acetobacter (Peiseler and Rohmer, 1992), an oxygenic phototroph (Simonin et al., 1996), planctomycetes (Sinninghe Damsté et al., 2004), and ammonia oxidising bacteria (Talbot et al., 2007).

Unsaturated BHT was identified in 14 samples within ODP 1075. This compound has only previously been reported in the acetic acid bacterium *Gluconacetobacter xylinus* (Peiseler and Rohmer, 1992; Talbot et al., 2007b).

5.4.1.2. BH Cyclitol Ether

High concentrations of BHT cyclitol ether are observed in ODP 1075. BHT cyclitol ether is a widespread BHP that has been identified in plant/soil bacteria, including *Burkholderia* spp. (Cvejic et al., 2000a; Joyeux et al., 2004; Talbot et al., 2007a), *Methylobacterium* spp. (Renoux and Rohmer, 1985; Knani et al., 1994; Talbot et al., 2007b) and *Acetobacter* spp. (Herrmann et al., 1996), within marine N fixing bacteria (*Trichodesmium* sp. and *Prochlorococcus* sp.; Talbot et al., 2008b), and within *Geobacter* spp. (Eickhoff et al., 2013a; *G. metallireducen* isolated from freshwater river sediments, *G. sulfurreducens* isolated from surface sediment of a ditch). Due to BHT cyclitol ether's multiple bacterial sources, this BHP is often found in many different environments and has been reported in soils (Chapter 3; e.g. Cooke et al., 2008a; Xu et al., 2009; Kim et al., 2011; Wagner et al., 2014), marine sediments (e.g. Pearson et al., 2009; Blumenberg et al., 2010), coastal sediments (e.g. Wagner et al., 2014), permafrost and riverine sediment (e.g. Rethemeyer et al., 2010; Kim et al., 2011; Sáenz et al., 2011a; Zhu et al., 2011; Doğrul Selver et al., 2012; 2015). BHT cyclitol ether is often one of the three dominant compounds within environmental samples, along with aminotriol and adenosylhopane (in soils) or BHT (in marine samples).

BHpentol cyclitol ether is a widespread BHP within environmental samples and while this BHP has similar sources to BHT cyclitol ether, fewer bacteria have been reported to synthesise BHpentol cyclitol ether. BHpentol cyclitol ether has been identified in a cyanobacterium (*Chlorogloeopsis* sp. LA; Talbot et al., 2003c), and soil bacteria including *Azotobacter vinelandii* (Vilcheze et al., 1994), *Frauturia aurantia* (Joyeux et al., 2004) and members of the *Acetobacter* and *Gluconacetobacer* where they are typically accompanied by methylated and/or unsaturated homologues (Talbot et al., 2007a and references therein).

BHhexol cyclitol ether is also widespread in environmental samples, occurring alongside BHT cyclitol ether and BHpentol cyclitol ether, however, a source organism for BHhexol cyclitol ether has yet to be identified. In Chapter 3, strong correlation between BHhexol cyclitol ether and BHT cyclitol ether and BHpentol cyclitol ether was identified suggesting that these compounds probably have similar bacterial sources (section 3.6.6).

Unsaturated BHT cyclitol ether was identified intermittently within ODP 1075 samples. There are few known sources of unsaturated BHT cyclitol ether, which include, acetic acid bacteria (Talbot et al., 2007b) and the marine cyanobacteria *Trichodesmium erythraeum* (Talbot et al., 2008b) and three strains of phylogenetically related *Burkholderia cepacia* bacteria isolated from acidic grassland soil (Cvejic et al., 2000b; Talbot et al., 2007a,b).

Guanidine substituted BHT cyclitol ether was found intermittently throughout ODP 1075. This BHP has previously been reported in *Methylobacterium* spp. (Renoux and Rohmer, 1985; Knani et al., 1994; Talbot et al., 2007a), *Burkholderia cepacia* (Talbot et al., 2007a) and the *Geobacter* spp., *G. metallireducens* and *G. sulfurreducens* (Eickhoff et al., 2013a).

5.4.2. Environmental Sources of BHPs in ODP 1075

5.4.2.1. Saturated BH Cyclitol Ethers

High concentrations of BHT cyclitol ether and minor concentrations of BHpentol - and BHhexol cyclitol ether are observed in ODP 1075. In the Congo soils (Chapter 3) high concentrations of saturated BH cyclitol ethers were observed. Clear correlation between BHT -, BHpentol -, and BHhexol cyclitol ether suggests that factors controlling the distribution of these compounds are similar (e.g. source organisms) between the different soils (see Chapter 3; section 3.6.6 for further discussion). However, in ODP 1075, no correlation between BHT cyclitol ether, and BHpentol cyclitol ether (R_s 0.460, $p < 0.05$) or BHhexol cyclitol ether (R_s 0.637, $p < 0.05$) or between BHpentol cyclitol ether and BHhexol cyclitol ether (R_s 0.663, $p < 0.05$; Figure 5.4) is observed. This suggests that there are additional factors controlling the distribution of these BHPs within ODP 1075. A possible reason could be due to post depositional diagenesis affecting the distribution of cyclitol ethers. However, while a clear diagenetic trend is not observed for BH cyclitol ethers (Figure 5.2), as these compounds are of a mixed terrestrial and marine source, post depositional diagenesis cannot be ruled out.

The lack of correlation between saturated BH cyclitol ethers could suggest these compounds are from a mixture of both marine and terrestrial sources. No clear correlation between BH cyclitol ethers (total BHT -, BHpentol- and BHhexol cyclitol ether) and OC_{ter} proxies (BIT R_s 0.067, p 0.274; R_{soil} R_s -0.321, p <0.05; Figure 5.5) are observed in ODP 1075 sediments.

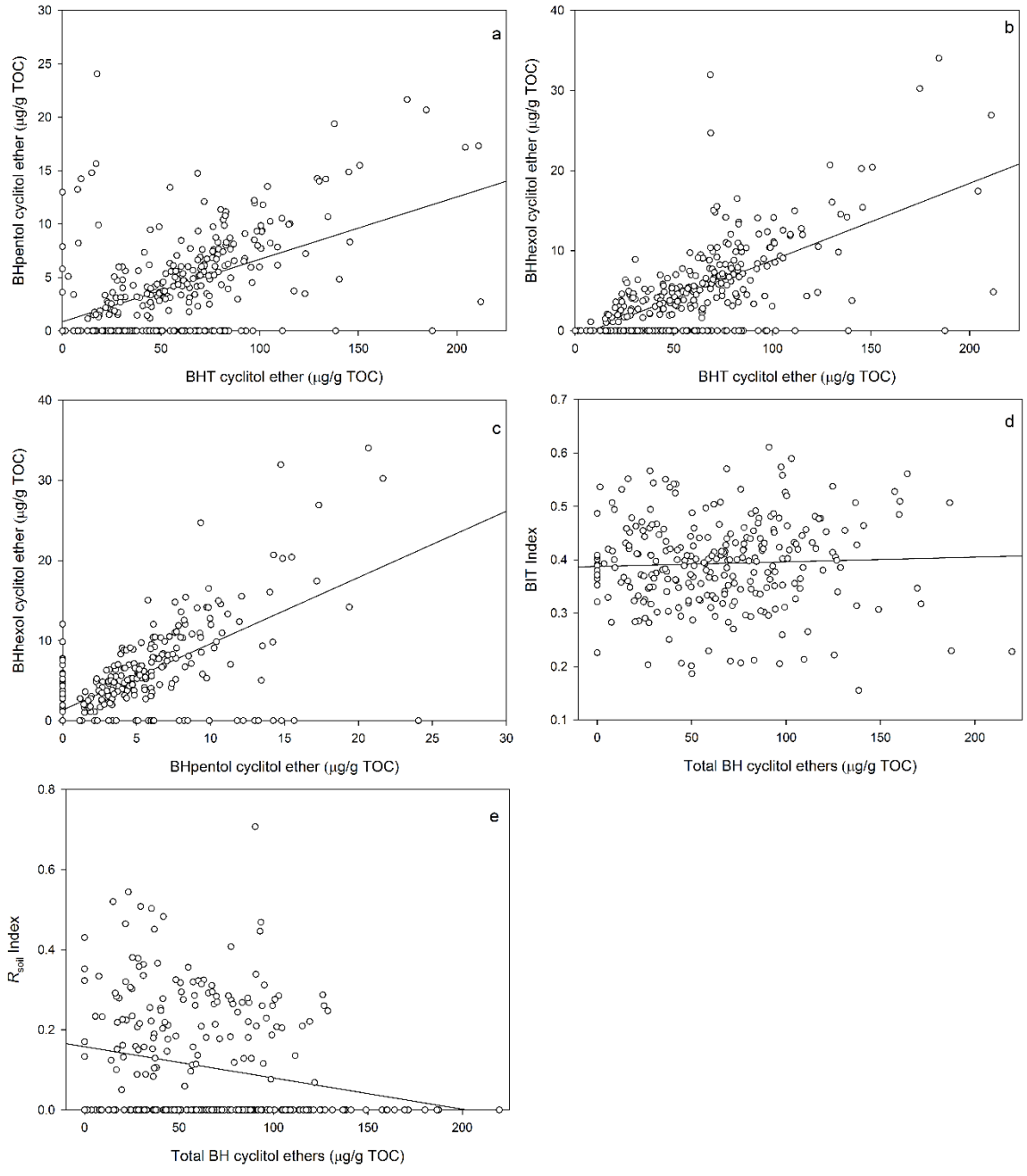

Figure 5.4. Correlation between the concentration of BHT cyclitol ether and BHpentol cyclitol ether (a), and BHhexol cyclitol ether (b); BHpentol cyclitol ether and BHhexol cyclitol ether (c); total BH cyclitol ether with BIT index (d) and Rsoil index (e).

Marine and terrestrial bacterial species that synthesise saturated BH cyclitol ethers, produce different proportions of BHT cyclitol ether, BHpentol cyclitol ether, and BHhexol cyclitol ether. The relative proportion of BHT cyclitol ether against BHpentol

cyclitol ether and BHhexol cyclitol ether is presented as an index (BH cyclitol ether index; Equation 5.1; Figure 5.6).

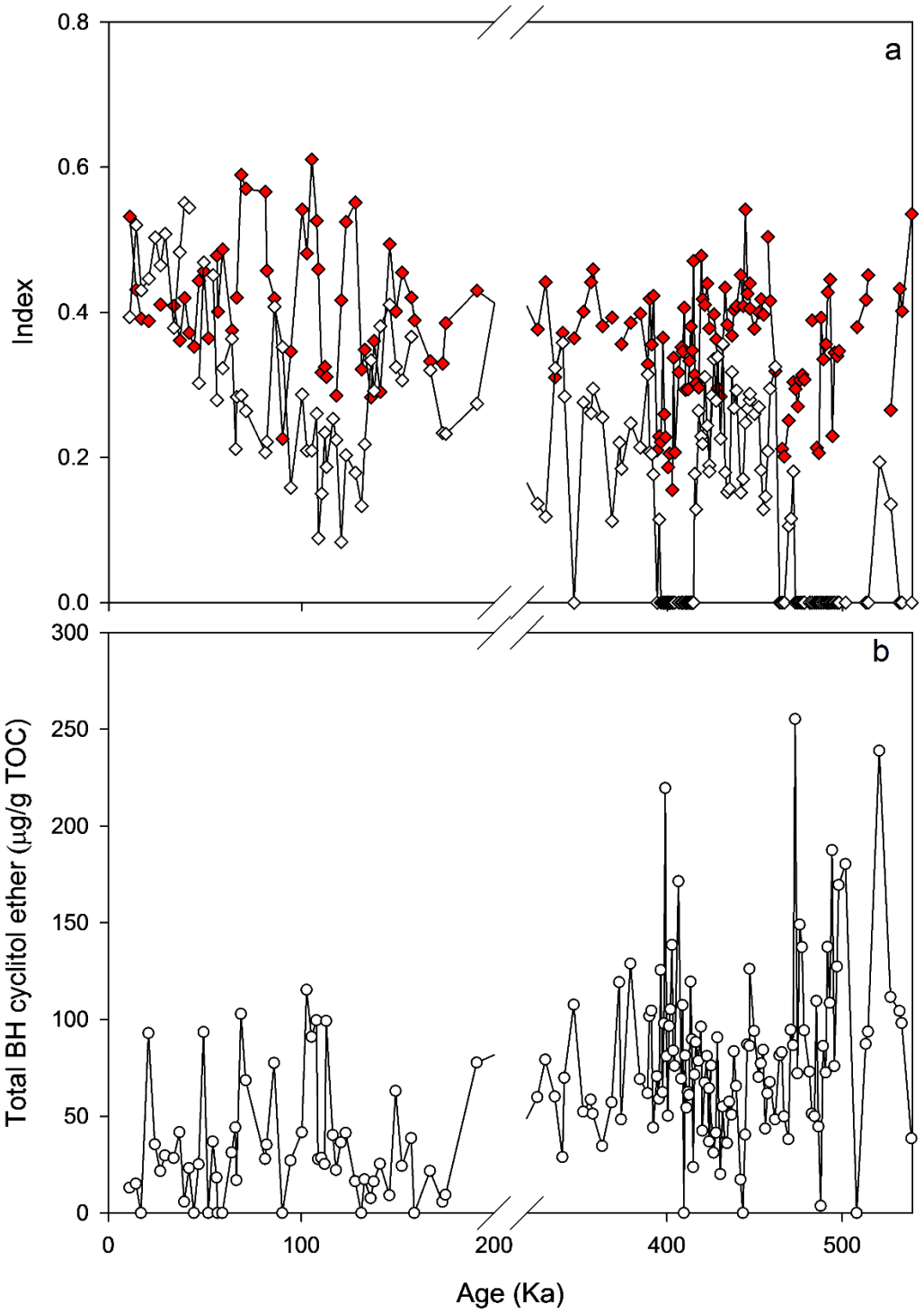

Figure 5.5. a; OC_{ter} indices including BIT (red) and R_{soil} (open). b; Comparison of total BH cyclitol ethers (µg/g TOC; BHT cyclitol ether, BHpentol cyclitol ether-, BHhexol cyclitol ether).

A low mean BH cyclitol ether index was observed for ODP 1075 samples compared with the Congo soils. The mechanisms that transport CH_4 oxidation – and soil marker BHPs to the Congo fan will similarly affect terrestrially derived saturated BH cyclitol ether BHPs (as described in section 3.6.4 and 3.6.8). Therefore, the difference in

cyclitol ether index values between the terrestrial and ODP 1075 samples could be due to higher contributions of BHT cyclitol ether at ODP 1075 site. To date, there are no known marine sources of BHpentol cyclitol ether, however, BHT cyclitol ether has been reported in marine bacteria (Talbot et al., 2008a). Furthermore BHT cyclitol ether is more common in river, coast, shelf and marine sites compared with BHpentol- and BHhexol cyclitol ether (e.g. Blumenberg et al., 2010; Zhu et al., 2011).

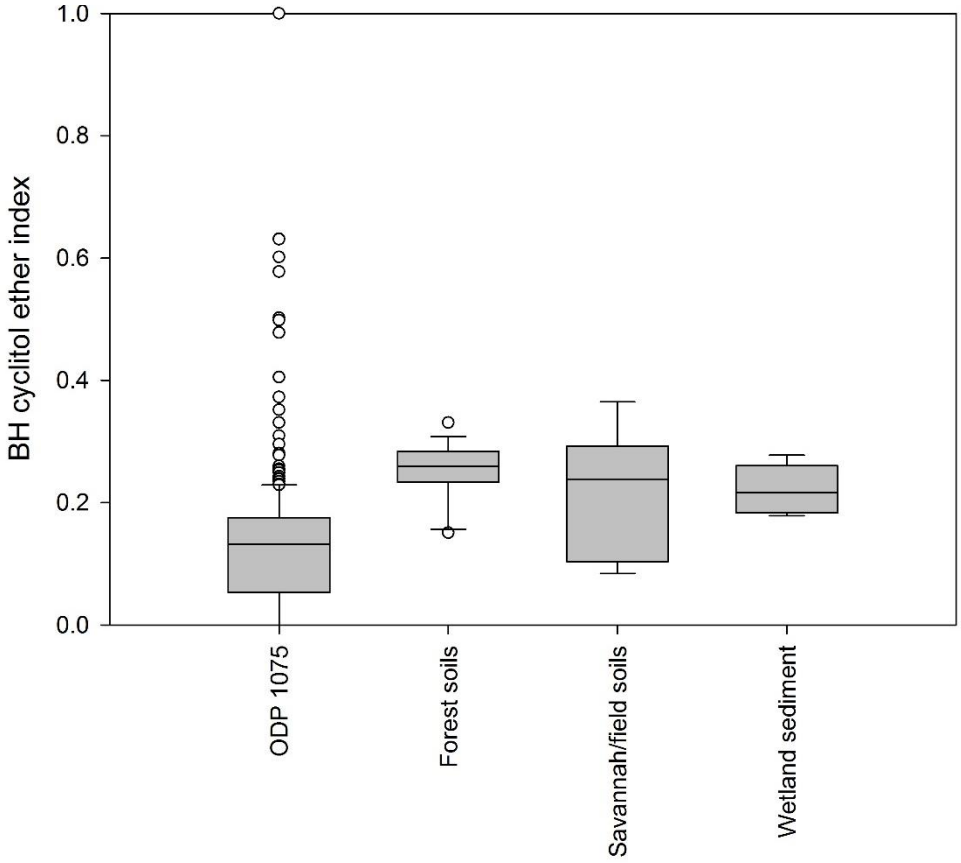

Figure 5.6. BH cyclitol ether index for ODP 1075 and Congo forest and savannah/field soil and wetland (Malebo pool) sediment.

Both BHpentol - and BHhexol cyclitol ether were found to be minor components of the overall BHP suite in the Congo Hinterland samples (relative abundance range from 1.42% - 8.29 and 0% to 6.54% of total BHPs respectively; Chapter 3). In contrast, BHT cyclitol ether was found to be a dominant BHP in the Congo hinterland samples. In addition, BHT cyclitol ether has also been found as the only cyclitol ether within some marine sediment (e.g. Blumenberg et al., 2010; Zhu et al., 2011). Previous analysis of suspended particulate material along a river transect suggests that terrestrial derived OC has significantly higher hopanoid content (by mass) than marine OC, and therefore, terrestrial derived BHP signatures could overprint marine BHP signals (Sáenz et al., 2011a). Furthermore, terrestrial BHPs transported in

association with mineral grains would more likely sink and be preserved (the ballast effect) compared with fresh (labile) marine produced material (Kennedy and Wagner, 2011). This therefore, suggests while there could be terrestrial inputs of these compounds (see section 3.6.6 for discussion of marine sources) there could also be significant marine inputs of BH cyclitol ethers, most notable BHT cyclitol ether, to the Congo Fan.

5.4.2.2. Unsaturated BHT Cyclitol Ether

High concentrations of unsaturated BHT cyclitol ether were first reported within the 521 (250 µg/g TOC) to 580 Ka (250 µg/g TOC) region of ODP 1075 by Handley et al. (2010). In this chapter, we observe unsaturated BHT cyclitol ether to persist throughout ODP 1075 (Figure 5.3) with lower concentrations of unsaturated BHT observed in older sediments during 1562 (170 µg/g TOC) and 1917 Ka (210 µg/g TOC). As discussed in section 5.4.1.2, possible source bacteria include terrestrial acetic acid bacteria and *Burkholderia* spp. (Talbot et al., 2007b and references therein) and marine cyanobacteria (Talbot et al., 2008b). Unsaturated BHT cyclitol ether was not observed in any of the Congo soil samples which included acidic grasslands (Chapter 3). Unsaturated BHT cyclitol ether has rarely been reported in other soils, with this compound notably absent from other tropical samples (e.g. Person et al., 2009; Wagner et al., 2014). This therefore suggests that acetic acid bacteria are unlikely to be the source of this BHP in the Congo fan (Handley et al., 2010).

The marine cyanobacteria *Trichodesmium erythraeum*, a known producer of unsaturated BHT cyclitol ether (Talbot et al., 2008b), could be the source organism of this BHP in the Congo Fan. *Trichodesmium* spp. are marine pelagic N fixing bacteria that occur extensively in the North Atlantic subtropical gyre where nitrate and phosphate nutrient concentrations are low (Tyrrell, 1999; Sohm and Capone, 2006). In the low nutrient waters of the North Atlantic, nitrate and phosphate are typically limited at the surface with phosphate consumption attributed to *Trichodesmium* spp. The intermittent presence of unsaturated BHT cyclitol ether within ODP 1075 suggests a major shift in the marine bacterial community and could be attributed to periods of low nutrients to the Congo fan as proposed by Handley et al. (2010).

5.4.2.3. BHT and Unsaturated BHT

High concentrations of BHT are present throughout ODP 1075. BHT is a common BHP that has been reported in most published soils and sediments (e.g. Cooke et al., 2008; Pearson et al., 2009; Xu et al., 2009; Rethemeyer et al., 2010; Zhu et al., 2011; Doğrul Selver et al., 2012; 2015; van Winden et al., 2012a; Kim et al., 2011; Sáenz et al., 2011 a,b; Wagner et al., 2014). Therefore, BHT identified within the Congo fan is likely from both terrestrial and marine sources. While no clear diagenetic trend is observed in BHT concentrations within ODP 1075, due to the mixed sources of this compound, post deposition diagenesis cannot be rule out.

Low concentrations of unsaturated BHT were identified in 14 ODP 1075 samples. Low concentrations of this BHP in the Congo Fan has also previously been reported by Handley et al. (2010). In this study, unsaturated BHT is observed to persist beyond 1.2 Ma (Figure 5.3). Unsaturated BHT has rarely been reported in pure culture with the only known source (to date) being a soil acetic acid bacterium G. xylinus (Peiseler and Rohmer, 1992; Talbot et al., 2007b). Previously, unsaturated BHT has been reported at low concentrations in soils from Northern England (Cooke et al., 2008) and Canada (Xu et al., 2009). The absence of this compound from the Congo soils and wetlands (Chapter 3) suggests that unsaturated BHT identified in ODP 1075 is not of terrestrial origin but could be produced in the Congo River or within the fan, potentially in the water column and/or sediment. Additionally, peak concentrations in unsaturated BHT show similar patterns to unsaturated BHT cyclitol ether (Figure 5.3) suggesting these compounds to have either similar sources or the synthesis of these relatively unusual BHPs is stimulated by similar environmental conditions. Unsaturated BHT has also been reported in non – soil environments including hypoliths (Talbot et al., 2008b), shelf sediments (Taylor and Harvey, 2011) peatlands (Talbot et al., *in prep*.). All three of these studies used samples collected from the Arctic, suggesting, that unsaturated BHT may be limited by temperature. However, unsaturated BHT has not been reported in all arctic BHP studies (e.g. Rethemeyer et al., 2010; Doğrul Selver et al., 2012, 2015; Hölfe et al., 2015), suggesting that occurrence of this BHP is not widespread.

5.4.2.4. Guanidine Substituted BHT Cyclitol Ether

Guanidine substituted BHT cyclitol ether was found intermittently throughout ODP 1075 (Figure 5.3). This BHP has previously been reported in soil and plant

associated bacteria (Renoux and Rohmer, 1985; Knani et al., 1994; Talbot et al., 2007a) and anaerobic bacteria found in soils and sediments (*Geobacter* spp. Eickhoff et al., 2013a), therefore, suggesting that guanidine substituted BHT cyclitol ether found in Congo fan could have marine and/or terrestrial origins. Guanidine substituted BHT cyclitol ether has not been reported in many modern terrestrial environmental samples and was absent in both the Congo hinterland samples (Chapter 3) and within other tropical samples (e.g. Amazon hinterland; Wagner et al., 2014), therefore suggesting that, at least in this setting, this BHP is not derived from a terrestrial source.

Guanidine substituted BHT cyclitol ether has been identified in two *Geobacter* spp. including *G. metallireducens* and *G. sulfurreducens* (Eickhoff et al., 2013a). Bacteria of the *Geobacteraceae* family are ubiquitous in the environment and have been identified in various anoxic settings including, soil, freshwater, marine and estuarine settings (Cummings et al., 2003 and references therein). *Geobacter* spp. are potentially important sources of marine sedimentary BHPs (Fischer and Pearson, 2007). Marine *Geobacter* spp. could be the source of Guanidine substituted BHT cyclitol ether in ODP 1075 in addition to BHT cyclitol ether and BHT glucosamine. Guanidine substituted BHT cyclitol ether has previously been identified in anoxic water column suspended particulate material samples from the Peru Margin (Sáenz et al., 2011b). This suggests that this compound could be used to suggest periods of water column anoxia. However, the potential of this compound as a biomarker remains to be elucidated.

5.5. Conclusions

The aim of this Chapter was to test the hypothesis “All BHPs found in ODP 1075 are of terrestrial origin”. The sources of soil marker BHPs and C-35 amine BHPs has previously been discussed in Chapters 3 and 4 and are clearly terrestrial. In addition to the presence of C-35 amine and soil marker BHPs, high concentrations of saturated BH cyclitol ethers and low concentrations of an unsaturated BHT have also been identified in ODP 1075. BH cyclitol ethers persist throughout ODP 1075 with no clear degradation signature at a maximum age of 2.5 Ma. This suggests that BH cyclitol ethers are recalcitrant BHPs in the sedimentary record.

Of the saturated BH cyclitol ethers, BHT cyclitol ether is the most abundant compound, with BHpentol – and BHhexol cyclitol ether present at minor

concentrations. High concentrations of saturated BHT cyclitol ethers in the Congo hinterland samples (Chapter 3) support a terrestrial source (or sources; soils, wetlands), however, lower values of the BH cyclitol ether index in ODP 1075 compared to the terrestrial materials indicate an additional contribution from marine sources.

Low concentrations of unsaturated BHT and unsaturated BHT cyclitol ether were identified in ODP 1075. Both unsaturated BHT and unsaturated BHT cyclitol ether were found to be present at similar intervals, suggesting that these compounds could have a similar source organism/s or that environmental conditions affect the synthesis of these compounds to a similar extent. Neither unsaturated BHT nor unsaturated BHT cyclitol ether have been identified in the Congo hinterland samples (Chapter 3) suggesting these compounds are not of terrestrial origin. However, no common bacterial source for these compounds has been identified, however unsaturated BHT may be an early stage degradation product of unsaturated BHT cyclitol ether. We therefore hypothesise that the presence of both compounds is due to blooms of the marine N fixing cyanobacterium *Trichodesmium* spp.

Low concentrations of guanidine substituted BHT cyclitol ether were identified in ODP 1075. This compound was also absent from the terrestrial Congo samples (Chapter 3) suggesting that guanidine substituted BHT cyclitol ether in ODP 1075 is of marine origins.

These results indicate that the origins of BHPs can be elucidated when terrestrial and marine end members are known. We can conclude that CH_4 oxidation – and soil marker BHPs appear to be of exclusively terrestrial origins in ODP 1075 and potentially within other Fan systems. Unsaturated BHT, unsaturated BHT cyclitol ether and guanidine substituted BHT cyclitol ether have known marine and terrestrial biological sources, however, as these compounds were not identified in the Congo hinterland samples and have not been widely reported in published modern soil studies. This suggests that a marine source is the most likely explanation for the presence of unsaturated BHT, unsaturated BHT cyclitol ether and guanidine substituted BHT cyclitol ether in this setting. However, a greater survey of BHPs within Congo soils, including samples from the largely unstudied mangroves systems, is required to confirm this conclusion.

Chapter 6:

High Resolution Record of Terrestrial Aerobic Methane Oxidation Reveals Intense Methane Cycling During MIS 11 and 5

Chapter 6. High Resolution Record of Terrestrial Aerobic Methane Oxidation Reveals Intense Methane Cycling During MIS 11 and 5

6.1. Introduction

During the past century, Earth has experienced rapid rise in surface temperature with instrumental record showing the past 30 years to have been successively warmer than the previous decades. In parallel with this rise, significant increase in the atmospheric concentrations of several greenhouse gasses has also been recorded (Hartmann et al., 2013). CH_4 is a potent greenhouse gas and is a potential driver of climate change. Recent measurements of atmospheric CH_4 show a tripling on pre-industrial levels with concentrations of 1803.2 ppbv recorded (Hartmann et al., 2013). Atmospheric CH_4 has been steadily increasing since 2007 (Hartmann et al., 2013); this rise in CH_4 is primarily due to anthropogenic influences and has the potential to destabilise vulnerable sources of terrestrial C (IPCC, 2013).

6.2. Modern Tropical CH_4 Cycling

Modern estimates suggest that between 2 200 and 3 060 Pg C is stored in the terrestrial biosphere (Lal, 2004). The implications and feedbacks of rapid release of terrrestrial C to the atmosphere are not fully understood. Modern wetlands are the largest single natural source of CH_4 to the atmosphere (Hartmann et al., 2013). These environments cover approximately 5 to 8% of the world's surface (Mitsch and Gosselink, 2007) with total emissions around 177 and 284 Tg CH_4 $year^{-1}$ (IPCC, 2013; Mitsch and Gosselink, 2007). CH_4 emissions, however, vary on a regional basis with the tropical wetlands thought to contribute approximately 60% of CH_4 to the global CH_4 budget (Bartlett and Harriss, 1993; Ortiz-Llorente and Alvarez-Cobelas, 2012). The modern Congo basin contains a significant proportion of wetlands, comprising approximately 56% of the land cover (Bwangoy et al. 2010).

Modern wetlands have an important role in biogeochemical cycling of C. Within the anoxic sediment and pore water of wetlands, CH_4 is produced through the microbial mediated process of methanogenesis. The CH_4 produced is then oxidised through either anaerobic oxidation of CH_4 (AOM; Equation 1.1) or aerobic CH_4 oxidation (AMO; Equation 1.2). AOM and AMO act as a buffer for CH_4 flux to the atmosphere, however, the effectiveness of this buffer depends on many factors including; wetland type, the presence of macrophytes, concentrations of nutrients, temperature, water

level, and seasonality (see Chapter 1, section 1.2 for full discussion). Therefore, global estimates of how much CH_4 is prevented from reaching the atmosphere are unclear with some estimates suggesting that oxidation within wetlands can consume up to 90% of CH_4 (e.g. King et al. 1990; Conrad and Rothfuss, 1991; Frenzel et al., 1992; Van Der Gon and Neue, 1996; Bosse and Frenzel, 1997, 1998; Gilbert and Frenzel, 1998). The role of tropical CH_4 sources in future climate change including potential feedbacks are not fully understood. However, records of high atmospheric CH_4 concentrations have the potential to provide information about biogeochemical cycles and feedbacks during geological periods characterised by high atmospheric CH_4 and warm global temperatures.

6.2.1. Paleo CH_4 Cycling

High atmospheric CH_4 concentrations have been observed during the Pleistocene. Loulergue et al. (2008) identified maximum atmospheric CH_4 concentrations of ~800 ppbv during MIS 9.3. The expansion of wetlands/floodplain lakes during humid periods is a prominent hypothesis for the source of paleo CH_4 within ice core records (Brook et al., 2000; Dallenbach et al., 2000). However, CH_4 concentrations from ice core records have yet to be reconciled with sedimentary archives.

Sedimentary records from central Africa suggest large scale shifts in vegetation during the Pleistocene. Marine and terrestrial palynological evidence suggests the expansion of mangrove swamps and tropical rainforest typically during warm – humid MIS within West Africa for the past 150 000 years (Dupont et al., 2000). In agreement, palynology records from Lake Edward (Uganda – Democratic Republic of Congo border) during the last glacial maximum suggest extensive semi-deciduous forest compared to typically drier grassland type environments that are present today (Beuning and Russell, 2004). To date, the shifts in wetland extent during the Pleistocene remain unknown; this is largely due to a lack of appropriate proxies including biomarkers.

Distribution of vegetation within the Congo is determined by moisture availability. In central Africa, precipitation maxima occurs twice a year with the movement of the inter-tropical convergence zone (ITCZ; Kazadi and Kaoru, 1996). Meteorological observations also suggest a relationship between central African rainfall and the meridional South Atlantic SST pattern, with negative correlation between rainfall with equatorial SST and a positive correlation with South Atlantic SSTs (Nicholson and

Entekhabi, 1987; Camberlin et al., 2001). Humidity and aridity in central Africa are controlled by variations in trade winds, SST and sea level pressure gradients. The tropical-subtropical SST gradient corresponds to a sea level pressure gradient, which in turn, controls the intensity of the southern hemisphere trade winds counteracting the inflow of moist air from the Atlantic Ocean on the African continent. High central African precipitation results when this gradient is low, i.e. when the equatorial Atlantic was relatively cool and the subtropical south Atlantic is relatively warm leading to weak trade winds (Schefuß et al., 2005; Figure 6.1).

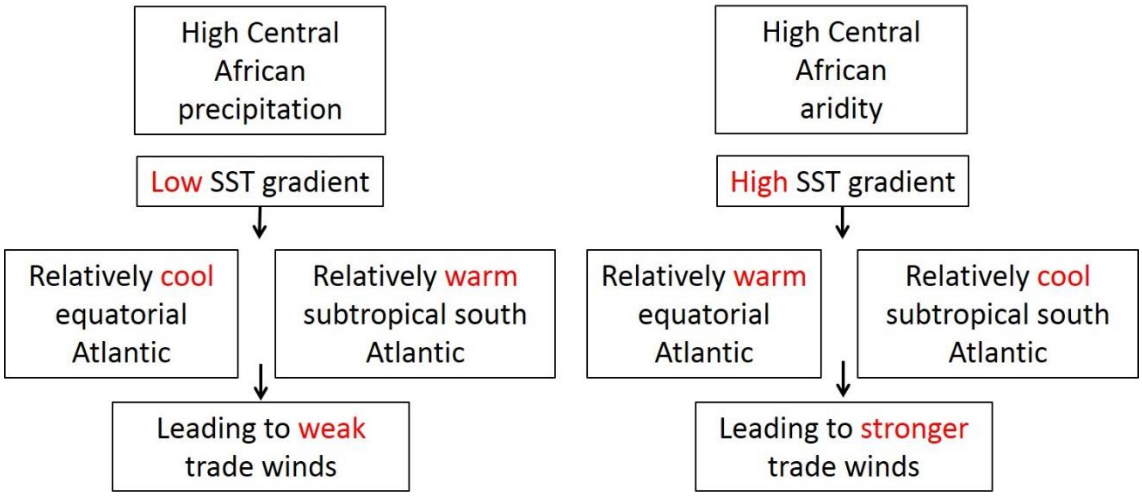

Figure 6.1. Diagram showing the relationship between tropical -, and subtropical SST and humidity and aridity cycles as described by Schefuß et al. (2005).

The reverse situation, relatively cold subtropics and relatively warm tropics corresponded to stronger trade winds and arid periods in equatorial Africa (Schefuß et al., 2005). This relationship between tropical and subtropical SST has led to the development of the alkenone $U^{K'}_{37}$ based Δ-SST proxy which can be used to describe humid and arid periods in West African geological history where increased West African humidity results in a low Δ-SST (Schefuß et al., 2005). Schefuß et al. (2005) determined that over the past 20 000 years, central African precipitation was mainly controlled by differences in tropical and subtropical SST of the south Atlantic ocean with little evidence for large-scale shifts in the position of the ITCZ. Large scale shifts in vegetation could suggest variations in wetland extent and therefore tropical CH_4 emissions. Beuning and Russell (2004) suggest that large scale shifts in vegetation observed in Lake Edward would require a much wetter Pleistocene climate compared to the present day and with a potential 25-60% increase in annual precipitation.

6.2.2. Analogues for Modern Climate: Marine Isotope Stages 5 & 11

Two different periods in Earth history have been suggested as analogues to modern Earth climate. MIS 5 and 11 are both considered warm stages in the geologic record with a duration of 58 Ka and 64 Ka respectively (Howard, 1997; Kukla et al., 1997; Spahni et al., 2005). MIS 5 and 11 are characterised as periods of reduced ice volume with an interglacial and numerous interstials and stidals (Loutre et al., 2003). However, insolation patterns, which partly control the duration and degree of incoming warmth, have not been similar throughout geological history. MIS 5e is the interglacial of the MIS 5 warm period and is the most recent pre Holocene interglacial. However, despite MIS 5 being well represented within marine, ice core and terrestrial sediment records, the insolation patterns during this warm stage are not similar to modern day insolation (Berger and Loutre, 2002; Loutre and Berger, 2003). Conversely, MIS 11 is considered a much better analogue for the Holocene. Incoming solar insolation during MIS 11 matches more closely with modern insolation than any other warm stage during the past 500 Ka (Berger and Loutre, 2002; Loutre and Berger, 2003). MIS 11 is characterised by relatively low eccentricity resulting from a circular earth orbit (Berger and Loutre, 2002; Loutre and Berger, 2003). Low eccentricity results in a more constant amount of insolation during the year, with no strong seasonal contrast (Candy et al., 2014). This phenomenon occurs every 413 Ka and characterises MIS 1 (modern day), 11, and 19 (Berger and Loutre, 2002; Loutre and Berger, 2003; Tzedakis, 2010).

6.2.3. Aims, Objectives and Scope

Previous work, (see Chapter 3 and Talbot et al., 2014), suggests large scale flux of CH_4 during warm climate stages as interpreted through biomarker records. Sediments from Congo fan represent an integrated terrestrial and oceanic climate signature (Holtvoeth et al., 2001; 2003; Jahn et al., 2005; Weijers et al., 2009). Flux of CH_4 during the Pleistocene has been linked with expansion of tropical wetlands within the Congo (Talbot et al., 2014).

In this chapter we test the hypothesis; "*Temporal changes in the concentration of biomarkers down core occur due to variations in terrestrial AMO intensity*".

The aim of this chapter is to determine short term variability in terrestrial CH_4 cycling within the Congo fan during MIS 5 and MIS 11. The objectives of this study are to

increase the sampling resolution of ODP 1075 to address the short term variability in CH_4 cycling and analyse various biomarker/proxies to determine orbitally driven climate controls on tropical CH_4 cycling.

The scope of this chapter will be to;

- Determine C-35 amine BHP inventory in ODP 1075.
- Determine diagenetic controls on biomarker concentrations including correlation of these biomarkers with TOC.
- Determine environmental controls on C-35 amine BHPs by clarifying the source of C-35 amine BHPs in ODP 1075 (correlation of aminopentol with aminotetrol and aminotriol) and determine influence of OM supply on C-35 amine concentrations in ODP 1075 through correlation with OC_{ter} proxies (BIT and R_{soil}).
- Determine the suitability of C-35 amine BHPs in paleoclimate reconstructions by assessing results of diagenetic and environmental controls.
- Determine if variations in CH_4 oxidation marker concentrations in the Congo fan track fluctuations in global CH_4 concentrations.
- Determine if orbitally forced climatic signals influence C-35 amine signatures within the Congo fan during MIS 11 and 5.

6.3. Overview of Methodology and Study site

6.3.1. Study Site

The study site has previously been described in Chapter 2. Briefly, Ocean drilling program (ODP) site 1075 was drilled as part of ODP leg 175 and is situated on the Northern part of the Congo deep-sea fan (4°47.1198'S, 10°4.4989'E; Figure 2.4) at 2996 m water depth. Total organic carbon ranges from 1.47 to 3.33% (mean TOC, 2.27%) within the high resolution section (Holtvoeth et al., 2001).

6.3.2. Bulk and Geochemical Analysis

Bulk and geochemical analysis has previously been described in Chapter 2. Briefly, TOC (%) of ODP 1075 sediments was measured as detailed in Holtvoeth et al. (2001) and Chapter 2. Total lipids were extracted from approximately 3 g of freeze-dried sediment using a modified Bligh and Dyer extraction method as described by Talbot et al. (2007a) and further modified by Osborne, (PhD thesis, Submitted). An

aliquot (one third) of the TLE was used for BHP analysis (Chapter 2, section 2.5) and one third was used for GDGT analysis.

6.3.3. Compound Classification and Statistics

The abbreviated names of the compounds identified, characteristic base peak ions (*m/z*) and structure numbers are given in Chapter 2. AminoBHPs include aminotriol (**1h**), unsaturated (**4/5h**) and methylated aminotriol (**2/3h**), aminotetrol (**1c**) and unsaturated aminotetrol (**4/5c**) and aminopentol (**1d**), unsaturated (**4/5d**) and aminopentol isomer (**1d'**; van Winden et al., 2012b). BHPs diagnostic for AMO (hereafter referred to as "CH_4 oxidation markers") include aminopentol, unsaturated and aminopentol isomer and aminotetrol. Statistical analysis was performed using Minitab 17.1.0. Spearmans Rho (R_s) correlation index was performed on BHP abundances.

6.4. Data Citation

In addition to the 87 new samples analysed in this study, BHP data from 20 ODP 1075 samples (see Table 6.1) previously reported in Talbot et al. (2014) are also used the results and discussion. Both the Talbot et al. (2014) data set and the high resolution data set were analysed at Newcastle University on the same instrument therefore it can be assumed that there should not be any offsets between the data. $U^{K'}_{37}$ (ΔSST) data have previously been reported in Jahn, (2002).

Table 6.1: 20 samples analysed from the high resolution section of ODP 1075 as reported in Talbot et al., 2014.

Core number	Section number	Interval (cm)	Ka	Core number	Section number	Interval (cm)	Ka
6	1	115	341.5	7	1	15	424.1
6	2	115	357.7	7	1	85	433
6	3	65	368.5	7	2	25	444.6
6	3	105	372.8	7	2	125	457.4
6	4	115	390.1	7	3	75	470.6
6	5	35	397.5	7	4	5	481.4
6	5	115	403.6	7	4	55	487.8
6	6	115	415	7	5	15	501.9
6	7	25	419.5	7	6	15	521.1
6	7	74	425.2	7	6	105	532.7

6.5. Results

Aminotriol (**1h**), aminotetrol (**1c**), aminopentol (**1d**) and unsaturated aminopentol (**4/5d**) and aminopentol isomer (**1d'**) are present in the high resolution sections of ODP 1075 (Figure 6.2). Aminotriol is the most abundant C-35 amine BHP with concentrations ranging from 4.6 to 270 µg/g TOC (Table 6.2).

Table 6.2. Mean concentration aminotriol, aminotetrol, aminopentol, unsaturated aminopentol and aminopentol isomer (µg/g TOC) in high resolution MIS (N=number of samples in MIS).

MIS	N	Aminotriol	Aminotetrol	Aminopentol	Unsaturated aminopentol	Aminopentol isomer
3	9	16	0.58	7.7	0	0
	Range	10-25	0-2.9	0-15	0-0	0-0
4	5	33	3.7	28	0	3.4
	Range	8.6-83	0-12	6.5-69	0-0	0-15
5	19	58	11	50	0.61	4.7
	Range	12-120	0-26	5.7-140	0-6.7	0-23
6	9	18	2.5	12	0	1.6
	Range	4.6-33	0-6.4	0-29	0-0	0-4.7
10	10	58	7.2	36	0	1.9
	Range	14-100	0-16	2.9-73	0-2.7	0-7.5
11	36	100	16	80	0.58	1.7
	Range	19-270	0-48	13-200	0-5.5	0-11
12	38	63	8.1	42	0	0.64
	Range	9.5-250	0-32	0-180	0-4.1	0-6.8
13	21	160	21	110	1.3	4.3
	Range	59-250	2.4-48	34-210	0-12	0-23

Aminopentol is the second most abundant C-35 amine and the most abundant CH_4 oxidation marker (see section 6.3.3 for definition) with concentrations ranging between 0 and 210 µg/g TOC (Table 6.2; Figure 6.2, Figure 6.3, and Figure 6.4).

Unsaturated aminopentol is present in 2 samples within MIS 2 to 8 and 11 samples within MIS 10 to 13, with concentrations between 0 and 12 µg/g TOC. Aminotriol, aminotetrol and aminopentol concentrations fluctuate down core. High concentrations of aminopentol are seen to occur during MIS 5, 8, 11, 12 and 13 (Figure 6.3 and Figure 6.4).

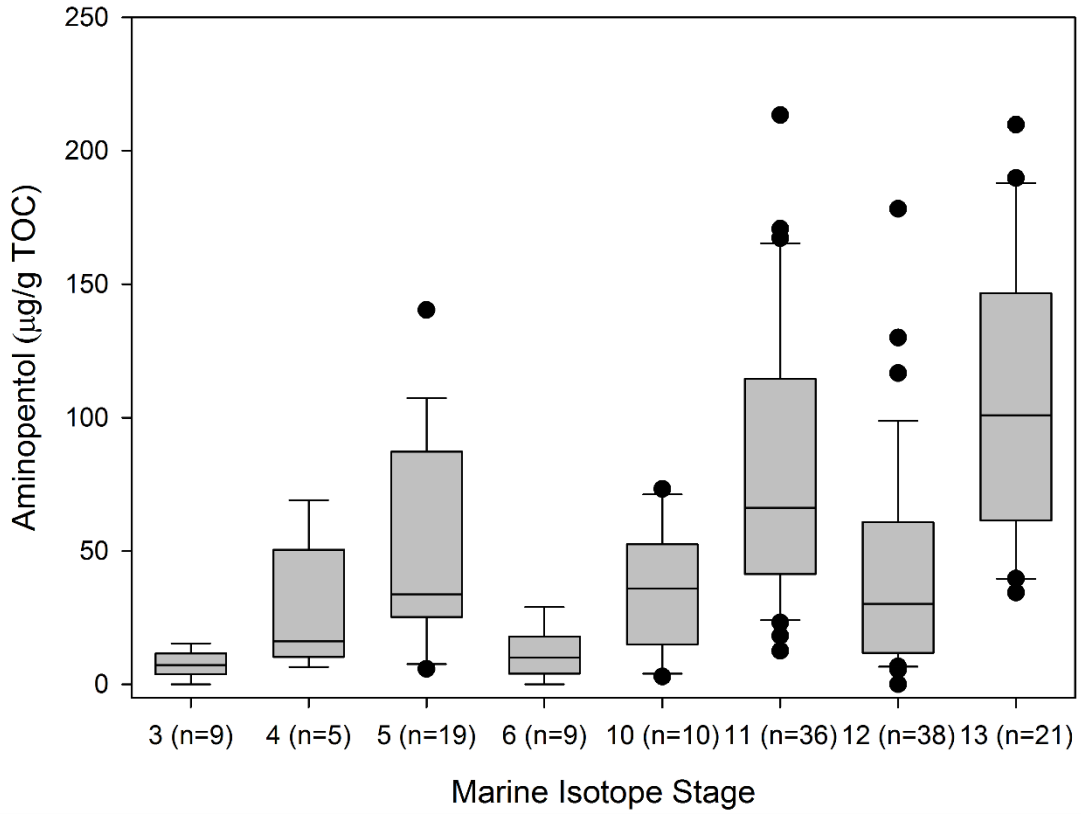

Figure 6.2. Distribution of aminopentol within high resolution MIS stages of ODP 1075 (µg/g TOC).

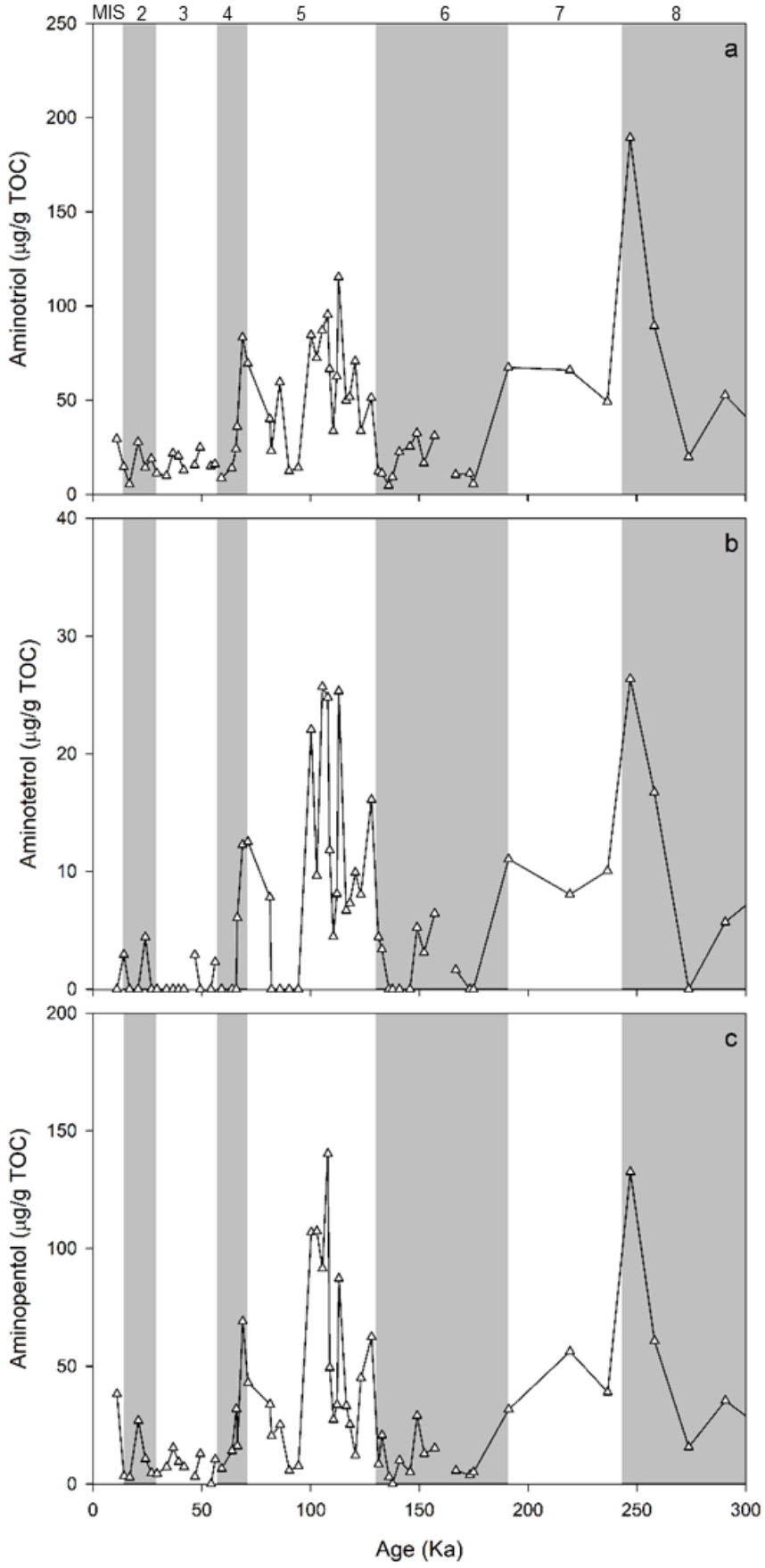

Figure 6.3. Concentration (µg/g TOC) of aminotriol (a), aminotetrol (b), and aminopentol (c) within ODP 1075 from 10 Ka to 300 Ka. Grey bars indicate MIS 2, 4, 6, and 8 (±20% error).

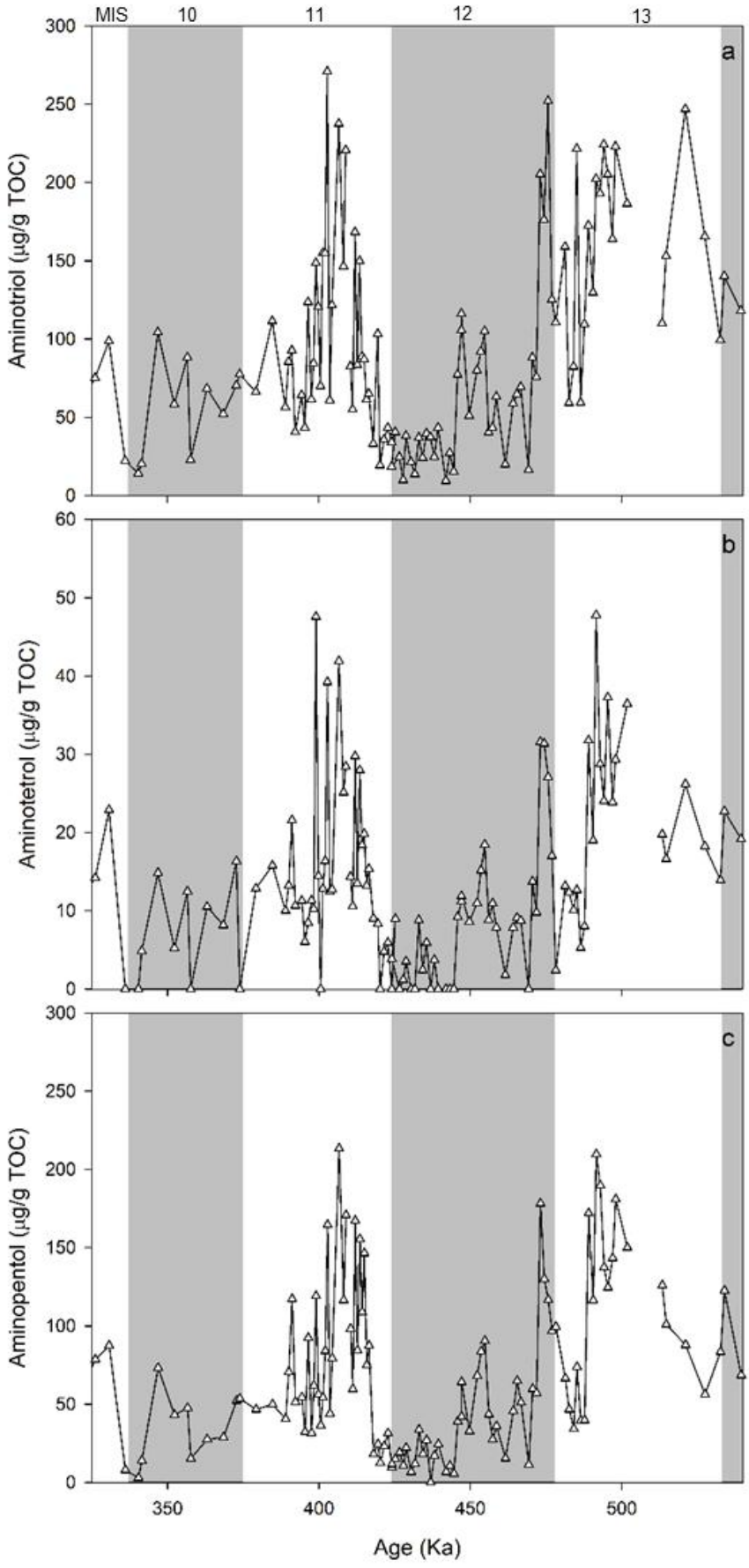

Figure 6.4. Concentration (µg/g TOC) of aminotriol (a), aminotetrol (b), and aminopentol (c) within ODP 1075 from 325 Ka to 540 Ka. Grey bars indicate MIS 10 and 12 (±20% error).

6.6. Discussion

6.6.1. C-35 Amine Inventory

Aminotriol (**1h**), aminotetrol (**1c**), aminopentol (**1d**), unsaturated aminopentol (**4/5d**) and aminopentol isomer (**1d'**) are identified within high resolution sections of ODP 1075. Aminotriol has several different microbial sources, including the N fixing bacteria (Vilcheze et al., 1994; Bravo et al., 2001), purple non-sulfur bacteria (Neunlist et al., 1988; Talbot et al., 2007a), ammonia oxidising bacteria (Talbot et al., 2007a), type I and II methanotrophs, (Cvejic et al., 2000a; Talbot et al., 2001; van Winden et al., 2012b), and SRB *Desulfovibrio* spp. (Blumenberg et al., 2006). The diversity in microbial sources is thus reflected in the large range in habitats aminotriol has been identified in including terrestrial (Cooke et al., 2008a; Pearson et al., 2009; Xu et al., 2009; Rethemeyer et al., 2010; Kim et al., 2011; Sáenz et al., 2011b; Zhu et al., 2011; Doğrul Selver et al., 2012; Wagner et al., 2014), riverine sediments (Rethemeyer et al., 2010; Kim et al., 2011; Zhu et al., 2011; Doğrul Selver et al., 2012; Wagner et al., 2014) and riverine water column samples (Sáenz et al., 2011b), lacustrine (Talbot et al., 2003a; Talbot et al., 2003b; Talbot and Farrimond, 2007; Coolen et al., 2008; Wagner et al., 2014), shelf (Wagner et al., 2014) and marine sediments (Cooke et al., 2008b; Handley et al., 2010; Sáenz et al., 2011a; Blumenberg et al., 2013; Wagner et al., 2014; Doğrul Selver et al., 2015) and marine water column samples (Blumenberg et al., 2007; Berndmeyer et al., 2013).

Aminotetrol, aminopentol, unsaturated aminopentol and early eluting aminopentol isomer have been predominantly identified in type I and II methanotrophs (Neunlist and Rohmer, 1985a,b; Cvejic et al., 2000a; Talbot et al., 2001; van Winden et al., 2012b; Osborne, PhD thesis submitted; see chapter 2 for full discussion) and are, therefore, considered biomarkers (termed CH_4 oxidation markers) for AMO.

Significantly lower concentrations of unsaturated aminopentol and aminopentol isomer are present in the high resolution sections compared to aminopentol and aminotetrol in this study (Table 6.2). Unsaturated aminopentol and aminopentol isomer have only been reported from *Methylovulum*-like strain M200 and *Methylomonas* like strain M5 (van Winden et al., 2012b), although a C-3 methylated unsaturated aminopentol was identified in *Methylocaldum szegediense* (Cvejic et al., 2000a). Low concentrations of unsaturated and aminopentol isomer have also been reported in environmental samples including Amazonian shelf and fan sediments

(GeoB 1514 and GeoB 3918; Wagner et al., 2014). When present in environmental samples and culture material, both unsaturated aminopentol and aminopentol isomer are reported as minor components of the total BHP suite (van Winden et al., 2012a; Wagner et al., 2014). This suggests that low concentrations of these two compounds is a general feature of environmental samples which only occur when aminopentol is present at higher concentrations.

6.6.2. Diagenetic Controls on C-35 amines in ODP 1075

Visual analysis of aminotriol, aminotetrol and aminopentol down core profiles (Figure 6.3 and Figure 6.4) show no clear diagenetic trends. Correlation of C-35 amine BHPs with TOC records (previously reported in Chapter 4) in ODP 1075 identify no correlation between TOC and; aminotriol (R_s 0.127, p 0.104; Figure 6.5), aminotetrol (R_s -0.029, p 0.715), or aminopentol (R_s 0.002, p 0.978) concentration (µg/g dry sediment). The lack of correlation between C-35 amine BHPs and TOC suggests that variations in C-35 amine BHP signatures are not driven by variations in TOC.

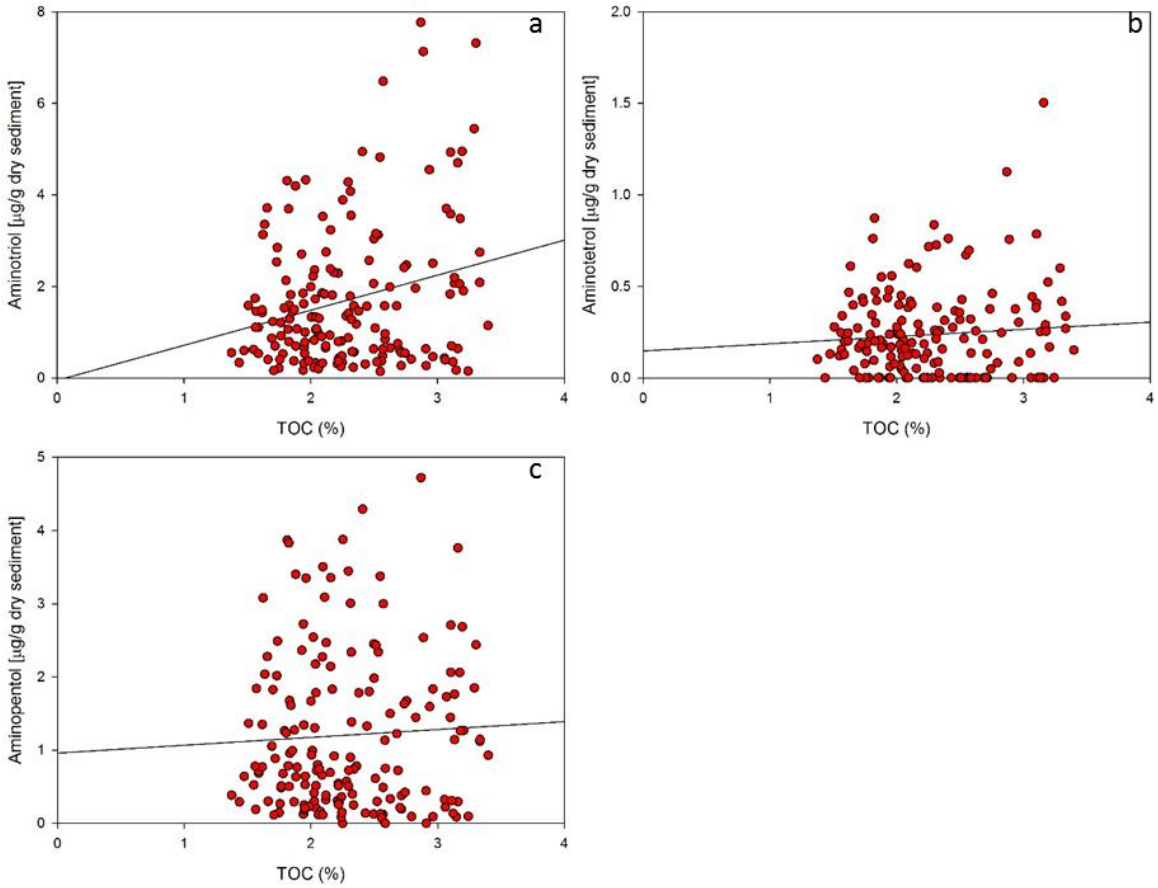

Figure 6.5. Correlations between TOC (%) and aminotriol (a), aminotetrol (b) and aminopentol (c; µg/g dry sediment).

6.6.3. Environmental Controls on C-35 Amines

As discussed in Chapter 3 and Talbot et al. (2014) the origin of CH_4 oxidation markers on the Congo fan could be due to (1) allochthonous production of these biomarkers due to intense aerobic methane oxidation occurring within wetlands/flood plain lakes, or (2) autochthonous production of CH_4 oxidation markers due to the destabilisation of shallow gas hydrates. Strong correlation is found between aminotriol and aminotetrol (R_s 0.878, $p<0.05$; Figure 6.6), aminotetrol and aminopentol (R_s 0.895, $P<0.05$) and aminotriol and aminopentol (R_s 0.917, <0.05), suggesting a similar microbial source. Due to the similarities in CH_4 oxidation signatures within ODP 1075 and within the Congo wetland samples (see Chapter 3), an allochthonous origin for these biomarkers is considered the most likely source.

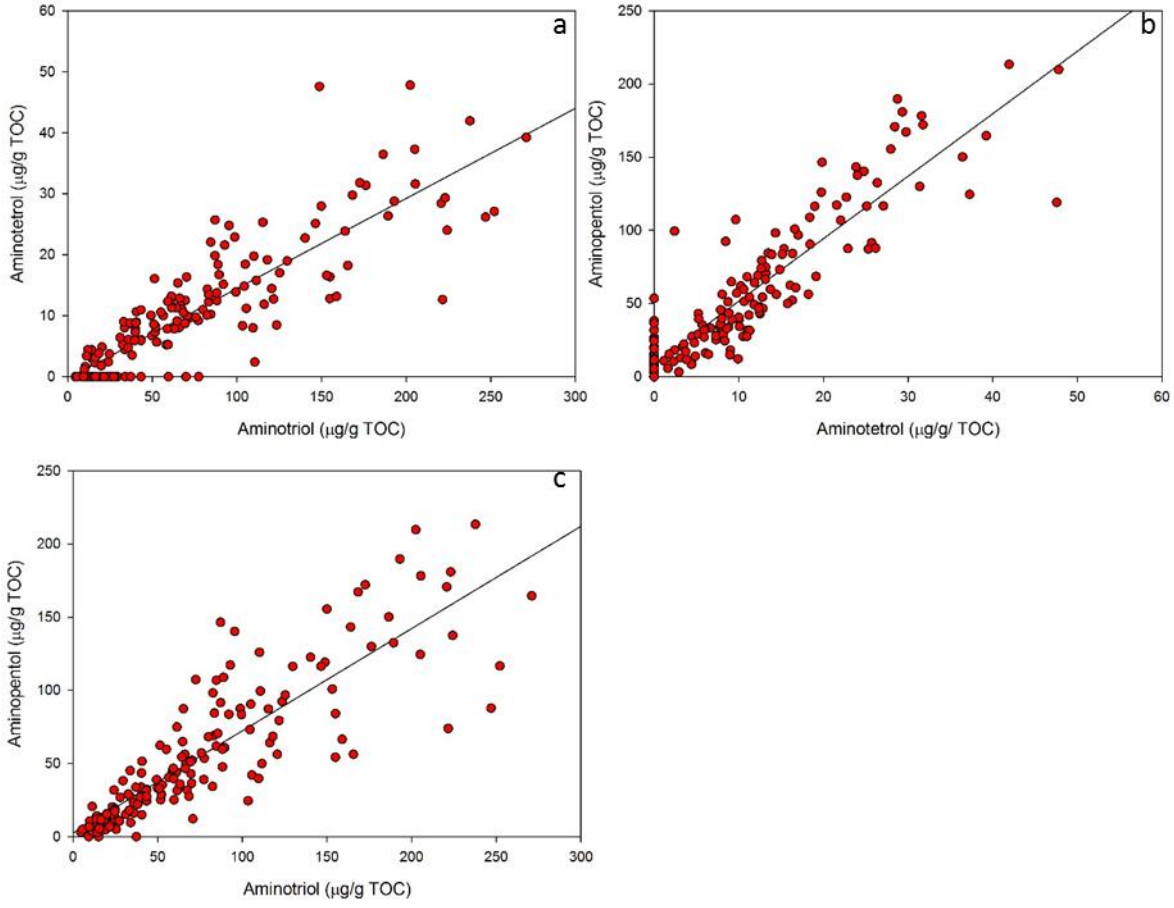

Figure 6.6. Correlation between concentration (µg/g TOC) of aminotriol and aminotetrol (a; R_s 0.878, $p<0.05$), aminotetrol and aminopentol (b; R_s 0.895, $P<0.05$), and aminotriol and aminopentol (c; R_s 0.917, <0.05).

Supply of CH_4 oxidation markers to the Congo fan could be a feature of massive fluvial wash out events (Hughes et al., 2011; Spencer et al., 2012). During favourable environmental conditions, OM containing organic biomarkers (including BHPs and

GDGTs) could be stored on the Congo shelf. During conditions favouring high river discharge or coastal erosion, the stored OM could be washed further into the fan and deposited at ODP site 1075. In this scenario, both GDGTs and BHPs are expected to be affected in a similar way and would therefore correlate. However, no correlation between CH_4 oxidation markers (µg/g TOC) and BIT index (R_s -0.180, $p < 0.05$; Figure 6.7) was found suggesting that while these biomarkers are supplied to the Congo fan by the River Congo, the factors controlling the supply, deposition and burial on the Congo fan are not similar. This is likely due to CH_4 oxidation markers being sourced from specifically wetland environments (Chapter 3; Talbot et al., 2014), whereas, br-GDGTs within the Congo will be supplied from a range of different soil and sediment environments (Weijers et al., 2006b)

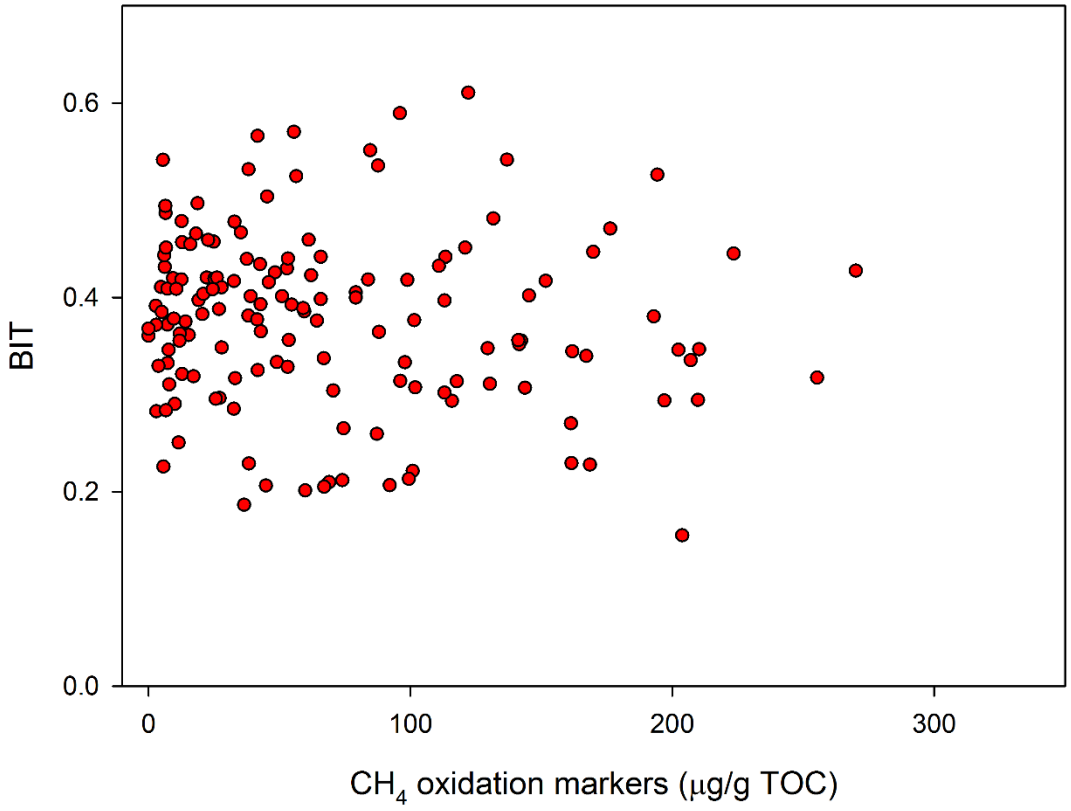

Figure 6.7. Correlation between CH_4 oxidation markers [µg/g TOC] and BIT index within high resolution sections of ODP 1075.

6.6.4. Suitability of C-35 amine BHPs in Paleoclimate Reconstructions

In order to assess the suitability of C-35 amine BHPs in terrestrial paleo CH_4 cycling reconstructions, both diagenetic and environmental controls on biomarker distributions must be determined.

Results from section 6.6.2 suggest that there are no clear diagenetic trends in C-35 amine profiles. This suggests that the C-35 amine signature preserved in ODP 1075 sediments is similar to the C-35 amine biomarker signature at the time of deposition. This is in contrast to adenosylhopane signatures reported in Chapter 4, suggesting that C-35 amine BHPs are potentially more recalcitrant than soil marker BHPs.

Aminotetrol and aminopentol signatures identified in ODP 1075 are likely from a similar terrestrial microbial source as indicated by the strong correlations between aminotriol, aminotetrol and aminopentol (Figure 6.6). These C-35 amine BHPs are all produced to some extent by aerobic methanotrophs with aminopentol the most diagnostic BHP for AMO (Talbot and Farrimond, 2007; Zhu et al., 2010; van Winden et al., 2012b; Berndmeyer et al., 2013; Talbot et al., 2014). Results from Chapter 3 suggest C-35 amine BHPs are largely from a terrestrial source. The proposed terrestrial origin of aminotetrol and aminopentol is inferred from the strong similarities between these biomarker signatures within ODP 1075 and wetland samples from Malebo pool (Congo). Wagner et al. (2014) also found strong similarities between C-35 amine signatures identified in Amazon shelf and fan sediments and those identified within Amazon wetland (várzea) sediments inferring a similar source and transport mechanism as proposed here.

In section 6.6.3 no correlation between CH_4 oxidation markers and BIT index was identified. Additionally, high concentrations of CH_4 oxidation markers do not always coincide with instances of high BIT, suggesting that high concentrations of these biomarkers in ODP 1075 are not a function of high fluvial inputs or coastal erosion. Instead, variations in CH_4 oxidation makers in ODP 1075 directly relate to variations in terrestrial source areas of these biomarkers (i.e. wetlands) in the Congo.

These results, therefore, suggest that in ODP 1075 CH_4 oxidation markers represent a diagentically stable record of terrestrial CH_4 cycling during the Pleistocene within the Congo.

6.6.5. Climatic Controls and CH_4 cycling During MIS 11 and 5

High concentrations of CH_4 oxidation markers are observed throughout the high resolution sections of ODP 1075. High concentrations of CH_4 oxidation markers are seen to correspond to warm climate stages including MIS 5, 11 and 13. Similar concentrations of CH_4 oxidation markers are observed within high resolution MIS sections (Figure 6.2; Figure 6.8; Figure 6.9). However the climate dynamics during MIS 5, 11 and 13 are not the same.

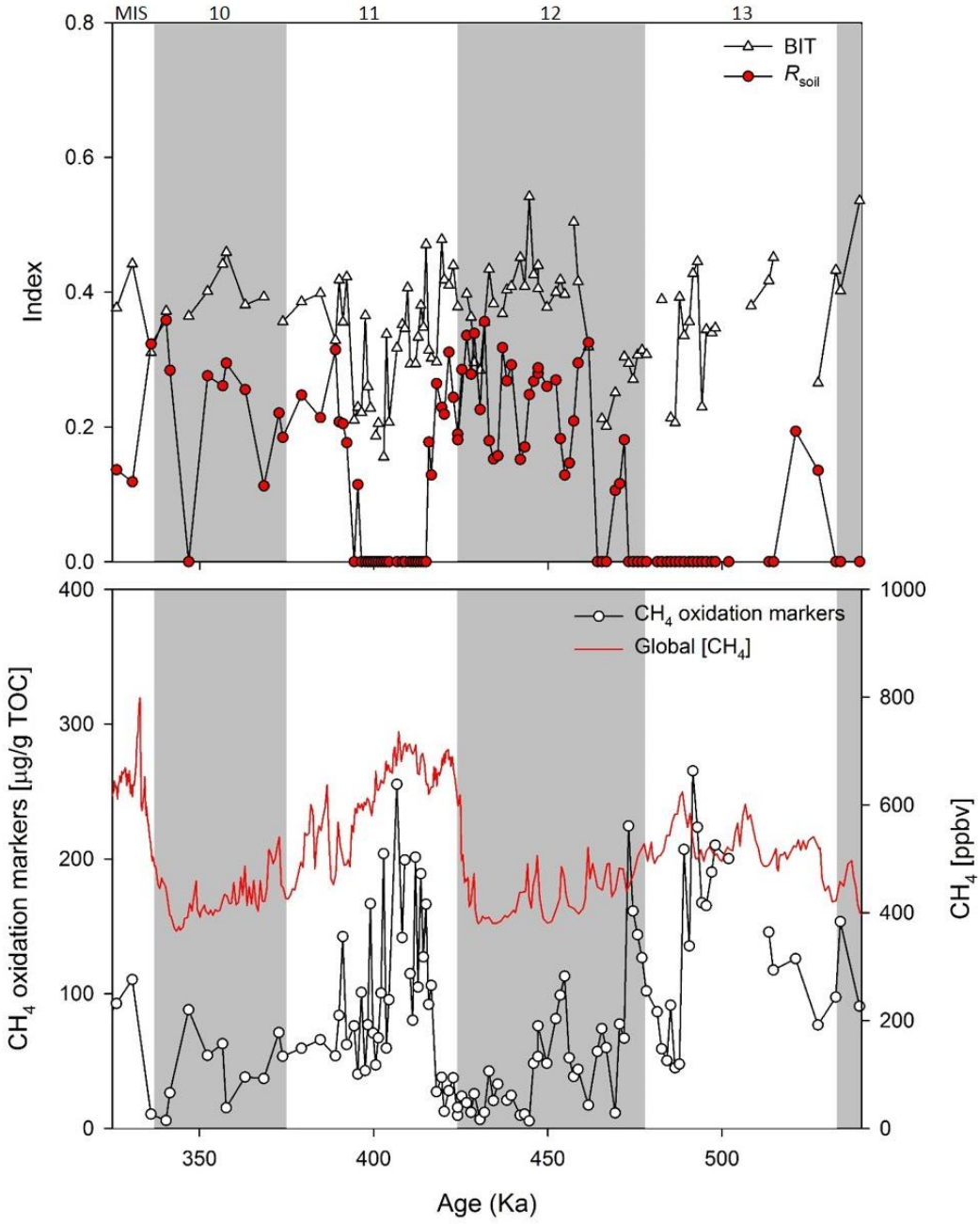

Figure 6.8. Concentration of CH_4 oxidation markers (µg/g TOC; ODP 1075), global CH_4 (Loulergue et al., 2008; Spahni et al., 2005), and BIT and R_{soil} indices (as reported in Chapter 4; ODP 1075). Grey bars indicate MIS 10 and 12.

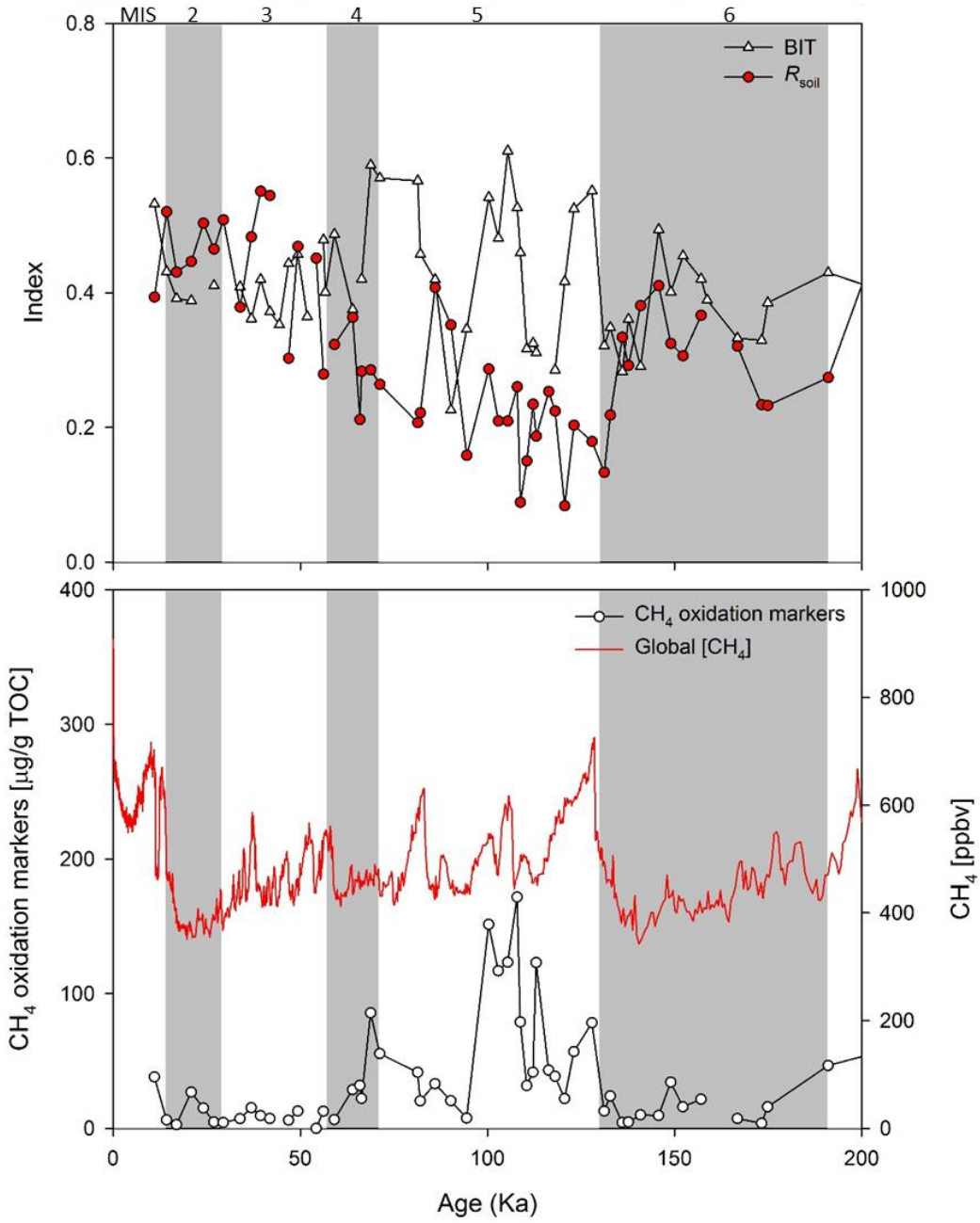

Figure 6.9. Concentration of CH_4 oxidation markers (µg/g TOC; ODP 1075), global CH_4 (Loulergue et al., 2008; Spahni et al., 2005), BIT and R_{soil} indices (as reported in Chapter 4; ODP 1075), from 10 Ka to 200 Ka. Grey bars indicate MIS 2, 4 and 6.

6.6.5.1. MIS 11-13

CH_4 oxidation marker signatures spanning MIS 13, the glaciation at MIS 12, and termination V (424 Ka; Lisiecki and Raymo, 2005) at MIS 11 show coherency with global CH_4 concentrations (Figure 6.8). During MIS 13, high concentrations of CH_4 oxidation markers are observed, followed by a reduction in CH_4 oxidation markers during the glaciation. An increase in CH_4 oxidation markers is then observed following termination V. During MIS 13, global CH_4 concentration increased to a maximum of 615 ppbv (Spahni et al., 2005) which is low compared to concentrations

during the LGM. Spahni et al. (2005) suggest the cause of the small rise in CH_4 could be due to colder interglacial temperatures during MIS 13, which, would have favoured methanotrophy over methanogenesis and thus contributing to lower net CH_4 emissions in the northern extra tropics, and/or the subtropical and tropical regions. The following glaciation during MIS 12 was cold with millennial timescale variations similar to those observed in the LGM. CH_4 concentrations during MIS 12 were low owing to glaciation of boreal CH_4 sources and the aridification of tropical CH_4 sources (Spahni et al., 2005). At termination V, global atmospheric CH_4 concentrations increased rapidly and were overall much higher during MIS 11 than during MIS 13 (Spahni et al., 2005). However, in our study a similar range in CH_4 oxidation markers is observed during both MIS 11 and 13. The BIT index also shows a similar range in values for both MIS 13 and 11 suggesting a similar supply of OM to the Congo fan during these warm intervals (Figure 6.8). Similarities in biomarker supply during MIS 11 and 13 could suggest that either (1) the total size of CH_4 oxidation marker source areas (i.e. wetlands) were comparable during both intervals; (2) the total size of CH_4 oxidation marker source areas were of a different but total CH_4 oxidation was similar; and (3) CH_4 oxidation during both MIS 11 and 13 had reached a threshold where maximal CH_4 had been consumed.

(1) total size of CH_4 oxidation marker source areas (i.e. wetlands) were comparable during both intervals

MIS 13 is a generally cooler warm stage with the interglacial of MIS 13 not fully reaching the high temperatures of other interglacials and is therefore described as an intermediate warm period (Spahni et al., 2005). The presence of high latitude ice sheets would reduce boreal CH_4 emissions resulting in a net reduction in global CH_4 emissions. Tropical CH_4 sources could have remained unaffected during this time and continued to produce CH_4 to be oxidised through methanotrophy. Miller and Gosling (2014) integrated palynological evidence from various sediment cores from the African west coast and found that, during MIS 11 and 13, Congo vegetation and habitat types were similar with palynology evidence for montane grassland and shrubland present during both time intervals. Miller and Gosling (2014) suggest minimum temperature within the Congo could have been as low as 12 and 22 °C during MIS 11 and 13 respectively. However, maximum temperatures are suggested to reach as high as 34 °C during both intervals. Precipitation could have ranged between 1000 and 3300 mm/yr during both MIS 11 and 13 (Miller and Gosling,

2014). This further suggests that generally cooler temperatures during MIS 13 may not have affected wetland extent and therefore CH_4 emissions within the Congo.

To date, few modelling and proxy studies exists comparing deglaciations and ice sheet collapse (of Greenland and Antarctica) of MIS 13 and 11, thus hindering our understanding of potentially non-linear responses during warm climate intervals. Isotope mixing model estimates of silt flux derived from each of Greenland's terrenes suggests the near complete deglaciation of Greenland during MIS 11 with the development of boreal forests (Reyes et al., 2014). Permafrost decomposition may not have been a general feature of MIS 11 with Siberian permafrost thought to have thawed (Vaks et al., 2013), but the discontinuous permafrost zone of the Yukon Territory (Canada) is thought to have persisted (Froese et al., 2008). Major ice rafting events have also been documented in North Atlantic sediment records (Vázquez Riveiros et al., 2013). This further suggests that high CH_4 concentrations present in ice core records during MIS 11 may be the result of northern hemisphere rather than tropical C sources thus explaining the similar range of concentrations of CH_4 oxidation markers in ODP 1075 during MIS 13 and 11

(2) total size of CH_4 oxidation marker source areas were of a different size but total CH_4 oxidation was similar

Spahni et al. (2005) suggest that cool climate conditions of MIS 13 could have favoured CH_4 oxidation over methanogenesis. Conversely, the warmer climate conditions of MIS 11 could have favoured methanogenesis over CH_4 oxidation. This simplistic analysis of microbial recycling of C is likely more complicated and will depend on the type of habitat where methanogenesis and methanotrophy is occurring coupled with environmental parameters. However, methanogenesis and methanotrophy in wetlands are known to be affected by temperature and moisture fluctuations. Under the proposed cool – dry environmental conditions of MIS 13 wetland extent and therefore CH_4 emissions could have been reduced. Within wetland type environments, dry events favour methanotrophy over methanogenesis and thus reduce CH_4 flux to the atmosphere (Liu et al., 2009; Vishwakarma and Dubey, 2010). For example, the Hongyuan peat deposits of the Tibetan Plateau show a long term drying out of the peat, coupled with a pronounced dry period during the Holocene (Zheng et al., 2014). Biomarker evidence from the Hongyuan peats suggest a reduction in methanogenesis coupled with an increase in methanotrophy, resulting in a net reduction in CH_4 flux to the atmosphere (Zheng et al., 2014). During

the warmer – wetter climate of MIS 11, while wetland extent could have increased, methanotrophy may have decreased due to a reduction in oxic wetland conditions, thus resulting in a similar CH_4 oxidation marker signature between both MIS 11 and 13.

(3) CH_4 oxidation during both MIS 11 and 13 had reached a threshold where maximal CH_4 had been consumed.

An alternative explanation for the high CH_4 oxidation markers during both MIS 11 and 13 could be due to an AMO threshold situation. van Winden (2011) incubated peat cores containing live sphagnum at 5 temperatures (5 to 25 °C) and found that CH_4 oxidation peaked at 20 °C but reduced at 25 °C, likely owing to reduced methanotroph activity and CH_4 solubility. Additionally, concentrations of aminopentol and aminotetrol were not found to linearly correlated with CH_4 cycling, with relatively high abundances of CH_4 oxidation markers found within mesocosms incubated at 25 °C. This could suggest that abundances of aminopentol and aminotetrol do not directly correlate with methanotroph activity. Additionally, these results could suggest that there is a threshold whereby high CH_4 production overwhelms the methanotroph community where there are also high concentrations of CH_4 oxidation markers synthesised. During MIS 11 and 13, high concentration of CH_4 could have been produced within Congo wetlands which subsequently overwhelmed the BHP producing methanotroph community resulting in high concentrations of CH_4 oxidation markers. To date, there remains no studies looking at the effect of increased CH_4 production on BHP producing methanotrophs using tropical samples.

6.6.5.2. MIS 2-6

As observed in MIS 10 and 12, low concentrations of CH_4 oxidation markers are observed during cool periods during this interval MIS 2-6 (Figure 6.9). Low concentrations of CH_4 oxidation markers could result from (1) decreased supply of these biomarkers to the Congo fan due to reduced OC_{ter}, or (2) a reduction in CH_4 oxidation marker source areas, e.g. a reduction in wetland extent. During MIS 6 low concentrations of CH_4 oxidation markers coincide with relatively high BIT index. A high BIT index suggests enhanced riverine supply of br-GDGTs to the Congo fan (Hopmans et al., 2004; Weijers et al., 2009) and could indicate enhanced OC_{ter}. This, therefore, suggests that low concentrations of CH_4 oxidation markers may not be the result of reduced OC_{ter} and, therefore, low concentrations of CH_4 oxidation markers

are most likely due to a reduction in AMO within the Congo hinterland during MIS 6. Dalibard et al. (2014) suggests the development of dry conditions during MIS 6 with limited export of humidity from the ocean inland due to reduced evaporation. These dry conditions would prevent the development of lowland forests, restricting them to refuges along river banks (Dalibard et al., 2014). This is in accordance with ∆-SST results, where a high ∆-SST is the consequence of relatively cool subtropics and relatively warm tropics corresponding to stronger trade winds and arid periods in equatorial Africa (Schefuß et al, 2005). This further suggests wetland extent as well as AMO was reduced during this time interval.

Some inter-climate variability is evident in the CH_4 oxidation marker record of the very well-studied MIS 5 sub-stages. At termination II (130Ka, Lisiecki and Raymo, 2005), Dalibard et al. (2014) suggests an expansion of savannah environments suggesting a relatively dry phase. Dry phases in African climate could be due to a delayed West African monsoon. This short dry episode is represented within the BHP record with a decline in CH_4 oxidation marker concentrations and coincides with insolation minima (Figure 6.10). Following the dry episode at MIS 5.5, humid conditions develop and a spread in lowland forest is observed (Dalibard et al., 2014). The development of more humid conditions coincides with an increase in CH_4 oxidation markers suggesting the expansion of wetland environments in response to increase West African monsoon intensification. During MIS 5.2, low concentrations of CH_4 oxidation markers are observed within ODP 1075 suggesting a reduction in wetland extent. West African monsoon intensity is reduced during MIS 5.2 resulting in drier climatic conditions within the Congo. At the end of MIS 5, a peak in CH_4 oxidation markers is observed, this peak coincides with West African monsoon intensity and results from the expansion of Congo wetlands during a humid climate. During MIS 4, the progressive instillation of glacial conditions sees a decline in CH_4 oxidation markers likely due to the reduction in wetland environments due to a dry climate.

Unusually, the concentration of CH_4 oxidation markers remains low throughout MIS 3 and 2. During these 2 intervals, variability in the BIT index is reduced suggesting OC_{ter} is more constant. Dalibard et al. (2014) suggests that West African vegetation shows important fluctuations during MIS 3 and 2. At the onset of MIS 3, a compression of the ITCZ leads to an expansion of dry open environments. A reduction in West African monsoon strength continues to the middle of 3 (3.2) leading

to conditions that are unsuitable to maintaining aquatic ecosystems and rainforest. Dalibard et al. (2014) suggests evidence for the expansion of less water dependent ecosystems such as savannah. Both CH_4 oxidation markers and ∆-SST records agree with Dalibard et al. (2014) suggesting greater continental aridity during MIS 3 and 2.

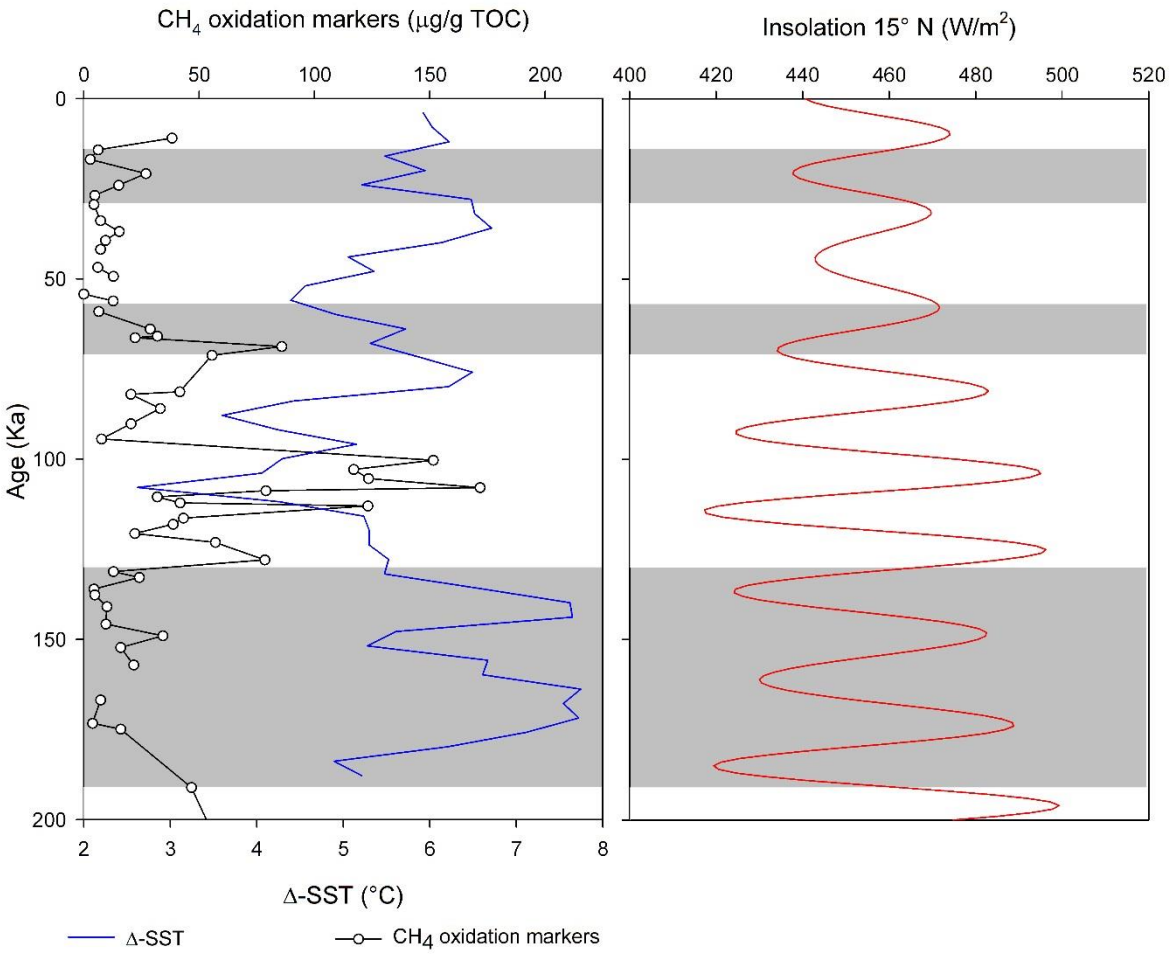

Figure 6.10. Concentration of CH_4 oxidation markers (µg/g TOC; black) compared with ∆-SST (°C; blue) and July insolation (15°N, W/m^2; red).

6.6.6. Potential as a CH_4 oxidation proxy

In chapter 4, high concentrations of adenosylhopane were found in ODP 1075. In this chapter we observe high concentrations of CH_4 oxidation markers to coincide with the absence of adenosylhopane (Figure 6.11).

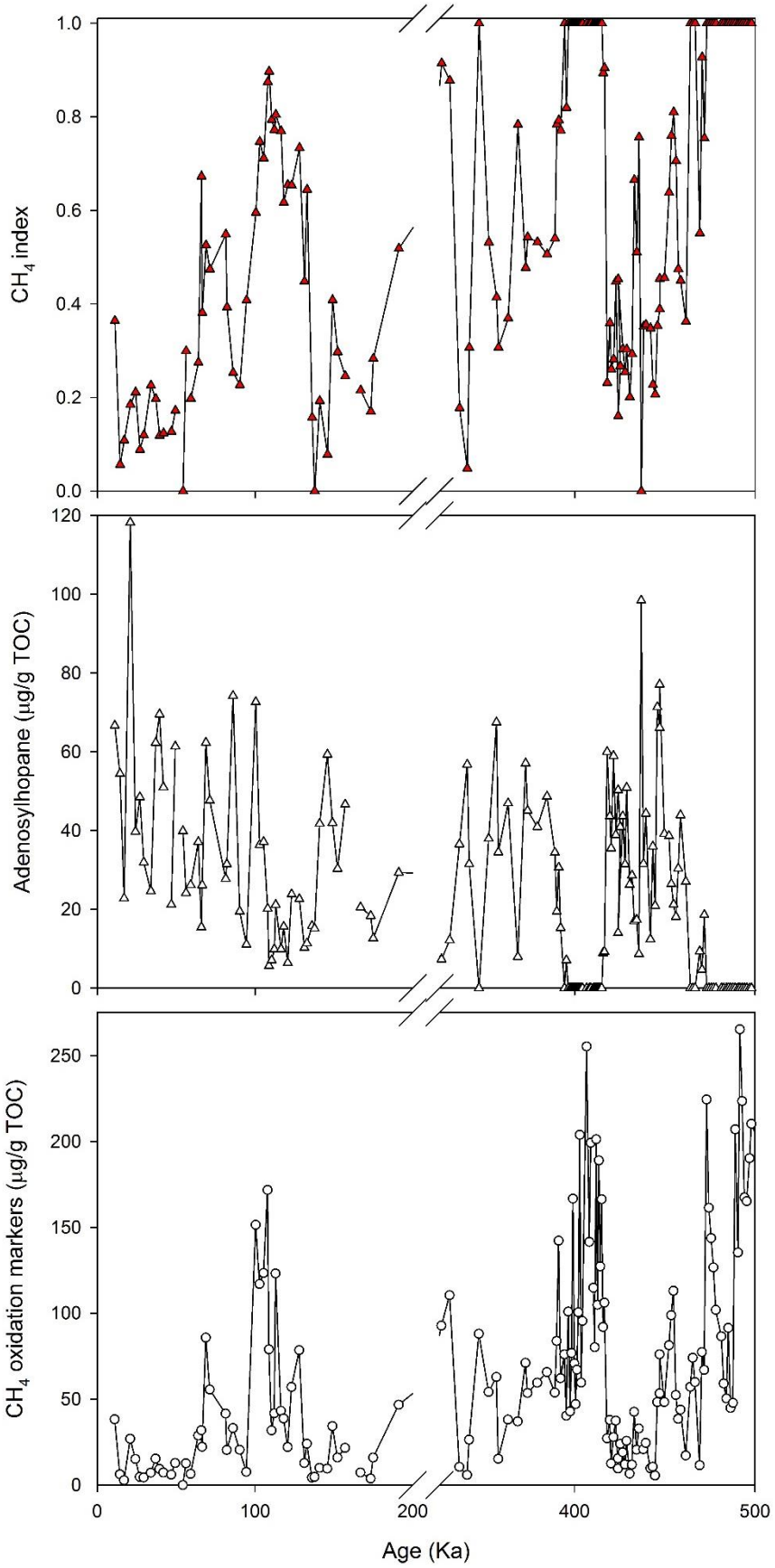

Figure 6.11. CH_4 oxidation marker and adenosylhopane concentration (µg/g TOC) and CH_4 index. Results from 200 – 325 Ka (i.e. low resolution sections) have been excluded from the plot.

This co-variance in adenosylhopane and CH_4 oxidation markers could represent two environmental end members. In Chapter 3, high concentrations of CH_4 oxidation markers were found to be limited to the Malebo pool wetland samples. Similarly Wagner et al., (2014) also found high concentrations of these biomarkers to be limited to wetland environments. In addition to this, the wetland samples analysed in Chapter 3 and Wagner et al. (2014) also contain low concentrations of adenosylhopane relative to other soils analysed in these studies. In contrast, the soil and savannah samples analysed in Chapter 3 had relatively high concentrations of adenosylhopane with CH_4 oxidation markers apparently absent. The contrast between adenosylhopane and CH_4 oxidation markers observed in ODP 1075 could be due to the expansion of wetland type environments resulting in a flux of CH_4 oxidation markers during wetland expansion (humid periods) and a flux in adenosylhopane during the expansion of soil/savannah environments (dry periods).

We suggest that where modern local BHP end members are constrained, the contrast between these two biomarker has the potential to be applied as a proxy for relative wetland expansion.

6.7. Conclusions

The aim of this chapter was to test the hypothesis "*Temporal changes in the concentration of biomarkers down core occur due to variations in terrestrial AMO intensity".* A range of C-35 amine BHPs are observed in ODP 1075 sediments, including aminotriol, aminotetrol and aminopentol (including unsaturated aminopentol and aminopentol isomer). In contrast to the record of adenosylhopane (Chapter 4), concentrations of the C-35 amines do not appear to show a strong degradation signature down core. Additionally, C-35 amine BHPs do not correlate with TOC further suggesting that concentrations of these compounds are not subject to enhanced diagenesis within ODP 1075. C-35 amine BHPs are also not found to correlate with OC_{ter} proxies (BIT and R_{soil} indices) suggesting that fluctuations of these primarily terrestrial compounds may not be due to variations in fluvial transport or coastal erosion. These results suggest that additional processes (i.e. climatic factors) may be determining distribution of C-35 amine BHPs in Congo fan sediments and these compounds are suitable biomarkers for reconstructing paleoclimate.

High concentrations of CH_4 oxidation markers were found during MIS 13, 11 and 5 and suggests enhanced C cycling during warm – humid time periods. Similar

concentrations of CH_4 oxidation marker signatures were found during both MIS 13 and 11 despite higher global CH_4 concentrations during MIS 11. The cause of this disparity between CH_4 oxidation markers in ODP 1075 and global CH_4 concentrations remains unclear. However, the similarity in CH_4 oxidation markers could suggest; (1) CH_4 sources in the Congo remained consistent during both MIS 11 and 13, with fluctuations in boreal CH_4 emissions driving variations in CH_4 concentrations observed in ice core records; (2) Congo wetlands experienced aridification during MIS 13 which enhanced AMO, producing high concentrations of CH_4 oxidation markers; or (3) a threshold has been reached, where, methanogenesis has overwhelmed the AMO buffer and CH_4 oxidation is high during both MIS 11 and 13, resulting in high concentrations of CH_4 oxidation markers. Similar biomarker signatures are observed during MIS 5, with high concentrations again suggesting enhanced CH_4 cycling.

These results indicate that production of CH_4 oxidation markers occurred in response to climatic conditions which favoured the expansion of wetland ecosystems. Similarly, high concentrations of these biomarkers correspond with a strengthening of the West African monsoon system, suggesting that these fluctuations in AMO were part of a larger orbitally forced response to climate.

Chapter 7:

Exploring Stratigraphic Limits of Aerobic Methane Oxidation Biomarkers: The Pleistocene Record from the Congo Fan

Chapter 7. Exploring Stratigraphic Limits of Aerobic Methane Oxidation Biomarkers: The Pleistocene Record from the Congo Fan

7.1. Introduction

Sedimentary archives from offshore West Africa reveal pronounced fluctuations in biomarker supply throughout the Pleistocene, recording fluctuations in insolation-driven African vegetation patterns (deMenocal, 2004) and carbon cycling (Jahn et al., 2005; Talbot et al., 2014). Of particular importance are sediments off major river mouths as they record almost directly climate and hydrological fluctuations in continental watersheds, via fluvial supply of mineral matter, including key nutrients, and terrigenous OC (e.g. Hinrichs and Rullkötter, 1997; Holtvoeth et al., 2001; Boot et al., 2006; Zhu et al., 2008; Wagner et al., 2014). Previous research has shown terrestrial derived OC as an important contributor to the bulk OM within Congo fan sediments (Holtvoeth et al., 2001; 2005; Schefuß et al., 2001; 2003; Spencer et al., 2012). What is not addressed is the relative importance of AMO in terrestrial C cycling in response to the Pleistocene aridity-humidity cycles of tropical Africa.

7.1.1. Pliocene-Pleistocene Climate Evolution

African climate records show a coupling between high and low latitude forcing after the onset of northern hemisphere glaciation near 2.8 Ma (deMenocal et al., 1993; 1995; Tiedemann et al., 1994; Clemens et al., 1996). Before the development of these high latitude ice sheets, early Pleistocene sedimentary records show West African climate to have varied at precessional timescales (19-23 Kyr) (deMenocal, 1995). The intensification of high latitude ice sheets and the influence of the cooling of sub polar oceans led to longer variations in West African climate (Raymo et al., 1990; Shackleton et al., 1990) at the orbital 41 and 100 Kyr periodicities (deMenocal, 2004). Throughout the Pleistocene, marine productivity has experienced significant changes at glacial-interglacial time scales (Holtvoeth et al., 2003; Jahn et al., 2005). During interglacial periods, marine productivity was mainly controlled enhanced siliceous production due to intense monsoonal runoff that maintained persistent high levels of nutrients off the Congo. Support for this scenario comes from Jahn et al. (2005), who observed high TOC MAR co-occurring with periods of low $\delta^{13}C_{org}$ values, high Fe intensities and increased boreal summer insolation suggesting increased OC accumulation consistent with enhanced fluvial supply during intense monsoonal

periods. Similarly, Holtvoeth et al. (2001) shows strong evidence that OM supply to the Congo deep sea fan was closely linked to precessional variations in the intensity of low – latitude African climate patterns. These orbital forced fluctuations in atmospheric circulation primarily controlled upwelling and productivity along the West African equatorial margin in addition to moisture supply to the continent, which influenced vegetation and weathering patterns and thus the export of terrigenous material by the Congo River (Holtvoeth et al., 2001). According to Head and Gibbard (2005) low Fe supply indicate that marine productivity shifted to primarily wind driven upwelling processes, consistent with strengthening of the trade winds and aridification of tropical Africa after the onset of the MPT. Enhancement of monsoon activity during interglacial periods is attributed to the northward migration of the ITCZ and consequently weakening of the NE trade winds. Conversely, the weakening of monsoon activity and strengthening of the NE trade winds during glacial periods limited zonal migration of the ITCZ and lead to smaller pressure gradients between the eastern South Atlantic and North Africa.

7.1.2. Pleistocene C Cycling

The global water cycle is an important control on terrestrial C cycling. Modulation of this cycle is achieved through glacial – interglacial climate cycles, which in the tropics is manifested by fluctuations of the monsoonal system (Guo et al., 2012). Such variations in the global and zonal water cycle results in important feedbacks on the C cycle, with earth system modelling identifying continental wetlands as important C sources and sinks (Beerling et al., 2011).

Paleoclimate analysis of West African marine sedimentary archives suggests significant variations in continental aridity and humidity cycles leading to the destabilisation of vegetation zones during the Pleistocene (Schefuß et al., 2003). Furthermore, high resolution biomarker analysis of sedimentary archives from the West African coast reveal a clear expansion in mangrove swamps during humid periods of the Pleistocene (Dalibard et al., 2014). The impact of habitat expansion during humid and arid periods on the C cycle, however, remains to be elucidated. It has been proposed that the expansion of mangroves and wetland environments during MIS 1 and 5 could have resulted in a significant increase in CH_4 flux to the atmosphere (Dalibard et al., 2014). Indeed, large-scale fluctuations in atmospheric CH_4 concentration have been observed in ice core records from Vostok station in

East Antarctica spanning the past 420 000 years with minimum concentrations of CH_4 within ice core records ranging from 320 to 350 ppbv and maximum CH_4 concentrations between 650 to 770 ppbv (Petit et al., 1999). Further support comes from a study by Loulergue et al. (2008) showing that changes in the strength of tropical CH_4 sources and sinks had an important control on the global atmospheric CH_4 budget during the past 800 000 years. However, direct measurements of atmospheric CH_4 concentration beyond 800 Ka are not available from ice cores, requiring a proxy approach to explore older time periods. Specific biomarker records are powerful proxies for reconstructing C cycling beyond this time period of direct measurements.

To date, determination of tropical CH_4 cycling via proxies has been difficult, largely due to a lack of appropriate diagenetically stable biomarkers (see Chapter 2, section 2.1 for further discussion). C-35 amine BHPs have been proposed as diagnostic biomarkers for AMO, due to the specificity of these compounds to methanotrophic bacteria (Neunlist and Rohmer, 1985a; Cvejic et al., 2000a; Talbot et al., 2003; Talbot and Farrimond, 2007; Zhang et al., 2007; Coolen et al., 2008; Cooke, 2010; Zhu et al., 2010; Kim et al., 2011; Sáenz et al., 2011a; van Winden et al., 2012a,b; Berndmeyer et al., 2013; Wagner et al., 2014). As these compounds are recalcitrant, previous work (Chapter 6) has shown C-35 amine BHPs to be highly suitable biomarkers for paleo reconstructions in sediments dated to 540 Ka. Furthermore, results summarised in Chapter 6 reveal high concentrations of these biomarkers during MIS 10 – 13, with a clear trend in high concentrations during humid MIS stages and periods of high atmospheric levels of CH_4.

7.2. Aims, Objectives and Scope

In this chapter we further test the suitability of C-35 amine biomarkers in paleoclimate reconstructions in ODP 1075 sediments and continue to explore the climate controls on these biomarkers. Chapter 7 tests the hypothesis; "*Ancient marine sediments record past terrestrial aerobic methane oxidation activity".* The aim of this chapter is to determine long term variability in terrestrial CH_4 cycling within the Congo fan for the entire Pleistocene. The objectives of this study are to increase the BHP analyses of ODP 1075 samples beyond 1.2 Ma to the maximum depth of 234 mcd (equivalent to about 2.5 Ma) to determine possible limitations of these unique biomarkers and to determine orbital driven climate controls on tropical CH_4 cycling far back in time.

The scope of this chapter will be to;

- Determine C-35 amine BHP inventory in ODP 1075 in samples >1.2 Ma
- Determine diagenetic controls on biomarker concentrations including correlation of these biomarkers with TOC.
- Determine if the relationship between C-35 amine BHPs (as discussed in Chapter 6) is maintained within the deeper core sections of ODP 1075.
- Determine the suitability of C-35 amine BHPs in deeper time paleoclimate reconstructions by assessing results of diagenetic and environmental controls.
- To determine if orbital forced climatic signals influence C-35 amine signatures within the Congo fan during the Pleistocene.

7.3. Overview of Methodology and Study Site

The study site has previously been described in Chapter 2. Briefly, Ocean drilling program (ODP) site 1075 was drilled as part of ODP leg 175 and is situated on the Northern part of the Congo deep-sea fan (4°47.1198'S, 10°4.4989'E; Figure 2.4) at 2996 m water depth.

7.3.1. Bulk and Geochemical Analysis

Bulk and geochemical analysis has previously been described in Chapter 2. Briefly, TOC (%) of ODP 1075 sediments was measured as detailed in Holtvoeth et al. (2001) and Chapter 2. Total lipids were extracted from approximately 3 g of freeze-dried sediment using a modified Bligh and Dyer extraction method as described by Talbot et al. (2007a) and further modified by Osborne, (PhD thesis, Submitted). An aliquot (one third) of the TLE was used for BHP analysis (Chapter 2, section 2.5) and one third was used for GDGT analysis. BHP analyses for 120 data points has previously been published in Talbot et al. (2014).

7.3.2. Compound Classification and Statistics

The abbreviated names of the compounds identified, characteristic base peak ions (*m/z*) and structure numbers are given in Chapter 2 (Table 2.7, Table 2.8, Table 2.9, Table 2.10). AminoBHPs include aminotriol (**1h**), unsaturated (**4/5h**) and methylated aminotriol (**2/3h**), aminotetrol (**1c**) and unsaturated aminotetrol (**4/5c**) and aminopentol (**1d**), unsaturated aminopentol (**4/5d**) and aminopentol isomer (**1d'**; van Winden et al., 2012b). BHPs diagnostic for AMO (hereafter referred to as "CH_4

oxidation markers") include aminotetrol, aminopentol, unsaturated aminopentol, and aminopentol isomer. Statistical analysis was performed using Minitab 17.1.0. CH_4 oxidation marker (μg/g TOC) data was found not to follow a Gaussian distribution, therefore, data was transformed using Box Cox. Upper and lower λ confidence limits are 0.20 and 0.39, rounded λ = 0.29. CH_4 oxidation marker concentration data was transformed using the optimal λ (0.29). Therefore Y (untransformed data) = $Y^{0.29}$. Following Box Cox transformation, CH_4 oxidation marker data was found to have a normal distribution. ANOVA with post hoc (Tukey) analysis was performed on transformed CH_4 oxidation marker data. Spearmans Rho (R_s) correlation index was performed on BHP abundances. The "aminopentol isomer index" is a ratio between aminopentol isomer and aminopentol (Equation 7.1).

Equation 7.1. "Aminopentol isomer index".

$$"Aminopentol\ isomer\ index" = \frac{(aminopentol\ isomer)}{(aminopentol\ isomer + aminopentol)}$$

An "aminopentol isomer index" >0.5 indicates a sample where aminopentol isomer concentration exceeds the concentration of aminopentol. An "aminopentol isomer index" <0.5 indicates a sample where the concertation of aminopentol exceeds the concentration of aminopentol isomer.

7.4. Results

High concentrations of C-35 amine BHPs persist within sediments beyond 1.2 Ma. Aminotriol (**1h**), aminotetrol (**1c**), aminopentol (**1d**) and unsaturated (**4/5d**) and aminopentol isomer (**1d'**) are present down to the bottom of ODP 1075, reaching >2.5 Ma (Figure 7.1 and Figure 7.2). Aminotriol is the most abundant C-35 amine BHP while aminopentol is the second most abundant C-35 amine and the most abundant CH_4 oxidation marker (Figure 7.1).

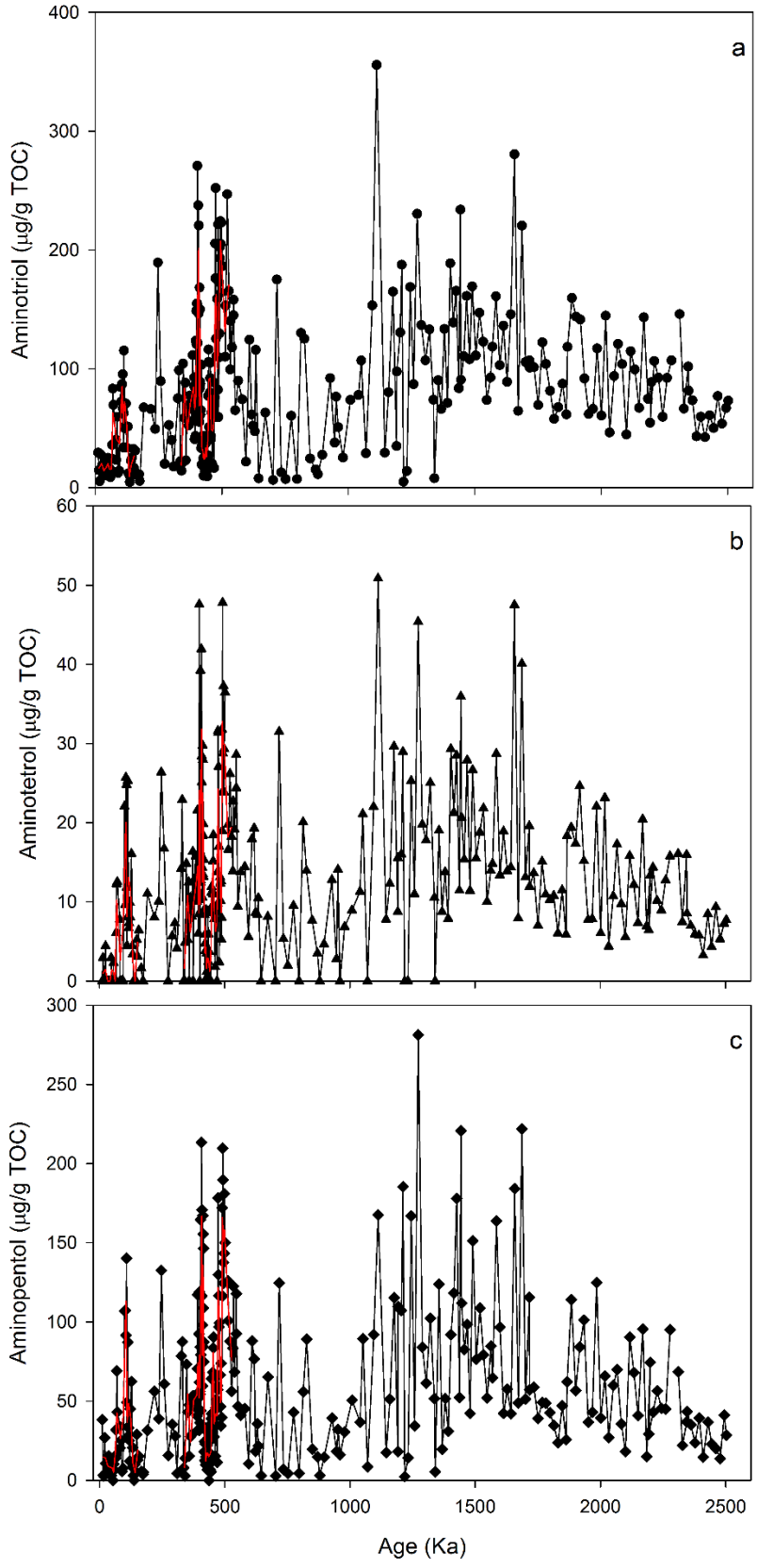

Figure 7.1. Concentration (µg/g TOC) of aminotriol (a), aminotetrol (b) and aminopentol (c) within ODP 1075 from 10 Ka to 2.5 Ma, error bar shows +/- 20% analytical error, red line indicates 3 point rolling average within high resolution sections.

In addition to the intermittent presence of unsaturated aminopentol (**4/5d**) in the high resolution sections (see chapter 6), this compound persists beyond 1.2 Ma (Figure 7.2). High concentrations of aminopentol isomer are also observed throughout the studied section of ODP 1075 (Figure 7.2).

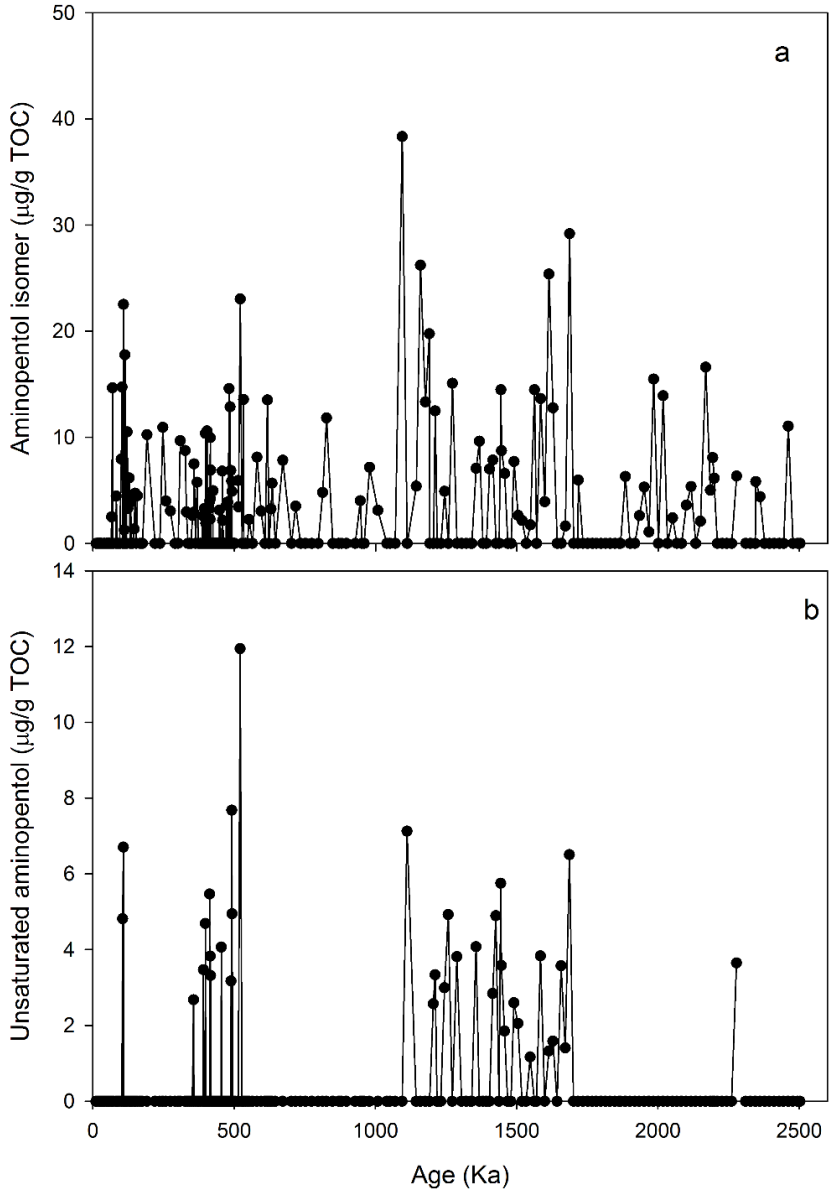

Figure 7.2. Concentration (µg/g TOC) of unsaturated aminopentol and aminopentol isomer within ODP 1075 from 10 Ka to 2.5 Ma, error bars show a 20% analytical error.

7.5. Discussion

7.5.1. Preservation of C-35 Amine BHPs

No clear diagenetic trends in aminotriol, aminotetrol, aminopentol and aminopentol isomer are evident, with all of these compounds present within ODP 1075 sediments dated to > 2.5 Ma. No correlation was found between TOC and aminotriol (R_S 0.101, p 0.079; Figure 7.3), aminotetrol (R_S -0.042, p 0.463), or aminopentol (R_S 0.006, p 0.920) concentration (µg/g dry sediment), suggesting that variations in C-35 amine BHP signatures are not driven by variations in TOC.

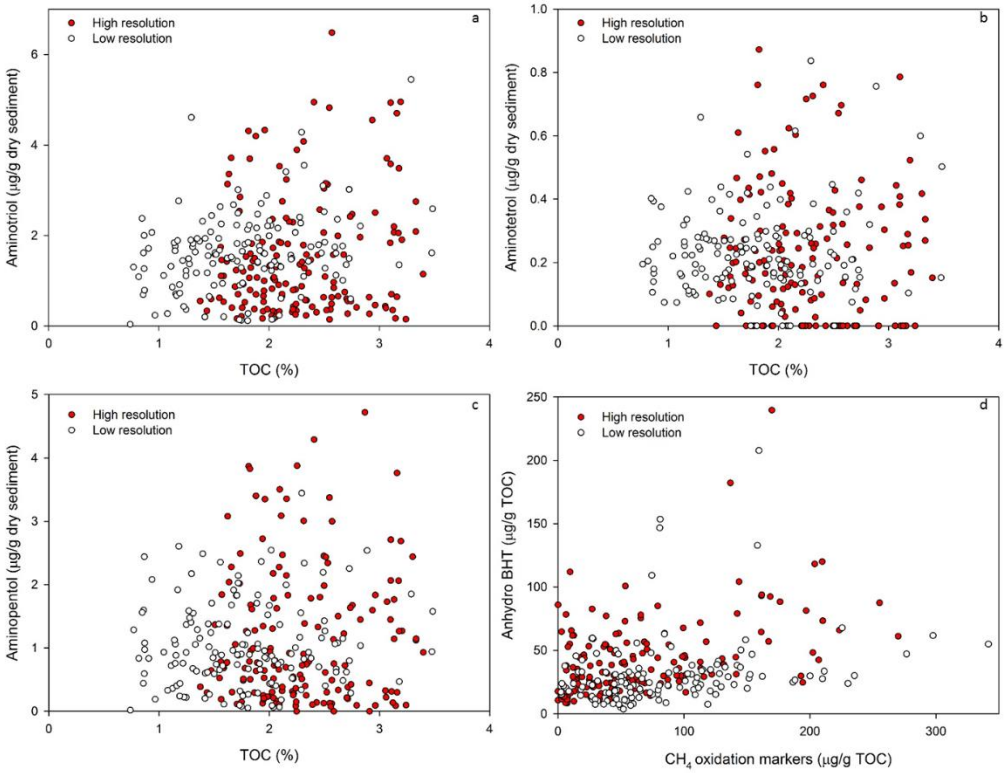

Figure 7.3. Correlation between TOC (%) and concentration (µg/g dry sediment) of aminotriol (a), aminotetrol (b) and aminopentol (c), and correlation between CH4 oxidation markers and anhydro BHT (µg/g TOC; d) in ODP 1075 within the high (red circles) and low (open circles) resolution sections.

Few published studies exist detailing the preservation of C-35 amine BHPs in ancient sediments. Wagner et al. (2014) identified CH_4 oxidation markers in Amazon fan and shelf sediments to a maximum core depth of 708 cm and dated to approximately 30 Ka. However, our results in the Congo deep sea fan represent the oldest and longest continuous record of CH_4 oxidation markers in sediments to date. As no clear diagenetic trend in CH_4 oxidation markers is evident we propose that these biomarkers may well be examined within potentially much older sediments. Furthermore, we also report the occurrence of unsaturated aminopentol and

aminopentol isomer within sediments dating to 2.2 Ma and 2.4 Ma, respectively. The presence of unsaturated aminopentol and aminopentol isomer in ODP 1075 is the oldest reported occurrence of these two compounds within marine sediments.

7.5.2. Environmental Controls

As discussed in Chapter 3 and Talbot et al. (2014) the origin of CH_4 oxidation markers on the Congo deep sea fan could be due to (1) allochthonous production of these biomarkers due to intense AMO occurring within wetlands/flood plain lakes, or (2) autochthonous production of CH_4 oxidation markers due to the destabilisation of shallow gas hydrates. Strong correlation is found between aminotriol and aminotetrol (R_S 0.904, p<0.05; Figure 7.4), aminotetrol and aminopentol (R_S 0.908, P<0.05) and aminotriol and aminopentol (R_S 0.891, <0.05), suggesting a common microbial source.

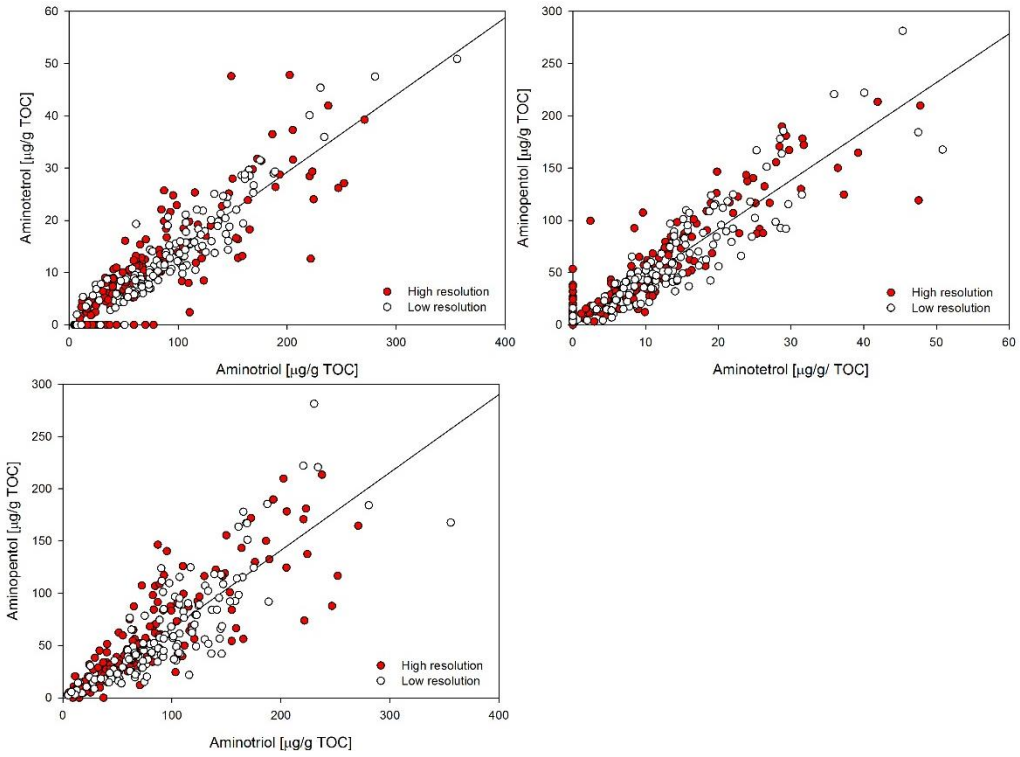

Figure 7.4. Correlation between aminotriol and aminotetrol (R_S 0.904, p<0.05), aminotetrol and aminopentol (R_S 0.908, P<0.05), and aminotriol and aminopentol (R_S 0.891, <0.05) within high (red circles) and low (open circles) resolution sections of ODP 1075.

Due to relatively heavy $\delta^{13}C$ of BHPs in ODP 1075 and the similarities in CH_4 oxidation signatures between ODP 1075 (Talbot et al., 2014) and the Congo wetland samples and (see Chapter 3), an allochthonous origin is considered the most likely source.

The sources of unsaturated aminopentol has been discussed in Chapter 6. Unsaturated aminopentol has similar type I methanotroph sources to aminopentol (van Winden et al., 2012b; Osborne, PhD thesis submitted). Generally, low concentrations of unsaturated aminopentol are present within 2 intervals in ODP 1075 (350 – 521 Ka and 1111 – 1686 Ka; Figure 7.2). Within ODP 1075 the relative abundance of unsaturated aminopentol ranges from 0 – 1.8% of total BHPs. Similarly, low relative abundance of this BHP is also found in modern Malebo pool wetland sediments (0.63 – 0.96% of total BHPs) and estuarine sediment (0.87% of total BHPs). Therefore, the Congo Malebo pool wetlands (and similar environments) remains as the source of unsaturated aminopentol in deeper parts of ODP 1075.

One study reports the presence of aminopentol isomer (**1d'**) within environmental samples (Wagner et al., 2014) and bacterial cultures. Aminopentol isomer has, to date, only been identified in 2 bacteria; *Methylovulum*-like strain M200 and *Methylomonas* like strain M5 (van Winden et al., 2012b). In both of these bacteria, aminopentol isomer is ~1.5% relative to aminopentol (van Winden et al., 2012b). The relative proportion of aminopentol isomer : aminopentol is higher within the modern Malebo pool wetland samples, where it ranges between 5.6% and 38%. However, within ODP 1075 samples, the relative abundance of aminopentol isomer to aminopentol ranges between 0 (where there is no aminopentol isomer present) to 222% (where the concentration of aminopentol isomer largely exceeds aminopentol; Figure 7.5). Aminopentol isomer relative abundance is greater than aminopentol relative abundance in 2 samples (Figure 7.5; sample at 37 mcd and 126.5 mcd). When these two samples are excluded aminopentol isomer : aminopentol does not exceed 100% with maximum values of 86%. To date, such high abundance of aminopentol isomer has not been reported in the literature. Further research into the provenance of aminopentol isomer is required to fully investigate the down core signatures of this BHP.

The relative abundance of aminotetrol, aminopentol, and aminopentol isomer is shown in Figure 7.6. Samples from ODP 1075 reveal a greater range in the relative abundance of aminopentol isomer compared with the modern Congo hinterland soil and wetland samples (Figure 7.6). One forest soil (closed evergreen lowland forest C18B) and the estuarine sediment show comparatively high relative abundance of aminopentol isomer (>10%) which could suggest a difference in microbial/environmental source compared to the other soils and wetlands samples.

However, it should be noted that analysis of a wider range of Congo soils is required to confirm this.

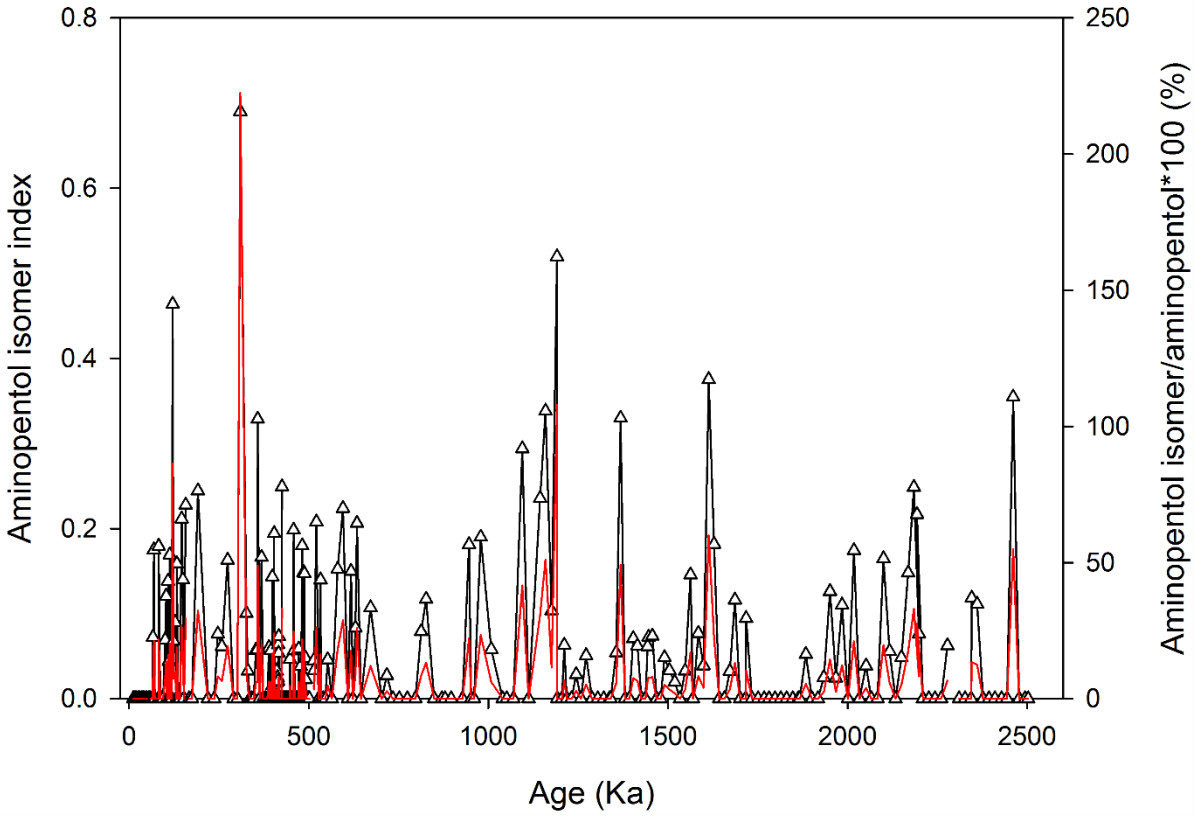

Figure 7.5. Aminopentol isomer index (= aminopentol isomer / (aminopentol isomer + aminopentol); triangles) within ODP 1075. An aminopentol isomer index of above 0.5 indicates a sample where aminopentol isomer concentration exceeds the concentration of aminopentol. An aminopentol isomer index below 0.5 indicates a sample where aminopentol concentration exceeds aminopentol isomer concentration. Aminopentol isomer as a percentage of aminopentol (%; red line).

CH_4 oxidation marker concentration does not correlate with BIT (µg/g TOC; R_s 0.174, $p < 0.05$; Figure 7.7) suggesting that factors controlling supply of CH_4 oxidation marker and BIT compounds to the Congo fan are not similar. These results are in agreement with results from Chapter 6 indicating that CH_4 oxidation markers and BIT index represent different reservoirs of the terrestrial carbon pool. CH_4 oxidation marker signatures in ODP 1075 are proposed to be primarily controlled by fluctuations in aridity and humidity cycles due to resulting changes in wetland extent (see discussion in Chapter 6, section 6.6.5). While some of the br-GDGTs identified in ODP 1075 will be sourced from Congo soil environments, the GDGT composition of the Congo fan will also be influenced by export of br-GDGTs from aquatic systems (e.g. rivers and lakes)..

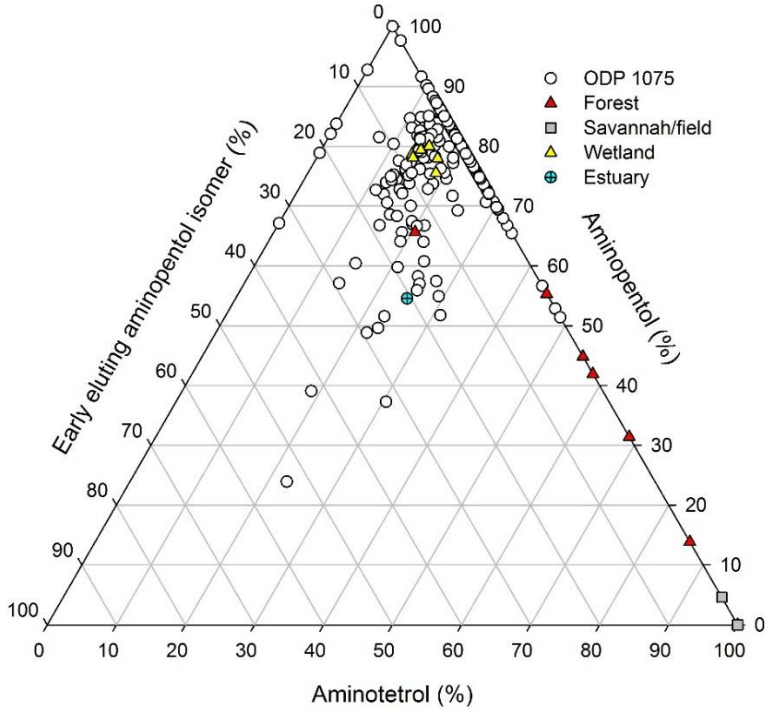

Figure 7.6. Relative abundance of aminotetrol, aminopentol and aminopentol isomer within ODP 1075 (open circles; n = 304) compared with modern Congo hinterland samples including forest soil (red triangles; n= 16), savannah/field soil (grey squares overlapping at right vertex; n = 6), wetland (Malebo pool) sediment (yellow triangles; n = 6) and estuarine sediment (blue circle; n = 1).

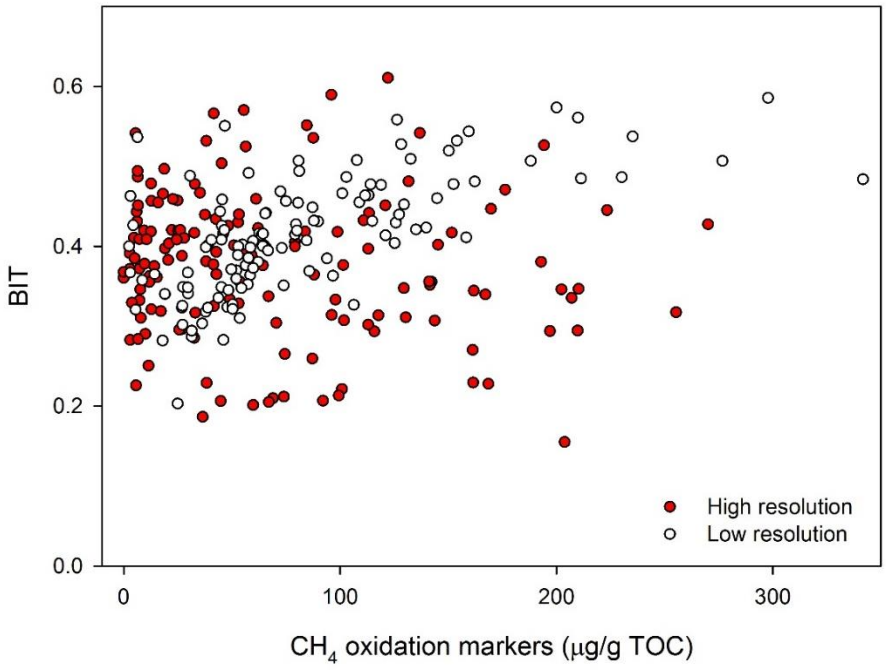

Figure 7.7. Correlation between concentration of CH_4 oxidation markers (µg/g TOC) and BIT index in high resolution sections (red; 10 Ka – 200 Ka and 350 Ka – 540 Ka) and low (open; remaining samples) resolution sections in ODP 1075.

7.5.3. Climate Controls

Concentrations of CH_4 oxidation markers are highly variable down core. Peak concentrations in CH_4 oxidation markers occur at 1686 Ka (270 µg/g TOC), 1271 Ka (330 µg/g TOC) and 491 Ka (270 µg/g TOC). Starting at the Pliocene/Pleistocene transition (2.5 Ma), a steady increase in CH_4 oxidation marker concentration is observed (Figure 7.8). This coincides with an increase in the relative abundance of CH4 oxidation markers compared to total BHPs (%; Figure 7.8). The increase in both the concentration and relative abundance (%) of CH_4 oxidation markers suggests a shift in the terrestrial BHP producing community, and an increase in AMO.

Between 1865 and 1713 Ka (hereafter referred to as interval 'a') a clear decrease in CH_4 oxidation marker concentration is observed. This reduction in CH_4 oxidation marker concentration does not correlate with the BIT index (Figure 7.9). The absence of a clear correlation between CH_4 oxidation markers and the BHP degradation product anhydro BHT (**1o**; Figure 7.3d) over this interval also excludes differences in preservation. A similar reduction in CH_4 oxidation markers (µg/g TOC) is also observed during 1099 Ka and 826 Ka (hereafter referred to as interval 'b'; Figure 7.8). Previous analysis of marine sediments from offshore Africa reveals that subtropical African climate periodically oscillated between wet and dry climate conditions (deMenocal, 2004). Furthermore, a marked increase in African climate variability and aridity has been documented near 1.7 Ma and 1 Ma (deMenocal, 2004; Trauth et al., 2007). These observations suggest that the reduction in CH_4 oxidation markers at intervals 'a' and 'b' within ODP 1075 may document a widespread change in African ecology. Increased continental African aridity could have reduced wetland extent and therefore reduced the production and supply of CH_4 oxidation markers to the Congo fan. These arid intervals are consistent with the onset and amplification of high latitude glacial conditions (deMenocal et al., 1993; Tiedemann et al., 1994; deMenocal, 1995; Clemens et al., 1996).

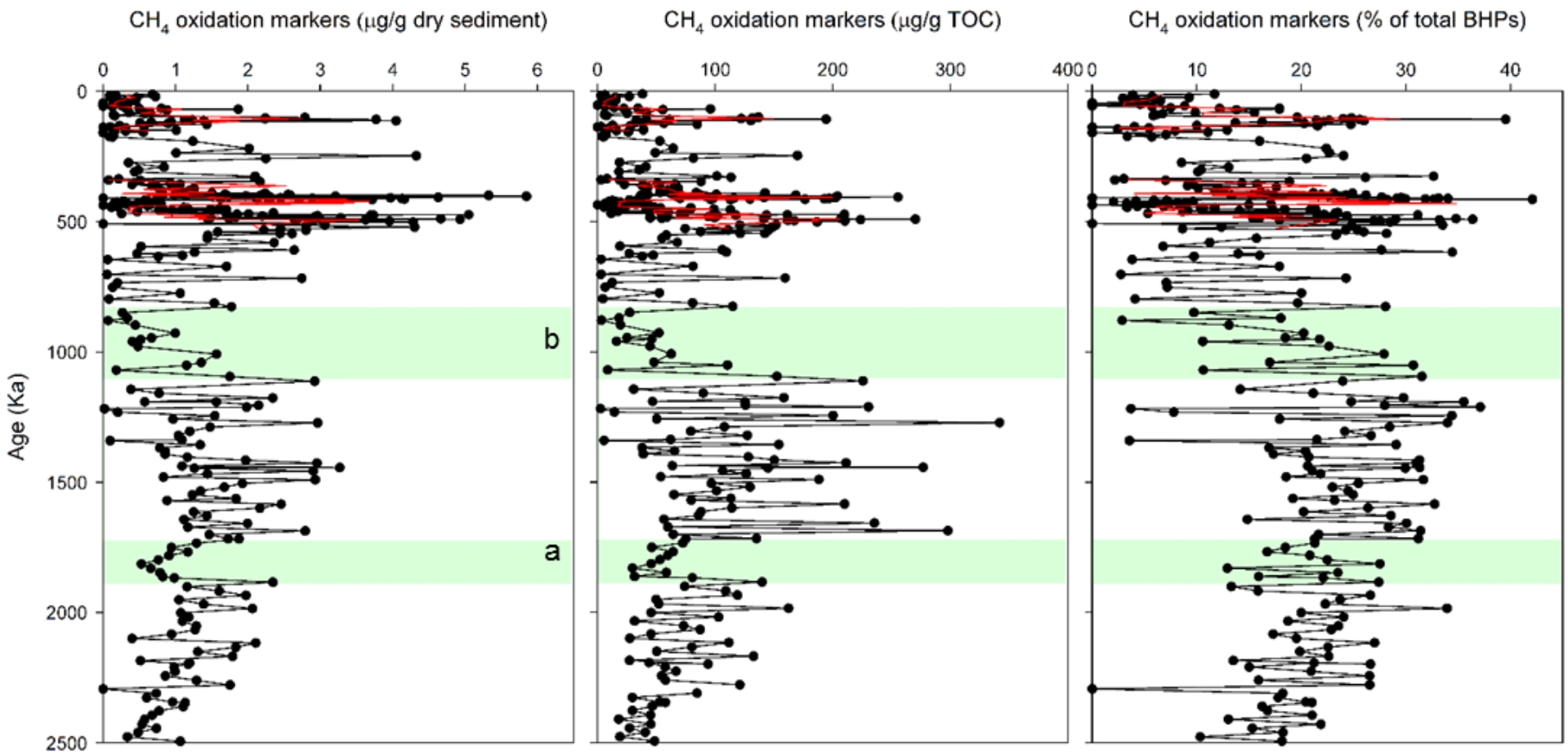

Figure 7.8. CH_4 oxidation marker concentration (μg/g sediment and μg/g TOC) and relative abundance (% of total BHPs) in ODP 1075, red line indicates 3 point rolling average. Green panel 'a' represents an interval from 1865-1713 Ka and green panel 'b' represents an interval from 1099-826 Ka.

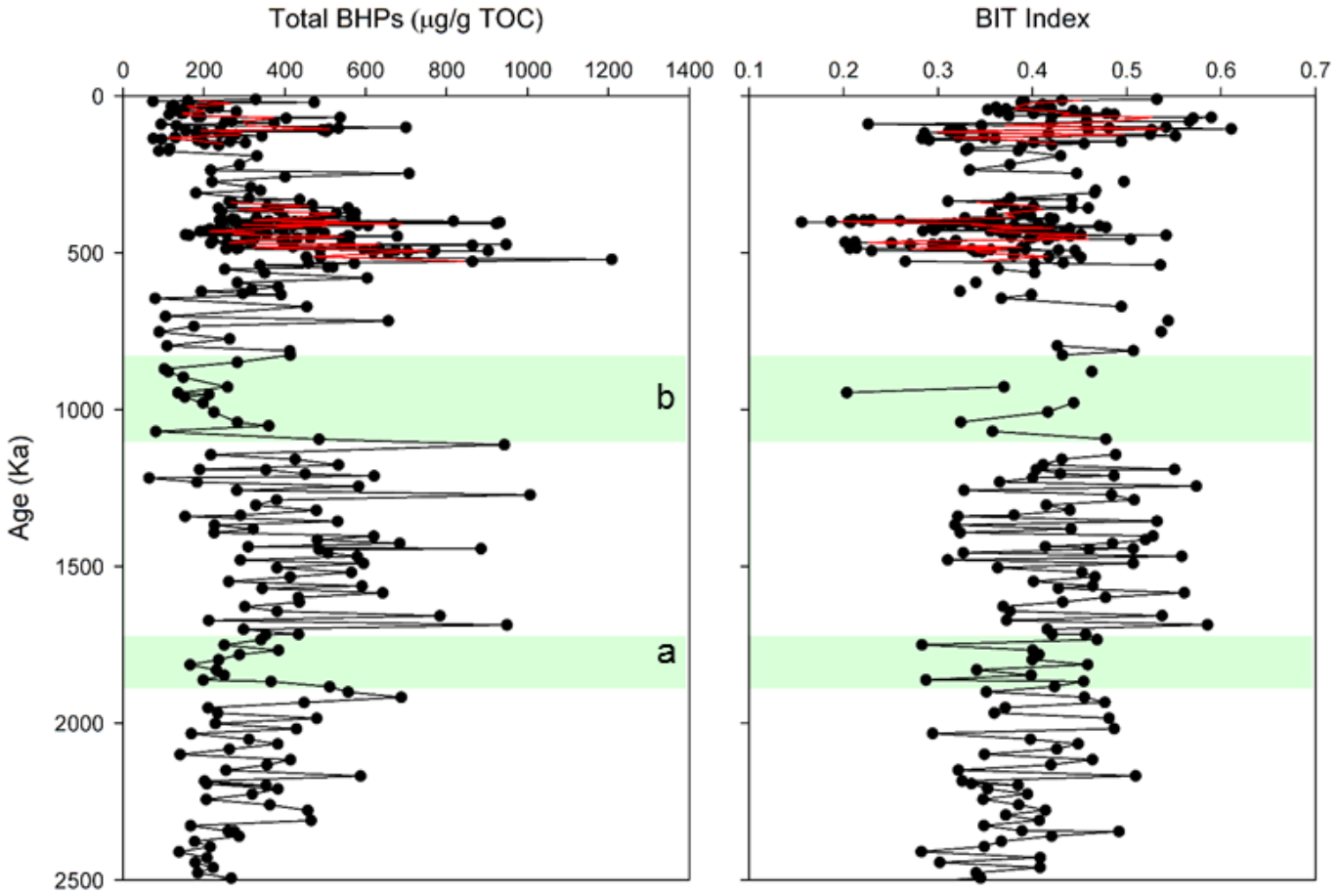

Figure 7.9. Concentration of total BHPs (µg/g TOC) and BIT index in ODP 1075, red line indicates 3 point rolling average. Green panel 'a' represents an interval from 1865-1713 Ka and green panel 'b' represents an interval from 1099-826 Ka.

In addition, mean CH_4 oxidation marker signatures (µg/g TOC) for the Jahn et al. (2005) intervals (as described in Chapter 4) show significant variability during the Pleistocene (ANOVA F 18.53, P <0.05; Figure 7.10), with marked increases in mean CH_4 oxidation marker concentrations for the 2.5 – 1.7 Ma and 1.7 – 1.1 Ma intervals. CH_4 oxidation marker concentrations following 1.7 Ma are shown to significantly decrease with the lowest mean CH_4 oxidation marker concentrations occurring during the 0 – 0.3 Ma interval (Table 7.1).

Table 7.1. ANOVA Post Hoc Tukey results (T and P values) mean CH_4 oxidation marker concentration (µg/g TOC), transformed using box-cox of λ 0.29 between intervals 0 – 0.3 Ma, 0.3 – 1.1 Ma, 1.1 – 1.7 Ma and 1.7 – 2.5 Ma.

Interval	0 - 0.3 Ma		0.3 - 1.1 Ma		1.1 - 1.7 Ma	
	T	P	T	P	T	P
0.3 - 1.1 Ma	5.23	<0.05				
1.1 - 1.7 Ma	7.36	<0.05	3.69	<0.05		
1.7 - 2.5 Ma	4.22	<0.05	-0.08	1	-3.12	<0.05

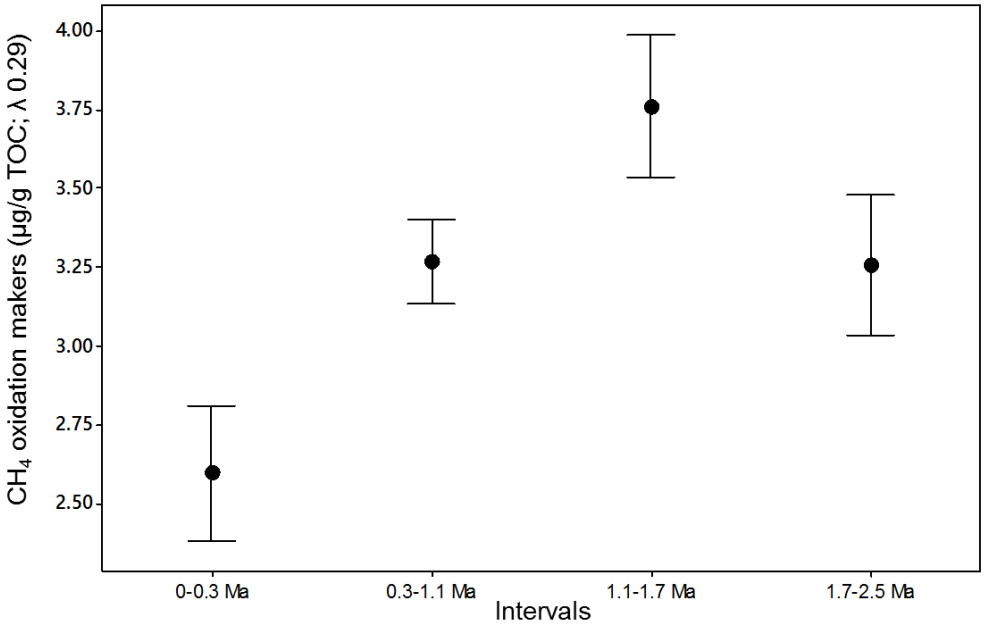

Figure 7.10. Interval plot showing mean and 95% confidence interval bar for CH_4 oxidation marker concentration (µg/g TOC), transformed using box-cox of λ 0.29 (see section 7.3.2 for further details), between intervals 0 – 0.3 Ma, 0.3 – 1.1 Ma, 1.1 – 1.7 Ma and 1.7 – 2.5 Ma.

Integrated terrestrial and marine paleoclimate records from Africa suggest a trend towards greater aridity during the Pleistocene (deMenocal, 2004). Consistent with this, Trauth et al. (2009) observe higher dust fluxes at approximately 1.4 – 1.9 Ma and significantly higher dust fluxes at 1 Ma. Strong increases in dust fluxes document an overall increase in African aridity, consistent with shifts in vegetation from C3

(trees and shrubs) to C4 (tropical grasses) plants observed within Pleistocene paleosol records (Ségalen et al., 2007). We therefore suggest that the pronounced decrease in CH_4 oxidation marker concentration between 1.7 Ma and 0.3 Ma (Figure 7.10) in ODP 1075 document a reduction in wetland and wetland type environments. Within the wider Congo catchment, continental aridity and humidity cycling is controlled by contrasts in tropical and subtropical SST (Schefuß et al., 2003). During the mid-Pleistocene (1.2 Ma – 0.45 Ma), a lower tropical Atlantic SST is observed to reduce evaporation and atmospheric moisture content, leading to large scale aridification (Schefuß et al., 2003). During these periods of enhanced aridity, C4 plant habitats should have expanded and persisted leading to a reduction in terrestrial CH_4 oxidation and consequently a reduction in CH_4 oxidation markers.

7.6. Conclusions

The aim of this chapter was to test the hypothesis "*Ancient marine sediments record past terrestrial aerobic methane oxidation activity".* A range of C-35 amine BHPs were identified in ODP 1075, including aminotriol, aminotetrol, aminopentol, unsaturated aminopentol and aminopentol isomer and were found to persist within sediments dated up to 2.5 Ma. To date, this is the oldest known occurrence of C-35 amine BHPs within sedimentary records. Similar to Chapter 6, aminotriol, aminotetrol, aminopentol and aminopentol isomer do not show a clear down core degradation trend. Furthermore, no clear correlation is observed between TOC and C-35 amine BHPs suggesting that variations in BHP concentration within ODP 1075 are not driven by this parameter. In agreement with Chapter 6, strong correlation is observed between aminotriol, aminotetrol and aminopentol suggesting a similar microbial source for these compounds. Similar to Chapter 6, no correlation between BIT and CH_4 oxidation markers (µg/g TOC) is observed, suggesting that while BHPs and GDGTs are supplied to the Congo fan by the Congo River, the factors controlling the supply, deposition and burial on the Congo fan are not similar.

CH_4 oxidation marker concentration is highly variable down core within ODP 1075. Low concentrations of CH_4 oxidation markers are observed during two intervals (1865 and 1713 Ka, 'a'; 1099 and 826 Ka, 'b') supporting a reduction in wetland extent in response to more arid tropical African environments, consistent with an increase in climate variability and aridity near 1.7 Ma and 1 Ma (deMenocal, 2004), possibly connected to an amplification of high latitude glacial cycles. Furthermore, a

long term reduction in the concentration of CH_4 oxidation markers is observed within ODP 1075 sediments. This decrease in biomarkers supports a long term trend towards greater continental aridity within the Congo and could, therefore, suggest further changes in vegetation zones.

Chapter 8:

Conclusions and Future Work

Chapter 8. Conclusions and Future Work

8.1. Conclusions

The overall aim of this thesis was to identify the microbial response to short term climate fluctuations within the continental catchment of the tropical Congo deep sea fan. This project builds on existing biomarker records from the Congo Fan, which suggests intense AMO (high concentration of BHP CH_4 oxidation markers) from an unknown source during Pleistocene interglacial periods (see Talbot et al., 2014). Bacteriohopanepolyol signatures within soils and sediments from the Congo catchment were analysed in order to determine modern BHP end members and terrestrial sources of BHPs within the deep sea fan deposits (Chapter 3). R_{soil} and BIT indices were measured within ODP 1075 sediments to determine soil OC transport during the Pleistocene. Further, amino BHP signatures were analysed to trace fluctuations in CH_4 cycling in the past. This project extends the BHP record back to ~ 2.5 Ma and demonstrates that amino BHP biomarkers provide an invaluable record of CH_4 cycling in geological sediments.

8.1.1. Sources of BHPs in the Congo Fan

Bacteriohopanepolyols have been identified in many environmental samples including soils, wetland sediments, suspended particulate matter, and continental shelf and marine sediments (see Table 2.1). Past environmental studies identify greater BHP structural diversity and high BHP concentrations within terrestrial samples compared with marine samples (for examples see; Cooke et al., 2008a; Zhu et al., 2011; Wagner et al., 2014). However, sediments analysed from continental margins and fans contradict this general trend in that they contain comparatively high concentrations of BHPs and include higher BHP structural diversity than entirely marine samples (Wagner et al., 2014). Sediments from the Congo fan have previously been found to contain high concentrations of BHPs (Cooke et al., 2008b; Handley et al., 2010; Talbot et al., 2014), of either autochthonous or allochthonous sources. Under modern and late Quaternary climate conditions, Congo fan sediments are significantly impacted by terrestrial OC transport (Holtvoeth et al., 2001; Holtvoeth et al., 2005; Jahn et al., 2005) suggesting that the BHP biomarkers observed could be transported from terrestrial source areas. BHP analysis of modern soil and sediment from the Congo catchment found a high abundance of similar

BHPs identified within both the Congo catchment samples and the fan samples (Chapter 3). CH_4 oxidation markers (**1d**, **4/5d**, **1d'**, **1c**) were found in high concentrations in both the Congo wetland, the estuary and the Congo fan, supporting the conclusion that these BHPs are of terrestrial origin (Talbot et al., 2014; Chapter 3). Furthermore, relatively light compound specific $\delta^{13}C$ of C-30 and C-31 hopanols mainly derived from BHP CH_4 oxidation markers suggest these compounds are not primarily of marine origin (Talbot et al., 2014).

Saturated BH cyclitol ethers (**1i**, **1j**, **1k** and methylated homologues) were also found to be relatively abundant in both the catchment (Chapter 3) and the Congo fan samples arguing for a terrestrial origin of these BHPs (Chapter 5). However, BH cyclitol ethers have also been found to be synthesised by marine bacteria. BH cyclitol ether signatures are, therefore, likely an integrated terrestrial and marine signal.

Within ODP 1075 low concentrations of unsaturated BHT (**4/5g**) and unsaturated BHT cyclitol ether (**4/5i**) and guanidine substituted cyclitol ether (**1p**) were identified (Chapter 5). These three compounds were not detected in the Congo hinterland samples suggesting a marine source. Additionally, the presence of unsaturated BHT and unsaturated BHT cyclitol ether in the Congo fan deposits have previously been attributed to marine cyanobacterial blooms (*Trichodesmium* spp; Handley et al., 2010).

Wetlands are a major sink of CH_4 emissions from sediments preventing its release to the atmosphere (Wuebbles and Hayhoe, 2002). The primary mechanism is AMO from a diverse group of methanotrophs, including many hopanoid synthesising bacteria (Henckel et al., 2001; Dedysh, 2009; van Winden et al., 2012b). Sediment from Malebo pool wetland was found to contain high concentration and high relative abundance of CH_4 oxidation markers, identifying this site as a location of intense AMO (Chapter 3). The data agrees with recent investigations of BHP signatures within the Amazon where Wagner et al. (2014) suggest wetland type environments as source areas for BHP CH_4 oxidation markers signatures. This Congo study is the second to document such high abundance of CH_4 oxidation markers within tropical wetland samples. We speculate that high concentrations of CH_4 oxidation markers may be a more general feature of tropical and possibly other wetlands.

8.1.2. Global Distributions of BHPs

BHP signatures determined in Congo soil and wetland sediment are compared with signatures reported from other published soils. The data presented here suggest that BHP relative abundance may be controlled by large scale climate trends. Within the soils and wetlands from the Congo Basin, a narrow range in soil marker BHP relative abundance (7.9-36% of total BHPs) and tetrafunctionalised BHP relative abundance (52-81% of total BHPs) was observed (Chapter 3 Figure 3.8). The range is much smaller in comparison with studies from other less stable (higher latitude) climatic zones, where surface soil marker BHP relative abundance varies between 0% and 66% of total BHPs and tetrafunctionalised BHP relative abundance varies between 34% and 100% of total BHPs (Cooke et al., 2008a; Xu et al., 2009; Rethemeyer et al., 2010; Kim et al., 2011). Furthermore, mean soil marker BHP relative abundance for Congo soils (17%) is distinctly lower than that for temperate soils from northern and eastern Europe (28%; Cooke et al., 2008a; Redshaw et al., 2008). These differences may indicate that the main factors controlling BHP distributions in tropical climate zones are different from those from temperate and polar climate zones. Our initial observations on BHP variation across climate zones leads us to propose that variation in BHP relative abundance in soils is controlled by the magnitude of local seasonal temperature contrasts. This hypothesis suggests that, in addition to in situ environmental parameters (e.g. pH), contrasts in MAAT impact on hopanoid producing microbial communities and their BHP signatures preserved in soils, on a regional scale.

8.1.3. BHP degradation

Bacteriohopanepolyols are recalcitrant biomarkers, however, the structural diversity of these compounds (unsaturation, methylation, amine and sugar moieties) may suggest differences in terms of preservation in sediments. Degradation of adenosylhopane in ODP 1075 has previously been reported with this BHP absent below 900 Ka (55 mbsf; Handley et al., 2010). Adenosylhopane (**1a**) is the only soil marker BHP detected in ODP 1075 with methylated adenosylhopane (**2a**), and group 2 (**1e**) and 3 (**1f**) soil marker BHPs absent (Chapter 4). In stark contrast, a full suite of soil marker BHPs (including methylated and group 2 and 3 soil markers) were identified in the soil and wetland samples (Chapter 3). As group 2 and 3 soil marker BHPs were likely be transported down the Congo catchment through similar transport

mechanisms as adenosylhopane, the absence of these compounds in ODP 1075 may point to degradation. BHP data from GeoB 6518-1 (a gravity core located on the Congo shelf; 40 Ka; Spencer-Jones et al., in prep; Schefuß et al., in prep.) shows the presence of a full suite of soil marker BHPs suggesting that these compounds are transported down the catchment. We speculate that different soil marker BHPs have different reactivities and thus degrade at different rates during fluvial transport and deposition within the marine sediments. Differences in the provenances of the different soil marker BHPs could, therefore, be due to differences in the moieties at C-35, however, the structures of group 2 and 3 adenosylhopane has yet to be fully elucidated.

C-35 amine BHPs and BH cyclitol ether BHPs are the other major group of BHPs within the Congo catchment. These samples do not show a clear down core degradation pattern suggesting C-35 amine BHPs can be used to trace past CH_4 cycling in sediments deeper/older than ODP 1075. C-35 amine BHPs and BH cyclitol ethers were identified to a maximum depth of 226 mcd (2.5 Ma; Chapters 5 and 7).

8.1.4. Soil Organic Carbon Transport During the Pleistocene

Congo fan sediments contain an integrated signal of both marine and terrestrial biomarkers. Previous studies have shown Congo fan sediments to be significantly impacted by terrestrial OC inputs (Holtvoeth et al., 2001; 2005). Results summarised in Chapter 3 show the Malebo pool R_{soil} end member to be 0.67, with the mean R_{soil} for ODP 1075 sediments to be 0.33. This suggests ODP 1075 sediments to be significantly impacted by microbial soil OC transport.

As anticipated variations in BIT and R_{soil} indices correspond with orbital cycling, as a result of large scale changes in Congo hydrology and vegetation zones, which in combination, impact on the type and abundance of OC_{ter} exported to the Congo fan. However, as has been shown for MIS 5 and MIS 11, the amplitude in precessional forcing needs to pass a threshold level to translate into biomarker signatures in the fan sediments.

8.1.5. A Record of Intense CH_4 Cycling During the Pleistocene

High concentrations of aminotriol (**1h**), aminotetrol (**1c**) and aminopentol (**1d**) were found throughout ODP 1075 sediments. Strong correlation between C-35 amine BHPs suggests these compounds have similar environmental origins. High

concentrations of CH_4 oxidation markers were found during MIS 13, 11 and 5. High concentrations of CH_4 oxidation markers suggests enhanced C cycling during at glacial-interglacial timescales. Similar concentrations of CH_4 oxidation marker signatures were found during both MIS 13 and 11 despite higher global CH_4 concentrations during MIS 11. The cause of this disparity between CH_4 oxidation markers ODP 1075 and global CH_4 concentrations remains unclear. However, the similarity in CH_4 oxidation markers could suggest; (1) CH_4 sources in the Congo remained consistent during both MIS 11 and 13, with fluctuations in boreal CH_4 emissions driving variations in CH_4 concentrations observed in ice core records; (2) Congo wetlands experienced aridification during MIS 13 which enhanced AMO, producing high concentrations of CH_4 oxidation markers; or (3) a threshold has been reached, where, methanogenesis has overwhelmed the AMO buffer and CH_4 oxidation is high during both MIS 11 and 13, resulting in high concentrations of CH_4 oxidation markers. Similar biomarker signatures are observed during MIS 5, with high concentrations again suggesting enhanced CH_4 cycling.

Furthermore, high concentrations of CH_4 oxidation markers persist beyond 1.2 Ma to 2.5 Ma. Two intervals of low CH_4 oxidation marker concentration are observed between 1865 and 1713 Ka (‘a’) and between 1099 and 826 Ka, (‘b’). This reduction in CH_4 oxidation marker concentration may suggest a reduction in wetland extent in response to a more arid environment. These interpretations are consistent with an increase in climate variability and aridity recorded near 1.7 Ma and 1 Ma, and the onset and amplification of high latitude glacial cycles. Furthermore, a long term reduction in the concentration of CH_4 oxidation markers is observed within ODP 1075 sediments. This decrease in biomarkers supports a long term trend towards greater continental aridity within the Congo and could, therefore, suggest further changes in vegetation zones.

8.2. Recommendations

The research conducted during this PhD has raised some relevant questions, which, require further work.

This PhD has analysed BHPs within the most extensive set of tropical soils and sediments, to date. This has extended our understanding of BHP production within the Congo and potentially other tropical sites. However, the Congo hinterland is also host to a number of extensive peatlands and mangrove habitats, which, we have not

been able to analyse. Additional analysis of these environments would further improve our understanding of BHP production within the Congo.

This work has aimed to address the input of BHPs from terrestrial and marine sources. However, without suspended particulate matter from both the Congo River and the Congo fan, it has not been possible to fully understand the proportions of terrestrial vs. marine BHPs deposited and preserved on the Congo fan site. We, therefore, recommend the analysis of BHPs within suspended particulate material at various points down the Congo River and within the Congo fan at various seasonal time points to gain a full understanding of the proportions of marine vs. terrestrial derived BHPs being preserved within the Congo fan.

The spatial – temporal variability in BHP distributions has yet to be fully realised. Chapter 3 presents some initial ideas suggesting BHP distributions may vary between different climate zones and present the hypothesis; “Variation in BHP relative abundance in soils is controlled by the magnitude of local seasonal temperature contrasts”. Both culture and micro/mesocosm approaches should be used in the future to fully test this hypothesis. Using a culture based approach, exposing hopanoid producing bacteria to a variety of growth conditions and testing a gene level response will further constrain both the role of BHPs in bacteria and the response to perturbations. Further to this, analysing BHP distributions across environmental transects encompassing a range of temperature and other environmental parameters will continue to link the laboratory scale bacterial responses to larger scale environmental response.

Isotopic variations between BHPs within both the modern and paleo samples are not addressed in this thesis. Previous studies have suggested differences in fractionation of C within methanotrophs (Summons et al., 1994; Jahnke et al., 1999). Furthermore, relatively few studies exist determining compound specific $\delta^{13}C$ of BHPs. Additionally, there are currently no published studies analysing D/H isotopes of BHPs. The systematic analysis of BHP isotopic signatures and the source CH_4 values is recommended as no literature data was identified providing values for tropical African wetlands

This work has shown clear differences in the preservation of BHPs within the Congo catchment and potentially within other catchments. However, the causes of preservation differences have not been determined. Potentially, some BHPs may

form mineral complexes during fluvial transport, which, may help with BHP preservation. We, therefore, recommend analysis of BHPs and the interaction of these compounds with minerals and the impact this has on preservation.

This PhD has shown terrestrial CH_4 cycling to be highly variable during the Pleistocene (Chapter 7) with high resolution records linking this variability to the global climate cycle (Chapter 6). The subsequent analysis of BHP signatures within both marine sediments and terrestrial paleoclimate records and analysis of ΔSST within marine records will further improve our understanding of local variations in terrestrial CH_4 cycling. Furthermore, statistical spectral analysis is required to fully understand the variability of these biomarkers on orbital timescales.

References

Anka, Z., Seranne, M., 2004. Reconnaissance study of the ancient Zaire (Congo) deep-sea fan (ZaiAngo Project). Marine Geology 209, 1-4.

Ashkenazy, Y., Tziperman, E., 2004. Are the 41 kyr glacial oscillations a linear response to Milankovitch forcing? Quaternary Science Reviews 23, 1879-1890.

Auman, A.J., Stolyar, S., Costello, A.M., Lidstrom, M.E., 2000. Molecular characterization of methanotrophic isolates from freshwater lake sediment. Applied and Environmental Microbiology 66, 5259-5266.

Auman, A.J., Lidstrom, M.E., 2002. Analysis of sMMO-containing Type I methanotrophs in Lake Washington sediment. Environmental Microbiology 4, 517-524.

Bartlett, K.B., Harriss, R.C., 1993. Review and assessment of methane emissions from wetlands. Chemosphere 26, 261-320.

Bechtel, A., Smittenberg, R.H., Bernasconi, S.M., Schubert, C.J., 2010. Distribution of branched and isoprenoid tetraether lipids in an oligotrophic and a eutrophic Swiss lake: Insights into sources and GDGT-based proxies. Organic Geochemistry 41, 822-832.

Beerling, D.J., Fox, A., Stevenson, D.S., Valdes, P.J., 2011. Enhanced chemistry-climate feedbacks in past greenhouse worlds. Proceedings of the National Academy of Sciences of the United States of America 108, 9770-9775.

Bender, M., Conrad, R., 1992. Kinetics of CH_4 oxidation in oxic soils exposed to ambient air or high CH_4 mixing ratios. FEMS Microbiology Letters 101, 261-270.

Bender, M., Conrad, R., 1993. Kinetics of methane oxidation in oxic soils. Chemosphere 26, 687-696.

Bentaleb, I., Grimalt, J.O., Vidussi, F., Marty, J.C., Martin, V., Denis, M., Hatté, C., Fontugne, M., 1999. The C37 alkenone record of seawater temperature during seasonal thermocline stratification. Marine Chemistry 64, 301-313.

Berger, W.H., Lange, C.B., Wefer, G., 2002. Upwelling history of the Benguela-Namibia system: A synthesis of Leg 175 Results. *In* Wefer, G., Berger, W.H., Richter, C (Eds.), Proceedings of the Ocean Drilling Program. Available from the World Wide Web: <http://www-odp.tamu.edu/publications/175_SR/synth/synth.htm> [Cited 2015-03-05].

Berger, A., Loutre, M.F., 2002. An exceptionally long interglacial ahead? Science 297, 1287-1288.

Berke, M.A., Johnson, T.C., Werne, J.P., Grice, K., Schouten, S., Sinninghe Damsté, J.S., 2012. Molecular records of climate variability and vegetation response since the Late Pleistocene in the Lake Victoria basin, East Africa. Quaternary Science Reviews 55, 59-74.

Berndmeyer, C., Thiel, V., Schmale, O., Blumenberg, M., 2013. Biomarkers for aerobic methanotrophy in the water column of the stratified Gotland Deep (Baltic Sea). Organic Geochemistry 55, 103-111.

Berndmeyer, C., Thiel, V., Schmale, O., Wasmund, N., Blumenberg, M., 2014. Biomarkers in the stratified water column of the Landsort Deep (Baltic Sea). Biogeosciences 11, 7009-7023.

Berry, A.M., Moreau, R.A., Jones, A.D., 1991. Bacteriohopanetetrol - Abundant lipid in *Frankia* cells and in nitrogen-fixing nodule tissue. Plant Physiology 95, 111-115.

Beuning, K.R.M., Russell, J.M., 2004. Vegetation and sedimentation in the Lake Edward Basin, Uganda-Congo during the late Pleistocene and early Holocene. Journal of Paleolimnology 32, 1-18.

Birgel, D., Feng, D., Roberts, H.H., Peckmann, J., 2011. Changing redox conditions at cold seeps as revealed by authigenic carbonates from Alaminos Canyon, northern Gulf of Mexico. Chemical Geology 285, 82-96.

Birgel, D., Thiel, V., Hinrichs, K.U., Elvert M., Campbell, K.A., Reitner, J., Farmer, J.D., Peckmann, J., 2006a. Lipid biomarker patterns of methane-seep microbialites from the Mesozoic convergent margin of California. Organic Geochemistry 37, 1289-1302.

Birgel, D., Peckmann, J., Klautzsch, S., Thiel, V., Reitner, J., 2006b. Anaerobic and aerobic oxidation of methane at late cretaceous seeps in the western interior seaway, USA. Geomicrobiology Journal 23, 565-577.

Bisseret, P., Zundel, M., Rohmer, M., 1985. Prokaryotic triterpenoids .2. 2-Beta-methylhopanoids from *Methylobacterium organophilum* and *Nostoc muscorum*, A new series of prokaryotic triterpenoids. European Journal of Biochemistry 150, 29-34.

Bligh, E.G., Dyer, W.J., 1959. A rapid method of total lipid extraction and purification. Canadian Journal of Biochemistry and Physiology 37, 911-917.

Blumenberg, M., Berndmeyer, C., Moros, M., Muschalla, M., Schmale, O., Thiel, V., 2013. Bacteriohopanepolyols record stratification, nitrogen fixation and other biogeochemical perturbations in Holocene sediments of the central Baltic Sea. Biogeosciences 10, 2725-2735.

Blumenberg, M., Hoppert, M., Kruger, M., Dreier, A., Thiel, V., 2012. Novel findings on hopanoid occurrences among sulfate reducing bacteria: Is there a direct link to nitrogen fixation? Organic Geochemistry

Blumenberg, M., Kruger, M., Nauhaus, K., Talbot, H.M., Oppermann, B.I., Seifert, R., Pape, T., Michaelis, W., 2006. Biosynthesis of hopanoids by sulfate-reducing bacteria (genus *Desulfovibrio*). Environmental Microbiology 8, 1220-1227.

Blumenberg, M., Mollenhauer, G., Zabel, M., Reimer, A., Thiel, V., 2010. Decoupling of bio- and geohopanoids in sediments of the Benguela Upwelling System (BUS). Organic Geochemistry 41, 1119-1129.

Blumenberg, M., Oppermann, B.I., Guyoneaud, R., Michaelis, W., 2009. Hopanoid production by *Desulfovibrio bastinii* isolated from oilfield formation water. FEMS Microbiology Letters 293, 73-78.

Blumenberg, M., Seifert, R., Michaelis, W., 2007. Aerobic methanotrophy in the oxic-anoxic transition zone of the Black Sea water column. Organic Geochemistry 38, 84-91.

Boot, C.S., Ettwein, V.J., Maslin, M.A., Weyhenmeyer, C.E., Pancost, R.D., 2006. A 35,000 year record of terrigenous and marine lipids in Amazon Fan sediments. Organic Geochemistry 37, 208-219.

Borowski, C., Giere, O., Krieger, J., Amann, R., Dubilier, N., 2002. New aspects of the symbiosis in the provannid snail *Ifremeria nautilei* from the North Fiji Back Arc Basin. Cahiers de Biologie Marine 43, 321-324.

Bosse, U., Frenzel, P., 1997. Activity and distribution of methane-oxidizing bacteria in flooded rice soil microcosms and in rice plants (*Oryza sativa*). Applied and Environmental Microbiology 63, 1199-1207.

Bosse, U., Frenzel, P., 1998. Methane emissions from rice microcosms: The balance of production, accumulation and oxidation. Biogeochemistry 41, 199-214.

Bouloubassi, I., Nabais, E., Pancost, R.D., Lorre, A., Taphanel, M.-H., 2009. First biomarker evidence for methane oxidation at cold seeps in the Southeast Atlantic (REGAB pockmark). Deep Sea Research Part II: Topical Studies in Oceanography 56, 2239-2247.

Bowman, J.P., Sly, L.I., Nichols, P.D., Hayward, A.C., 1993. Revised taxonomy of the methanotrophs: Description of *Methylobacter* gen. nov., emendation of *Methylococcus*, validation of *Methylosinus* and *Methylocystis* species, and a proposal that the family *Methylococcacea*e includes only the group I methanotrophs. International Journal of Systematic Bacteriology 43, 735-753.

Bowman, J.P., Sly, L.I., Stackebrandt, E., 1995. The phylogenetic position of the family *Methylococcaceae*. International Journal of Systematic Bacteriology 45, 182-185.

Boyle, E.A., Keigwin, L.D., 1982. Deep circulation of the North Atlantic over the last 200,000 Years: Geochemical evidence. Science 218, 784-787.

Bradley, A.S., Pearson, A., Sáenz, J.P., Marx, C.J., 2010. Adenosylhopane: The first intermediate in hopanoid side chain biosynthesis. Organic Geochemistry 41, 1075-1081.

Brassell, S.C., Eglinton, G., Marlowe, I.T., Pflaumann, U., Sarnthein, M., 1986. Molecular stratigraphy: A new tool for climatic assessment. Nature 320, 129-133.

Bravo, J.M., Perzl, M., Härtner, T., Kannenberg, E.L., Rohmer, M., 2001. Novel methylated triterpenoids of the gammacerane series from the nitrogen-fixing bacterium *Bradyrhizobium japonicum* USDA 110. European Journal of Biochemistry 268, 1323-1331.

Brocks, J.J., Love, G.D., Summons, R.E., Knoll, A.H., Logan, G.A., Bowden, S.A., 2005. Biomarker evidence for green and purple sulphur bacteria in a stratified Palaeoproterozoic sea. Nature 437, 866-870.

Brook, E.J., Harder, S., Severinghaus, J., Steig, E.J., Sucher, C.M., 2000. On the origin and timing of rapid changes in atmospheric methane during the last glacial period. Global Biogeochemical Cycles 14, 559-572.

BS ISO 10390, 2005. Soil quality. Determination of pH. BSI, ISBN 0 580 45659 5.

Buckles, L.K., Weijers, J.W.H., Verschuren, D., Sinninghe Damsté, J.S., 2014. Sources of core and intact branched tetraether membrane lipids in the lacustrine environment: Anatomy of Lake Challa and its catchment, equatorial East Africa. Geochimica et Cosmochimica Acta 140, 106-126.

Bull, I.D., Parekh, N.R., Hall, G.H., Ineson, P., Evershed, R.P., 2000. Detection and classification of atmospheric methane oxidizing bacteria in soil. Nature 405, 175-178.

Burhan, R.Y.P., Trendel, J.M., Adam, P., Wehrung, P., Albrecht, P., Nissenbaum, A., 2002. Fossil bacterial ecosystem at methane seeps: origin of organic matter from Be'eri sulphur deposit, Israel. Geochimica et Cosmochimica Acta 66, 4085-4101.

Burwicz, E.B., Rüpke, L.H., Wallmann, K., 2011. Estimation of the global amount of submarine gas hydrates formed via microbial methane formation based on numerical reaction-transport modeling and a novel parameterization of Holocene sedimentation. Geochimica et Cosmochimica Acta 75, 4562-4576.

Bwangoy, J.R.B., Hansen, M.C., Roy, D.P., De Grandi, G., Justice, C.O., 2010. Wetland mapping in the Congo Basin using optical and radar remotely sensed data and derived topographical indices. Remote Sensing of Environment 114, 73-86.

Camberlin, P., Janicot, S., Poccard, I., 2001. Seasonality and atmospheric dynamics of the teleconnection between African rainfall and tropical sea-surface temperature: Atlantic vs. ENSO. International Journal of Climatology 21, 973-1005.

Cambon-Bonavita, M.A., Nadalig, T., Roussel, E., Delage, E., Duperron, S., Caprais, J.C., Boetius, A., Sibuet, M., 2009. Diversity and distribution of methane-oxidizing microbial communities associated with different faunal assemblages in a giant pockmark of the Gabon continental margin. Deep Sea Research Part II: Topical Studies in Oceanography 56, 2248-2258.

Candy, I., Schreve, D.C., Sherriff, J., Tye, G.J., 2014. Marine Isotope Stage 11: Palaeoclimates, palaeoenvironments and its role as an analogue for the current interglacial. Earth-Science Reviews 128, 18-51.

Cao-Hoang, L., Dumont, F., Marechal, P. A., Gervais, P., 2010. Inactivation of *Escherichia coli* and *Lactobacillus plantarum* in relation to membrane permeabilization due to rapid chilling followed by cold storage. Archives of Microbiology 192, 299-305.

Carrillo-Hernandez, T., Schaeffer, P., Adam, P., Albrecht, P., Derenne, S., Largeau, C., 2003. Remarkably well-preserved archaeal and bacterial membrane lipids in 140 million year old sediments from the Russian platform (Kashpir Oil Shales, Upper Jurassic), In: 21st International Meeting on Organic Geochemistry, Krakow pp. 77-78 (Abstract).

Charlou, J.L., Donval, J.P., Fouquet, Y., Ondreas, H., Knoery, J., Cochonat, P., Levaché, D., Poirier, Y., Jean-Baptiste, P., Fourré, E., Chazallon, B., 2004. Physical and chemical characterization of gas hydrates and associated methane plumes in the Congo-Angola Basin. Chemical Geology 205, 405-425.

Chiang, J.C.H., Biasutti, M., Battisti, D.S., 2003. Sensitivity of the Atlantic Intertropical Convergence Zone to Last Glacial Maximum boundary conditions. Paleoceanography 18, 18-11.

Chowdhury, T.R., Dick, R.P., 2013. Ecology of aerobic methanotrophs in controlling methane fluxes from wetlands. Applied Soil Ecology 65, 8-22.

Clemens, S.C., Murray, D.W., Prell, W.L., 1996. Nonstationary phase of the Plio-Pleistocene Asian monsoon. Science 274, 943-948.

Collister, J.W., Summons, R.E., Lichtfouse, E., Hayes, J.M., 1992. An isotopic biogeochemical study of the Green River oil shale. Organic Geochemistry 19, 265-276.

Conte, M.H., Volkman, J.K., Eglinton, G., 1994. Lipid biomarkers of the haptophyta. Claredon Press, Oxford. 351-377.

Conrad, R., Rothfuss, F., 1991. Methane oxidation in the soil surface layer of a flooded rice field and the effect of ammonium. Biology and Fertility of Soils 12, 28-32.

Conrad, R., 2005. Quantification of methanogenic pathways using stable carbon isotopic signatures: a review and a proposal. Organic Geochemistry 36, 739-752.

Conrad, R., Erkel, C., Liesack, W., 2006. Rice Cluster I methanogens, an important group of Archaea producing greenhouse gas in soil. Current Opinion in Biotechnology 17, 262-267.

Cook, M.S., Keigwin, L.D., Birgel, D., Hinrichs, K.U., 2011. Repeated pulses of vertical methane flux recorded in glacial sediments from the southeast Bering Sea. Paleoceanography 26, DOI: 10.1029/2010pa001993

Cooke, M.P., 2010. The Role of Bacteriohopanepolyols as Biomarkers for Soil Bacterial Communities and Soil Derived Organic Matter, PhD Thesis, Civil Engineering and Geoscience. Newcastle University. Available from the World Wide Web: <https://theses.ncl.ac.uk/dspace/> [Cited 2013-03-09].

Cooke, M.P., Talbot, H.M., Farrimond, P., 2008a. Bacterial populations recorded in bacteriohopanepolyol distributions in soils from Northern England. Organic Geochemistry 39, 1347-1358.

Cooke, M.P., Talbot, H.M., Wagner, T., 2008b. Tracking soil organic carbon transport to continental margin sediments using soil-specific hopanoid biomarkers: A case study from the Congo fan (ODP site 1075). Organic Geochemistry 39, 965-971.

Cooke, M.P., van Dongen, B.E., Talbot, H.M., Semiletov, I., Shakhova, N., Guo, L., Gustafsson, O., 2009. Bacteriohopanepolyol biomarker composition of organic matter exported to the Arctic Ocean by seven of the major Arctic rivers. Organic Geochemistry 40, 1151-1159.

Coolen, M.J.L., Talbot, H.M., Abbas, B.A., Ward, C., Schouten, S., Volkman, J.K., Sinninghe Damsté, J.S., 2008. Sources for sedimentary bacteriohopanepolyols as revealed by 16S rDNA stratigraphy. Environmental Microbiology 10, 1783-1803.

Costantino, V., Fattorusso, E., Imperatore, C., Mangoni, A., 2001. A biosynthetically significant new bacteriohopanoid present in large amounts in the Caribbean sponge Plakortis simplex. Tetrahedron 57, 4045-4048.

Crossman, Z.M., Ineson, P., Evershed, R.P., 2005. The use of 13C labelling of bacterial lipids in the characterisation of ambient methane-oxidising bacteria in soils. Organic Geochemistry 36, 769-778.

Crossman, Z.M., Wang, Z.P., Ineson, P., Evershed, R.P., 2006. Investigation of the effect of ammonium sulfate on populations of ambient methane oxidising bacteria by 13C-labelling and GC/C/IRMS analysis of phospholipid fatty acids. Soil Biology and Biochemistry 38, 983-990.

Cummings, D.E., Snoeyenbos-West, O.L., Newby, D.T., Niggemyer, A.M., Lovley, D.R., Achenbach, L.A., Rosenzweig, R.F., 2003. Diversity of *Geobacteraceae* species inhabiting metal-polluted freshwater lake sediments ascertained by 16S rDNA analyses. Microbial Ecology 46, 257-269.

Cvejic, J.H., Bodrossy, L., Kovács, K.L., Rohmer, M., 2000a. Bacterial triterpenoids of the hopane series from the methanotrophic bacteria *Methylocaldum* spp.: Phylogenetic implications and first evidence for an unsaturated aminobacteriohopanepolyol. FEMS Microbiology Letters 182, 361-365.

Cvejic, J.H., Putra, S.R., El-Beltagy, A., Hattori, R., Hattori, T., Rohmer, M., 2000b. Bacterial triterpenoids of the hopane series as biomarkers for the chemotaxonomy of *Burkholderia*, *Pseudomonas* and *Ralstonia* spp. FEMS Microbiology Letters 183, 295-299.

Dalibard, M., Popescu, S.M., Maley, J., Baudin, F., Melinte-Dobrinescu, M.C., Pittet, B., Marsset, T., Dennielou, B., Droz, L., Suc, J.P., 2014. High-resolution vegetation history of West Africa during the last 145 ka. Geobios 47, 183-198.

Dallenbach, A., Blunier, T., Fluckiger, J., Stauffer, B., Chappellaz, J., Raynaud, D., 2000. Changes in the atmospheric CH_4 gradient between Greenland and Antarctica during the Last Glacial and the transition to the Holocene. Geophysical Research Letters 27, 1005-1008.

De Jonge, C., Stadnitskaia, A., Hopmans, E.C., Cherkashov, G., Fedotov, A., Sinninghe Damsté, J.S., 2014. In situ produced branched glycerol dialkyl glycerol tetraethers in suspended particulate matter from the Yenisei River, Eastern Siberia. Geochimica et Cosmochimica Acta 125, 476-491.

De Jonge, C., Stadnitskaia, A., Hopmans, E.C., Cherkashov, G., Fedotov, A., Streletskaya, I.D., Vasiliev, A.A., Sinninghe Damsté, J.S., 2015. Drastic changes in the distribution of branched tetraether lipids in suspended matter and sediments from the Yenisei River and Kara Sea (Siberia): Implications for the use of brGDGT-based proxies in coastal marine sediments. Geochimica et Cosmochimica Acta 165, 200-225.

de Leeuw, J.W., van der Meer, F.W., Rijpstra, W.I.C., Schenck, P.A., 1980. On the occurrence and structural identification of long chain unsaturated ketones and hydrocarbons in sediments. Physics and Chemistry of the Earth 12, 211-217.

De Rosa, M., Gambacorta, A., Gliozzi, A., 1986. Structure, Biosynthesis, and Physicochemical Properties of Archaebacterial Lipids. Microbiological Reviews 50, 70-80.

DeConto, R.M., Galeotti, S., Pagani, M., Tracy, D., Schaefer, K., Zhang, T.J., Pollard, D., Beerling, D.J., 2012. Past extreme warming events linked to massive carbon release from thawing permafrost. Nature 484, 87-92.

Dedysh, S.N., 2009. Exploring methanotroph diversity in acidic northern wetlands: Molecular and cultivation-based studies. Microbiology 78, 655-669.

Dedysh, S.N., Belova, S.E., Bodelier, P.L.E., Smirnova, K.V., Khmelenina, V.N., Chidthaisong, A., Trotsenko, Y.A., Liesack, W., Dunfiel, P.F., 2007. *Methylocystis heyeri* sp. nov., a novel type II methanotrophic bacterium possessing 'signature' fatty acids of type I methanotrophs. International Journal of Systematic and Evolutionary Microbiology 57, 472-479.

deMenocal, P.B., 1995. Plio-Pleistocene African climate. Science 270, 53-59.

deMenocal, P.B., 2004. African climate change and faunal evolution during the Pliocene-Pleistocene. Earth and Planetary Science Letters 220, 3-24.

deMenocal, P.B., Ruddiman, W.F., Pokras, E.M., 1993. Influence of high- and low-latitude processes on African terrestrial climate: Pleistocene Eolian records from equatorial Atlantic Ocean Drilling Program Site 663. Paleoceanography 8, 209-242.

Deng, Y., Cui, X., Lüke, C., Dumont, M.G., 2013. Aerobic methanotroph diversity in Riganqiao peatlands on the Qinghai-Tibetan Plateau. Environmental Microbiology Reports 5, 566-574.

Devol, A.H., Richey, J.E., Forsberg, B.R., Martinelli, L.A., 1990. Seasonal dynamics in methane emissions from the Amazon River floodplain to the troposphere. Journal of Geophysical Research-Atmospheres 95, 16417-16426.

Dickens, G.R., Castillo, M.M., Walker, J.C.G., 1997. A blast of gas in the latest Paleocene: Simulating first-order effects of massive dissociation of oceanic methane hydrate. Geology 25, 259-262.

Dickens, G.R., O'Neil, J.R., Rea, D.K., Owen, R.M., 1995. Dissociation of oceanic methane hydrate as a cause of the carbon-isotope excursion at the end of the Paleocene. Paleoceanography 10, 965-971.

Distel, D.L., Cavanaugh, C.M., 1994. Independent phylogenetic origins of methanotrophic and chemoautotrophic bacterial endosymbioses in marine bivalves. Journal of Bacteriology 176, 1932-1938.

Doğrul Selver, A., Sparkes, R.B., Bischoff, J., Talbot, H.M., Gustaffson, Ö., Semilitov, I., Dudarev, O., Boult, S., van Dongen, B.E., 2015. Distributions of bacterial and archaeal membrane lipids in surface sediments across the Kolyma River transect. Organic Geochemistry 83-84, 16-26.

Doğrul Selver, A., Talbot, H.M., Gustafsson, Ö., Boult, S., van Dongen, B.E., 2012. Soil organic matter transport along an sub-Arctic river-sea transect. Organic Geochemistry 51, 63-72.

Dörr, H., Katruff, L., Levin, I., 1993. Soil texture parameterization of the methane uptake in aerated soils. Chemosphere 26, 697-713.

Doughty, D.M., Hunter, R.C., Summons, R.E., Newman, D.K., 2009. 2-Methylhopanoids are maximally produced in akinetes of *Nostoc punctiforme*: Geobiological implications. Geobiology 7, 524-532

Dubilier, N., Bergin, C., Lott, C., 2008. Symbiotic diversity in marine animals: the art of harnessing chemosynthesis. Nature Reviews Microbiology 6, 725-740.

Dumont, M.G., Pommerenke, B., Casper, P., 2013. Using stable isotope probing to obtain a targeted metatranscriptome of aerobic methanotrophs in lake sediment. Environmental Microbiology Reports 5, 757-764.

Dupont, L.M., 2009. The Congo deep-sea fan as an archive of Quaternary change in Africa and the eastern tropical south Atlantic (a review), in: Kneller, B., Martinsen, O.J., McCaffrey, B. (Eds.), External Controls on Deep-Water Depositional Systems. S E P M – Society for Sedimentary Geology, Tulsa, pp. 79-87.

Dupont, L.M., Jahns, S., Marret, F., Ning, S., 2000. Vegetation change in equatorial West Africa: Time-slices for the last 150 ka. Palaeogeography, Palaeoclimatology, Palaeoecology 155, 95-122.

Dutaur, L., Verchot, L.V., 2007. A global inventory of the soil CH4 sink. Global Biogeochemical Cycles 21, DOI: 10.1029/2006GB002734

Duvold, T., Rohmer, M., 1999. Synthesis of ribosylhopane, the putative biosynthetic precursor of bacterial triterpenoids of the hopane series. Tetrahedron 55, 9847-9858.

Eickhoff, M., Birgel, D., Talbot, H.M., Peckmann, J., Kappler, A., 2013a. Bacteriohopanoid inventory of *Geobacter sulfurreducens* and *Geobacter metallireducens*. Organic Geochemistry 58, 107-114.

Eickhoff, M., Birgel, D., Talbot, H.M., Peckmann, J., Kappler, A., 2013b. Oxidation of Fe(II) leads to increased C-2 methylation of pentacyclic triterpenoids in the anoxygenic phototrophic bacterium *Rhodopseudomonas palustris* strain TIE-1. Geobiology 11, 268-278.

Eickhoff, M., Birgel, D., Talbot, H.M., Peckmann, J., Kappler, A., 2014. Diagenetic degradation products of bacteriohopanepolyols produced by *Rhodopseudomonas palustris* strain TIE-1. Organic Geochemistry 68, 31-38.

Eigenbrode, J.L., Freeman, K.H., Summons, R.E., 2008. Methylhopane biomarker hydrocarbons in Hamersley Province sediments provide evidence for Neoarchean aerobiosis. Earth and Planetary Science Letters 273, 323-331.

Eisma, D., Kalf, J., Van Der Gaast, S.J., 1978. Suspended matter in the Zaire estuary and the adjacent Atlantic Ocean. Netherlands Journal of Sea Research 12, 3-4.

Emerson, S., Hedges, J.I., 1988. Processes controlling the organic carbon content of open ocean sediments. Paleoceanography 3, 621-634.

Eswaran, H., Van Den Berg, E., Reich, P., 1993. Organic carbon in soils of the World. Soil Science Society of America Journal 57, 192-194.

Fan, Z., Neff, J.C., Hanan, N.P., 2015. Modeling pulsed soil respiration in an African savanna ecosystem. Agricultural and Forest Meteorology 200, 282-292.

Farrimond, P., Talbot, H.M., Watson, D.F., Schulz, L.K., Wilhelms, A., 2004. Methylhopanoids: Molecular indicators of ancient bacteria and a petroleum correlation tool. Geochimica et Cosmochimica Acta 68, 3873-3882.

Fersht, A.R., Jencks, W.P., 1970. Acetylpyridinium ion intermediate in pyridine-catalyzed hydrolysis and acyl transfer reactions of acetic anhydride - observations, kinetics, structure-reactivity correlations, and effects of concentrated salt solutions Journal of the American Chemical Society 92, 5432-5442.

Fietz, S., Huguet, C., Bendle, J., Escala, M., Gallacher, C., Herfort, L., Jamieson, R., Martínez-Garcia, A., McClymont, E.L., Peck, V.L., Prahl, F.G., Rossi, S., Rueda, G., Sanson-Barrera, A., Rosell-Melé, A., 2012. Co-variation of crenarchaeol and branched GDGTs in globally-distributed marine and freshwater sedimentary archives. Global and Planetary Change 92-93, 275-285.

Fischer, W.W., Pearson, A., 2007. Hypotheses for the origin and early evolution of triterpenoid cyclases. Geobiology 5, 19-34.

Flesch, G., Rohmer, M., 1988. Biosynthesis of a carbocyclic pentos analogue linked to bacteriohopanetetrol from the bacterium Methylobacterium organophilum. Journal of the Chemical Society-Chemical Communications, 868-870.

Formolo, M.J., Salacup, J.M., Petsch, S.T., Martini, A.M., Nusslein, K., 2008. A new model linking atmospheric methane sources to Pleistocene glaciation via methanogenesis in sedimentary basins. Geology 36, 139-142.

Freeman, C., Fenner, N., Ostle, N.J., Kang, H., Dowrick, D.J., Reynolds, B., Lock, M.A., Sleep, D., Hughes, S., Hudson, J., 2004. Export of dissolved organic carbon from peatlands under elevated carbon dioxide levels. Nature 430, 195-198.

Frenzel, P., Rothfuss, F., Conrad, R., 1992. Oxygen profiles and methane turnover in a flooded rice microcosm. Biology and Fertility of Soils 14, 84-89.

Froese, D.G., Westgate, J.A., Reyes, A.V., Enkin, R.J., Preece, S.J., 2008. Ancient permafrost and a future, warmer arctic. Science 321, 1648.

Gasse, F., Téhet, R., Durand, A., Gibert, E., Fontes, J.C., 1990. The arid-humid transition in the Sahara and the Sahel during the last deglaciation. Nature 346, 141-146.

Gay, A., Lopez, M., Cochonat, P., Séranne, M., Levaché, D., Sermondadaz, G., 2006. Isolated seafloor pockmarks linked to BSRs, fluid chimneys, polygonal faults and stacked Oligocene-Miocene turbiditic palaeochannels in the Lower Congo Basin. Marine Geology 226, 25-40.

Geymonat, E., Ferrando, L., Tarlera, S.E., 2011. *Methylogaea oryzae* gen. nov., sp. nov., a mesophilic methanotroph isolated from a rice paddy field. International Journal of Systematic and Evolutionary Microbiology 61, 2568-2572.

Gibson, R.A., Talbot, H.M., Kaur, G., Pancost, R.D., Mountain, B., 2008. Bacteriohopanepolyol signatures of cyanobacterial and methanotrophic bacterial populations recorded in a geothermal vent sinter. Organic Geochemistry 39, 1020-1023.

Gilbert, B., Frenzel, P., 1998. Rice roots and CH_4 oxidation: The activity of bacteria, their distribution and the microenvironment. Soil Biology and Biochemistry 30, 1903-1916.

Gong, C., Hollander, D.J., 1999. Evidence for differential degradation of alkenones under contrasting bottom water oxygen conditions: Implication for paleotemperature reconstruction. Geochimica et Cosmochimica Acta 63, 405-411.

Goñi, M.A., Ruttenberg, K.C., Eglinton, T.I., 1998. A reassessment of the sources and importance of land-derived organic matter in surface sediments from the Gulf of Mexico. Geochimica et Cosmochimica Acta 62, 3055-3075.

Graumann, P., Schröder, K., Schmid, R., Marahiel, M.A., 1996. Cold shock stress-induced proteins in *Bacillus subtilis*. Journal of Bacteriology 178, 4611-4619.

Grice, K., Klein Breteler, W.C.M., Schouten, S., Grossi, V., De Leeuw, J.W., Sinninghe Damsté, J.S., 1998. Effects of zooplankton herbivory on biomarker proxy records. Paleoceanography 13, 686-693.

Gulledge, J., Hrywna, Y., Cavanaugh, C., Steudler, P.A., 2004. Effects of long-term nitrogen fertilization on the uptake kinetics of atmospheric methane in temperate forest soils. FEMS Microbiology Ecology 49, 389-400.

Guo, Z.T., Zhou, X., Wu, H.B., 2012. Glacial-interglacial water cycle, global monsoon and atmospheric methane changes. Climate Dynamics 39, 1073-1092.

Haines, R.B., 1938. The Effect of Freezing on Bacteria. Proceedings of the Royal Society of London. Series B, Biological Sciences 124, 451-463.

Handley, L., Talbot, H.M., Cooke, M.P., Anderson, K.E., Wagner, T., 2010. Bacteriohopanepolyols as tracers for continental and marine organic matter supply and phases of enhanced nitrogen cycling on the late Quaternary Congo deep sea fan. Organic Geochemistry 41, 910-914.

Hanson, R.S., Hanson, T.E., 1996. Methanotrophic bacteria. Microbiological Reviews 60, 439-471.

Hart, T.J., Currie, R.T., 1960. The Benguela Current. Discovery Reports 31, 123-298.

Hartmann, D.L., Klein Tank, A.M.G., Rusticucci, M., Alexander, L.V., Bronnimann, S., Charabi, Y., Denterner, F.J., Dlugokencky, E.J., Easterling, D.R., Kaplan, A., B.J., S., Thorne, P.W., Wild, M., Zhai, P.M., 2013. Obervations: Atmosphere and Surface. Cambridge University Press, Cambridge, United Kingdom and New York, NY, USA.

Head, M.J., Gibbard, P.L., 2005. Early-Middle Pleistocene transitions: An overview and recommendation for the defining boundary, in: Head, M.J., Gibbard, P.L. (Eds.), Early-Middle Pleistocene Transitions: The Land-Ocean Evidence. Geological Society of London Publishing House, Bath, pp. 1-18.

Hébraud, M., Potier, P., 1999. Cold shock response and low temperature adaptation in psychrotrophic bacteria. Journal of Molecular Microbiology and Biotechnology 1, 211-219.

Hedges, J.I., Keil, R.G., Benner, R., 1997. What happens to terrestrial organic matter in the ocean? Organic Geochemistry 27, 195-212.

Henckel, T., Jackel, U., Conrad, R., 2001. Vertical distribution of the methanotrophic community after drainage of rice field soil. FEMS Microbiology Ecology 34, 279-291.

Henckel, T., Jäckel, U., Schnell, S., Conrad, R., 2000. Molecular analyses of novel methanotrophic communities in forest soil that oxidize atmospheric methane. Applied and Environmental Microbiology 66, 1801-1808.

Herrmann, D., Bisseret, P., Connan, J., Rohmer, M., 1996b. A non-extractable triterpenoid of the hopane series in *Acetobacter xylinum*. FEMS Microbiolgy Letters 135, 323-326.

Higgins, J.A., Schrag, D.P., 2006. Beyond methane: Towards a theory for the Paleocene-Eocene Thermal Maximum. Earth and Planetary Science Letters 245, 523-537.

Hinrichs, K.U., Hmelo, L.R., Sylva, S.P., 2003. Molecular fossil record of elevated methane levels in late Pleistocene coastal waters. Science 299, 1214-1217.

Hinrichs, K.-U., Rullkötter, J., 1997. Terrigenous and marine lipids in Amazon Fan sediments: implications for sedimentological reconstructions., in: Flood, R.D., Piper, D.J.W., Klaus, A., Peterson, L.C.E. (Eds.), Proceedings of the Ocean Drilling Program, Scientific Results, 155. Ocean Drilling Program, College Station, TX, , pp. 539-553.

Hinrichs, J., Schnetger, B., Schale, H., Brumsack, H.J., 2001. A high resolution study of NE Atlantic sediments at station Bengal: Geochemistry and early diagenesis of Heinrich layers. Marine Geology 177, 79-92.

Hirayama, H., Abe, M., Miyazaki, M., Nunoura, T., Furushima, Y., Yamamoto, H., Takai, K., 2014. *Methylomarinovum caldicuralii* gen. nov., sp. nov., a moderately thermophilic methanotroph isolated from a shallow submarine hydrothermal system, and proposal of the family Methylothermaceae fam. nov. International Journal of Systematic and Evolutionary Microbiology 64, 989-999.

Hirayama, H., Fuse, H., Abe, M., Miyazaki, M., Nakamura, T., Nunoura, T., Furushima, Y., Yamamoto, H., Takai, K., 2013. *Methylomarinum vadi* gen. nov., sp. nov., a methanotroph isolated from two distinct marine environments. International Journal of Systematic and Evolutionary Microbiology 63, 1073-1082.

Hoefman, S., van der Ha, D., Iguchi, H., Yurimoto, H., Sakai, Y., Boon, N., Vandamme, P., Heylen, K., De Vos, P., 2014. *Methyloparacoccus murrellii* gen. nov., sp. nov., a methanotroph isolated from pond water. International Journal of Systematic and Evolutionary Microbiology 64, 2100-2107.

Hoefs, M.J.L., Versteegh, G.J.M., Rijpstra, W.I.C., De Leeuw, J.W., Sinninghe Damsté, J.S., 1998. Postdepositional oxic degradation of alkenones: Implications for the measurement of Palaeo Sea surface temperatures. Paleoceanography 13, 42-49.

Hoehler, T.M., Alperin, M.J., Albert, D.B., Martens, C.S., 1994. Field and laboratory studies of methane oxidation in an anoxic marine sediment: Evidence for a methanogen-sulfate reducer consortium. Global Biogeochemical Cycles 8, 451-463.

Höfle, S.T., Kusch, S., Talbot, H.M., Mollenhauer, G., Zubrzycki, S., Burghardt, S., Rethemeyer, J., 2015. Characterisation of bacterial populations in Arctic permafrost soils using bacteriohopanepolyols. Organic Geochemistry 88, 1-16.

Holmes, A.J., Roslev, P., McDonald, I.R., Iversen, N., Henriksen, K., Murrell, J.C., 1999. Characterization of methanotrophic bacterial populations in soils showing atmospheric methane uptake. Applied and Environmental Microbiology 65, 3312-3318.

Holtvoeth, J., Kolonic, S., Wagner, T., 2005. Soil organic matter as an important contributor to late Quaternary sediments of the tropical West African continental margin. Geochimica et Cosmochimica Acta 69, 2031-2041.

Holtvoeth, J., Wagner, T., Horsfield, B., Schubert, C.J., Wand, U., 2001. Late-quaternary supply of terrigenous organic matter to the Congo deep-sea fan (ODP site 1075): Implications for equatorial African paleoclimate. Geo-Marine Letters 21, 23-33.

Holtvoeth, J., Wagner, T., Schubert, C.J., 2003. Organic matter in river-influenced continental margin sediments: The land-ocean and climate linkage at the Late Quaternary Congo fan (ODP Site 1075). Geochemistry Geophysics Geosystems 4, DOI: 10.1029/2003gc000590.

Hopmans, E.C., Schouten, S., Pancost, R.D., van der Meer, M.T.J., Sinninghe Damsté, J.S., 2000. Analysis of intact tetraether lipids in archaeal cell material and sediments by high performance liquid chromatography/atmospheric pressure chemical ionization mass spectrometry. Rapid Communications in Mass Spectrometry 14, 585-589.

Hopmans, E.C., Weijers, J.W.H., Schefuß, E., Herfort, L., Sinninghe Damsté, J.S., Schouten, S., 2004. A novel proxy for terrestrial organic matter in sediments based on branched and isoprenoid tetraether lipids. Earth and Planetary Science Letters 224, 107-116.

Howard, W.R., 1997. A warm future in the past. Nature 388, 418-419.

Huang, T.-H., Fu, Y.-H., Pan, P.-Y., Chen, C.-T.A., 2012. Fluvial carbon fluxes in tropical rivers. Current Opinion in Environmental Sustainability 4, 162-169.

Hughes, H.J., Sondag, F., Cocquyt, C., Laraque, A., Pandi, A., Andre, L., Cardinal, D., 2011. Effect of seasonal biogenic silica variations on dissolved silicon fluxes and isotopic signatures in the Congo River. Limnology and Oceanography 56, 551-561.

Huguet, C., de Lange, G.J., Gustafsson, O., Middelburg, J.J., Sinninghe Damsté, J.S., Schouten, S., 2008. Selective preservation of soil organic matter in oxidised marine sediments (Madeira Abyssal Plain). Geochimica et Cosmochimica Acta 72, 6061-6068.

Huguet, C., Hopmans, E.C., Febo-Ayala, W., Thompson, D.H., Sinninghe Damsté, J.S., Schouten, S., 2006. An improved method to determine the absolute abundance of glycerol dibiphytanyl glycerol tetraether lipids. Organic Geochemistry 37, 1036-1041.

Huguet, C., Schimmelmann, A., Thunell, R., Lourens, L.J., Sinninghe Damsté, J.S., Schouten, S., 2007. A study of the TEX86 paleothermometer in the water column and sediments of the Santa Barbara Basin, California. Paleoceanography 22, DOI: 10.1029/2006PA001310.

Huybers, P., 2007. Glacial variability over the last two million years: an extended depth-derived age model, continuous obliquity pacing, and the Pleistocene progression. Quaternary Science Reviews 26, 37-55.

Imbrie, J., Berger, A., Boyle, E.A., Clemens, S.C., Duffy, A., Howard, W.R., Kukla, G., Kutzbach, J., Martinson, D.G., McIntyre, A., Mix, A.C., Molfino, B., Morley, J.J., Peterson, L.C., Pisias, N.G., Prell, W.L., Raymo, M.E., Shackleton, N.J., Toggweiler, J.R., 1993. On the structure and origin of major glaciation cycles .2. The 100,000-year cycle. Paleoceanography 8, 699-735.

Imbrie, J., Boyle, E.A., Clemens, S.C., Duffy, A., Howard, W.R., Kukla, G., Kutzbach, J., Martinson, D.G., McIntyre, A., Mix, A.C., Molfino, B., Morley, J.J., Peterson, L.C., Pisias, N.G., Prell, W.L., Raymo, M.E., Shackleton, N.J., Toggweiler, J.R., 1992. On the structure and origin of major glaciation cycles 1. Linear responses to Milankovitch forcing. Paleoceanography 7, 701-738.

Imbrie, J., Imbrie, J.Z., 1980. Modeling the climatic response to orbital variations. Science 207, 943-953.

IPCC, 2013. Climate change 2013: The Physical Science Basis. Contribution of working group I to the fifth assessment report of the intergovernmental panel on climate change, Cambridge university press, Cambridge, United Kingdom and New York, NY, USA.

Jahn, B., Schneider, R.R., Müller, P.J., Donner, B., Rohl, U., 2005. Response of tropical African and East Atlantic climates to orbital forcing over the last 1.7 Ma, in: Head, M.J., Gibbard, P.L. (Eds.), Early-Middle Pleistocene Transitions: The Land-Ocean Evidence. Geological Soc Publishing House, Bath, pp. 65-84.

Jahnke, L.L., Summons, R.E., Dowling, L.M., Zahiralis, K.D., 1995. Identification of methanotrophic lipid biomarkers in cold-seep mussle gills - chemical and isotopic analysis. Applied and Environmental Microbiology 61, 576-582.

Jahnke, L.L., Summons, R.E., Hope, J.M., Des Marais, D.J., 1999. Carbon isotopic fractionation in lipids from methanotrophic bacteria II: the effects of physiology and environmental parameters on the biosynthesis and isotopic signatures of biomarkers. Geochimica et Cosmochimica Acta 63, 79-93.

Jenkyns, H.C., Schouten-Huibers, L., Schouten, S., Sinninghe Damsté, J.S., 2012. Warm Middle Jurassic–Early Cretaceous high-latitude sea-surface temperatures from the Southern Ocean. Climate of the Past 8, 215-226.

Jones, P.G., Inouye, M., 1994. The cold-shock response - A hot topic. Molecular Microbiology 11, 811-818.

Joyeux, C., Fouchard, S., Llopiz, P., Neunlist, S., 2004. Influence of the temperature and the growth phase on the hopanoids and fatty acids content of *Frateuria aurantia* (DSMZ 6220). FEMS Microbiology Ecology 47, 371-379.

Kates, M., 1972. Techniques of lipidology: isolation, analysis and identification of lipids. North-Holland Publishing Company, Amsterdam.

Kannenberg, E.L., Poralla, K., 1999. Hopanoid biosynthesis and function in bacteria. Naturwissenschaften 86, 168-176.

Kasting, J.F., 2005. Methane and climate during the Precambrian era. Precambrian Research 137, 119-129.

Kazadi, S.N., Kaoru, F., 1996. Interannual and long-term climate variability over the Zaire River Basin during the last 30 years. Journal of Geophysical Research: Atmospheres 101, 21351-21360.

Kennedy, M.J., Wagner, T., 2011. Clay mineral continental amplifier for marine carbon sequestration in a greenhouse ocean. Proceedings of the National Academy of Sciences of the United States of America 108, 9776-9781.

Kennett, J.P., Cannariato, K.G., Hendy, I.L., Behl, R.J., 2003. Methane Hydrates in Quaternary Climate Change: The Clathrate Gun Hypothesis. AGU, Washington, DC.

Kessler, J.D., Valentine, D.L., Redmond, M.C., Du, M., Chan, E.W., Mendes, S.D., Quiroz, E.W., Villanueva, C.J., Shusta, S.S., Werra, L.M., Yvon-Lewis, S.A., Weber, T.C., 2011. A persistent oxygen anomaly reveals the fate of spilled methane in the deep Gulf of Mexico. Science 331, 312-315.

Khalil, M., Shearer, M.J., 2000. Sources of methane: an overview. Springer-Verlag, New York, NY.

Kiese, R., Wochele, S., Butterbach-Bahl, K., 2008. Site specific and regional estimates of methane uptake by tropical rainforest soils in north eastern Australia. Plant and Soil 309, 211-226.

Kim, S.Y., Freeman, C., Fenner, N., Kang, H., 2012. Functional and structural responses of bacterial and methanogen communities to 3-year warming incubation in different depths of peat mire. Applied Soil Ecology 57, 23-30.

Kim, J.H., Talbot, H.M., Zarzycka, B., Bauersachs, T., Wagner, T., 2011. Occurrence and abundance of soil-specific bacterial membrane lipid markers in the Tet watershed (southern France): Soil-specific BHPs and branched GDGTs. Geochemistry Geophysics Geosystems 12, DOI: 10.1029/2010gc003364

Kim, J.-H., Zell, C., Moreira-Turcq, P., Pérez, M.A.P., Abril, G., Mortillaro, J.-M., Weijers, J.W.H., Meziane, T., Sinninghe Damsté, J.S., 2012. Tracing soil organic carbon in the lower Amazon River and its tributaries using GDGT distributions and bulk organic matter properties. Geochimica et Cosmochimica Acta 90, 163-180.

Kip, N., Ouyang, W., van Winden, J., Raghoebarsing, A., van Niftrik, L., Pol, A., Pan, Y., Bodrossy, L., van Donselaar, E.G., Reichart, G.J., Jetten, M.S.M., Damsté, J.S.S., den Camp, H.J.M.O., 2011. Detection, isolation, and characterization of acidophilic methanotrophs from sphagnum mosses. Applied and Environmental Microbiology 77, 5643-5654.

King, G.M., Roslev, P., Skovgaard, H., 1990. Distribution and rate of methane oxidation in sediments of the Florida Everglades. Applied and Environmental Microbiology 56, 2902-2911.

Knani, M., Corpe, W.A., Rohmer, M., 1994. Bacterial hopanoids from pink-pigmented facultative methylotrophs (PPFMS) and from green plant-surfaces. Microbiology-Uk 140, 2755-2759.

Kroeger, K.F., di Primio, R., Horsfield, B., 2011. Atmospheric methane from organic carbon mobilization in sedimentary basins - The sleeping giant? Earth-Science Reviews 107, 423-442.

Kukla, G., McManus, J.F., Rousseau, D.D., Chuine, I., 1997. How long and how stable was the last interglacial? Quaternary Science Reviews 16, 605-612.

Kulkarni, G., Wu, C.H., Newmana, D.K., 2013. The general stress response factor EcfG regulates expression of the C-2 hopanoid methylase HpnP in *Rhodopseudomonas palustris* TIE-1. Journal of Bacteriology 195, 2490-2498.

Kutzbach, J.E., 1981. Monsoon climate of the early Holocene: Climate experiment with the Earth's orbital parameters for 9000 years ago. Science 214, 59-61.

Kvenvolden, K.A., Lorenson, T.D., 2001. The global occurrence of natural gas hydrate, in: Paull, C.K., Dillon, W.P. (Eds.), Natural gas hydrates: occurrence, distribution and detection. AGU, Washington, D.C, Geophysical Monograph Series, pp. 3-18.

Lal, R., 2004. Soil carbon sequestration impacts on global climate change and food security. Science 304, 1623-1627.

Laraque, A., Bricquet, J.P., Pandi, A., Olivry, J.C., 2009. A review of material transport by the Congo River and its tributaries. Hydrological Processes 23, 3216-3224.

Lin, H.-L., Lin, C.-Y., Meyers, P.A., 2001. Data report: Carbonate, organic carbon, and opal concentrations and organic d13C values of sediments from Sites 1075-1082 and 1084, southwest African margin. Wefer, G., Berger, W.H., Richter, C., (Eds). Proceedings of the Ocean Drilling Program, Scientific Results, 175 [Online], World Wide Web: <http://www-odp.tamu.edu/publications/175_SR/chap_17/chap_17.htm> [Cited 2015-03-05]

Lisiecki, L.E., Raymo, M.E., 2005. A Pliocene-Pleistocene stack of 57 globally distributed benthic delta O-18 records. Paleoceanography 20, doi:10.1029/2004PA001071.

Lisiecki, L.E., Raymo, M.E., 2007. Plio-Pleistocene climate evolution: trends and transitions in glacial cycle dynamics. Quaternary Science Reviews 26, 56-69.

Liu, Z., Herbert, T.O., 2004. High-latitude influence on the eastern equatorial Pacific climate in the early Pleistocene epoch. Nature 427, 720-723.

Liu, Z., Otto-Bliesner, B., Kutzbach, J., Li, L., Shields, C., 2003. Coupled climate simulation of the evolution of global monsoons in the Holocene. Journal of Climate 16, 2472-2490.

Liu, W., Sakr, E., Schaeffer, P., Talbot, H.M., Donisi, J., Hartner, T., Kannenberg, E., Takano, E., Rohmer, M., 2014. Ribosylhopane, a Novel Bacterial Hopanoid, as Precursor of C35 Bacteriohopanepolyols in *Streptomyces coelicolor* A3(2). ChemBioChem: a European Journal of Chemical Biology 15, 2156-2161.

Loomis, S.E., Russell, J.M., Sinninghe Damsté, J.S., 2011. Distributions of branched GDGTs in soils and lake sediments from western Uganda: Implications for a lacustrine paleothermometer. Organic Geochemistry 42, 739-751.

Loulergue, L., Schilt, A., Spahni, R., Masson-Delmotte, V., Blunier, T., Lemieux, B., Barnola, J.-M., Raynaud, D., Stocker, T.F., Chappellaz, J., 2008. Orbital and millennial-scale features of atmospheric CH_4 over the past 800,000 years. Nature 453, 383-386.

Loutre, M.F., Berger, A., 2003. Marine Isotope Stage 11 as an analogue for the present interglacial. Global and Planetary Change 36, 209-217.

Lowe, D.C., 2006. Global change: A green source of surprise. Nature 439, 148-149.

Ludwig, W., Amiotte-Suchet, P., Probst, J.L., 1996. River discharges of carbon to the world's oceans: Determining local inputs of alkalinity and of dissolved and particulate organic carbon. Comptes Rendus de l'Academie de Sciences - Serie IIa: Sciences de la Terre et des Planetes 323, 1007-1014.

Marani, L., Alvalá, P.C., 2007. Methane emissions from lakes and floodplains in Pantanal, Brazil. Atmospheric Environment 41, 1627-1633.

Marlowe, I.T., Brassell, S.C., Eglinton, G., Green, J.C., 1984. Long chain unsaturated ketones and esters in living algae and marine sediments. Organic Geochemistry 6, 135-141.

Martins, O., Probst, J.-L., 1991. Biogeochemistry of major African rivers: Carbon and mineral transport, Biogeochemistry of Major World Rivers. Wiley, Chichester, pp. 129-157.

Martinson, G.O., Werner, F.A., Scherber, C., Conrad, R., Corre, M.D., Flessa, H., Wolf, K., Klose, M., Gradstein, S.R., Veldkamp, E., 2010. Methane emissions from tank bromeliads in neotropical forests. Nature Geoscience 3, 766-769.

Maslin, M.A., Thomas, E., 2003. Balancing the deglacial global carbon budget: the hydrate factor. Quaternary Science Reviews 22, 1729-1736.

Maslin, M.A., Ridgwell, A.J., 2005. Mid-Pleistocene revolution and the 'eccentricity myth', in: Head, M.J., Gibbard, P.L. (Eds.), Early-Middle Pleistocene Transitions: The Land-Ocean Evidence. Geological Society of London Publishing House, Bath, pp. 19-34.

Maslin, M.A., Pancost, R.D., Wilson, K.E., Lewis, J., Trauth, M.H., 2012. Three and half million year history of moisture availability of South West Africa: Evidence from ODP site 1085 biomarker records. Palaeogeography, Palaeoclimatology, Palaeoecology 317-318, 41-47.

McIntyre, A., Ruddiman, W.F., Karlin, K., Mix, A.C., 1989. Surface water response of the equatorial Atlantic Ocean to orbital forcing. Paleoceanography 4, 19-55.

Menot, G., Bard, E., 2010. Geochemical evidence for a large methane release during the last deglaciation from Marmara Sea sediments. Geochimica et Cosmochimica Acta 74, 1537-1550.

Meyers, P.A., 1997. Organic geochemical proxies of paleoceanographic, paleolimnologic, and paleoclimatic processes. Organic Geochemistry 27, 213-250.

Miller, C.S., Gosling, W.D., 2014. Quaternary forest associations in lowland tropical West Africa. Quaternary Science Reviews 84, 7-25.

Milliman, J.D., Syvitski, J.P.M., 1992. Geomorphic/tectonic control of sediment discharge to the ocean: the importance of small mountainous rivers. Journal of Geology 100, 525-544.

Mitsch, W.J., Gosselink, J.G., 2007. Wetlands of the world, 4th ed. John Wiley & Sons, Inc., Hoboken, New Jersey.

Molfino, B., McIntyre, A., 1990. Nutricline variation in the equatorial Atlantic coincident with the Younger Dryas. Paleoceanography 5, 997-1008.

Mondamert, L., Labanowski, J., N'Goye, F., Talbot, H.M., Croué, J.P., 2011. High pressure membrane foulants of seawater, brackish water and river water: Origin assessed by sugar and bacteriohopanepolyol signatures. Biofouling 27, 21-32.

Müller, P.J., Kirst, G., Ruhland, G., Von Storch, I., Rosell-Melé, A., 1998. Calibration of the alkenone paleotemperature index U37K based on core-tops from the eastern South Atlantic and the global ocean (60°N-60°S). Geochimica et Cosmochimica Acta 62, 1757-1772.

Müller, P.J., Suess, E., 1979. Productivity, sedimentation rate, and sedimentary organic matter in the oceans-I. Organic carbon preservation. Deep Sea Research Part A, Oceanographic Research Papers 26, 1347-1362.

Naeher, S., Peterse, F., Smittenberg, R.H., Niemann, H., Zigah, P.K., Schubert, C.J., 2014. Sources of glycerol dialkyl glycerol tetraethers (GDGTs) in catchment soils, water column and sediments of Lake Rotsee (Switzerland) - Implications for the application of GDGT-based proxies for lakes. Organic Geochemistry 66, 164-173.

Nahlik, A.M., Mitsch, W.J., 2011. Methane emissions from tropical freshwater wetlands located in different climatic zones of Costa Rica. Global Change Biology 17, 1321-1334.

Neunlist, S., Bisseret, P., Rohmer, M., 1988. The hopanoids of the purple non-sulfur bacteria *Rhodopseudomonas-palustris* and *Rhodopseudomonas-acidophila* and the absolute-configuration of bacteriohopanetetrol. European Journal of Biochemistry 171, 245-252.

Neunlist, S., Rohmer, M., 1985a. Novel hopanoids from the methylotrophic bacteria *Methylococcus capsulatus* and *Methylomonas methanica* - (22*S*)-35-Aminobacteriohopane-30,31,32,33,34-pentol and (22*S*)-35-amino-3-β-methylbacteriohopane-30,31,32,33,34-pentol. Biochemical Journal 231, 635-639.

Neunlist, S., Rohmer, M., 1985b. The hopanoids of *'Methylosinus trichosporium'*: Aminobacteriohopanetriol and aminobacteriohopanetetrol. Journal of General Microbiology 131, 1363-1367.

Nicholson, S.E., 1996. A review of climate dynamics and climate variability in Eastern Africa, in: Johnson, T.C., Odada, E.O. (Eds.), The liminology, climatology and paleoclimatology of East African lakes. Gordon and Breach Science Publishers SA., The Netherlands, pp. 25-56.

Nicholson, S.E., Entekhabi, D., 1987. Rainfall variability in equatorial and southern Africa: relationships with sea surface temperatures along the southwestern coast of Africa. Journal of Climate & Applied Meteorology 26, 561-578.

Nkounkou, R.-R., Probst, J.-L., 1987. Hydrology and geochemistry of the Congo River system. SCOPE/UNEP - Sonderband 64, 483-508.

Ochs, D., Kaletta, C., Entian, K.D., Becksickinger, A., Poralla, K., 1992. Cloning, expression, and sequencing of squalene hopene cyclase, a key enzyme in triterpenoid metabolism. Journal of Bacteriology 174, 298-302.

Offre, P., Spang, A., Schleper, C., 2013. Archaea in biogeochemical cycles, Annual Review of Microbiology, pp. 437-457.

Ortiz-Llorente, M.J., Alvarez-Cobelas, M., 2012. Comparison of biogenic methane emissions from unmanaged estuaries, lakes, oceans, rivers and wetlands. Atmospheric Environment 59, 328-337.

Osborne, K.A., PhD Thesis Submitted. Environmental Controls on Bacteriohopanepolyol Signatures in Estuarine Sediment. Newcastle University (UK).

Ourisson, G., Albrecht, P., 1992. Hopanoids. 1. Geohopanoids: the most abundant natural products on Earth? Accounts of Chemical Research 25, 398-402.

Ourisson, G., Rohmer, M., Poralla, K., 1987. Prokaryotic hopanoids and other polyterpenoid sterol surrogates. Annual Review of Microbiology 41, 301-333.

Pancost, R.D., Hopmans, E.C., Sinninghe Damsté, J.S., 2001. Archaeal lipids in Mediterranean cold seeps: Molecular proxies for anaerobic methane oxidation. Geochimica et Cosmochimica Acta 65, 1611-1627.

Pancost, R.D., Pressley, S., Coleman, J.M., Talbot, H.M., Kelly, S.P., Farrimond, P., Schouten, S., Benning, L., Mountain, B.W., 2006. Composition and implications of diverse lipids in New Zealand geothermal sinters. Geobiology 4, 71-92.

Pancost, R.D., Steart, D.S., Handley, L., Collinson, M.E., Hooker, J.J., Scott, A.C., Grassineau, N.V., Glasspool, I.J., 2007. Increased terrestrial methane cycling at the Palaeocene-Eocene thermal maximum. Nature 449, 332-335.

Pancost, R.D., Zhang, C.L., Tavacoli, J., Talbot, H.M., Farrimond, P., Schouten, S., Sinninghe Damsté, J.S., Sassen, R., 2005. Lipid biomarkers preserved in hydrate-associated authigenic carbonate rocks of the Gulf of Mexico. Palaeogeography, Palaeoclimatology, Palaeoecology 227, 48-66.

Parkin, D.W., Shackleton, N.J., 1973. Trade wind and temperature correlations down a deep-sea core off the Saharan coast. Nature 245, 455-457.

Pearson, A., Leavitt, W.D., Sáenz, J.P., Summons, R.E., Tam, M.C.M., Close, H.G., 2009. Diversity of hopanoids and squalene-hopene cyclases across a tropical land-sea gradient. Environmental Microbiology 11, 1208-1223.

Pearson, A., Page, S.R.F., Jorgenson, T.L., Fischer, W.W., Higgins, M.B., 2007. Novel hopanoid cyclases from the environment. Environmental Microbiology 9, 2175-2188.

Pearson, E.J., Juggins, S., Talbot, H.M., Weckstrom, J., Rosen, P., Ryves, D.B., Roberts, S.J., Schmidt, R., 2011. A lacustrine GDGT-temperature calibration from the Scandinavian Arctic to Antarctic: Renewed potential for the application of GDGT-paleothermometry in lakes. Geochimica et Cosmochimica Acta 75, 6225-6238.

Peckmann, J., Thiel, V., 2004. Carbon cycling at ancient methane-seeps. Chemical Geology 205, 443-467.

Peiseler, B., Rohmer, M., 1992. Prokaryotic triterpenoids of the hopane series - Bacteriohopanetetrols of new side-chain configuration from *Acetobacter* species. Journal of Chemical Research-S, 298-299.

Peters, K.E., Walters, C.C., Moldowan, J.M., 2005. The Biomarker Guide: Biomarkers and Isotopes in the Environment and Human History, Second ed. Cambridge University Press, Cambridge, UK.

Petit, J.R., Jouzel, J., Raynaud, D., Barkov, N.I., Barnola, J.M., Basile, I., Bender, M., Chappellaz, J., Davis, M., Delaygue, G., Delmotte, M., Kotlyakov, V.M., Legrand, M., Lipenkov, V.Y., Lorius, C., Pepin, L., Ritz, C., Saltzman, E., Stievenard, M., 1999. Climate and atmospheric history of the past 420,000 years from the Vostok ice core, Antarctica. Nature 399, 429-436.

Pimenov, N.V., Savvichev, A.S., Rusanov, I.I., Lein, A.Y., Ivanov, M.V., 2000. Microbiological processes of the carbon and sulfur cycles at cold methane seeps of the North Atlantic. Microbiology 69, 709-720.

Poger, D., Mark, A.E., 2013. The relative effect of sterols and hopanoids on lipid bilayers: When comparable is not identical. Journal of Physical Chemistry B 117, 16129-16140.

Pokras, E.M., Mix, A.C., 1985. Eolian evidence for spatial variability of late Quaternary climates in tropical Africa. Quaternary Research 24, 137-149.

Poralla, K., Hartner, T., Kannenberg, E., 1984. Effect of temperature and pH on the hopanoid content of *Bacillus acidocaldarius*. FEMS Microbiology Letters 23, 253-256.

Poralla, K., Muth, G., Härtner, T., 2000. Hopanoids are formed during transition from substrate to aerial hyphae in *Streptomyces coelicolor* A3(2). FEMS Microbiology Letters 189, 93-95.

Post, W.M., 1993. Organic carbon in soils and the global carbon cycle. Springer, New York.

Prahl, F.G., Collier, R.B., Dymond, J., Lyle, M., Sparrow, M.A., 1993. A biomarker perspective on prymnesiophyte productivity in the northeast Pacific Ocean. Deep-Sea Research Part I 40, 2061-2076.

Prahl, F.G., Wakeham, S.G., 1987. Calibration of unsaturation patterns in long-chain ketone compositions for palaeotemperature assessment. Nature 330, 367-369.

Prell, W.L., Kutzbach, J.E., 1987. Monsoon variability over the past 150 000 years. Journal of Geophysical Research 92, 8411-8425.

Purbopuspito, J., Veldkamp, E., Brumme, R., Murdiyarso, D., 2006. Trace gas fluxes and nitrogen cycling along an elevation sequence of tropical montane forests in Central Sulawesi, Indonesia. Global Biogeochemical Cycles 20, DOI: 10.1029/2005GB002516

Raggi, L., Schubotz, F., Hinrichs, K.U., Dubilier, N., Petersen, J.M., 2013. Bacterial symbionts of *Bathymodiolus* mussels and *Escarpia* tubeworms from Chapopote, an asphalt seep in the southern Gulf of Mexico. Environmental Microbiology 15, 1969-1987.

Raghoebarsing, A.A., Smolders, A.J.P., Schmid, M.C., Rijpstra, W.I.C., Wolters-Arts, M., Derksen, J., Jetten, M.S.M., Schouten, S., Sinninghe Damsté, J.S., Lamers, L.P.M., Roelofs, J.G.M., Op den Camp, H.J.M., Strous, M., 2005. Methanotrophic symbionts provide carbon for photosynthesis in peat bogs. Nature 436, 1153-1156.

Ramsar Convention Secretariat, 2013. The Ramsar Convention Manual: a guide to the Convention on Wetlands (Ramsar, Iran, 1971), 6th ed. Ramsar Convention Secretariat, Gland, Switzerland.

Randlett, M.E., Coolen, M.J.L., Stockhecke, M., Pickarski, N., Litt, T., Balkema, C., Kwiecien, O., Tomonaga, Y., Wehrli, B., Schubert, C.J., 2014. Alkenone distribution in Lake Van sediment over the last 270ka: Influence of temperature and haptophyte species composition. Quaternary Science Reviews 104, 53-62.

Raymo, M.E., Ruddiman, W.F., Shackleton, N.J., Oppo, D.W., 1990. Evolution of Atlantic-Pacific δ13C gradients over the last 2.5 m.y. Earth and Planetary Science Letters 97, 353-368.

Reagan, M.T., Moridis, G.J., 2007. Oceanic gas hydrate instability and dissociation under climate change scenarios. Geophysical Research Letters 34.

Redshaw, C.H., Cooke, M.P., Talbot, H.M., McGrath, S., Rowland, S.J., 2008. Low biodegradability of fluoxetine HCl, diazepam and their human metabolites in sewage sludge-amended soil. Journal of Soils and Sediments 8, 217-230.

Reeburgh, W.S., 2007. Oceanic methane biogeochemistry. Chemical Reviews 107, 486-513.

Renoux, J.M., Rohmer, M., 1985. Prokaryotic triterpenoids - New Bacteriohopanetetrol cyclitol ethers from the methylotrophic bacterium *Methylobacterium organophilum*. European Journal of Biochemistry 151, 405-410.

Rethemeyer, J., Schubotz, F., Talbot, H.M., Cooke, M.P., Hinrichs, K.U., Mollenhauer, G., 2010. Distribution of polar membrane lipids in permafrost soils and sediments of a small high Arctic catchment. Organic Geochemistry 41, 1130-1145.

Reyes, A.V., Carlson, A.E., Beard, B.L., Hatfield, R.G., Stoner, J.S., Winsor, K., Welke, B., Ullman, D.J., 2014. South Greenland ice-sheet collapse during Marine Isotope Stage 11. Nature 510, 525-528.

Ricci, J.N., Coleman, M.L., Welander, P.V., Sessions, A.L., Summons, R.E., Spear, J.R., Newman, D.K., 2014. Diverse capacity for 2-methylhopanoid production correlates with a specific ecological niche. ISME Journal 8, 675-684.

Rohmer, M., 1993. The biosynthesis of triterpenoids of the hopane series in the Eubacteria - a mine of new enzyme-reactions. Pure and Applied Chemistry 65, 1293-1298.

Rohmer, M., Bouviernave, P., Ourisson, G., 1984. Distribution of hopanoid triterpenes in prokaryotes. Journal of General Microbiology 130, 1137-1150.

Rontani, J.F., Cuny, P., Grossi, V., Beker, B., 1997. Stability of long-chain alkenones in senescing cells of *Emiliania huxleyi*: effect of photochemical and aerobic microbial degradation on the alkenone unsaturation ratio ($U_{37}^{k'}$). Organic Geochemistry 26, 503-509.

Rosa-Putra, S., Nalin, R., Domenach, A.M., Rohmer, M., 2001. Novel hopanoids from Frankia spp. and related soil bacteria - Squalene cyclization and significance of geological biomarkers revisited. European Journal of Biochemistry 268, 4300-4306.

Rosell-Melé, A., 1998. Interhemispheric appraisal of the value of alkenone indices as temperature and salinity proxies in high-latitude locations. Paleoceanography 13, 694-703.

Rossignol-Strick, M., 1983. African monsoons, an immediate climate response to orbital insolation. Nature 304, 46-49.

Ruddiman, W.F., McIntyre, A., 1984. Ice-age thermal response and climatic role of the surface Atlantic Ocean, 40°N to 63°N. Geological Society of America Bulletin 95, 381-396.

Ruddiman, W.F., Janecek, T.R., 1989. Pliocene-Pleistocene biogenic and terrigenous fluxes at equatorial Atlantic Sites 662, 663, and 664. Proc., Scientific Results, ODP, Leg 108, eastern tropical Atlantic, 211-240.

Ruddiman, W.F., Raymo, M.E., Martinson, D.G., Clement, B.M., Backman, J., 1989. Pleistocene evolution: Northern Hemisphere ice sheets and North Atlantic Ocean. Paleoceanography 4, 353-412.

Ruddiman, W.F., 2003. Orbital insolation, ice volume, and greenhouse gases. Quaternary Science Reviews 22, 1597-1629.

Runge, J., 2007. The Cong River, Central Africa, In: Gupta, A. (ed.), Large Rivers: Geomorphology and Management. John Wiley & Sons, Ltd, Chichester, UK. doi:10.1002/9780470723722.ch14.

Rush, D., Osborne, K.A., Birgel, D., Kalyuzhnaya, M.G., Boetius, A., Nickel, J.C., Mangelsdorf, K., di Primo, R. et al. Talbot, H.M. In Preparation. "*Methylocaldum* and other novel bugs – BHP distribution explains absence of aminopentol in marine systems".

Rush, D., Sinninghe Damsté, J.S., Poulton, S.W., Thamdrup, B., Garside, A.L., Acuña González, J., Schouten, S., Jetten, M.S.M., Talbot, H.M., 2014. Anaerobic ammonium-oxidising bacteria: A biological source of the bacteriohopanetetrol stereoisomer in marine sediments. Geochimica et Cosmochimica Acta 140, 50-64.

Sáenz, J.P., Eglinton, T.I., Summons, R.E., 2011a. Abundance and structural diversity of bacteriohopanepolyols in suspended particulate matter along a river to ocean transect. Organic Geochemistry 42, 774-780.

Sáenz, J.P., Sezgin, E., Schwille, P., Simons, K., 2012. Functional convergence of hopanoids and sterols in membrane ordering. Proceedings of the National Academy of Sciences of the United States of America 109, 14236-14240.

Sáenz, J.P., Wakeham, S.G., Eglinton, T.I., Summons, R.E., 2011b. New constraints on the provenance of hopanoids in the marine geologic record: Bacteriohopanepolyols in marine suboxic and anoxic environments. Organic Geochemistry 42, 1351-1362.

Saito, H., Suzuki, N., 2007. Distributions and sources of hopanes, hopanoic acids and hopanols in Miocene to recent sediments from ODP Leg 190, Nankai Trough. Organic Geochemistry 38, 1715-1728.

Šantl-Temkiv, T., Finster, K., Hansen, B.M., Pašić, L., Karlson, U.G., 2013. Viable methanotrophic bacteria enriched from air and rain can oxidize methane at cloud-like conditions. Aerobiologia 29, 373-384.

Schaeffer, P., 1993. Marqueurs biologiques de milieux e´vaporitiques. PhD Thesis. Université Louis Pasteur, Strasbourg, France.

Schaeffer, P., Schmitt, G., Adam, P., Rohmer, M., 2008. Acid catalysed formation of 32,35-anhydrobacteriohopanetetrol from bacteriohopanetetrol. Organic Geochemistry 39, 1479-1482.

Schaeffer, P., Schmitt, G., Adam, P., Rohmer, M., 2010. Abiotic formation of 32,35-anhydrobacteriohopanetetrol: A geomimetic approach. Organic Geochemistry 41, 1005-1008.

Schefuß, E., Eglington, T.I., Spencer-Jones, C.L., Rullkötter, J., Se Pol-Holz, R., Talbot, H.M., Grootes, P.M., Schneider, R.R., In Preparation. Hydrologic control of carbon release from tropical wetlands.

Schefuß, E., Kuhlmann, H., Mollenhauer, G., Prange, M., Patzold, J., 2011. Forcing of wet phases in southeast Africa over the past 17,000 years. Nature 480, 509-512.

Schefuß, E., Schouten, S., Jansen, J.H.F., Sinninghe Damsté, J.S., 2003. African vegetation controlled by tropical sea surface temperatures in the mid-Pleistocene period. Nature 422, 418-421.

Schefuß, E., Schouten, S., Schneider, R.R., 2005. Climatic controls on central African hydrology during the past 20,000 years. Nature 437, 1003-1006.

Schefuß, E., Sinninghe Damsté, J.S., Jansen, J.H.F., 2004a. Forcing of tropical Atlantic sea surface temperatures during the mid-Pleistocene transition. Paleoceanography 19.

Schefuß, E., Versteegh, G.J.M., Jansen, J.H.F., Sinninghe Damsté, J.S., 2004b. Lipid biomarkers as major source and preservation indicators in SE Atlantic surface sediments. Deep Sea Research Part I: Oceanographic Research Papers 51, 1199-1228.

Schefuß, E., Versteegh, G.J.M., Jansen, J.H.F., Sinninghe Damsté, J.S., 2001. Marine and terrigenous lipids in southeast Atlantic sediments (Leg 175) as paleoenvironmental indicators: initial results. Eds: Wefer, G., Berger, A., Richter, C. (Eds.) In: Proceedings of the Ocean Drilling Program, Scientific Results, 175. , Available from: http://www-odp.tamu.edu/publications/175_SR/chap_10/chap_10.htm.

Schmerk, C.L., Bernards, M.A., Valvano, M.A., 2011. Hopanoid production is required for low-pH tolerance, antimicrobial resistance, and motility in Burkholderia cenocepacia. Journal of Bacteriology 193, 6712-6723.

Schmidt, G.A., Shindell, D.T., Harder, S., 2004. A note on the relationship between ice core methane concentrations and insolation. Geophysical Research Letters 31, 1-4.

Schouten, S., Hopmans, E.C., Baas, M., Boumann, H., Standfest, S., Konneke, M., Stahl, D.A., Sinninghe Damsté, J.S., 2008. Intact membrane lipids of "Candidatus *Nitrosopumilus maritimus*," a cultivated representative of the cosmopolitan mesophilic group I crenarchaeota. Applied and Environmental Microbiology 74, 2433-2440.

Schouten, S., Hopmans, E. C., Pancost, R. D., Sinninghe Damsté, J. S., 2000. Widespread occurrence of structurally diverse tetraether membrane lipids: Evidence for the ubiquitous presence of low-temperature relatives of hyperthermophiles. Proceedings of the National Academy of Sciences of the United States of America 97, 14421-14426.

Schouten, S., Hopmans, E.C., Rosell-Melé, A., Pearson, A., Adam, P., Bauersachs, T., Bard, E., Bernasconi, S.M., Bianchi, T.S., Brocks, J.J., Carlson, L.T., Castañeda, I.S., Derenne, S., Selver, A.D., Dutta, K., Eglinton, T., Fosse, C., Galy, V., Grice, K., Hinrichs, K.U., Huang, Y., Huguet, A., Huguet, C., Hurley, S., Ingalls, A., Jia, G., Keely, B., Knappy, C., Kondo, M., Krishnan, S., Lincoln, S., Lipp, J., Mangelsdorf, K., Martínez-García, A., Ménot, G., Mets, A., Mollenhauer, G., Ohkouchi, N., Ossebaar, J., Pagani, M., Pancost, R.D., Pearson, E.J., Peterse, F., Reichart, G.J., Schaeffer, P., Schmitt, G., Schwark, L., Shah, S.R., Smith, R.W., Smittenberg, R.H., Summons, R.E., Takano, Y., Talbot, H.M., Taylor, K.W.R., Tarozo, R., Uchida, M., Van Dongen, B.E., Van Mooy, B.A.S., Wang, J., Warren, C., Weijers, J.W.H., Werne, J.P., Woltering, M., Xie, S., Yamamoto, M., Yang, H., Zhang, C.L., Zhang, Y., Zhao, M., Sinninghe Damsté, J.S., 2013a. An interlaboratory study of TEX86 and BIT analysis of sediments, extracts, and standard mixtures. Geochemistry, Geophysics, Geosystems 14, 5263-5285.

Schouten, S., Hopmans, E.C., Sinninghe Damsté, J.S., 2013b. The organic geochemistry of glycerol dialkyl glycerol tetraether lipids: A review. Organic Geochemistry 54, 19-61.

Schouten, S., van der Meer, M.T.J., Hopmans, E.C., Rijpstra, W.I.C., Reysenbach, A.L., Ward, D.M., Sinninghe Damsté, J.S., 2007. Archaeal and bacterial glycerol dialkyl glycerol tetraether lipids in hot springs of Yellowstone National Park. Applied and Environmental Microbiology 73, 6181-6191.

Ségalen, L., Lee-Thorp, J.A., Cerling, T., 2007. Timing of C4 grass expansion across sub-Saharan Africa. Journal of Human Evolution 53, 549-559.

Seipke, R.F., Loria, R., 2009. Hopanoids are not essential for growth of *Streptomyces scabies* 87-22. Journal of Bacteriology 191, 5216-5223.

Serrano-Silva, N., Sarria-Guzmán, Y., Dendooven, L., Luna-Guido, M., 2014. Methanogenesis and Methanotrophy in Soil: A Review. Pedosphere 24, 291-307.

Sessions, A.L., Zhang, L., Welander, P.V., Doughty, D., Summons, R.E., Newman, D.K., 2013. Identification and quantification of polyfunctionalized hopanoids by high temperature gas chromatography-mass spectrometry. Organic Geochemistry 56, 120-130.

Shackleton, N.J., Berger, A., Peltier, W.R., 1990. An alternative astronomical calibration of the Lower Pleistocene timescale based on ODP Site 677. Transactions - Royal Society of Edinburgh: Earth Sciences 81, 251-261.

Shannon, L.V., Agenbag, J.J., Buys, M.E.L., 1987. Large- and mesoscale features of the Angola-Benguela front, In: Payne, A.I.L., Gulland, J.A., Brink, K.H., (Eds), The Benguela and comparable ecosystems. South African Journal of Marine Science 5, 11-34.

Sharp, Z., 2007. Principles of Stable Isotope Geochemistry, 1st ed. Pearson Education, Inc., Upper Saddle River, NJ 07458.

Shipboard Scientific Party, 1998. Proceedings of the Ocean Drilling Program, Initial Reports, 175. Ocean Drilling Program. College Station, Texas. doi:10.2973/odp.proc.ir.175.1998.

Simonin, P., Jurgens, U.J., Rohmer, M., 1996. Bacterial triterpenoids of the hopane series from the Prochlorophyte *Prochlorothrix hollandica* and their intracellular localization. European Journal of Biochemistry 241, 865-871.

Singarayer, J.S., Valdes, P.J., Friedlingstein, P., Nelson, S., Beerling, D.J., 2011. Late Holocene methane rise caused by orbitally controlled increase in tropical sources. Nature 470, 82-91.

Sinninghe Damsté, J.S., Ossebaar, J., Abbas, B., Schouten, S., Verschuren, D., 2009. Fluxes and distribution of tetraether lipids in an equatorial African lake: Constraints on the application of the TEX86 palaeothermometer and BIT index in lacustrine settings. Geochimica et Cosmochimica Acta 73, 4232-4249.

Sinninghe Damsté, J.S., Rijpstra, W.I.C., Hopmans, E.C., Weijers, J.W.H., Foesel, B.U., Overmann, J., Dedysh, S.N., 2011. 13,16-Dimethyl Octacosanedioic Acid (iso-Diabolic Acid), a Common Membrane-Spanning Lipid of Acidobacteria Subdivisions 1 and 3. Applied and Environmental Microbiology 77, 4147-4154.

Sinninghe Damsté, J.S., Rijpstra, W.I.C., Schouten, S., Fuerst, J.A., Jetten, M.S.M., Strous, M., 2004. The occurrence of hopanoids in planctomycetes: implications for the sedimentary biomarker record. Organic Geochemistry 35, 561-566.

Smith, L.K., Lewis, W.M., Chanton, J.P., Cronin, G., Hamilton, S.K., 2000. Methane emissions from the Orinoco River floodplain, Venezuela. Biogeochemistry 51, 113-140.

Sohm, J.A., Capone, D.G., 2006. Phosphorus dynamics of the tropical and subtropical north Atlantic: *Trichodesmium* spp. versus bulk plankton. Marine Ecology Progress Series 317, 21-28.

Spahni, R., Chappellaz, J., Stocker, T.F., Loulergue, L., Hausammann, G., Kawamura, K., Fluckiger, J., Schwander, J., Raynaud, D., Masson-Delmotte, V., Jouzel, J., 2005. Atmospheric methane and nitrous oxide of the late Pleistocene from Antarctic ice cores. Science 310, 1317-1321.

Sparkes, R.B., Doğrul Selver, A., Bischoff, J., Talbot, H.M., Gustafsson, Ö., Semiletov, I.P., Dudarev, O.V., van Dongen, B.E., 2015. GDGT distributions on the East Siberian Arctic Shelf: implications for organic carbon export, burial and degradation. Biogeosciences 12, 3753-3768.

Spencer, R.G.M., Hernes, P.J., Aufdenkampe, A.K., Baker, A., Gulliver, P., Stubbins, A., Aiken, G.R., Dyda, R.Y., Butler, K.D., Mwamba, V.L., Mangangu, A.M., Wabakanghanzi, J.N., Six, J., 2012. An initial investigation into the organic matter biogeochemistry of the Congo River. Geochimica et Cosmochimica Acta 84, 614-627.

Spencer-Jones, C.L., Schefuß, E., Talbot, H.M. In Preparation. Bacteriohopanepolyol signatures in Congo fan sediments (GeoB 6518-1).

Spencer, R.G.M., Stubbins, A., Gaillardet, J., 2014. Geochemistry of the Congo River, estuary and plume. In: Biogeochemical Dynamics at Large River-Coastal Interfaces: Linkages with Global Climate Change. Bianchi, T.S., Allison, M.A., Cai, W.J. (Ed.). Cambridge University Press. pp.554-583.

Stein, R., 1985. Late Neogene changes of paleoclimate and paleoproductivity off northwest Africa (D.S.D.P. Site 397). Palaeogeography, Palaeoclimatology, Palaeoecology 49, 47-59.

Street, F.A., Grove, A.T., 1976. Environmental and climatic implications of late Quaternary lake-level fluctuations in Africa. Nature 261, 385-390.

Strous, M., Jetten, M.S.M., 2004. Anaerobic oxidation of methane and ammonium, Annual Review of Microbiology 58, 99–117.

Sugihara, S., Shibata, M., Mvondo Ze, A.D., Araki, S., Funakawa, S., 2015. Effects of vegetation on soil microbial C, N, and P dynamics in a tropical forest and savanna of Central Africa. Applied Soil Ecology 87, 91-98.

Summons, R.E., Jahnke, L.L., Roksandic, Z., 1994. Carbon isotopic fractionation in lipids from methanotrophic bacteria: Relevance for interpretation of the geochemical record of biomarkers. Geochimica et Cosmochimica Acta 58, 2853-2863.

Sun, Y.Y., Zhang, K.X., Liu, J., He, Y.X., Song, B.W., Liu, W.G., Liu, Z.H., 2012. Long chain alkenones preserved in Miocene lake sediments. Organic Geochemistry 50, 19-25.

Syvitski, J.P.M., Vörösmarty, C.J., Kettner, A.J., Green, P., 2005. Impact of humans on the flux of terrestrial sediment to the global coastal ocean. Science 308, 376-380.

Talbot, H.M., Coolen, M.J.L., Sinninghe Damsté, J.S., 2008a. An unusual 17α,21β(H)-bacteriohopanetetrol in Holocene sediments from Ace Lake (Antarctica). Organic Geochemistry 39, 1029-1032.

Talbot, H.M., Farrimond, P., 2007. Bacterial populations recorded in diverse sedimentary biohopanoid distributions. Organic Geochemistry 38, 1212-1225.

Talbot, H.M., Farrimond, P., Schaeffer, P., Pancost, R.D., 2005. Bacteriohopanepolyols in hydrothermal vent biogenic silicates. Organic Geochemistry 36, 663-672.

Talbot, H.M., Handley, L., Spencer-Jones, C.L., Bienvenu, D.J., Schefuß, E., Mann, P.J., Poulsen, J.R., Spencer, R.G.M., Wabakanghanzi, J.N., Wagner, T., 2014. Variability in aerobic methane oxidation over the past 1.2Myrs recorded in microbial biomarker signatures from Congo fan sediments. Geochimica et Cosmochimica Acta 133, 387-401.

Talbot, H.M., Rohmer, M., Farrimond, P., 2007a. Rapid structural elucidation of composite bacterial hopanoids by atmospheric pressure chemical ionisation liquid chromatography/ion trap mass spectrometry. Rapid Communications in Mass Spectrometry 21, 880-892.

Talbot, H.M., Rohmer, M., Farrimond, P., 2007b. Structural characterisation of unsaturated bacterial hopanoids by atmospheric pressure chemical ionisation liquid chromatography/ion trap mass spectrometry. Rapid Communications in Mass Spectrometry 21, 1613-1622.

Talbot, H.M., Squier, A.H., Keely, B.J., Farrimond, P., 2003a. Atmospheric pressure chemical ionisation reversed-phase liquid chromatography/ion trap mass spectrometry of intact bacteriohopanepolyols. Rapid Communications in Mass Spectrometry 17, 728-737.

Talbot, H.M., Summons, R.E., Jahnke, L.L., Cockell, C.S., Rohmer, M., Farrimond, P., 2008b. Cyanobacterial bacteriohopanepolyol signatures from cultures and natural environmental settings. Organic Geochemistry 39, 232-263.

Talbot, H.M., Summons, R., Jahnke, L., Farrimond, P., 2003c. Characteristic fragmentation of bacteriohopanepolyols during atmospheric pressure chemical ionisation liquid chromatography/ion trap mass spectrometry. Rapid Communications in Mass Spectrometry 17, 2788-2796.

Talbot, H.M., Watson, D.F., Murrell, J.C., Carter, J.F., Farrimond, P., 2001. Analysis of intact bacteriohopanepolyols from methanotrophic bacteria by reversed-phase high-performance liquid chromatography-atmospheric pressure chemical ionisation mass spectrometry. Journal of Chromatography A 921, 175-185.

Talbot, H.M., Bischoff, J., Collinson, M.E., Pancost, R.D., In Preparation. Remarkable preservation of polyfunctionalised hopanoids in the Eocene Cobham lignite (UK). Newcastle University, UK.

Tathy, J.P., Cros, B., Delmas, R.A., Marenco, A., Servant, J., Labat, M., 1992. Methane emission from flooded forest in central Africa. Journal of Geophysical Research-Atmospheres 97, 6159-6168.

Tavormina, P.L., Ussler, W., Joye, S.B., Harrison, B.K., Orphan, V.J., 2010. Distributions of putative aerobic methanotrophs in diverse pelagic marine environments. ISME Journal 4, 700-710.

Taylor, K.A., Harvey, H.R., 2011. Bacterial hopanoids as tracers of organic carbon sources and processing across the western Arctic continental shelf. Organic Geochemistry 42, 487-497.

Teece, M.A., Getliff, J.M., Leftley, J.W., Parkes, R.J., Maxwell, J.R., 1998. Microbial degradation of the marine prymnesiophyte *Emiliania huxleyi* under oxic and anoxic conditions as a model for early diagenesis: Long chain alkadienes, alkenones and alkyl alkenoates. Organic Geochemistry 29, 863-880.

Tiedemann, R., Sarnthein, M., Shackleton, N.J., 1994. Astronomic timescale for the Pliocene Atlantic δ18O and dust flux records of Ocean Drilling Program site 659. Paleoceanography 9, 619-638.

Tierney, J.E., Russell, J.M., 2009. Distributions of branched GDGTs in a tropical lake system: Implications for lacustrine application of the MBT/CBT paleoproxy. Organic Geochemistry 40, 1032-1036.

Tierney, J.E., Russell, J.M., Eggermont, H., Hopmans, E.C., Verschuren, D., Sinninghe Damsté, J.S., 2010. Environmental controls on branched tetraether lipid distributions in tropical East African lake sediments. Geochimica et Cosmochimica Acta 74, 4902-4918.

Tierney, J.E., Schouten, S., Pitcher, A., Hopmans, E.C., Sinninghe Damsté, J.S., 2012. Core and intact polar glycerol dialkyl glycerol tetraethers (GDGTs) in Sand Pond, Warwick, Rhode Island (USA): Insights into the origin of lacustrine GDGTs. Geochimica et Cosmochimica Acta 77, 561-581.

Topp, E., Pattey, E., 1997. Soils as sources and sinks for atmospheric methane. Canadian Journal of Soil Science 77, 167-178.

Torn, M.S., Chapin III, F.S., 1993. Environmental and biotic controls over methane flux from arctic tundra. Chemosphere 26, 357-368.

Trauth, M.H., Larrasoaña, J.C., Mudelsee, M., 2009. Trends, rhythms and events in Plio-Pleistocene African climate. Quaternary Science Reviews 28, 399-411.

Trauth, M.H., Maslin, M.A., Deino, A.L., Strecker, M.R., Bergner, A.G.N., Dühnforth, M., 2007. High- and low-latitude forcing of Plio-Pleistocene East African climate and human evolution. Journal of Human Evolution 53, 475-486.

Tyrrell, T., 1999. The relative influences of nitrogen and phosphorus on oceanic primary production. Nature 400, 525-531.

Tzedakis, P.C., 2010. The MIS 11 - MIS 1 analogy, southern European vegetation, atmospheric methane and the "early anthropogenic hypothesis. Climate of the Past 6, 131-144.

Uchida, M., Shibata, Y., Ohkushi, K., Ahagon, N., Hoshiba, M., 2004. Episodic methane release events from Last Glacial marginal sediments in the western North Pacific. Geochemistry Geophysics Geosystems 5, doi: 10.1029/2004GC000699.

Vaks, A., Bar-Matthews, M., Matthews, A., Ayalon, A., Frumkin, A., 2013. Corrigendum to Middle-Late Quaternary paleoclimate of northern margins of the Saharan-Arabian Desert: Reconstruction from speleothems of Negev Desert, Israel [Quat. Sci. Rev. 29 (2010), 2647-2662]. Quaternary Science Reviews 65, 144.

Valentine, D.L., 2007. Adaptations to energy stress dictate the ecology and evolution of the Archaea. Nature Reviews Microbiology 5, 316-323.

Valentine, D.L., Blanton, D.C., Reeburgh, W.S., Kastner, M., 2001. Water column methane oxidation adjacent to an area of active hydrate dissociation, Eel River Basin. Geochimica et Cosmochimica Acta 65, 2633-2640.

Valentine, D.L., Reeburgh, W.S., 2000. New perspectives on anaerobic methane oxidation. Environmental Microbiology 2, 477-484.

Van Der Gon, D.H.A.C., Neue, H.U., 1996. Oxidation of methane in the rhizosphere of rice plants. Biology and Fertility of Soils 22, 359-366.

van Dongen, B.E., Talbot, H.M., Schouten, S., Pearson, P.N., Pancost, R.D., 2006. Well preserved Palaeogene and Cretaceous biomarkers from the Kilwa area, Tanzania. Organic Geochemistry 37, 539-557.

van Winden, J.F., 2011. Methane Cycling in Peat Bogs: Environmental Relevance of Methanotrophs Revealed by Microbial Lipid Chemistry. LPP Contribution Series (35). Utrecht University.

van Winden, J.F., Talbot, H.M., De Vleeschouwer, F., Reichart, G.-J., Sinninghe Damsté, J.S., 2012a. Variation in methanotroph-related proxies in peat deposits from Misten Bog, Hautes-Fagnes, Belgium. Organic Geochemistry 53, 73-79.

van Winden, J.F., Talbot, H.M., Kip, N., Reichart, G.J., Pol, A., McNamara, N.P., Jetten, M.S.M., den Camp, H., Sinninghe Damsté, J.S., 2012b. Bacteriohopanepolyol signatures as markers for methanotrophic bacteria in peat moss. Geochimica et Cosmochimica Acta 77, 52-61.

Vázquez Riveiros, N., Waelbroeck, C., Skinner, L., Duplessy, J.C., McManus, J.F., Kandiano, E.S., Bauch, H.A., 2013. The "MIS 11 paradox" and ocean circulation: Role of millennial scale events. Earth and Planetary Science Letters 371-372, 258-268.

Vecherskaya, M.S., Galchenko, V.F., Sokolova, E.N., Samarkin, V.A., 1993. Activity and species composition of aerobic methanotrophic communities in tundra soils. Current Microbiology 27, 181-184.

Versteegh, G.J.M., Schefuß, E., Dupont, L., Marret, F., Sinninghe Damsté, J.S., Jansen, J.H.F., 2004. Taraxerol and *Rhizophora* pollen as proxies for tracking past mangrove ecosystems. Geochimica et Cosmochimica Acta 68, 411-422.

Vigneron, A., Cruaud, P., Pignet, P., Caprais, J.C., Cambon-Bonavita, M.A., Godfroy, A., Toffin, L., 2013. Archaeal and anaerobic methane oxidizer communities in the Sonora Margin cold seeps, Guaymas Basin (Gulf of California). ISME Journal 7, 1595-1608.

Vilcheze, C., Llopiz, P., Neunlist, S., Poralla, K., Rohmer, M., 1994. Prokaryotic triterpenoids - New hopanoids from the nitrogen fixing bacteria *Azobacter vinelandii*, *Beijerinckia indica* and *Beijerinckia mobilis*. Microbiology 140, 2749-2753.

Vishwakarma, P., Dubey, S.K., 2010. DNA microarray analysis targeting pmoA gene reveals diverse community of methanotrophs in the rhizosphere of tropical rice soils. Current Science 99, 1090-1095.

Volkman, J.K., Eglinton, G., Corner, E.D.S., Sargent, J.R., 1980. Novel unsaturated straight-chain C37 C39 methyl and ethyl ketones in marine sediments and a coccolithophore *Emiliania huxleyi*. Physics and Chemistry of the Earth 12, 219-227.

Volkman, J.K., Barrerr, S.M., Blackburn, S.I., Sikes, E.L., 1995. Alkenones in *Gephyrocapsa oceanica*: Implications for studies of paleoclimate. Geochimica et Cosmochimica Acta 59, 513-520.

Wagner, T., 2000. Control of organic carbon accumulation in the late Quaternary equatorial Atlantic (Ocean Drilling Program sites 664 and 663): Productivity versus terrigenous supply. Paleoceanography 15, 181-199.

Wagner, T., Kallweit, W., Talbot, H.M., Mollenhauer, G., Boom, A., Zabel, M., 2014. Microbial biomarkers support organic carbon transport from methane-rich Amazon wetlands to the shelf and deep sea fan during recent and glacial climate conditions. Organic Geochemistry 67, 85-98.

Wakeham, S.G., Amann, R., Freeman, K.H., Hopmans, E.C., Jørgensen, B.B., Putnam, I.F., Schouten, S., Sinninghe Damsté, J.S., Talbot, H.M., Woebken, D., 2007. Microbial ecology of the stratified water column of the Black Sea as revealed by a comprehensive biomarker study. Organic Geochemistry 38, 2070-2097.

Walsh, E.M., Ingalls, A.E., Keil, R.G., 2008. Sources and transport of terrestrial organic matter in Vancouver Island fjords and the Vancouver-Washington Margin: A multiproxy approach using $\delta^{13}C_{org}$, lignin phenols, and the ether lipid BIT index. Limnology and Oceanography 53, 1054-1063.

Watson, D.F., 2002. Environmental Distribution and Sedimentary Fate of Hopanoid Biological Marker Compounds, Fossil Fuels and Environmental Geochemistry (Postgraduate Institute). University of Newcastle upon Tyne, Online.

Weijers, J.W.H., Schouten, S., Hopmans, E.C., Geenevasen, J.A.J., David, O.R.P., Coleman, J.M., Pancost, R.D., Sinninghe Damsté, J.S., 2006a. Membrane lipids of mesophilic anaerobic bacteria thriving in peats have typical archaeal traits. Environmental Microbiology 8, 648-657.

Weijers, J.W.H., Schouten, S., Spaargaren, O.C., Sinninghe Damsté, J.S., 2006b. Occurrence and distribution of tetraether membrane lipids in soils: Implications for the use of the TEX(86) proxy and the BIT index. Organic Geochemistry 37, 1680-1693.

Weijers, J.W.H., Schouten, S., Schefuß, E., Schneider, R.R., Sinninghe Damsté, J.S., 2009. Disentangling marine, soil and plant organic carbon contributions to continental margin sediments: A multi-proxy approach in a 20 000 year sediment record from the Congo deep-sea fan. Geochimica et Cosmochimica Acta 73, 119-132.

Weiser, R.S., Osterud, C.M., 1945. Studies on the Death of Bacteria at Low Temperatures: I. The Influence of the Intensity of the Freezing Temperature, Repeated Fluctuations of Temperature, and the Period of Exposure to Freezing Temperatures on the Mortality of Escherichia coli. Journal of Bacteriology 50, 413-439.

Welander, P.V., Coleman, M.L., Sessions, A.L., Summons, R.E., Newman, D.K., 2010. Identification of a methylase required for 2-methylhopanoid production and implications for the interpretation of sedimentary hopanes. Proceedings of the National Academy of Sciences of the United States of America 107, 8537-8542.

Welander, P.V., Hunter, R.C., Zhang, L.C., Sessions, A.L., Summons, R.E., Newman, D.K., 2009. Hopanoids Play a Role in Membrane Integrity and pH Homeostasis in Rhodopseudomonas palustris TIE-1. Journal of Bacteriology 191, 6145-6156.

Welander, P.V., Summons, R.E., 2012. Discovery, taxonomic distribution, and phenotypic characterization of a gene required for 3-methylhopanoid production. Proceedings of the National Academy of Sciences of the United States of America 109, 12905-12910.

Westbrook, G.K., Thatcher, K.E., Rohling, E.J., Piotrowski, A.M., Pälike, H., Osborne, A.H., Nisbet, E.G., Minshull, T.A., Lanoisellé, M., James, R.H., Hühnerbach, V., Green, D., Fisher, R.E., Crocker, A.J., Chabert, A., Bolton, C., Beszczynska-Möller, A., Berndt, C., Aquilina, A., 2009. Escape of methane gas from the seabed along the West Spitsbergen continental margin. Geophysical Research Letters 36, doi:10.1029/2009GL039191.

Whalen, S.C., 2005. Biogeochemistry of methane exchange between natural wetlands and the atmosphere. Environmental Engineering Science 22, 73-94.

Wolf, K., Flessa, H., Veldkamp, E., 2012. Atmospheric methane uptake by tropical montane forest soils and the contribution of organic layers. Biogeochemistry 111, 469-483.

Wuebbles, D.J., Hayhoe, K., 2002. Atmospheric methane and global change. Earth-Science Reviews 57, 177-210.

Xu, Y.P., Cooke, M.P., Talbot, H.M., Simpson, M.J., 2009. Bacteriohopanepolyol signatures of bacterial populations in Western Canadian soils. Organic Geochemistry 40, 79-86.

Yang, G., Zhang, C.L., Xie, S., Chen, Z., Gao, M., Ge, Z., Yang, Z., 2013. Microbial glycerol dialkyl glycerol tetraethers from river water and soil near the Three Gorges Dam on the Yangtze River. Organic Geochemistry 56, 40-50.

Zabel, M., Wagner, T., deMenocal, P.B., 2004. Terrigenous signals in sediments of the low-latitude Atlantic - Indications to environmental variations during the Late Quaternary: Part II: Lithogenic matter, in: Wefer, G., Mulitza, S., Ratmeyer, V. (Eds.), The South Atlantic in the Late Quaternary. Springer -Verlag, Berlin Heidelberg.

Zachos, J., Pagani, H., Sloan, L., Thomas, E., Billups, K., 2001. Trends, rhythms, and aberrations in global climate 65 Ma to present. Science 292, 686-693.

Zachos, J.C., Wara, M.W., Bohaty, S., Delaney, M.L., Petrizzo, M.R., Brill, A., Bralower, T.J., Premoli-Silva, I., 2003. A transient rise in tropical sea surface temperature during the Paleocene-Eocene Thermal Maximum. Science 302, 1551-1554.

Zell, C., Kim, J.-H., Abril, G., Sobrinho, R., Dorhout, D., Moreira-Turcq, P., Sinninghe Damsté, J., 2013a. Impact of seasonal hydrological variation on the distributions of tetraether lipids along the Amazon River in the central Amazon basin: Implications for the MBT/CBT paleothermometer and the BIT index. Frontiers in Microbiology 4, DOI: 10.3389/fmicb.2013.00228

Zell, C., Kim, J.-H., Hollander, D., Lorenzoni, L., Baker, P., Silva, C.G., Nittrouer, C., Sinninghe Damsté, J.S., 2014a. Sources and distributions of branched and isoprenoid tetraether lipids on the Amazon shelf and fan: Implications for the use of GDGT-based proxies in marine sediments. Geochimica et Cosmochimica Acta 139, 293-312.

Zell, C., Kim, J.-H., Moreira-Turcq, P., Abril, G., Hopmans, E.C., Bonnet, M.-P., Sobrinho, R.L., Sinninghe Damsté, J.S., 2013b. Disentangling the origins of branched tetraether lipids and crenarchaeol in the lower Amazon River: Implications for GDGT-based proxies. Limnology and Oceanography 58, 343-353.

Zell, C., Kim, J.H., Balsinha, M., Dorhout, D., Fernandes, C., Baas, M., Sinninghe Damsté, J.S., 2014b. Transport of branched tetraether lipids from the Tagus River basin to the coastal ocean of the Portuguese margin: consequences for the interpretation of the MBT'/CBT paleothermometer. Biogeosciences 11, 5637-5655.

Zhang, C.L., Huang, Z., Li, Y.-L., Romanek, C.S., Mills, G., Gibson, R.A., Talbot, H.M., Wiegel, J., Noakes, J., Culp, R., White, D.C., 2007. Lipid biomarkers, carbon isotopes and phylogenetic characterisation of bacteria in California and Nevada hot springs. Geomicrobiology Journal 24, 519–534.

Zhang, C., Wang, J., Wei, Y., Zhu, C., Huang, L., Dong, H., 2012. Production of branched tetraether lipids in the lower Pearl River and estuary: effects of extraction methods and impact on bGDGT proxies. Frontiers in Microbiology 2, DOI: 10.3389/fmicb.2011.00274

Zhang, Y.G., Zhang, C.L.L., Liu, X.L., Li, L., Hinrichs, K.U., Noakes, J.E., 2011. Methane Index: A tetraether archaeal lipid biomarker indicator for detecting the instability of marine gas hydrates. Earth and Planetary Science Letters 307, 525-534.

Zhao, J., An, C., Longo, W.M., Dillon, J.T., Zhao, Y., Shi, C., Chen, Y., Huang, Y., 2014. Occurrence of extended chain length C41 and C42 alkenones in hypersaline lakes. Organic Geochemistry 75, 48-53.

Zheng, Y., Singarayer, J.S., Cheng, P., Yu, X., Liu, Z., Valdes, P.J., Pancost, R.D., 2014. Holocene variations in peatland methane cycling associated with the Asian summer monsoon system. Nature Communications 5, DOI: 10.1038/ncomms5631.

Zhu, C., Talbot, H.M., Wagner, T., Pan, J.M., Pancost, R.D., 2010. Intense aerobic methane oxidation in the Yangtze Estuary: A record from 35-aminobacteriohopanepolyols in surface sediments. Organic Geochemistry 41, 1056-1059.

Zhu, C., Talbot, H.M., Wagner, T., Pan, J.M., Pancost, R.D., 2011. Distribution of hopanoids along a land to sea transect: Implications for microbial ecology and the use of hopanoids in environmental studies. Limnology and Oceanography 56, 1850-1865.

Zhu, C., Wagner, T., Talbot, H.M., Weijers, J.W.H., Pan, J.M., Pancost, R.D., 2013. Mechanistic controls on diverse fates of terrestrial organic components in the East China Sea. Geochimica et Cosmochimica Acta 117, 129-143.

Zhu, C., Weijers, J.W.H., Wagner, T., Pan, J.-M., Chen, J.-F., Pancost, R.D., 2011. Sources and distributions of tetraether lipids in surface sediments across a large river-dominated continental margin. Organic Geochemistry 42, 376-386.

Zhu, C., Xue, B., Pan, J., Zhang, H., Wagner, T., Pancost, R.D., 2008. The dispersal of sedimentary terrestrial organic matter in the East China Sea (ECS) as revealed by biomarkers and hydro-chemical characteristics. Organic Geochemistry 39, 952-957.

Appendices

Appendix I. Data Citation

Amazon Basin soils are cited from Wagner et al., (2014) and include; sample 5 seasonally inundated soils (0-20 cm depth), sample 6 Terra Firme soil (0-20 cm depth). Amazon wetland samples are cited from Wagner et al., (2014) and include; sample 1 wetland sediment (0-10 and 200-250 cm depth), sample 2 wetland sediment (0-10 and 25-30 cm depth), sample 3 wetland sediment (0-25 cm depth). San Salvador upland soil is cited from Pearson et al., (2009). Têt watershed soil is cited from Kim et al., (2010) and includes; TESO1 (soil 2-7 cm depth), TESO5 (soil 2-7 cm depth), TESO15 (soil 1-5 cm depth), TESO17 (soil upper 10 cm depth), TESO19 (soil upper 10 cm depth), TESO 32 (soil upper 10 cm depth), TESO35 (soil upper 10 cm depth), TESO36 (soil 0-5 cm depth), TESO39 (soil upper 10 cm depth), TESO41 (soil upper 10 cm depth), TESO47 (upper 10 cm depth), TESO 48 (soil 0-20 cm depth). Têt watershed peat samples are cited from Kim et al., (2010) and include; TESO2 (Peat 0-10 cm depth), TESO49 (Peat 0-10 cm depth). Soils from East China are cited from Zhu et al., (2011) and include; Arable farm, Grassland, Afforestation. Canadian soils are cited from Xu et al., (2009) and include: Grassland soil 1 Ah horizon 0-15 cm depth, Grassland soil 2 Ah horizon 0-15cm depth, Grassland 3 Ah horizon 0-15 cm depth, Aspen forest-grassland transition soil Ah horizon 0-10 cm depth, Aspen forest soil O horizon 0-15 cm depth. Arctic permafrost soils are cited from Rethemeyer et al., (2010) and include; Kolhaugen Hill trough 0-30 cm depth, Kolhaugen Hill centre 0-30 cm depth, Leierhaugen Hill 0-30 cm depth, Upper Drainage Area 0-20cm depth, Upper Drainage Area 0-20 cm depth, Lower Drainage Area 0-20 cm depth. Northern UK soils are cited from Cooke et al., (2008) and include; University garden DSNM 0-10 cm, Arable TFWC 0-10 cm, Pasture WNBC9 0-10 cm, Palace Leas Plot 7 0-5 cm.

Appendix II. Concentration (µg/g TOC) of bacteriohopanepolyols in 16 forest soils from the Congo (bdl, below detection limit).

Structure	CELF JP6	CELF C6B	CELF C17B	CELF C18B	CELF C19B	CELF C27B	LTF 7-1	LTF 8-1	LTF 10-1	TMF 12-1	GF 9-1	SF 11-1	TSFF 6-1	SFS 3-1	FSFM 4-1	MF C8B
1m	bdl	bdl	bdl	bdl	bdl	bdl	10	5.0	6.1	8.7	5.3	10	20	bdl	bdl	bdl
1k	bdl	bdl	8.0	6.1	6.2	2.0	11	19	15	8.6	20	16	12	5.6	5.4	bdl
1b	22	34	55	64	71	30	230	190	210	130	270	210	390	79	180	55
2b	13	4.1	18	24	42	11	81	130	130	45	160	63	52	46	26	15
1n	bdl	bdl	bdl	bdl	bdl	bdl	bdl	bdl	bdl	bdl	bdl	bdl	bdl	bdl	bdl	bdl
4/5g	96	28	92	55	270	69	70	66	110	35	21	240	110	16	22	240
1g	940	270	740	720	1300	440	790	1600	1500	590	1300	770	730	340	540	1000
2g	22.0	8.3	20	30	42	19	16	40	25	10	31	19	7.6	9	12	26
3g	5.3	2.3	5.6	8.7	5.4	6.0	bdl	30	28	14	21	19	21	bdl	7.7	9.4
4/5e	bdl	bdl	bdl	bdl	7.7	bdl	bdl	bdl	bdl	bdl	bdl	bdl	bdl	bdl	bdl	bdl
1e	42	18	38	81	87	16	26	59	67	17	23	47	30	8.6	16	24
4/5f	1.2	bdl	bdl	13	1.9	bdl	bdl	bdl	bdl	bdl	bdl	bdl	bdl	bdl	bdl	bdl
1f	bdl	13	47	260	14	13	bdl	bdl	bdl	bdl	bdl	bdl	bdl	bdl	bdl	11
1f'	bdl	bdl	bdl	55	bdl	bdl	bdl	bdl	bdl	bdl	bdl	bdl	bdl	bdl	bdl	bdl
1a	197	59	180	170	300	69	570	800	700	290	540	580	520	380	230	120
2a	19	8.0	13	15	37	2.9	35	69	52	17	34	53	37	52	25	13
1c	20	8.7	95	100	130	56	35	28	44	22	48	130	55	91	20	130
2c	4.8	4.8	17	24	60	37	5.9	8	10	5.8	12	48	15	19	15	10
1d	5.5	5.1	10	6.1	16	bdl	17	27	19	12	bdl	22	24	16	22	8.9
2d	bdl	1.1	1.9	3.5	4.4	bdl	7.3	26	14	4.1	bdl	bdl	12	6.9	14	5.6
4/5l	bdl	bdl	bdl	bdl	bdl	bdl	33	57	68	19	35	27	58	15	38	bdl
1l	24	10	26	28	20	15	86	100	120	44	130	30	110	16	30	27
2l	bdl	bdl	bdl	bdl	bdl	bdl	30	100	26	26	96	bdl	bdl	bdl	35	bdl
1h	260	250	270	970	740	400	870	1400	1500	530	1000	1400	1600	360	290	390
1h	120	bdl	360	bdl	370	bdl	bdl	bdl	bdl	bdl	bdl	bdl	bdl	bdl	bdl	270
2h	120	23	89	100	220	97	84	290	360	97	86	230	170	bdl	bdl	120
3h	bdl	4.6	bdl	11	42	6.1	bdl	bdl	bdl	bdl	bdl	bdl	bdl	bdl	bdl	22
1o	bdl	9.2	25	24	23	7.5	23	25	48	13	24	bdl	25	11	bdl	14
1i	76	54	120	95	190	53	170	180	270	95	210	180	340	43	55	110
1i	20	12	77	18	44	14	bdl	bdl	bdl	bdl	bdl	bdl	bdl	bdl	bdl	38
2i	10	3.2	12	5.4	12	5.9	40	71	73	24	35	32	56	19	bdl	5.9
3i	bdl	bdl	bdl	bdl	bdl	bdl	23	57	40	6	18	22	10	21	41	bdl
1j	92	26	41	54	100	37	150	280	280	100	190	240	340	25	42	55
1j	bdl	6.6	12	5.4	22	bdl	bdl	bdl	bdl	bdl	bdl	bdl	bdl	bdl	bdl	7.1
2j	bdl	bdl	bdl	4.5	3.3	bdl	14	57	bdl	12	bdl	bdl	bdl	bdl	bdl	3.1
3j	19	bdl	3.0	4.2	8.8	1.7	bdl	bdl	bdl	bdl	bdl	bdl	bdl	bdl	bdl	2.8

Appendix III. Concentration (µg/g TOC) of bacteriohopanepolyols in 6 Savannah/field soils from the Congo (bdl, below detection limit).

Structure	SB C38B	CG C46B	SBZV 1-1	SS 1-1	SS 5-1	F 13-1
1m	bdl	bdl	bdl	bdl	bdl	bdl
1k	bdl	bdl	bdl	bdl	bdl	bdl
1b	14	30	160	160	76	220
2b	4.2	5.0	24	32	24	74
1n	bdl	bdl	bdl	bdl	bdl	bdl
4/5g	11	38	9.1	20	42	31
1g	300	550	210	410	480	360
2g	17	15	10	bdl	20	11
3g	2.0	7.3	bdl	bdl	bdl	bdl
4/5e	1.8	bdl	bdl	bdl	bdl	bdl
1e	19	14	bdl	2.1	12	15
4/5f	bdl	bdl	bdl	bdl	bdl	bdl
1f	0.92	bdl	bdl	bdl	bdl	bdl
1f’	bdl	bdl	bdl	bdl	bdl	bdl
1a	47	61	200	160	33	460
2a	10	10	38	36	21	84
1c	23	10	26	18	25	140
2c	13	26	26	18	16	71
1d	bdl	8.2	13	13	11	16
2d	bdl	3.7	bdl	bdl	bdl	bdl
4/5l	bdl	bdl	bdl	bdl	22	49
1l	bdl	3.9	bdl	bdl	bdl	bdl
2l	bdl	bdl	bdl	bdl	bdl	bdl
1h	50	200	97	250	370	900
1h	47	bdl	bdl	bdl	bdl	bdl
2h	3.3	29	bdl	45	bdl	130
3h	2.6	9.2	bdl	bdl	bdl	bdl
1o	bdl	2.1	bdl	bdl	bdl	19
1i	39	42	12	23	55	140
1i	7.0	11	bdl	bdl	bdl	bdl
2i	1.6	4.3	6.7	14	bdl	42
3i	bdl	bdl	11	48	67	31
1j	10	18	bdl	bdl	70	120
1j	bdl	2.2	bdl	bdl	bdl	bdl
2j	bdl	0.48	bdl	bdl	bdl	13
3j	0.9	1.2	bdl	bdl	bdl	bdl

Appendix IV. Concentration (µg/g TOC) of bacteriohopanepolyols in 6 Malebo pool wetland and 1 estuarine sediment from the Congo (bdl, below detection limit).

Structure	PS 0-5	PS 5-10	RE 0-5	RE 5-10	EF 0-5	EF 5-10	Estuary
1m	bdl	bdl	bdl	bdl	bdl	bdl	bdl
1k	bdl	bdl	bdl	bdl	bdl	bdl	bdl
1b	490	590	400	370	460	390	320
2b	53	84	70	81	41	36	24
1n	40	65	46	49	33	34	bdl
4/5g	bdl	bdl	bdl	bdl	bdl	bdl	bdl
1g	960	1100	420	360	950	710	320
2g	bdl	bdl	bdl	bdl	bdl	bdl	bdl
3g	bdl	bdl	bdl	bdl	bdl	bdl	bdl
4/5e	bdl	bdl	bdl	bdl	bdl	bdl	bdl
1e	270	270	110	89	230	200	82
4/5f	58	56	31	27	58	52	12
1f	1200	1100	640	500	1200	1100	180
1f’	69	86	64	51	70	86	68
1a	640	910	520	560	640	520	81
2a	100	110	100	91	64	50	bdl
1c	45	48	31	33	37	29	bdl
2c	17	19	22	13	11	5.6	bdl
1d	16	23	14	13	18	14	bdl
2d	bdl	bdl	bdl	bdl	bdl	bdl	bdl
4/5l	bdl	bdl	bdl	bdl	bdl	bdl	bdl
1l	bdl	bdl	bdl	bdl	bdl	bdl	bdl
2l	bdl	bdl	bdl	bdl	bdl	bdl	bdl
1h	2000	2200	1200	1300	1700	1700	230
1h	bdl	bdl	bdl	bdl	bdl	bdl	bdl
2h	230	260	170	170	130	120	bdl
3h	bdl	bdl	bdl	bdl	bdl	bdl	bdl
1o	bdl	bdl	bdl	bdl	bdl	bdl	12
1i	280	250	190	220	170	220	33
1i	bdl	bdl	bdl	bdl	bdl	bdl	bdl
2i	38	41	42	29	12	15	bdl
3i	59	59	38	48	18	23	bdl
1j	260	250	220	280	200	260	21
1j	bdl	bdl	bdl	bdl	bdl	bdl	bdl
2j	bdl	bdl	bdl	bdl	bdl	bdl	bdl
3j	bdl	bdl	bdl	bdl	bdl	bdl	bdl

Appendix V. ***Spearmans Rho correlation coefficient (r_s) and p values of cyclitol ethers, bold indicates significant correlation at the 0.05 level, BHT cyclitol ether BHpentol cyclitol ether and BHhexol cyclitol ether are presented as a total of the two isomers.***

		BHT cyclitol ether	BHpentol cyclitol ether	BHT glucosamine	BHhexol cyclitol ether	2-methyl BHT cyclitol ether	3-methyl BHT cyclitol ether	2-methyl BHpentol cyclitol ether	3-methyl BHpentol cyclitol ether	2-methyl BHhexol cyclitol ether
BHT cyclitol ether	r_s									
	p									
BHpentol cyclitol ether	r_s	.903								
	p	<0.05								
BHT glucosamine	r_s	.119	.279							
	p	.539	.143							
BHhexol cyclitol ether	r_s	.921	.896	.171						
	p	<0.05	<0.05	.374						
2-methyl BHT cyclitol ether	r_s	.864	.830	.169	.833					
	p	<0.05	<0.05	.381	<0.05					
3-methyl BHT cyclitol ether	r_s	-.274	-.160	.184	-.373	-.089				
	p	.150	.407	.340	.046	.647				
2-methyl BHpentol cyclitol ether	r_s	.713	.686	.309	.758	.732	-.483			
	p	<0.05	<0.05	.103	<0.05	<0.05	<0.05			
3-methyl BHpentol cyclitol ether	r_s	.443	.283	-.300	.491	.303	-.646	.502		
	p	<0.05	.136	.114	<0.05	.110	<0.05	<0.05		
2-methyl BHhexol cyclitol ether	r_s	.026	.010	.511	.060	.165	.330	.168	-.126	
	p	.892	.960	<0.05	.757	.393	.081	.384	.514	
3-methyl BHhexol cyclitol ether	r_s	-.237	-.068	.187	-.325	-.019	.705	-.419	-.704	.223
	p	.216	.725	.331	.085	.921	<0.05	<0.05	<0.05	.245

Appendix VI. One way ANOVA post hoc (Tukey) results for comparisons of mean BIT at four intervals (T, T value; P, significance value).

BIT intervals		2.5-1.7	1.7-1.1	1.1-0.3
2.5-1.7	T			
	P			
1.7-1.1	T	-3.24		
	P	<0.05		
1.1-0.3	T	1.95	5.68	
	P	0.208	<0.05	
0.3-0	T	-1.74	1.58	-4.05
	P	0.302	0.389	<0.05

Appendix VII. ANOVA with post hoc analysis (Tukey) for TOC divided into 100 Ka intervals.

Interval		10-100	100-200	200-300	300-400	400-500	500-600	600-700	700-800	800-900	900-1000	1000-1100
10-100	T											
	Adj P											
100-200	T	-1.97										
	Adj P	0.962										
200-300	T	-1.33	0.42									
	Adj P	1	1									
300-400	T	-2.32	-0.56	-0.88								
	Adj P	0.819	1	1								
400-500	T	-1.63	0.54	<0.05	1.08							
	Adj P	0.997	1	1	1							
500-600	T	-2.04	-0.43	-0.75	0.06	-0.88						
	Adj P	0.943	1	1	1	1						
600-700	T	-4.13	-2.69	-2.78	-2.06	-3.24	-1.96					
	Adj P	0.009	0.547	0.475	0.938	0.173	0.963					
700-800	T	-3.89	-2.43	-2.55	-1.82	-2.97	-1.74	0.22				
	Adj P	0.022	0.745	0.66	0.985	0.327	0.991	1				
800-900	T	-5.38	-4.02	-3.98	-3.31	-4.65	-3.12	-1.14	-1.35			
	Adj P	<0.05	0.013	<0.05	0.145	<0.05	0.235	1	1			
900-1000	T	-4.8	-3.44	-3.46	-2.78	-4.01	-2.64	-0.71	-0.92	0.4		
	Adj P	<0.05	0.101	0.094	0.469	<0.05	0.583	1	1	1		
1000-1100	T	-4.38	-2.94	-3	-2.29	-3.52	-2.17	-0.19	-0.4	0.96	0.54	
	Adj P	<0.05	0.347	0.306	0.838	0.077	0.896	1	1	1	1	
1100-1200	T	-7.24	-5.98	-5.72	-5.11	-6.74	-4.77	-2.71	-2.93	-1.55	-1.93	-2.55
	Adj P	<0.05	<0.05	<0.05	<0.05	<0.05	<0.05	0.527	0.357	0.998	0.97	0.657

Appendix VIII. ANOVA with post hoc analysis (Tukey) for TOC divided into 100 Ka intervals.

Interval		10-100	100-200	200-300	300-400	400-500	500-600	600-700	700-800	800-900	900-1000	1000-1100	1100-1200	1200-1300	1300-1400	1400-1500
1200-1300	T	-6.14	-5.2	-5.21	-4.75	-5.57	-4.62	-3.21	-3.36	-2.41	-2.67	-3.1	-1.34			
	Adj P	<0.05	<0.05	<0.05	<0.05	<0.05	<0.05	0.189	0.125	0.763	0.564	0.249	1			
1300-1400	T	-4.54	-3.56	-3.64	-3.15	-3.89	-3.08	-1.69	-1.84	-0.89	-1.16	-1.57	0.19	1.24		
	Adj P	<0.05	<0.05	0.053	0.218	<0.05	0.259	0.994	0.982	1	1	0.998	1	1		
1400-1500	T	-5.48	-4.45	-4.47	-3.96	-4.85	-3.84	-2.32	-2.48	-1.44	-1.73	-2.19	-0.28	0.93	-0.38	
	Adj P	<0.05	<0.05	0.002	<0.05	<0.05	<0.05	0.823	0.711	0.999	0.992	0.89	1	1	1	
1500-1600	T	-4.5	-3.52	-3.6	-3.11	-3.85	-3.04	-1.65	-1.8	-0.85	-1.12	-1.53	0.23	1.27	0.03	0.42
	Adj P	<0.05	0.078	0.06	0.239	<0.05	0.282	0.996	0.986	1	1	0.999	1	1	1	1
1600-1700	T	-4.29	-3.41	-3.5	-3.06	-3.69	-3.01	-1.77	-1.91	-1.05	-1.3	-1.66	-0.09	0.93	-0.22	0.12
	Adj P	<0.05	0.109	0.082	0.27	<0.05	0.302	0.989	0.973	1	1	0.996	1	1	1	1
1700-1800	T	-3.04	-2.03	-2.18	-1.66	-2.33	-1.64	-0.26	-0.42	0.54	0.25	-0.14	1.63	2.4	1.16	1.61
	Adj P	0.281	0.948	0.895	0.995	0.816	0.996	1	1	1	1	1	0.997	0.765	1	0.997
1800-1900	T	-3.27	-2.37	-2.5	-2.04	-2.63	-2.02	-0.79	-0.93	-0.07	-0.33	-0.68	0.9	1.76	0.61	0.99
	Adj P	0.162	0.789	0.697	0.943	0.591	0.949	1	1	1	1	1	1	0.99	1	1
1900-2000	T	-2.88	-1.98	-2.12	-1.66	-2.23	-1.65	-0.42	-0.55	0.3	0.04	-0.3	1.27	2.07	0.92	1.32
	Adj P	0.392	0.96	0.918	0.996	0.868	0.996	1	1	1	1	1	1	0.934	1	1
2000-2100	T	-2.28	-1.3	-1.47	-0.97	-1.56	-0.98	0.32	0.18	1.09	0.8	0.45	2.13	2.8	1.6	2.05
	Adj P	0.844	1	0.999	1	0.998	1	1	1	1	1	1	0.915	0.456	0.997	0.941
2100-2200	T	-2.11	-1.12	-1.3	-0.8	-1.38	-0.81	0.49	0.34	1.25	0.97	0.61	2.3	2.94	1.74	2.16
	Adj P	0.923	1	1	1	1	1	1	1	1	1	1	0.835	0.352	0.992	0.887
2200-2300	T	-3.06	-2.22	-2.35	-1.93	-2.46	-1.91	-0.77	-0.89	-0.1	-0.34	-0.66	0.8	1.64	0.55	0.9
	Adj P	0.274	0.876	0.802	0.97	0.729	0.973	1	1	1	1	1	1	0.996	1	1
2300-2400	T	-2.67	-1.7	-1.86	-1.36	-1.97	-1.36	-0.05	-0.2	0.71	0.43	0.07	1.75	2.49	1.29	1.72
	Adj P	0.562	0.994	0.981	1	0.962	1	1	1	1	1	1	0.991	0.704	1	0.992
2400-2500	T	-1.65	-0.66	0.86	-0.35	-0.91	-0.38	0.92	0.78	1.68	1.4	1.05	2.73	3.3	2.1	2.57
	Adj P	0.996	1	1	1	1	1	1	1	0.995	1	1	0.511	0.15	0.926	0.641

Appendix IX. ANOVA with post hoc analysis (Tukey) for TOC divided into 100 Ka intervals.

Interval		1500-1600	1600-1700	1700-1800	1800-1900	1900-2000	2000-2100	2100-2200	2200-2300	2400-2500
1600-1700	T	-0.25								
	Adj P	1								
1700-1800	T	1.13	1.3							
	Adj P	1	1							
1800-1900	T	0.58	0.78	-0.47						
	Adj P	1	1	1						
1900-2000	T	0.9	1.07	-0.15	0.29					
	Adj P	1	1	1	1					
2000-2100	T	1.57	1.7	0.48	0.9	0.59				
	Adj P	0.998	0.994	1	1	1				
2100-2200	T	1.71	1.83	0.61	1.02	0.72	0.13			
	Adj P	0.993	0.984	1	1	1	1			
2200-2300	T	0.52	0.71	-0.47	-0.03	-0.31	-0.88	-1		
	Adj P	1	1	1	1	1	1	1		
2300-2400	T	1.26	1.41	0.17	0.61	0.3	-0.3	-0.43	0.61	
	Adj P	1	1	1	1	1	1	1	1	
2400-2500	T	2.07	2.16	0.97	1.36	1.05	0.48	0.35	1.32	0.78
	Adj P	0.936	0.901	1	1	1	1	1	1	1

Appendix X. BHP concentrations (μg/g TOC) for ODP 1075 [disc].